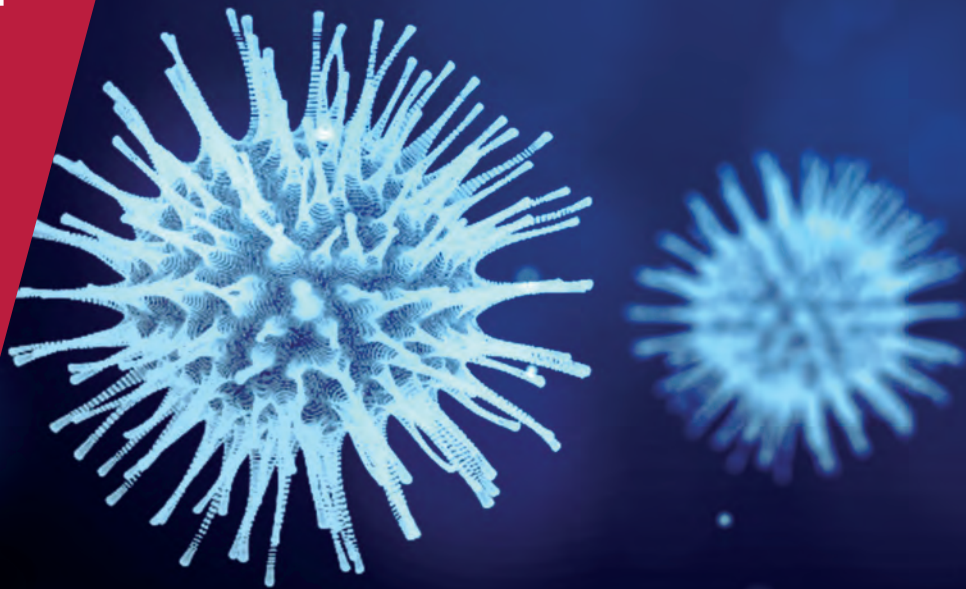


**CENTRE FOR  
ECONOMIC  
POLICY  
RESEARCH**

**CEPR PRESS**



**COVID ECONOMICS**  
VETTED AND REAL-TIME PAPERS

**PERSISTENCE OF PANDEMICS**

Peter Zhixian Lin and  
Christopher M. Meissner

**VOLUNTARY AND MANDATORY  
SOCIAL DISTANCING**

Alexander Chudik, M. Hashem Pesaran  
and Alessandro Rebucci

**WHO GOT HIT, WHEN AND WHY?**

Annette Alstadsæter, Bernt Bratsberg,  
Gaute Eielsen, Wojciech Kopczuk,  
Simen Markussen, Oddbjørn Raaum  
and Knut Røed

**LONG-RUN EFFECTS ON  
EMPLOYMENT**

Victoria Gregory, Guido Menzio  
and David Wiczer

**ISSUE 15**  
7 MAY 2020

**EQUILIBRIUM SOCIAL DISTANCING**

Flavio Toxvaerd

**THE US PAYCHECK PROTECTION  
PROGRAM**

Anna Cororaton and Samuel Rosen

**QUARANTINE: WHEN AND HOW  
LONG?**

Rikard Forslid and Mathias Herzing

**POVERTY IN AFRICA**

Gbêtondji Melaine Armel Nonvide

---

# Covid Economics

## Vetted and Real-Time Papers

*Covid Economics, Vetted and Real-Time Papers*, from CEPR, brings together formal investigations on the economic issues emanating from the Covid outbreak, based on explicit theory and/or empirical evidence, to improve the knowledge base.

**Founder:** Beatrice Weder di Mauro, President of CEPR

**Editor:** Charles Wyplosz, Graduate Institute Geneva and CEPR

**Contact:** Submissions should be made at <https://portal.cepr.org/call-papers-covid-economics-real-time-journal-cej>. Other queries should be sent to [covidecon@cepr.org](mailto:covidecon@cepr.org).

Copyright for the papers appearing in this issue of *Covid Economics: Vetted and Real-Time Papers* is held by the individual authors.

### **The Centre for Economic Policy Research (CEPR)**

The Centre for Economic Policy Research (CEPR) is a network of over 1,500 research economists based mostly in European universities. The Centre's goal is twofold: to promote world-class research, and to get the policy-relevant results into the hands of key decision-makers. CEPR's guiding principle is 'Research excellence with policy relevance'. A registered charity since it was founded in 1983, CEPR is independent of all public and private interest groups. It takes no institutional stand on economic policy matters and its core funding comes from its Institutional Members and sales of publications. Because it draws on such a large network of researchers, its output reflects a broad spectrum of individual viewpoints as well as perspectives drawn from civil society. CEPR research may include views on policy, but the Trustees of the Centre do not give prior review to its publications. The opinions expressed in this report are those of the authors and not those of CEPR.

Chair of the Board

Sir Charlie Bean

Founder and Honorary President

Richard Portes

President

Beatrice Weder di Mauro

Vice Presidents

Maristella Botticini

Ugo Panizza

Philippe Martin

Hélène Rey

Chief Executive Officer

Tessa Ogden

---

# Editorial Board

**Beatrice Weder di Mauro**, CEPR  
**Charles Wyplosz**, Graduate Institute  
Geneva and CEPR

**Viral V. Acharya**, Stern School of  
Business, NYU and CEPR

**Abi Adams-Prassl**, University of  
Oxford and CEPR

**Jérôme Adda**, Bocconi University  
and CEPR

**Guido Alfani**, Bocconi University and  
CEPR

**Franklin Allen**, Imperial College  
Business School and CEPR

**Oriana Bandiera**, London School of  
Economics and CEPR

**David Bloom**, Harvard T.H. Chan  
School of Public Health

**Tito Boeri**, Bocconi University and  
CEPR

**Markus K Brunnermeier**, Princeton  
University and CEPR

**Michael C Burda**, Humboldt  
Universitaet zu Berlin and CEPR

**Paola Conconi**, ECARES, Universite  
Libre de Bruxelles and CEPR

**Giancarlo Corsetti**, University of  
Cambridge and CEPR

**Fiorella De Fiore**, Bank for  
International Settlements and CEPR

**Mathias Dewatripont**, ECARES,  
Universite Libre de Bruxelles and  
CEPR

**Barry Eichengreen**, University of  
California, Berkeley and CEPR

**Simon J Evenett**, University of St  
Gallen and CEPR

**Antonio Fatás**, INSEAD Singapore  
and CEPR

**Francesco Giavazzi**, Bocconi  
University and CEPR

**Christian Gollier**, Toulouse School of  
Economics and CEPR

**Rachel Griffith**, IFS, University of  
Manchester and CEPR

**Timothy J. Hatton**, University of  
Essex and CEPR

**Ethan Ilzetzki**, London School of  
Economics and CEPR

**Beata Javorcik**, EBRD and CEPR

**Sebnem Kalemli-Ozcan**, University  
of Maryland and CEPR Rik Frehen

**Tom Kompas**, University of  
Melbourne and CEBRA

**Per Krusell**, Stockholm University  
and CEPR

**Philippe Martin**, Sciences Po and  
CEPR

**Warwick McKibbin**, ANU College of  
Asia and the Pacific

**Kevin Hjortshøj O'Rourke**, NYU  
Abu Dhabi and CEPR

**Evi Pappa**, European University  
Institute and CEPR

**Barbara Petrongolo**, Queen Mary  
University, London, LSE and CEPR

**Richard Portes**, London Business  
School and CEPR

**Carol Propper**, Imperial College  
London and CEPR

**Lucrezia Reichlin**, London Business  
School and CEPR

**Ricardo Reis**, London School of  
Economics and CEPR

**Hélène Rey**, London Business School  
and CEPR

**Dominic Rohner**, University of  
Lausanne and CEPR

**Moritz Schularick**, University of  
Bonn and CEPR

**Paul Seabright**, Toulouse School of  
Economics and CEPR

**Christoph Trebesch**, Christian-  
Albrechts-Universitaet zu Kiel and  
CEPR

**Karen-Helene Ulltveit-Moe**,  
University of Oslo and CEPR

**Jan C. van Ours**, Erasmus University  
Rotterdam and CEPR

**Thierry Verdier**, Paris School of  
Economics and CEPR

---

# Ethics

*Covid Economics* will publish high quality analyses of economic aspects of the health crisis. However, the pandemic also raises a number of complex ethical issues. Economists tend to think about trade-offs, in this case lives vs. costs, patient selection at a time of scarcity, and more. In the spirit of academic freedom, neither the Editors of *Covid Economics* nor CEPR take a stand on these issues and therefore do not bear any responsibility for views expressed in the journal's articles.

---

# Covid Economics

## Vetted and Real-Time Papers

Issue 15, 7 May 2020

### Contents

A note on long-run persistence of public health outcomes in pandemics <i>Peter Zhixian Lin and Christopher M. Meissner</i>	1
Voluntary and mandatory social distancing: Evidence on Covid-19 exposure rates from Chinese provinces and selected countries <i>Alexander Chudik, M. Hashem Pesaran and Alessandro Rebucci</i>	26
The first weeks of the coronavirus crisis: Who got hit, when and why? Evidence from Norway <i>Annette Alstadsæter, Bernt Bratsberg, Gaute Eielsen, Wojciech Kopczuk, Simen Markussen, Oddbjørn Raaum and Knut Røed</i>	63
Pandemic recession: L-shaped or V-shaped? <i>Victoria Gregory, Guido Menzio and David Wiczer</i>	88
Equilibrium social distancing <i>Flavio Toxvaerd</i>	110
Public firm borrowers of the US Paycheck Protection Program <i>Anna Cororaton and Samuel Rosen</i>	134
Assessing the consequences of quarantines during a pandemic <i>Rikard Forslid and Mathias Herzing</i>	159
Short-term impact of COVID-19 on poverty in Africa <i>Gbêtondji Melaine Armel Nonvide</i>	184

# A note on long-run persistence of public health outcomes in pandemics<sup>1</sup>

Peter Zhixian Lin<sup>2</sup> and Christopher M. Meissner<sup>3</sup>

Date submitted: 30 April 2020; Date accepted: 1 May 2020

*Covid-19 is the single largest threat to global public health since the Spanish Influenza pandemic of 1918-20. Was the world better prepared in 2020 than it was in 1918? After a century of public health and basic science research, pandemic response and mortality outcomes should be better than in 1918-20. We ask whether historical mortality from pandemics has any predictive content for mortality in the ongoing Covid-19 pandemic. We find a strong persistence in public health performance in the early days of the Covid-19 pandemic. Places that performed poorly in terms of mortality in 1918 were more likely to have higher mortality today. This is true across countries and across a sample of US cities. Experience with SARS is associated with lower mortality today. Distrust of expert advice, lack of cooperation at many levels, over-confidence, and health care supply shortages have likely promoted higher mortality today as in the past.*

<sup>1</sup> We thank Haoze Li and Jingxuan Ma for helpful research assistance. Guido Alfani, Matthias Blum, Gregori Galofré Vilà, and Alan M. Taylor provided helpful comments.

<sup>2</sup> Doctoral Candidate, University of California, Davis.

<sup>3</sup> Professor of Economics, University of California, Davis.

Copyright: Peter Zhixian Lin and Christopher M. Meissner

## 1. Introduction

The Covid-19 pandemic is the single largest threat to global public health and the global economy since the Spanish Influenza pandemic of 1918-1920. Was the world better prepared in 2020 than it was in 1918-20? It might be expected that in the intervening 100 years societies would have made great progress in predicting, containing, mitigating and managing pandemics (Morens and Fauci, 2007). However, public health specialists, even prior to 2020, were cautious, citing the threats arising from “hubris, isolationism and distrust” (Parmet and Rothstein, 2018).

The most recent global public health scares such as SARS, MERS, Ebola, and H1N1 influenza in 2009 were largely successfully contained without extraordinary levels of excess mortality at the global level. This track record suggests high preparedness and ability to manage pandemics. On the other hand, society has changed in the last 100 years and even in the last decade since the 2009 H1N1 pandemic.

Geographic mobility has increased dramatically over time and significantly so with respect to the years 1918-1920. International inter-connections have continued to grow even since 2002, but international cooperation is waning as exemplified by recent US policy. Modern methods of communication like social media, which have emerged in the last decade, complicate the search for accurate content and often create confusion. Distrust of expert opinion has also heightened in the last decade. In many western societies, including the US, experts have often been replaced with political appointees and civil servants have been granted minimal leeway. Moreover, health infrastructure and accessibility in many countries, even developed and advanced economies, was widely predicted to be incapable of meeting surging demands induced by a pandemic. Such bottlenecks can raise cumulative mortality when health care provides viable means of treatment.

In this regard, the public health response to the Covid-19 pandemic represents a significant test of whether modern public health systems can do better than they have done historically. Evidently, SARS-CoV-2 and the 1918 H1N1 influenza have different etiologies and epidemiology. Nevertheless, the two pandemics seem to be roughly similar in the magnitude of their case fatality ratios. An estimate of the case fatality rate (CFR) for Covid-19 is 1.34% while the CFR for the 1918-20 influenza has been estimated to be  $\geq 2.5\%$  (Verity et al. 2020 and Short et. al, 2018).<sup>1</sup>

Given these numbers, and modern levels of knowledge and know how, one might strongly expect better performance today. Given the estimated fatality rates, most would predict lower mortality at this point in the pandemic than in 1918-20. After all, humanity has a century of public health research and practice, along with experience gained from SARS,

---

<sup>1</sup> Case fatality ratios for the 1957 and 1968 influenza pandemics were roughly 0.27 and 0.15 (Centers for Disease Control and Prevention, 2007).

MERS and Ebola. Contingency plans have been formulated at the behest of the WHO and through national initiatives. Non-pharmaceutical interventions designed to lower peak mortality have been investigated and shown to be effective (Bootsma and Ferguson, 2007; Hatchett et. al, 2007; Markel et. al, 2007).

Recent data make us less sanguine. Figure 1 illustrates that many countries, especially advanced western countries, have had a difficult time in keeping mortality rates below the frontier defined by US mortality rates from flu and pneumonia in 1918 at similar stages in the pandemic. Similarly, Figure 2 shows a number of US states also witnessed mortality rates per 100,000 population above those witnessed in 1918 at a similar stage. These statistics give us pause to re-consider the persistence of pandemic mortality.

We emphasize that our goal in this paper is not to assess the level of mortality in one pandemic versus the other. There are obvious problems comparing distinct diseases and many data measurement issues. Neither do we wish to argue that Covid-19 will be worse than 1918-20. Instead, we compare relative outcomes across time. We ask whether historical public health performance has any predictive content for public health performance in a recent pandemic. We find that historical experience does help predict recent experience.

Our main findings correlate population mortality rates for Covid-19 today with mortality rates from influenza and pneumonia in the 1918-20 pandemic and with SARS in 2002-03. We do so in a broad sample of countries and for a large sample of US cities.

We find a strong persistence in public health performance in the early days of the Covid-19 pandemic. Places that performed poorly in terms of mortality during the “Spanish flu” were more likely to have higher mortality today. This is true across countries and across a sample of US cities.

On the other hand, there has been some recent success consistent with the possibility of learning over time. Countries that were more strongly affected by SARS in 2002-03 are likely to have lower mortality rates today, thus far, from Covid-19. These places are mainly in East Asia and have a recent memory of a potentially highly lethal pandemic. As we detail in the discussion, these successes (and failures) when compared to history depend upon a number of deeper social and political determinants. In short “mis-trust, isolationism and hubris” matter. These may not be persistent but, whether by coincidence or not, they are arguably present now in the case of the many nations, especially in many Western nations.

## 2. Methods

### 2.1 Data Collection

We collect data on country-level population mortality from influenza in 1918-20 and from Covid-19. Our baseline sample covers 22 countries. The sample is determined by availability of estimated mortality rates from 1918-20 influenza, other control variables, and

whether a country had established a first death case or confirmed case for Covid-19. Therefore, our sample for cross-country comparison covers those countries subjected to Covid-19 relatively early on.

Data on total deaths from Covid-19 are expressed in numbers per 100,000 (CSSE Johns Hopkins University, 2020). Data on mortality in the 1918-20 influenza pandemic are also expressed in numbers per 100,000 population (Johnson and Mueller, 2002). These latter figures refer to total mortality from influenza between 1918 and 1920. It should be noted that these are not always deaths from influenza and pneumonia nor are they excess deaths from all causes. Variable quality of underlying official statistics is our key constraint. We added several data points for the 1918 pandemic from secondary sources including Singapore, Hong Kong and Korea. Deaths and confirmed cases of Covid-19 were last updated for US cities on April 25, 2020 and on April 17, 2020 for our country-data. Our data begin on January 21, 2020. The inter-quartile range of mortality in 1918-20 is 430-710 deaths per 100,000 population with a median of 610 and a mean value of 649. This compares to the interquartile range (as of 17 April, 2020) for reported Covid-19 deaths of 0.39 to 15.44 per 100,000 and a median of 5.01.

We supplement the country mortality data with population mortality rates from SARS in 2002-03, GDP per capita in 2018, population density in 2019, some measures of cultural differences such as an index of individualism in a country, and a dummy variable for a tradition of Confucianism. Places coded as Confucianist include mainland China, Taiwan, Hong Kong, Singapore, Japan and South Korea.

We also explore a historical data base of 46 US cities (Collins et. al, 1930). Influenza became a 'reportable' in September 1918. Prior to this detailed only exist for a small handful of states and cities. The total population in these cities is equal to 20.4 million or about 18% of US population. Data cover all of the largest cities in the US.

The mortality from the 1918-1920 influenza pandemic in these cities is expressed as monthly or weekly excess mortality per 100,000 population of 1920. We use weekly data for the period 10 September 1918 to 13 November 1918, covering the first six weeks of the 1918-20 pandemic for US cities. The excess mortality rates were the differences between the actual mortality rates and median mortality rates from influenza and pneumonia in previous non-epidemic years in those cities. We refer to deaths from influenza and pneumonia since diagnoses were often inexact at the time with the influenza virus often causing apparent death from pneumonia. The excess mortality rate from influenza and pneumonia serves as a good measure of the severity of the 1918 pandemic. To make data even more comparable to our data from Covid-19, we convert the weekly excess deaths to daily observations by linear interpolation within the week and calculated daily cumulative excess deaths since the first week of September, 1918.

We match the cities with continuous historical data to modern city or county-level data. One issue associated with the long-run city-level comparison is that deaths and confirmed cases of Covid-19 are reported mostly at the county-level. While Covid-19 data

are separately reported for some cities in our sample (New York City, St. Louis, Richmond, etc.) most data is reported at the county level. For cities in the historical sample without separately reported Covid-19 data at the city-level, we use data from today for the corresponding counties where the cities are located in. For example, we pair the city of Detroit with Wayne County.

We set a threshold level of mortality at the city level of 0.5 per 100,000 for each pandemic. Event time and observations begin as per this threshold mortality rate. This threshold was chosen since this is the lowest recorded threshold for excess deaths from influenza and pneumonia we have available in the historical city-level data in 1918-20.

## 2.2 Data Analysis

Our first test finds significant persistence of public health performance across countries. In Figure 3, we plot the mortality rates from influenza 1918-20 against the average daily growth rates of the total reported deaths from Covid-19 in the first five weeks after each country reported their first death from Covid-19. We condition only on mortality 1918-20 finding a positive and statistically significant correlation (robust t-statistic = 2.74, adjusted  $R^2 = 0.21$ )

The scatter plot reveals that some countries performing poorly in terms of mortality in the 1918 pandemic, such as Spain and Italy, also experienced fast mortality growth in the recent Covid-19 pandemic. However, the persistence between 1918 influenza and current Covid-19 pandemic might not be a universal phenomenon for all countries. We note that some places such as Japan, South Korea, and Taiwan, fall well below the regression line, suggesting these countries are performing much better than what their 1918 performance predicted.

We carry out more formal regression analysis by controlling for several country-level economic, demographic, and cultural characteristics. Besides the country-level mortality in the 1918-20 pandemic, we also include these countries' mortality during the more 2002-03 SARS pandemic. Our baseline result is reported in column (3) of Table 1.

Mortality rates in 1918-20 are positively associated with the growth rates of reported deaths from Covid-19 in the first five weeks (point estimate: 0.166, p-value: 0.029, 95% C.I. 0.02 to 0.031). We also find that the mortality rate from SARS is negatively correlated with growth rates of reported deaths of Covid-19 (point estimate: -0.162, p-value: 0.003, 95% C.I. -0.255 to -0.068). Similar results on persistence emerge (columns 3-6 of Table 1) when we switch the dependent variable to be the growth of confirmed cases of Covid-19 in the six weeks after the 10th reported confirm case.

All of these findings suggest that, even after conditioning on a number of observable characteristics, countries performing poorly in the 1918-20 pandemic tended to fail to control mortality growth of Covid-19 in the first months of the outbreak. On the other hand. There is some evidence of learning. The negative correlation between SARS and Covid-19 performance reveals that the countries hit harder by the more recent epidemic have been

more successful in slowing down the development of Covid-19 in the first several weeks and months. This is suggestive evidence that countries learned from their more recent experience.

Next, we examine the persistence of public health performance in a group of large U.S. cities. We compare the early trajectories of population mortality rates in the 1918 influenza and the contemporary Covid-19 pandemic. Data are for 46 cities for which we have high frequency data in 1918.

In Figure 4, we plot the trajectory of the mortality rate (excess deaths per 100,000 population) from influenza and pneumonia and Covid-19 over the days after total deaths crossed the 0.5 per 100,000 people in those cities.<sup>2</sup> The city-by-city comparison of historical and contemporary mortality trajectories reveals high similarity of the two epidemics in most cities, particular in the early phase.

Regression results indicate that Covid-19 deaths are positively correlated with total excess deaths from 1918 influenza (point estimate: 0.341, p-value: 0.000, 95% C.I.: 0.193-0.488). Baseline results are presented in column (2) of Table 2. Regressions control for city fixed effects, event time and the square of event time.

We also compare the growth of total deaths from the 1918 flu and total deaths from Covid-19 in the early weeks of the latter pandemic. In Figure 5, we plot the average daily growth rate of total deaths during the two epidemics in the first three weeks after mortality reached 0.5 per 100,000 population. The positive correlation suggests that the cities experiencing faster mortality growth in 1918 tend to experience the same issue in the early phase of Covid-19. Regressions are reported in Table 3. We find that conditional on geographic location and contemporary population density, this positive correlation still holds significantly in the first two, three, and four weeks after mortality rates reached the given threshold.

### 3. Discussion

What factors inhibit prompt response and success in the midst of a pandemic? Let us assume that they include “distrust, isolationism and hubris” (Parmet and Rothstein, 2018). In our discussion it will become clear that all of these factors mattered for performance in both 1918 and in 2020. These factors seem to be correlated over time across countries. It is not clear however whether these factors are recurrent features of societies which have been unfortunately timed with the outbreak of a new infectious disease like Covid-19 or whether these factors indeed persist over time.

---

<sup>2</sup> Excess deaths rates serve as good measurement of the severity of the 1918 pandemic across cities with potentially different seasonal influenza patterns. The threshold of 0.5/100,000 is chosen to attain a comparable starting mortality rates for two epidemics across cities. Most cities in our sample reached this threshold early in both epidemics. Our results are robust to other alternative thresholds such as 1/100,000.

Whatever the case may be, history is surely not destiny nor does history repeat itself. We do not want to suggest either. The correlations we highlight in this paper emphasize that if public health objectives are to be met, societies must substitute innovative efforts to overcome adversity when other social and political forces such as “distrust, isolationism and hubris” handicap public health responses.

Still, historical experience has seemingly affected the path of mortality in the Covid-19 pandemic. First, in a positive sense. Experience with SARS is likely to have promoted societal learning and reaction. Meanwhile, where the mortality of the 1918 influenza was high, mortality is likely to be high today. Why? As we discuss below, local public health “traditions” may be historically persistent, but the timing of Covid-19 and the flu of 1918 have been somewhat unfortunate as well.

### 3.1 SARS and Recent History

East Asian nations, the places most affected by SARS in 2002-03 have been more likely to act quickly to mitigate spread and to have lower mortality from Covid-19 thus far. The searing lessons of SARS, along with particular national characteristics, appear to have positively influenced pandemic preparedness. The key national characteristics for success in battling a pandemic -- trust, cooperation, and a lack of hubristic over-confidence --- are present in these nations and they have provided a favorable environment for learning from the past. Are there other explanations?

It is plausible that experience with SARS obscures national characteristics since SARS had a limited geographic reach, largely affecting selected places in East Asia. Indeed, places in East Asia like Taiwan, Singapore, Hong Kong, South Korea, Japan, and mainland China have kept reported cumulative cases and deaths from Covid-19 at low levels especially when scaled by population. The population mortality rate has averaged 0.305 per 100,000 in these six places and if we exclude Japan and China it was 0.286. This is well below the average of 16.65 in other advanced economic nations in western Europe, the Americas and Australia as of 25 April, 2020 (Table 1).

We control for regional fixed effects and some religio-philosophical and cultural traditions including “Confucianism” and collectivism. None of these eliminate the statistically significant association between past pandemics and Covid-19. Neither of these “deep” cultural factors is statistically significant. Many of these places have been at the epicenter of recent pandemics like SARS but also including MERS and the recent Covid-19 pandemic. There is strong evidence that these places saw the threat of SARS due to recent experience. Meanwhile the western nations less affected by these recent pandemics “saw the threat through the lens of influenza” according to the editor of *The Lancet* Richard Horton. (Ahuja, 2020).

E. Asian nations appear to have used their trusted and competent technocratic civil services to learn from recent past experience, and to develop a high level of preparedness for a pandemic. The pandemic preparedness plans for the East Asian nations most affected

by SARS often mention recent local experience with SARS. Pandemic response to Covid-19 has been swift and forceful. A host of specialized protocols have been followed including border checks of travelers for illness, international travel bans from affected regions, high rates of testing and contact tracing, social distancing, using masks and raising public awareness.

Another plausible explanation for East Asian success in the recent period may be competency and trust in the civil service. China, Taiwan, Hong Kong, Japan and South Korea, the countries most affected by SARS, have an average percentage of people having “a great deal of trust” or “quite a lot of trust” in civil service of 56.68 % (std. dev. =13.96) according to the 2010-2014 World Values Survey. The average of western nations available in the sample (Australia, Germany, New Zealand, Spain, Sweden and the USA) was 45.9% (std. dev. = 5.06) and that for all other nations in the sample excluding these places was 42.5% (std. dev. = 19.18).

The salience of events in recent living memory combined with high trust and competence in the civil service most likely helped these nations to learn from past experience. East Asian success has been built upon the realization that a new pandemic was likely given the recent past experience. As one can see in Figure 1, many of these E. Asian nations are below the regression line implying better than expected performance during the early phases of Covid-19. In western nations pandemics had largely been relegated to history with influenza being the most recurrent issue. Population mortality rates from influenza have been significantly lower since 1918 and most influenza since then has had a CFR much lower than that of Covid-19.

### 3.2 Influenza Mortality in 1918-20 and Covid-19 Mortality: Countries

What then explains the positive correlation between influenza in 1918 and mortality in the early phases of Covid-19? At the country level, our regression analysis rules out individualist cultural explanations and geographic/regional unobservables. One explanation may rely on deep-rooted tendencies and capabilities of the government and civil service in solving the problems of infectious diseases. The issues of distrust, hubris and isolationism return to the forefront and are evident in 1918 and now. Unfortunate timing may play a role in the persistence of these enabling factors. Recent research argues that the greater mortality in the 1918-20 pandemic generates lower trust in the long-run (Aassve et. al. 2020).<sup>3</sup> This may help explain some of the persistence we see in the data both across countries and within the US.

---

<sup>3</sup> The measure of trust is based on the General Social Survey question: “Generally speaking, would you say that most people can be trusted or that you can’t be too careful in dealing with people?”

Today, many western nations have elected officials that have openly discussed abandoning international agreements of the post-World War 2 era. The US is not alone in this. So-called populist tendencies have emerged in many western democracies. Electoral success has risen, but many countries see this manifested in the strength of opposition parties like the AFD in Germany, the FN in France, and UKIP in the UK. These political movements also are amplifications of public mis-trust of officials and experts. The politicization of public health responses has been highlighted (Eichengreen, 2020).

In 1918 many countries in the west were involved in all-out war. Reporting on the influenza pandemic was minimized as most historians agree. The Italian interior minister was not alone in denying the spread of the pandemic (Martini et. al, 2019). In the US, politicians downplayed the menace of the flu. Similar responses have been heard today in Italy. The mayor of Milan promoted “Milan doesn’t stop” on day 6 of the Covid-19 outbreak leaving bars, restaurants, and cafes open (McCann et. al, 2020). In the United States, the president declared Covid-19 to be a “hoax” in late February, 2020.

Another unfortunate similarity between today and in the past was the inadequate preparation of many health care systems for surge demand. During World War I, the US military had 300,000 physicians on duty which is over 1/5 of the total number of physicians in the USA at the time.<sup>4</sup> Other nations fighting in the war also had skewed their health infrastructure to war efforts. Today, a nearly constant discussion about equipment shortages, lack of PPE and beds in ICUs has been a common theme. Access to health care in the United States is problematic especially in places where poverty is high, inequality is high, and the social safety net is over-stretched. This characterizes the health care system in New York but in other localities in the US as well.

Finally, politics was on a knife-edge and highly polarized in many western nations in 1918. Many countries were fighting in the war, facing imminent revolutions or momentous political changes or both. Mussolini and fascists in Italy were rising to power, Spain was unstable, Russia was recovering from recent revolution. Even in the US, Woodrow Wilson’s political mandate was handicapped by the narrow Republican victory in a New Mexico senate race leading to Republican control of the Senate.

### 3.3 US Cities in 1918 versus Today

Perhaps the most striking correlation that we have uncovered is the apparent long-run correlation between mortality in 1918 and today in US cities. Again, the role of politics is manifest. Historians have found evidence that that non-pharmaceutical interventions

---

<sup>4</sup> Number of medical personnel in the military as of November 1918 300,000 (Statistical Abstract of the United States of America, 1919, p. 728). Number of physicians in the United states in 1920 1.542 million according to Carter et. al. (2006).

(NPIs) mattered for peak mortality and cumulative death rates. Cities that adopted NPIs earlier and/or maintained them longer had some success in keeping these variables lower, especially peak mortality. Cities like Philadelphia which delayed and allowed a “Liberty Bond” rally to go ahead have been compared unfavorably to St. Louis which limited public gatherings and sustained school closures. St. Paul has been compared to Minneapolis and San Francisco has been compared to New York. In the former pair St. Paul delayed longer in implementing NPIs than Minneapolis suffering the consequences. San Francisco implemented a mask ordinance in mid-October 1918 while New York implemented light touch social distancing. At the time there was much debate about how far to go with these measures and about their effectiveness. For instance, the Anti-Mask League of San Francisco was a political force in late 1918. Opponents of William Hassler, the city Public Health Officer who promoted mask-wearing, also attempted to murder him such was their mis-trust and dislike of his public health policies. Dr. Anthony Fauci, director of the National Institute of Allergy and Infectious Disease, and a key proponent of social distancing, was given a security detail in late March against “un-specified threats” (Diamond, 2020).

Across US cities there has been political debate on the effectiveness of social distancing and NPIs. It is interesting that the mayors of San Francisco had opposing viewpoints in March on how to handle Covid-19. While mayor London Breed of San Francisco emphasized pandemic preparedness for a major disruption on 2 March, Mayor Bill de Blasio of New York was “encouraging New Yorkers to go on with your lives” on twitter even making a recommendation for watching a movie in a cinema. Historian John M. Barry has emphasized that Tammany (a corrupted political machine) was in control of New York in 1918 and had appointed a homeopath as president of the New York City Board of Health. Copeland went on to become a US Senator. Hassler would eventually become the president of the American Public Health Association.

None of this is to ascribe the correlations we have found to extreme persistence in public health capabilities and the politics of public. However, the coincidence of divergent opinions and political and social malaise in the west is notable. It is impossible to blame the disease on these issues. It may however be possible to credit slow response times and delayed action to these matters. In other words, while history has not repeated itself, certain outcomes are remarkably similar. The success of East Asian nations in combating the spread of Covid-19 so far is testament to the idea that history is not destiny.

## References

Aassve, A., Alfani, G., Gandolfi, F. and Le Moglie, M. 2020. "Epidemics and Trust: The Case of the Spanish Flu". IGER working paper no. 661.

Ahuja, Anjana. 2020. "Richard Horton: 'It's the biggest science policy failure in a generation'". Financial Times, 25 April, 2020.

Bootsma, M.C. and Ferguson, N.M., 2007. The effect of public health measures on the 1918 influenza pandemic in US cities. *Proceedings of the National Academy of Sciences*, 104(18), pp.7588-7593.

Carter, Susan B. et. al. (eds.) *Historical statistics of the United States* (Online) (Millennial edition). New York: Cambridge University Press.

Collins, S.D., Frost, W.H., Gover, M. and Sydenstricker, E., 1930. Mortality from influenza and pneumonia in 50 large cities of the United States, 1910-1929. Ann Arbor, Michigan: Michigan Publishing, University Library, University of Michigan.

Centers for Disease Control and Prevention 2007. "Interim Pre-Pandemic Planning Guidance: Community Strategy for Pandemic Influenza Mitigation in the United States—Early, Targeted, Layered Use of Nonpharmaceutical Interventions. Department of Health and Human Services. US Government.

Center for Systems Science and Engineering (CSSE) at Johns Hopkins University, Covid-19 Dashboard.

Eichengreen, Barry 2020. "Corononomics 101" Project Syndicate 10 March 2020.

Diamond, D. 2020. "Fauci gets security detail after receiving threats" Politico 1 April, 2020. Downloaded on 28 April, 2020 from <https://www.politico.com/news/2020/04/01/fauci-coronavirus-security-160901>

Hatchett, R.J., Mecher, C.E. and Lipsitch, M., 2007. "Public health interventions and epidemic intensity during the 1918 influenza pandemic." *Proceedings of the National Academy of Sciences*, 104(18), pp.7582-7587.

Johnson, N.P. and Mueller, J., 2002. "Updating the accounts: global mortality of the 1918-1920 'Spanish' influenza pandemic". *Bulletin of the History of Medicine*, pp.105-115.

Markel, H., Lipman, H.B., Navarro, J.A., Sloan, A., Michalsen, J.R., Stern, A.M. and Cetron, M.S., 2007. "Nonpharmaceutical interventions implemented by US cities during the 1918-1919 influenza pandemic". *JAMA*, 298(6), pp.644-654.

Martini, M., Gazzaniga, V., Bragazzi, N.L. and Barberis, I., 2019. "The Spanish Influenza Pandemic: a lesson from history 100 years after 1918". *Journal of Preventive Medicine and Hygiene*, 60(1), p.E64.

McCann, A., Popovich, N. and Wu, J. 2020 "Italy's Virus Shutdown Came Too Late. What Happens Now?" *New York Times* 5 April, 2020. Downloaded on 28 April, 2020.  
<https://www.nytimes.com/interactive/2020/04/05/world/europe/italy-coronavirus-lockdown-reopen.html>

Morens, D.M. and Fauci, A.S., 2007. "The 1918 influenza pandemic: insights for the 21st century." *The Journal of infectious diseases*, 195(7), pp.1018-1028.

Parmet, W.E. and Rothstein, M.A., 2018. "The 1918 Influenza Pandemic: Lessons Learned and Not—Introduction to the Special Section." *American Journal of Public Health* 108 (11) pp. 1435-1436.

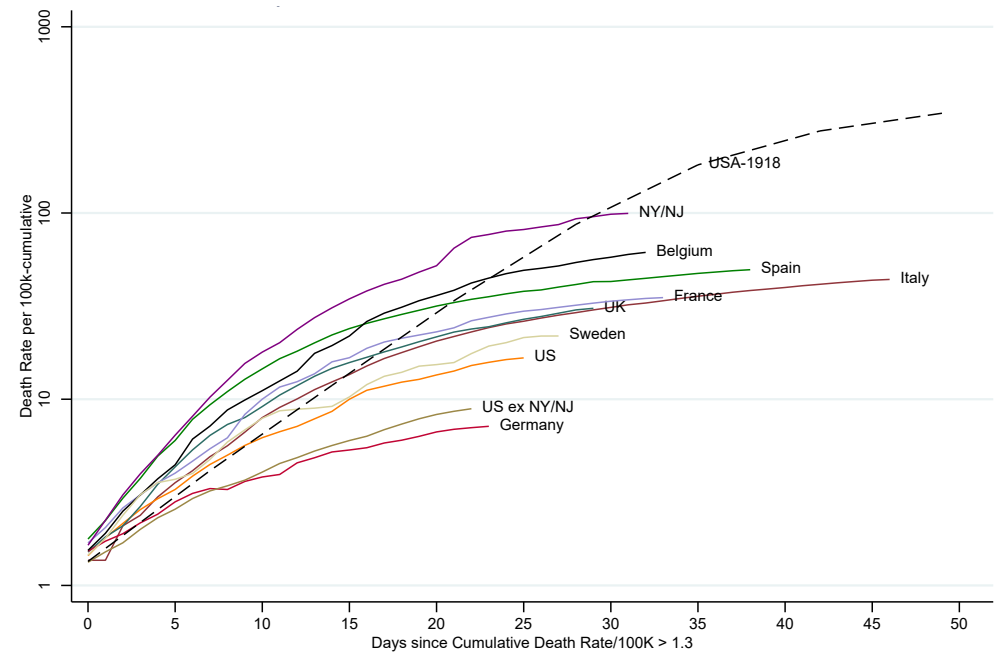
Short, K.R., Kedzierska, K. and van de Sandt, C.E., 2018. "Back to the future: lessons learned from the 1918 influenza pandemic". *Frontiers in cellular and infection microbiology*, 8, p.343.

Statistical Abstract of the United States of America. 1919. Bureau of the Census. Washington: Government Printing Office.

Verity et. al. 2020. "Estimates of the severity of COVID-19 disease". Medrxiv posted March 13, 2020. Downloaded 4/25/2020.

<https://www.medrxiv.org/content/10.1101/2020.03.09.20033357v1>

Figure 1 Mortality Rate per 100,000 Covid-19 and 1918-20 Influenza Pandemics: Cross-Country Evidence

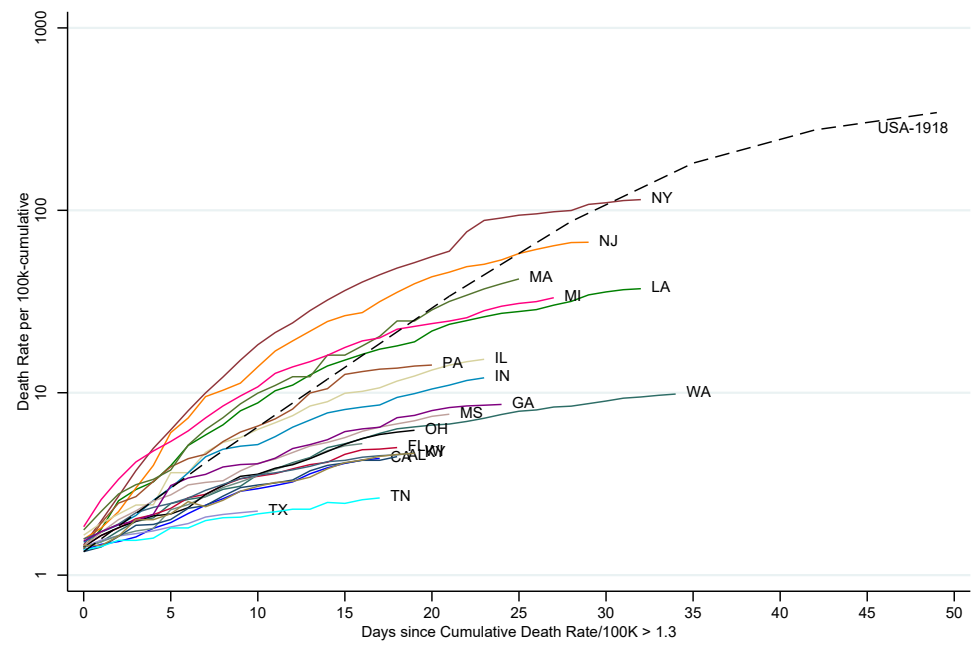


Notes: Figure shows the population mortality rates of Covid-19 based on data from CSSE Johns Hopkins. We break the data for the US into three parts: mortality for the entire US, mortality rates for the states of New York and New Jersey, the hardest hit states and for the US excluding these two states. Data for the Influenza pandemic of 1918 are for total weekly deaths per 100k from influenza and pneumonia for data from 46 cities in the USA (Collins et. al. 1930). Data are plotted for countries in 2020 that had reached a threshold of 1.34 deaths per 100,000. This is the first available level of mortality the mortality rate in the 1918 for the national level data for the USA.

Covid Economics 15, 7 May 2020: 1-25

**COVID ECONOMICS**  
VETTED AND REAL-TIME PAPERS

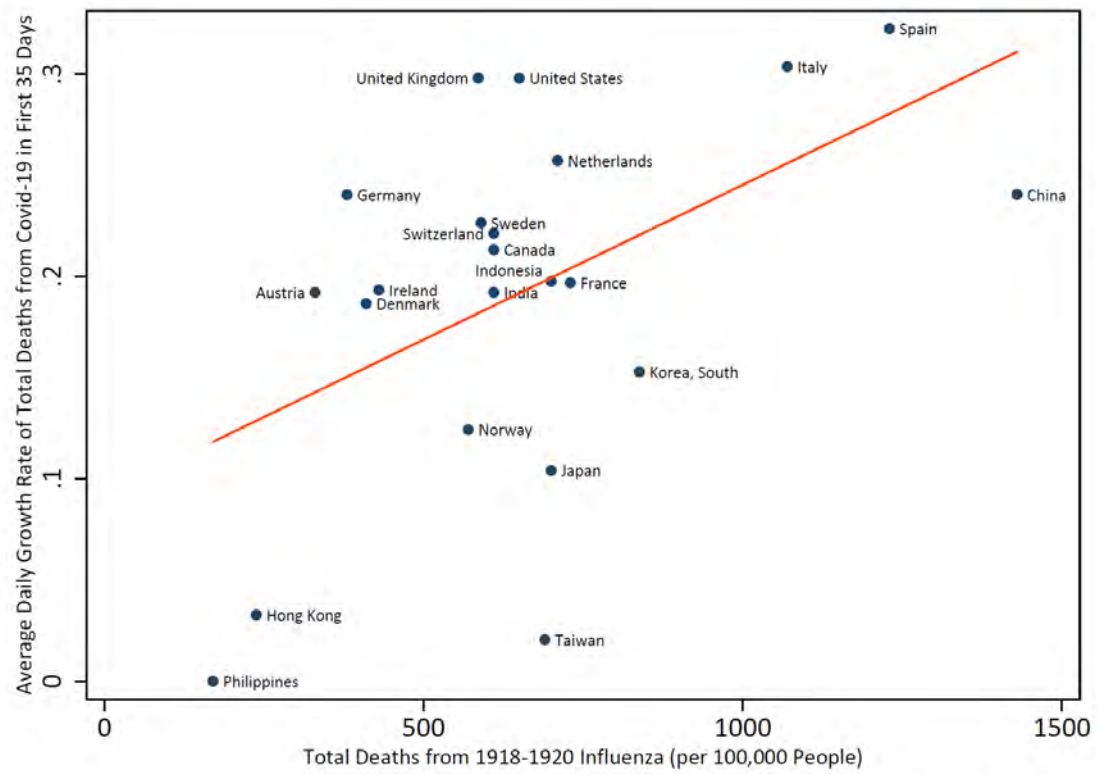
Figure 2 Mortality Rate per 100,000 Covid-19 and 1918-20 Influenza Pandemics: US States



Notes: Figure shows the population mortality rates of Covid-19 based on data from CSSE Johns Hopkins. Data for the Influenza pandemic of 1918 are as described in the notes to Figure 1.

Covid Economics 15, 7 May 2020: 1-25

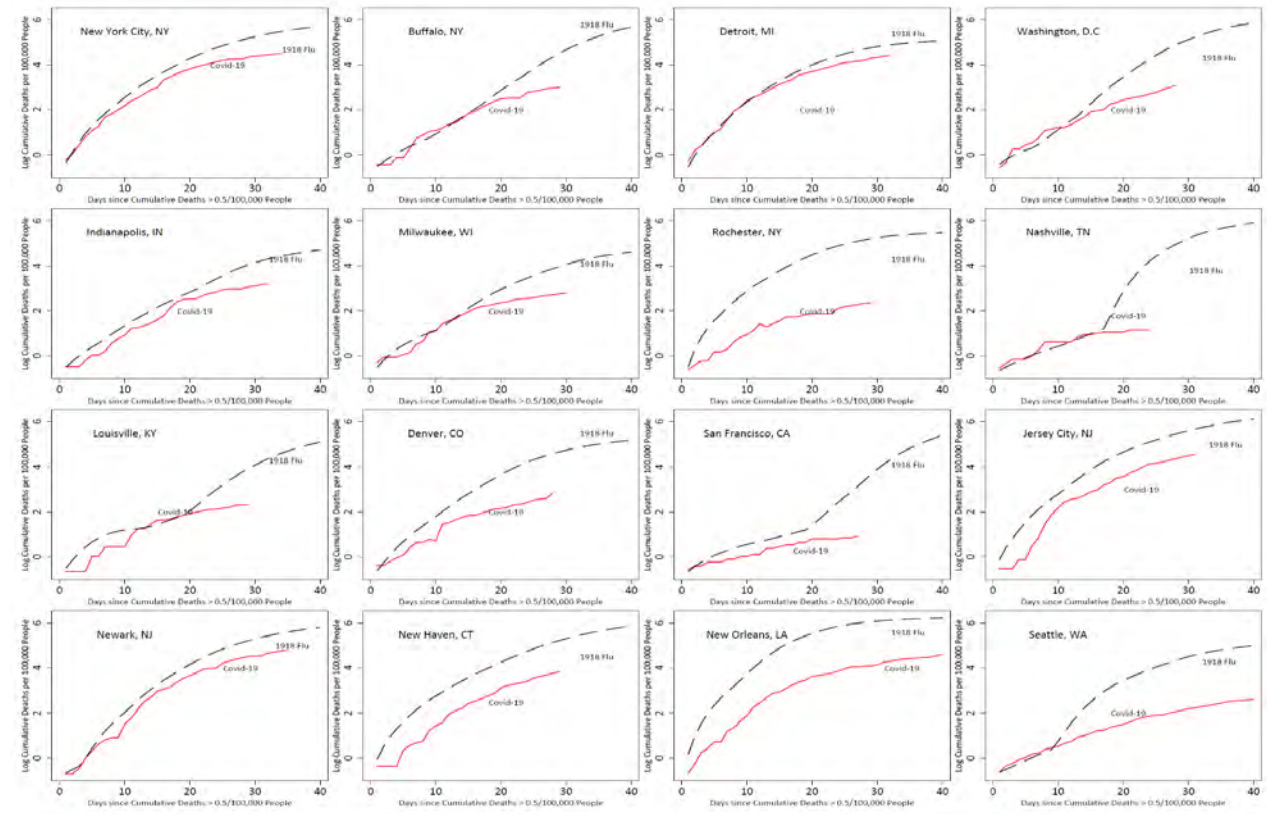
Figure 3 Mortality of 1918-20 Influenza and Covid-19 Pandemics, 22 Countries



Notes: This graph plots the average daily growth rate of cumulative deaths from Covid-19 in the first 35 days since the first death in each country against the country-specific overall mortality rate from the 1918 Influenza pandemic. Data are described in the data appendix. The average growth rate of cumulative deaths for Covid-19 is calculated as  $\sqrt[34]{cmdeath_{i35}/cmdeath_{i1}} - 1$ . We include 22 countries with a sufficiently established mortality trajectory in this graph. The robust t-statistic for the coefficient on deaths from influenza in 1918 is =2.74, and the regression has an adjusted R<sup>2</sup> = 0.21.

Covid Economics 15, 7 May 2020: 1-25

Figure 4 Mortality Curves for Covid-19 and Influenza and Pneumonia in 1918 in Selected U.S. Cities

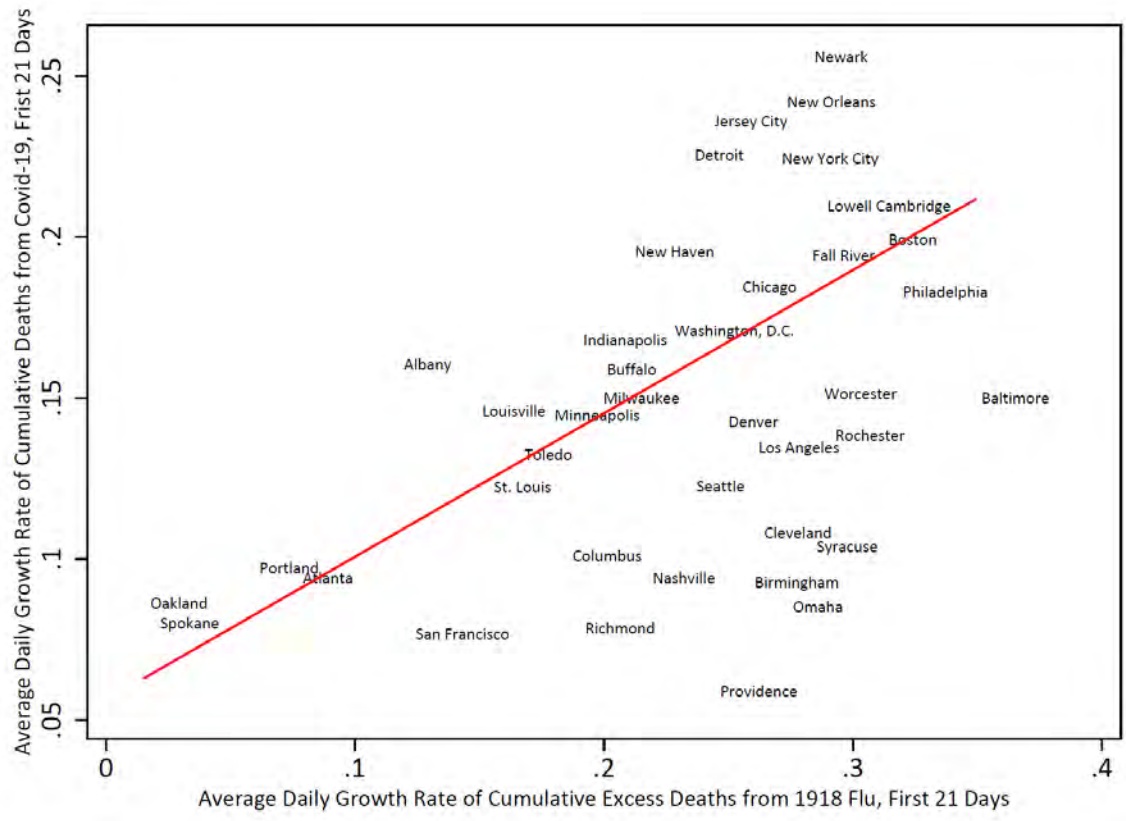


Notes: These charts provide city-by-city comparisons between the trajectory of the population mortality rate from influenza and pneumonia in 1918 and Covid-19 in 2020. We plot the logarithm of total deaths per 100,000 (for Covid-19) or total excess deaths per 100,000 (for influenza and pneumonia) on the y-axis versus the number of days since mortality rates reached 0.5/100,000 population. The 16 cities are selected here the cities with the longest Covid-19 trajectories. Trajectories for other cities are available upon request from authors.

Covid Economics 15, 7 May 2020: 1-25

Figure 5 Average Daily Growth of Total Deaths from Covid-19 and Influenza and Pneumonia in U.S. Cities: First 21 Days

Covid Economics 15, 7 May 2020: 1-25



Notes: Chart shows the unconditional relationship between the average daily growth rate of total deaths during Covid-19 in the first 21 days compared to the average growth rate of excess deaths in the first 21 days of the 1918-20 pandemic. The coefficient of the regression (which includes a constant) is 0.355 with a robust t-statistic of 4.09 and a 95% C.I. of 0.179 to 0.531. The average daily growth rates of total deaths (or total excess deaths for 1918 influenza) in the first 21 days are calculated by  $\sqrt[20]{cmdeath_{it}/cmdeath_{it-20}} - 1$ . The first 21 days refer to the 21 days since the total deaths (for Covid-19) or total excess deaths (for 1918 Influenza) reached 0.5 for every 100,000 population.

Table 1 Mortality Rates of for Three Pandemics: 1918-20 Influenza, 2002-03 SARS, and Covid-19

Country	Mortality Rates of 1918-20 Influenza (per 100,000)	Mortality Rates of 2002-2003 SARS (per 100,000)	Mortality Rates of Covid-19 by April 17, 2020 (per 100,000)
Austria	330	0	4.81
Canada	610	0.131	3.62
Denmark	410	0	5.82
Finland	580	0	1.48
France	730	0.002	28.68
Germany	380	0	5.21
Ireland	430	0	10.86
Italy	1070	0	37.56
Netherlands	710	0	20.23
Norway	570	0	2.99
Spain	1230	0	42.80
Sweden	590	0	13.95
Switzerland	610	0	15.45
United Kingdom	586	0	21.61
United States	650	0	11.11
Average	676	0.006	16.65
Asian Countries			
China	1430	0.027	0.32
India	610	0	0.04
Indonesia	700	0	0.19
Japan	700	0	0.15
Korea, South	838	0	0.45
Philippines	170	0.002	0.36
Singapore	706	0.79	0.19
Taiwan	690	0.799	0.03
Hong Kong	238	4.448	0.05
Average	1043	0.03	0.19
Average (ex. China and Japan)	620	0.04	0.09

Notes: Estimates of mortality rates of 1918 Influenza come from the recalculation and compilation by Johnson and Mueller (2002). See their paper for details. Mortality rates of 2002-2003 SARS come from WHO and include the deaths from cases from November 1, 2002 to July 31, 2003. Mortality rates for Covid-19 come from the CSSE of Johns Hopkins University. Population-weighted averages are presented for each region. Finland and Singapore are listed in this table, but not included in the regression in table 2, as these two countries have not reached their 35<sup>th</sup> day after first death.

Table 2 Covid-19 Pandemics and Mortality from 1918 Influenza and SARS, Country-Level Evidence

	(1)	(2)	(3)	(4)	(5)	(6)
	Average Daily Growth Rate of Total Deaths from Covid-19 35 Days since First Death	Average Daily Growth Rate of Total Deaths from Covid-19 35 Days since First Death	Average Daily Growth Rate of Total Deaths from Covid-19 35 Days since First Death	Average Daily Growth Rate of Total Cases of Covid-19 42 Days since 10 <sup>th</sup> Case	Average Daily Growth Rate of Total Cases of Covid-19 42 Days since 10 <sup>th</sup> Case	Average Daily Growth Rate of Total Cases of Covid-19 42 Days since 10 <sup>th</sup> Case
Total Mortality Rate from 1918-20 Influenza	0.165*** (0.0265)	0.167*** (0.0354)	0.165** (0.0666)	0.0957*** (0.0135)	0.0867*** (0.0106)	0.0677** (0.0226)
Total Mortality Rate from SARS	-0.199*** (0.0463)	-0.169*** (0.0276)	-0.161*** (0.0420)	-0.143*** (0.0290)	-0.130*** (0.0295)	-0.153*** (0.0260)
Population Density in 2019	0.0515*** (0.0116)	0.0459*** (0.00744)	0.0437*** (0.0100)	0.0367*** (0.00732)	0.0338*** (0.00753)	0.0394*** (0.00663)
Log (GDP per capita in 2018)		-0.0246* (0.0131)	-0.0286 (0.0415)		-0.0158** (0.00530)	-0.0261 (0.0163)
Confucianism Tradition (0/1)			0.0116 (0.123)			0.0315 (0.0545)
Individualism Index (0/100)			0.000305 (0.000984)			-0.000531 (0.000609)
Observations	22	22	22	20	20	20
R <sup>2</sup>	0.810	0.843	0.845	0.873	0.905	0.919

Notes: Dependent variables in columns (1)-(3) is the average daily growth rate of cumulative deaths from Covid-19 in the first 35 days since the first death case. Dependent variable in columns (4)-(6) is the average daily growth rate of cumulative cases of Covid-19 in the first 42 days since the 10<sup>th</sup> confirmed cases. Estimation is by OLS. The estimated coefficients and standard errors on the total mortality rate of 1918-20 influenza were multiplied by 1000 for presentational purposes. All regressions control for region fixed effects (we categorize countries into 7 regions: East Asia, South Asia, Africa, Europe, North America, South America, and Oceania). Robust standard errors reported in parentheses. \* p < 0.1, \*\* p < 0.05, \*\*\* p < 0.01.

Table 3 Total Deaths and Confirmed Cases from Covid-19 and 1918 Influenza in 46 U.S. Cities, Daily Data

	(1) Log Total Deaths per 100,000 Covid-19	(2) Log Total Deaths per 100,000 Covid-19	(3) Log Total Deaths per 100,000 Covid-19	(4) Log Total Cases per 100,000 Covid-19	(5) Log Total Cases per 100,000 Covid-19	(6) Log Total Cases per 100,000 Covid-19
Log Total Excess Deaths per 100,000, 1918 Flu	0.300*** (0.0547)	0.341*** (0.0733)	0.407*** (0.105)	0.224*** (0.0630)	0.232*** (0.0531)	0.188*** (0.0428)
Event Days	0.121*** (0.00968)	0.108*** (0.0121)		0.0544*** (0.0102)	0.0493*** (0.0138)	
(Event Days) <sup>2</sup>	-0.00150*** (0.000232)	-0.00137*** (0.000217)		-0.000355*** (0.0000848)	-0.000290 (0.000294)	
<i>Observations</i>	1244	1244	1235	1244	1244	1235
<i>R</i> <sup>2</sup>	0.931	0.962	0.974	0.899	0.964	0.981
Covid-19 Calendar Date Fixed Effects	No	No	Yes	No	No	Yes
State Fixed Effects	Yes	No	No	Yes	No	No
City Fixed Effects	No	Yes	Yes	No	Yes	Yes
# Cities	46	46	46	46	46	46

*Notes:* Dependent variables are listed at the top of each column. These and total excess death rates from the 1918-20 influenza are at the daily level. All specifications control for city fixed effects. Event days are defined as the days since cumulative death rates per 100,000 (for Covid-19) and cumulative excess deaths (for 1918 Influenza) reached 0.5/100,000 population. The data on Covid-19 were last updated on April 25, 2020. The full list of cities can be found in the public health reports by Collins et. al (1930). All regressions are weighted by population in 2019 and standard errors are clustered at the state level for column (1) and (4). For the rest of columns, standard errors are clustered at the city level. \*  $p < 0.1$ , \*\*  $p < 0.05$ , \*\*\*  $p < 0.01$ .

Table 4 Growth of Total Deaths from Covid-19 and 1918 Influenza in U.S. Cities

	(1)	(2)	(3)
	Average Daily Growth Rate of Total Deaths, Covid-19 First 14 Days	Average Daily Growth Rate of Total Deaths, Covid-19 First 21 Days	Average Daily Growth Rate of Total Deaths, Covid-19 First 28 Days
Average Daily Growth Rate of Total Excess Deaths, 1918 Flu, First 14 Days	0.242*** (0.0576)		
Average Daily Growth Rate of Total Excess Deaths, 1918 Flu, First 21 Days		0.269*** (0.0540)	
Average Daily Growth Rate of Total Excess Deaths, 1918 Flu, First 28 Days			0.511*** (0.135)
Population Density in 2019	0.214*** (0.0503)	0.170*** (0.0407)	0.0455 (0.0293)
# Cities	46	40	20
R <sup>2</sup>	0.616	0.682	0.792

Notes: The average daily growth rates of total deaths for first  $n$  days are calculated by  $\sqrt[n-1]{cmdeath_{it}/cmdeath_{in-1}} - 1$ . The first  $n$  days refers to the number of days since total deaths (for Covid-19) and total excess deaths (for 1918 Influenza) reached 0.5 for every 100,000 people. All specifications also control for latitude and longitude of cities. All regressions are also weighted by population in 2019. Robust standard errors are reported in the parentheses. \*  $p < 0.1$ , \*\*  $p < 0.05$ , \*\*\*  $p < 0.01$ .

## Data Appendix

### Cross-Country Data, 1918

Mortality rates: Johnson and Mueller (2002) . Data for UK are for England, Wales and Scotland. Date for Ireland are for Eire; Singapore deaths from Lee et. al. (2007); Korea from Hong et. al (2017); Hong Kong data from Cheng and Leung (2007). Hong Kong population in 1919 calculated from Swee-Hock and Wing King (1975); Singapore, population Dodge (1980)

Excess mortality: Murray, Lopez, Chin, Feehan, Hill (2006)

Population density, GDP per capita: Data underlying Clemens and Williamson (2004). All data for 1919.

Population (000s) and GDP per capita (1990 real US Dollars) from Maddison when unavailable Clemens and Williamson (2004). Interpolated where necessary.

Land Area from google searches when unavailable in Clemens and Williamson (2004). Land area in square miles.

### Covid-19 Data, 2020

Data for cases and deaths by country for Covid-19 on 16 April

<https://data.europa.eu/euodp/en/data/dataset/covid-19-coronavirus-data/resource/55e8f966-d5c8-438e-85bc-c7a5a26f4863> downloaded on April 27, 2020.

### DOL Initial jobless claims:

<https://oui.doleta.gov/unemploy/claims.asp>

### Employment by industry

US Bureau of Labor Statistics. "OES Research Estimates by State and Industry" all occupations.

Downloaded from [https://www.bls.gov/oes/current/oes\\_research\\_estimates.htm](https://www.bls.gov/oes/current/oes_research_estimates.htm)

(not sure about this)

[https://www.bls.gov/oes/current/oes\\_research\\_estimates.htm](https://www.bls.gov/oes/current/oes_research_estimates.htm) on 4/7/2020

### Employment for the following Industries:

Mining, Quarrying, and Oil and Gas Extraction, NAICS 21

Wholesale Trade, NAICS 42  
Retail Trade, NAICS 44-45  
Arts, Entertainment, and Recreation, NAICS 71  
Accommodation and Food Services, NAICS 72

### **Share of Jobs that can be “worked from home” or via telecommuting**

“How Many Jobs Can be Done at Home?” by Jonathan I. Dingel and Brent Neiman. NBER wp. 26948

Downloaded from github <https://github.com/jdingel/DingelNeiman-workathome>

For MSAs spanning state borders we simply use the population weight given by total MSA population in such an MSA relative to population all other MSAs including this cross-state MSA.

Populations for MSA from US Census bureau

<https://www.census.gov/data/tables/time-series/demo/popest/2010s-total-metro-and-micro-statistical-areas.html>

Metropolitan and Micropolitan Statistical Area Population Estimates and Estimated Components of Change: April 1, 2010 to July 1, 2019 (CBSA-EST2019-alldata.csv)

### **Employment by MSA**

<https://www.bls.gov/web/metro.supp.toc.htm>

Data file is ssamattab.zip .We use total employment for February 2020 to weight the telecommuting index from Dingel and Neiman.

### **1918-1919 Influenza Pandemic in U.S. Cities**

The mortality data in 47 major U.S. cities come from the public health reports (Collins, 1930). We calculate the cumulative deaths. We interpolate the weekly excess deaths and median deaths by linear interpolation. The cumulative deaths are calculated from the date of first officially reported case of influenza in the 1918-1919 influenza pandemic.

The timing of Nonpharmaceutical interventions across cities are from Markel et al. (2007).

## References for data appendix

- Cheng, K.F. and Leung, P.C., 2007. What happened in China during the 1918 influenza pandemic? *International Journal of Infectious Diseases*, 11(4), pp.360-364.
- Clemens, M.A. and Williamson, J.G., 2004. Wealth bias in the first global capital market boom, 1870–1913. *The Economic Journal*, 114(495), pp.304-337.
- Dodge, Nicholas N. "Population Estimates for the Malay Peninsula in the Nineteenth Century, with Special Reference to the East Coast States." *Population Studies* 34, no. 3 (1980): 437-75. Accessed April 4, 2020. doi:10.2307/2174803.
- Hong, S.C. and Yun, Y., 2017. Fetal exposure to the 1918 influenza pandemic in colonial Korea and human capital development. *Seoul Journal of Economics*, 30(4).
- Johnson, N.P. and Mueller, J., 2002. Updating the accounts: global mortality of the 1918-1920" Spanish" influenza pandemic. *Bulletin of the History of Medicine*, pp.105-115.
- Lee, V.J., Chen, M.I., Chan, S.P., Wong, C.S., Cutter, J., Goh, K.T. and Tambyah, P.A., 2007. Influenza pandemics in Singapore, a tropical, globally connected city. *Emerging infectious diseases*, 13(7), p.1052.
- Murray, C.J., Lopez, A.D., Chin, B., Feehan, D. and Hill, K.H., 2006. Estimation of potential global pandemic influenza mortality on the basis of vital registry data from the 1918–20 pandemic: a quantitative analysis. *The Lancet*, 368(9554), pp.2211-2218.
- Swee-Hock, Saw, and Chiu Wing Kin. "Population Growth and Redistribution in Hong Kong, 1841-1975." *Southeast Asian Journal of Social Science* 4, no. 1 (1975): 123-31.

# Voluntary and mandatory social distancing: Evidence on Covid-19 exposure rates from Chinese provinces and selected countries<sup>1</sup>

Alexander Chudik,<sup>2</sup> M. Hashem Pesaran<sup>3</sup> and Alessandro Rebucci<sup>4</sup>

Date submitted: 30 April 2020; Date accepted: 1 May 2020

*This paper considers a modification of the standard Susceptible-Infected-Recovered (SIR) model of epidemic that allows for different degrees of compulsory as well as voluntary social distancing. It is shown that the fraction of population that self-isolates varies with the perceived probability of contracting the disease. Implications of social distancing both on the epidemic and recession curves are investigated and their trade off is simulated under a number of different social distancing and economic participation scenarios. We show that mandating social distancing is very effective at flattening the epidemic curve but is costly in terms of employment loss. However, if targeted towards individuals most likely to spread the infection, the employment loss can be somewhat reduced. We also show that voluntary self-isolation driven by individual's perceived risk of becoming infected kicks in only towards the peak of the epidemic and has little or no impact on flattening the epidemic curve. Using available statistics and correcting for measurement errors, we estimate the rate of exposure to COVID-19 for 21 Chinese*

1 We thank Johns Hopkins University for assistance with the data. We also would like to acknowledge helpful comments by Ron Smith. The views expressed in this paper are those of the authors and do not necessarily reflect those of the Federal Reserve Bank of Dallas.

2 Economic Policy Advisor and Senior Economist, Federal Reserve Bank of Dallas.

3 John Elliot Distinguished Chair in Economics, Director, USC Dornsife Centre for Applied Financial Economics, Emeritus Professor of Economics, Cambridge University.

4 Associate Professor, Johns Hopkins University Carey Business School and CEPR Research Fellow.

Copyright: Alexander Chudik, M. Hashem Pesaran and Alessandro Rebucci

*provinces and a selected number of countries. The exposure rates are generally small but vary considerably between Hubei and other Chinese provinces as well as across countries. Strikingly, the exposure rate in Hubei province is around 40 times larger than the rates for other Chinese provinces, with the exposure rates for some European countries being 3-5 times larger than Hubei (the epicenter of the epidemic). The paper also provides country-specific estimates of the recovery rate, showing it to be about 21 days (a week longer than the 14 days typically assumed), and relatively homogeneous across Chinese provinces and for a selected number of countries.*

## 1 Introduction

The COVID-19 pandemic has already claimed many lives and is causing an unprecedented and widespread disruption to the world economy. China responded to the initial outbreak with draconian social distancing policies which are shown to be effective in containing the epidemic, but at the cost of large short term losses in employment and output. Other countries have responded more timidly, either by deliberate choice, as in the United States, or due to implementation constraints, as in some European countries. The purpose of this paper is to evaluate the impact of alternative mitigation or containment policies on both the epidemic and the so-called recession curves, and to empirically compare their implementation across countries.

Most importantly we consider both government-mandated social distancing policies, and voluntary self-isolation, and endogenize the fraction of the population that remain exposed to the virus within a standard Susceptible-Infected-Recovered model (SIR). Specifically, we distinguish between individuals exposed to COVID-19 and those isolated from the epidemic. We decompose the population,  $P$ , into two categories: those who are exposed to COVID-19 in the sense that they can contract the virus because they are not isolated and they have not been infected yet,  $P_E$ ; and the rest,  $P_I$ , that are isolated and therefore taken out of harm's way. We denote the strength of the mitigation policy by  $1 - \lambda$ , where  $\lambda$  is the proportion of population that is exposed to COVID-19, defined as  $\lambda = P_E/P$ . Initially we focus on the relatively simple case where  $\lambda$  is set at the outset of the spread of the epidemic, close to what we believe China did after the start of the epidemic in Wuhan. We also consider a variation of the SIR model where  $\lambda$  changes due to the voluntary decision to isolate at the micro level. Using a simple decision model we show that the proportion of the population that self-isolates rises with the probability of contracting the disease. We approximate this probability with the number of active cases and show (by simulation) that the effect of self-isolation occurs as the epidemic nears its peak, and is relatively unimportant during the early or late stages of the epidemic. A coordinated social policy is required from the early outset of the epidemic to flatten the epidemic curve.

We then model the short-term impact of the epidemic on employment. This permits an eval-

uation of the costs and benefits of alternative societal decisions on the degree and the nature of government-mandated containment policies by considering alternative values of  $\lambda$  in conjunction with an employment loss elasticity,  $\alpha$ , that allows a given social distancing policy to have different employment consequences. In the extreme case where the incidence of social distancing is uniform across all individuals and sectors, a fall in  $\lambda$  results in a proportionate fall in employment, and  $\alpha = 1$ . But by enabling individuals to isolate and to work from home, together with wide spread targeted testing for the virus plus the use of protective clothing and equipment, it is possible to mitigate somewhat the economic costs of social distancing policies. We simulate the employment loss for alternative values of  $\lambda$  and  $\alpha$  and find that, for sufficiently low values of  $\lambda$  required to manage the peak of hospitalization and death from COIVD-19, the economic costs could be substantial even with smart social distancing policies. We also simulate the duration of the epidemic to be around 120 days, with a sizeable part of the employment loss occurring close to the peak of the epidemic.

Whilst there is ample medical and biological evidence on the key parameters of the SIR model, namely the basic reproduction rate,  $R_0$ , and the recovery rate,  $\gamma$ , to our knowledge there are no direct estimates of  $\lambda$ . A recent report from the Imperial College COIVD-19 Response Team uses a Bayesian hierarchical model to infer the impact of social distancing policies implemented across 11 European countries, see Flaxman et al. (2020). They use the number of observed deaths to infer the number of infections and do not make use of confirmed infections that are subject to significant measurement errors due to limited testing. Whilst acknowledging the measurement problems, in this paper we provide estimates of  $\gamma$  and  $\lambda$  using daily data on confirmed, recovered and death cases from the Johns Hopkins University (JHU) hub.<sup>1</sup> Using a discretized version of our modified SIR model we derive reduced form regressions in confirmed recoveries and the number of active cases that allow for systematic and random measurement errors. We show that  $\gamma$  can be identified assuming that confirmed infected and recovery cases are subject to a similar degree of mis-measurement. We also show that, for a given value of  $R_0$ , the social distancing parameter,  $\lambda$ , can be identified up to a fraction which is determined by the scale of mis-measurement of reported

<sup>1</sup>Available at [https://github.com/CSSEGISandData/COVID-19/tree/master/csse\\_covid\\_19\\_data](https://github.com/CSSEGISandData/COVID-19/tree/master/csse_covid_19_data).

active cases. We calibrate this fraction using the data from the Diamond Princess cruise ship reported by Moriarty et al. (2020).

We first use daily data on Chinese provinces with complete history of the course of the epidemic. The estimates of the recovery rates are very similar across the Chinese provinces and lie in the range of 0.033 (for Beijing) and 0.066 (for Hebei). We also find that the random measurement in the underlying data is relatively unimportant for the estimation of  $\gamma$ . The mean estimate of  $\gamma$  across the Chinese provinces is around 0.046 which corresponds to around 22 days from infection to recovery (or death). This estimate is substantially larger than the 14 days typically assumed in designing quarantine policies. Setting  $\gamma = 0.046$  and  $R_0$ , we then proceed to estimate  $\lambda$  (up to the scaling fraction). We find that for Chinese provinces  $\lambda$  is very small even if we allow for a significant under-recording of infected and recovered cases. We find that, with the exception of Hubei province (the epicenter of the epidemic), the share of exposed population across other provinces was less than 1 individuals per 100,000! This is an astonishingly low rate and is consistent with dramatically falling estimates of the effective reproduction rate at the onset of the epidemic in China. In contrast, the estimates of  $\lambda$  which we have obtained for European countries are significantly higher even when compared to the relatively high exposure rates for Hubei, with a substantial heterogeneity across countries. In particular, we estimate exposure rates for Italy and Spain to be almost five times the rate estimated for Hubei.

To summarize, *our theoretical analysis shows that voluntary social distancing is likely to be effective only when the epidemic begins to approach its peak, and mandated social distancing to flatten the curve is required from the early phases of the epidemic. Our estimates show that in order to flatten the epidemic curve very strict mandatory policies are necessary, as in the case of the Chinese provinces excluding the Hubei epicenter show. Unfortunately, our estimates suggest that, despite the time-lag in the contagion from China to other countries, an inadequate and uncoordinated policy response resulted in exposure rates outside of China that are multiples of those documented at the epicenter of the epidemic in Hubei.*

### **Related Literature**

The characteristics and the economic consequences of the COVID-19 outbreak, and of policies

to contain its spread, are the subject of a fast growing body of research. Scientific evidence based on more accurate data at the local level has begun to document the rate of transmission and incubation periods. The literature has also begun to document the role of mitigation policies in reducing transmission, and the rate of asymptomatic transmission.

Kucharski et al. (2020) estimate that, in China, the effective reproductive rate  $R_t$  fell from 2.35 one week before travel restrictions were imposed on Jan 23, 2020, to 1.05 one week after travel restrictions. They use a SIR model and estimate it to forecast the epidemic in China, extending the model to explicitly account for infections arriving and departing via flights. Using data from Wuhan, Wang et al. (2020) report a baseline reproductive rate of 3.86, that fell to 0.32 after the vast lock-down intervention. They also find a high rate of asymptomatic transmission.

Work on the economic impact of the epidemic is just starting, as the data are only partially available. Atkeson (2020) explores the trade-off between the severity and timing of suppression of the disease, for example through social distancing, and the progression of the disease in the population in simulations of a SIR model like ours with exposed and not exposed population, but does not provide estimates and does not focus on the share of the exposed population, nor does he provides estimates of the model parameters.

Berger, Herkenhoff, and Mongey (2020) show that testing at a higher rate in conjunction with targeted quarantine policies can reduce both the economic impact of the COVID-19 and peak symptomatic infections. As noted above, by selectively applying social distancing policies (with different  $\alpha$  parameters) it is also possible to reduce both the economic impact of the epidemic and the peak symptomatic infections. Related to this, using data on the Spanish flu, Correia, Luck, and Verner (2020) find that cities that intervened earlier and more aggressively do not perform worse and, if anything, grow faster after the pandemic is over. These findings thus indicate that containment policies not only lower mortality, they also mitigate the adverse long term economic consequences of a pandemic.

Fang, Wang, and Yang (2020) analysis of Chinese efforts to contain the COVID-19 outbreak measures the effectiveness of the lock-down of Wuhan and enhanced social distancing policies in other cities. They produce evidence for all Chinese provinces and show that these policies con-

tributed significantly to reducing the total number of infections outside of Wuhan.

Stock (2020) focuses on measurement error and explores the benefits of randomly testing the general population to determine the asymptomatic infection rate.

Eichenbaum, Rebelo, and Trabandt (2020) discuss the trade off between the economic costs of containment policies — which could include a recession — and the number of lives saved in a model in which agents optimize and the probability of infection is endogenous. Barro, Ursua, and Weng (2020) estimate death rates and output losses based on 43 countries during the 1918-1920 Spanish flu. They find a very high death rate, with 39 million deaths, or 2.0 percent of world population, implying 150 million deaths when applied to current population. According to their estimates, the Spanish flu resulted in economic declines for GDP and consumption in the typical country of 6 and 8 percent, respectively.

Linton (2020) uses a reduced form quadratic time trend model in log of new cases and new deaths to predict the peak of COVID-19 for a large number of countries.

As far as we are aware, no study has modelled the difference between government-mandated and self-imposed isolation and their implication for the flattening of the economic and pandemic curves that we consider in this paper.

The rest of the paper is organized as follows. Section 2 sets out the modified SIR model with social distancing. Section 3 analyzes the distinction between mandatory and voluntary isolation. Section 4 discusses the trade off between containing the epidemic and the employment losses that depend on the share of exposed population. Section 5 sets out the econometric and measurement models and reports the estimation results. Section 6 concludes.

## 2 A Discrete-time SIR Model with Mitigation Policy

There are many approaches to modelling the spread of epidemics. The basic mathematical model used by many researchers is the susceptible-infective-removed (SIR) model advanced by Kermack and McKendrick (1927). This model, and its various extensions, has been the subject of a vast number of studies, and has been used extensively over the past few months to investigate the spread

of COVID-19. A comprehensive treatment is provided by Diekmann and Heesterbeek (2000) with further contributions by Metz (1978), Satsuma et al. (2004), Harko et al. (2014), Salje et al. (2016), amongst many others.

The basic SIR model considers a given population of fixed size  $P$ , composed of three distinct groups, those individuals in period  $t$  who have not yet contracted the disease and are therefore susceptible, denoted by  $S_t$ ; the ‘removed’ individuals who can no longer contract the disease, consisting of recovered and deceased, denoted by  $R_t$ ; and those who remain infected at time  $t$  and denoted by  $I_t$ . Thus

$$P = S_t + I_t + R_t. \quad (1)$$

As it stands, this is an accounting identity, and it is therefore sufficient to model  $S_t$  and  $I_t$  and obtain  $R_t$  as the remainder. The SIR model is typically cast in a set of differential equations, which we discretize and write as the following difference equations (for  $t = 1, 2, \dots, T$ )

$$S_{t+1} - S_t = -\beta s_t I_t, \quad (2)$$

$$I_{t+1} - I_t = (\beta s_t - \gamma) I_t, \quad (3)$$

$$R_{t+1} - R_t = \gamma I_t, \quad (4)$$

where  $\beta$  and  $\gamma$  are the key parameters of the epidemic.  $\beta$  is the rate of transmission and  $\gamma$  is the recovery rate. In this model it is assumed that an infected individual in period  $t$  causes  $\beta s_t$  secondary infections, where  $s_t = S_t/P$  is the share of susceptible individuals in the total population. The time profile of  $I_t$  critically depends on the basic reproduction number, defined as the expected number of secondary cases produced by a single infected individual in a completely susceptible population, denoted by  $R_0 = \beta/\gamma$ . The parameter  $\beta$  is determined by the biology of the virus, and is assumed to be constant over time and homogeneous across countries and regions. The recovery rate,  $\gamma$ , can also be written as  $\gamma = 1/d$ , where  $d$  denotes the number of days to recover or die from the infection. We assume that  $\gamma$  is constant over time, but allow it to vary across countries and regions, reflecting the differences in the capacity of the local health care systems to treat the infected population.

The epidemic begins with non-zero initial values  $I_1 > 0$  and  $S_1 > 0$ , and without any mitigation policies in place it will spread widely if  $R_0 > 1$ , ending up infecting a large fraction of the population if  $R_0$  is appreciably above unity. We show below that the steady state value of this proportion is given by  $\pi_0 = (R_0 - 1)/R_0$ . In the case of COVID-19, a number of different estimates have been suggested in the literature, placing  $R_0$  somewhere in the range of 2.4 to 3.9.<sup>2</sup>

In the simulations, and the empirical analysis to follow, we adopt a central estimate and set  $R_0 = 3$ . As we shall see the SIR model predicts that in the absence of social distancing as much as 2/3 of the population could eventually become infected before the epidemic runs its course—the so-called herd immunity solution to the epidemic. Such an outcome will involve unbearable strain on national health care systems and a significant loss of life, and has initiated unparalleled mitigation policies first by China and South Korea, and more recently by Europe, US and many other countries. Such interventions, which broadly speaking we refer to as "social distancing", include case isolation, banning of mass gatherings, closures of schools and universities, and even local and national lock-downs.

To investigate the economic implications of such policies we first modify the SIR model by decomposing the total population,  $P$  into two categories, those who are exposed to COVID-19 in the sense that they could catch the virus (they have not been infected yet),  $P_E$ , and the rest,  $P_I$ , who are isolated and therefore taken out of harm's way. We denote the strength of the mitigation policy by  $1 - \lambda$ , where  $\lambda$  is the proportion of population that is exposed to COVID-19, defined as  $\lambda = P_E/P$ . In practice,  $\lambda$  will be time-varying and most likely there will be feedbacks from the progress of the epidemic to the coverage of the intervention policies. Here we consider the relatively simple case where  $\lambda$  is set at the outset of the spread of the epidemics, close to what we believe China did after the start of the epidemic in Wuhan.

In the presence of the social distancing intervention characterized by  $\lambda$ , the equations of the

---

<sup>2</sup>Using data from Wuhan, Wang et al. (2020) report a pre-intervention reproductive rate of 3.86. Kucharski et al. (2020) estimate that, in China, the reproductive rate was 2.35 one week before travel restrictions were imposed on Jan 23, 2020. Ferguson et al. (2020) made baseline assumption of  $R_0 = 2.4$  based on the fits to early growth-rate of epidemic in Wuhan (and also examined values of 2.0 and 2.6) based on fits to the early growth-rate of the epidemic in Wuhan by Li et al. (2020) and Riou and Althaus (2020).

SIR model now become (noting that the population exposed to the virus is now  $P_E$ ):

$$\begin{aligned} S_{t+1} - S_t &= -\beta \left( \frac{S_t}{P_E} \right) I_t, \\ I_{t+1} - I_t &= \left[ \beta \left( \frac{S_t}{P_E} \right) - \gamma \right] I_t, \\ \lambda P &= S_t + I_t + R_t. \end{aligned}$$

Dividing both sides of the above equation by  $P$  and using the fractions  $s_t = S_t/P$ ,  $i_t = I_t/P$  and  $r_t = R_t/P$ , we have

$$s_{t+1} - s_t = - \left( \frac{\beta}{\lambda} \right) s_t i_t, \quad (5)$$

$$i_{t+1} - i_t = \left[ \left( \frac{\beta}{\lambda} \right) s_t - \gamma \right] i_t, \quad (6)$$

and

$$\lambda = s_t + i_t + r_t. \quad (7)$$

Given  $\beta$ , the fraction of total exposed population,  $\lambda$ , determines the effective transmission rate,  $\theta = \beta/\lambda$ . When  $\lambda = 1$ , the whole population is exposed, and the effective transmission rate coincides with the biological one,  $\beta$ .

The system equations (5) and (6) can be solved by iterating forward from some non-zero initial values, with  $i_1$  a small fraction and  $s_1 = \lambda - i_1$ , since at the start of the epidemic we can safely assume that  $r_1 = 0$ . Iterating (6) forward from  $i_1 > 0$ , and for given values of  $s_1, s_2, \dots, s_t$  we have (where we have replaced  $\theta = \beta/\lambda = \gamma(R_0/\lambda)$ )

$$i_{t+1} = \left( \prod_{\tau=1}^t \rho_\tau \right) i_1, \quad (8)$$

where  $\rho_\tau = 1 + \gamma [(R_0/\lambda) s_\tau - 1]$ . Initially, where few are infected and  $s_\tau$  is close to  $\lambda$ ,  $\rho_\tau > 1$  and the number of infected individuals rises exponentially fast so long as  $R_0 > 1$ . But as the disease spreads and recovered and/or deceased are removed, at some point in time  $t = t^*$ ,  $s_\tau$  starts to fall for  $\tau > t^*$  such that  $\rho_\tau < 1$  from  $\tau > t^*$ , and eventually  $\lim_{t \rightarrow \infty} \left( \prod_{\tau=1}^t \rho_\tau \right) = 0$ . Hence,  $\lim_{t \rightarrow \infty} (i_t) = i^* = 0$ .

Further,  $\lim_{t \rightarrow \infty} (i_{t+1}/i_t) = 1$ , and from (6) we have  $\lim_{t \rightarrow \infty} s_t = s^* = \lambda(\gamma/\beta) = \lambda/R_0$ , and using the identity  $\lambda = s^* + r^*$ , we finally obtain the following expression for the total number of infected cases as a fraction of the population ( $c^*$ ):

$$c^* = r^* = \lambda - \lambda/R_0 = \frac{\lambda(R_0 - 1)}{R_0}. \tag{9}$$

The choice of  $\lambda$  also has important implications for the steepness and the peak of the epidemic curve, and can be used to flatten the trajectory of  $i_t$ . To this end, and also for the purpose of estimating  $\lambda$  using data realizations from completed epidemics, we first eliminate  $s_t$  from the equation for  $i_t$  noting from (6) and (5) that

$$\frac{s_{t+1}}{s_t} = 1 - \theta i_t \quad \text{and} \quad \frac{i_{t+1}}{i_t} = 1 - \gamma + \theta s_t. \tag{10}$$

Since  $\theta > 0$ , solving for  $s_t$ , we have  $s_t = \theta \left( \frac{i_{t+1}}{i_t} - 1 + \gamma \right)$ , and hence

$$\frac{s_{t+1}}{s_t} = \frac{\left( \frac{i_{t+2}}{i_{t+1}} - 1 + \gamma \right)}{\left( \frac{i_{t+1}}{i_t} - 1 + \gamma \right)} = 1 - \theta i_t,$$

which yields the following second-order non-linear difference equation in  $i_t$

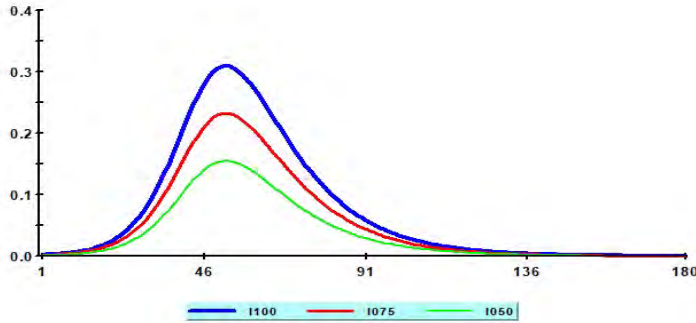
$$i_{t+1} = i_t^2/i_{t-1} + \theta [i_t i_{t-1} (1 - \gamma) - i_t^2], \quad t = 1, 2, \dots, T, \tag{11}$$

with the initial values  $i_1$  and  $i_2 = (1 - \gamma + \theta s_1) i_1$ , where  $s_1 = \lambda - i_1$ . Realizations on  $i_t$ , for  $t = 1, 2, \dots, T$ , can also be used to estimate  $\gamma$  and  $\theta$  from the above non-linear autoregression, but it is important to note that  $\beta$  and  $\lambda$  cannot be separately identified without further *a priori* knowledge. In the empirical analysis that follows we set  $R_0$  a priori and estimate  $\lambda$  from  $\gamma R_0/\theta$ , as  $\beta = \gamma R_0$  and  $\theta = \beta/\lambda$ .

As an illustration in Figure 1 we show the time profile of  $i_t(\lambda)$  using the parameter values  $R_0 = 3$  and  $\gamma = 1/d = 1/14$  and the initial values  $i_1(\lambda) = \lambda/1000$ , and  $i_2(\lambda) = [1 - \gamma + (\gamma R_0/\lambda) s_1(\lambda)] i_1(\lambda)$ , where  $s_1(\lambda) = \lambda - i_1$ . Consider the following social distancing coefficients,  $\lambda = 1, 0.75$ , and  $0.50$ .

The time profiles of the infected (as the fraction of population) peak after 52 days and does not seem to depend much on the choice of  $\lambda$ . But the choice of  $\lambda$  is clearly important for flattening the curve and reduces the peak of infected from 31 percent when  $\lambda = 1$ , to 23 per cent for  $\lambda = 0.75$ , and to 15 per cent for  $\lambda = 0.50$ .

**Figure 1:** Simulated values of  $i_t(\lambda)$  for different social distancing coefficients:  $\lambda = 1$  (blue), 0.75 (red), and 0.5 (green)



### 3 A voluntary model of social isolation: case of time-varying $\lambda$

So far we have assumed that  $\lambda$ , the proportion of population that can be infected is fixed and set exogenously by central authorities. In practice, the degree of social distancing also depends on the extent to which individuals follow the rules, which could depend on the fear of contracting the disease and most likely will depend on the number of those who are already infected, and an individual’s perception of the severity of the epidemic and its rate of spread. Even central authorities can be slow to respond when the number of active cases is small and they might delay or start with a low level of social distancing and then begin to raise it as the number of infected cases start to increase rapidly. In the context of our modified SIR model we can allow for such time variations in  $\lambda$  by relating the extent of social isolation in day  $t$ , measured by  $1 - \lambda_t$ , to the probability of contracting the disease.

More formally, consider an individual  $j$  from a fixed population of size  $P$  in the day  $t$  from the start of an epidemic, and suppose the individual in question is faced with the voluntary decision of whether to isolate or not. Under self-isolation the individual incurs the loss of wages net of transfers, amounting to  $(1 - \tau_j)w_j$ , plus the inconvenience cost,  $a_j$ , of being isolated. For those individuals who can work from home  $\tau_j$  is likely to be 1 or very close to it. But for many workers who are furloughed or become unemployed,  $\tau_j$  is likely to be close to zero, unless they are compensated by transfers from the government. On the other hand, if the individual decides not to self-isolate then he/she receives the uncertain pay-off of  $(1 - d_{jt})w_j - d_{jt}\phi_j$ , where  $d_{jt}$  is an indicator which takes the value of unity if the individual contracts the disease and zero otherwise.  $\phi_j$  represents the cost of contracting the disease and is expected to be quite high. We are ruling out the possibility of death as an outcome. In this setting the individual decides to self-isolate if the sure loss of self-isolating is less than the expected loss of not self-isolating, namely if

$$(1 - \tau_j)w_j + a_j < E[d_{jt}\phi_j - (1 - d_{jt})w_j | \mathcal{I}_{t-1}], \quad (12)$$

where  $\mathcal{I}_{t-1}$  is the publicly available information that includes  $i_{t-1}$ , the proportion of population being infected in day  $t-1$ . We assume that the probability of anyone contracting the disease is uniform across the population and this is correctly perceived to be given by  $\pi_{t-1}$ . Hence  $E(d_{jt} | \mathcal{I}_{t-1}) = \pi_{t-1}$ , and the condition for self-isolating can be written as

$$(2 - \tau_j)w_j + a_j < \pi_{t-1}(w_j + \phi_j),$$

or as

$$\frac{2 - \tau_j + (a_j/w_j)}{1 + (\phi_j/w_j)} = \mu_j < \pi_{t-1}. \quad (13)$$

Since  $\pi_{t-1} \leq 1$ , then for individual  $i$  to self-isolate we must have  $\mu_j < 1$ , (note that  $\mu_j \geq 0$ , with  $\mu_j = 0$  when  $\phi_j \rightarrow \infty$ ) or if

$$\phi_j/w_j > a_j/w_j + (1 - \tau_j). \quad (14)$$

Namely, if the relative cost of contracting the disease,  $\phi_j/w_j$  is higher than the inconvenience cost

of self-isolating plus the proportion of wages being lost due to self-isolation. Also, an individual is more likely to self-isolate voluntarily if the wage loss, measured by  $\tau_j$ , is low thus providing an additional theoretical argument in favor of compensating some workers for the loss of their wages, not only to maintain aggregate demand but to encourage a larger fraction of the population to self-isolate.

The above formulation also captures the differential incentive to self-isolate across different age groups and sectors of economic activity. Given that the epidemic affects the young and the old differently, with the old being more at risk as compared to the young, then  $\phi_{old} > \phi_{young}$ , and the old are more likely to self-isolate. Similarly, low-wage earners are more likely to self-isolate as compared to high-wage earners with the same preferences ( $\phi_j$  and  $\alpha_j$ ), and facing the same transfer rates,  $\tau_j$ . But the reverse outcome could occur if low-wage earners face a higher rate of transfer as compared to the high-wage earners. These and many other micro predictions of the theory can be tested. But here we are interested in the aggregate outcomes, in particular the fraction of the population that voluntarily self-isolates.

Denote the fraction of the population in day  $t$  who are self-isolating voluntarily by  $v_t(P)$  and using (13) note that

$$v_t(P) = P^{-1} \sum_{j=1}^P I(\mu_j < \pi_{t-1}).$$

Suppose now that condition (14) is met and  $0 \leq \mu_j < 1$ . Further suppose that the differences in  $\mu_j$  across  $j$  can be represented by a continuous distribution function,  $F_\mu(\cdot)$ . Then assuming that  $\mu_j$  are independently distributed across  $j$ , by the standard law of large numbers we have

$$v_t = \lim_{P \rightarrow \infty} [v_t(P)] = Pr(\mu_j < \pi_{t-1}) = F_\mu(\pi_{t-1}). \quad (15)$$

In practice, although  $P$  is fixed, it is nevertheless sufficiently large (in millions) and the above result holds, almost surely.<sup>3</sup>

In the case where a fixed fraction,  $1 - \lambda$ , of the population are placed under compulsory social

---

<sup>3</sup>This limiting result holds even if  $\mu_j$  are cross correlated so long as the degree of cross correlation across  $\mu_j$  is sufficiently weak.

distancing, and the remaining  $\lambda$  fraction of population decides to self-isolate voluntarily, the overall fraction of the population that isolates either compulsory or voluntarily is given by

$$1 - \lambda_t = (1 - \lambda) + \lambda F_\mu (\pi_{t-1}),$$

which yields the following expression for the fraction of population in day  $t$  that is not self-isolating

$$\lambda_t = \lambda [1 - F_\mu (\pi_{t-1})]. \tag{16}$$

Assuming that  $\mu_j$  is distributed uniformly over  $0 \leq \mu_j < 1$ , we have  $\lambda_t = \lambda(1 - \pi_{t-1})$ . Other distributions, such as Beta distribution can also be considered. But, as to be expected, it is clear that  $\lambda_t$  is inversely related to  $\pi_{t-1}$ . The higher the probability of contracting the disease the lower the fraction of the population that will be exposed to the disease.

In order to integrate the possibility of time variations in  $\lambda$  to the SIR model, we need to provide an approximate model for  $\pi_{t-1}$ , noting that  $\pi_{t-1}$  is not the true probability of contracting the disease (which itself depends on  $\lambda_t$  in a circular manner), but the subjective (or perceived) probability by individuals. As a simple, yet plausible approximation, we suppose that  $\pi_{t-1} = \kappa i_{t-1}$ , where  $\kappa > 0$ , and  $\kappa \sup_t(i_t) < 1$ , and write the modified SIR model as

$$s_{t+1} - s_t = - \left( \frac{\beta}{\lambda_t} \right) s_t i_t, \tag{17}$$

$$i_{t+1} - i_t = \left[ \left( \frac{\beta}{\lambda_t} \right) s_t - \gamma \right] i_t, \tag{18}$$

$$\lambda_t = \lambda(1 - \kappa i_{t-1}), \tag{19}$$

which can be solved iteratively from the initial values  $i_1$  and  $s_1$ . This formulation clearly reduces to the time-invariant case when  $\kappa = 0$ . Since  $i_{t-1} \geq 0$ , then  $\lambda_t \leq \lambda$  and the proportion of the population who are in harm's way declines as the epidemic spreads, and rises towards  $\lambda$ , as the epidemic starts to wane. Following a similar line of reasoning as before, it is easily established that  $i^* = \lim_{t \rightarrow \infty}(i_t) = 0$ , and  $\lambda^* = \lim_{t \rightarrow \infty}\lambda_t = \lambda$ , with the rest of the results for the case of fixed  $\lambda$  holding in the limit.

Figure 2 below shows the simulated values of  $\lambda_t$  from iterating equations (17), (18) and (19) forward with parameters  $R_0 = 3, \gamma = 1/14, \lambda = 0.5$  and  $\kappa = 1.5$ . The differences in the time profiles of  $i_t$  without feedback effects ( $\lambda = 0.5$ , and  $\kappa = 0$ ) and the ones with feedback effects ( $\lambda = 0.5$ , and  $\kappa = 1.5$ ) are shown in Figure 3. As can be seen, by relating  $\lambda_t$  to vary inversely with  $i_{t-1}$ , it is possible to flatten the peak of infected cases curve, and reduce the adverse public health and economic implications of the epidemic. But voluntary social distancing starts to have an effect only once the epidemic is already widely spread, and some coordinated social policy is clearly needed from the out-set, and before the epidemic begins to spread widely.

**Figure 2:** Simulated values of  $\lambda_t$  in the case of the SIR model with parameters

$$R_0 = 3, \gamma = 1/14, \lambda = 0.5 \text{ and } \kappa = 1.5.$$

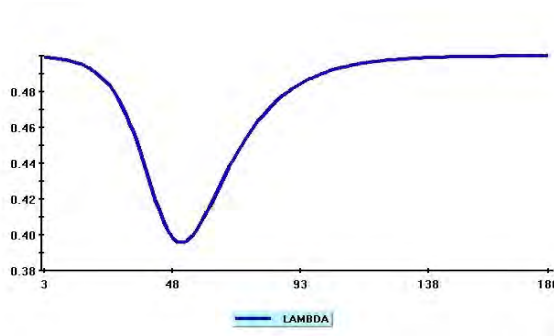
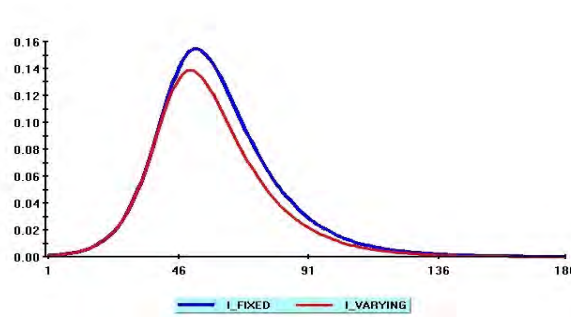


**Figure 3:** Time profiles of  $i_t$  with a fixed  $\lambda = 0.5$  and time-varying lambda with  $\kappa = 0$  (blue) and  $\kappa = 1.5$  (red)



## 4 The Economic Cost of Mitigating Epidemics

The choice of  $\lambda$  plays a critical role in establishing a balance between the height of the infection and the associated economic costs. The reduction in  $\lambda$  can be achieved through social distancing. There is a clear trade off between the adverse effects of reducing  $\lambda$  on the employment rate and its positive impact on reducing the fraction of the population infected,  $i_t(\lambda)$ , and hence removed from the work force. There is also the further trade off between the employment rate and the death rate due to the spread of the epidemic for different choices of  $\lambda$ . However, we do not model the death rate or take into account its economic or social cost.

Since the duration of the epidemic is expected to be relatively short, 3 to 4 months at most, it is reasonable to assume that the immediate economic impact of the epidemic will be on the rate of employment. In the absence of the epidemic, we assume that the rate of employment in day  $t$  is given by  $e_t = E_t/P$  where  $E_t$  is the counterfactual level of employment during day  $t$ , and  $P$  is the population taken as given. For the US economy the current value of  $e_t$  is around 60%, which we take to be the counterfactual employment rate.

Consider now the rate of employment during the spread of the epidemic,  $t = 1, 2, \dots, T$ , under the social distancing policy  $\lambda$  ( $0 < \lambda \leq 1$ ). The effect of the epidemic on the employment level is two-fold. First it reduces the number in employment directly by  $f(\lambda)$ , where  $f(1) = 1$ , and  $f(\lambda)$  is an increasing function of  $\lambda$ , with  $f''(\lambda) \leq 0$ , for  $\lambda$  in the range  $0 < \lambda \leq 1$ . In the extreme scenario where the incidence of social distancing is uniform across all individuals and all sectors of the economy, we have  $f(\lambda) = \lambda$ . But in practice the fall in employment is likely to be less than proportional since some who work from home are less affected by social distancing as compared to those who are fired because of down-sizing and firm closures. It is also possible to mitigate the negative employment effects of social distancing by focussing on sectors of the economy that are less affected by social distancing, by embarking on intensive and targeted testing, contract tracing, and by more extensive use of protective clothing and equipment. To capture such effects we set  $f(\lambda) = 1 - (1 - \lambda)^\alpha$ , with  $\alpha \geq 1$ . As required  $f(1) = 1$ , and  $f'(\lambda) = \alpha(1 - \lambda)^{\alpha-1} > 0$ . We refer to  $\alpha$  as the elasticity of employment loss with respect to the degree of social distancing,  $\lambda$ . The direct

employment effect of social distancing will be less adverse for values of  $a > 1$ . In what follows, in addition to the baseline value of  $\alpha = 1$ , we also consider  $\alpha = 2$ , under which a reduction of  $\lambda$  from 1 to  $1/2$ , for example, reduces the employment rate by  $1/4$  as compared to  $1/2$  if we set  $\alpha = 1$ .

In addition to this direct effect, the employment level also falls directly due to the number of infected individuals,  $I_t(\lambda)$ , which also depends on  $\lambda$ . Recall that  $I_t(\lambda)$  is increasing in  $\lambda$ . There will be more infected individuals the higher the level of exposure to the virus. Overall, the rate of employment during the spread of the epidemic is given by

$$e_t(\lambda) = f(\lambda)e_t - i_t(\lambda). \quad (20)$$

The associated employment loss is then

$$\ell_t(\lambda) = e_t - e_t(\lambda) = [1 - f(\lambda)]e_t + i_t(\lambda), \text{ for } t = 1, 2, \dots, T. \quad (21)$$

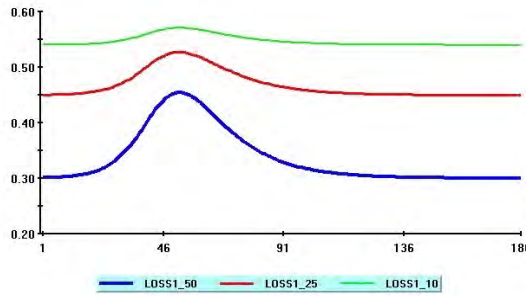
This relationship represents a trade off between the opposing effects of high and low exposures to the epidemic on the rate of employment. In the event of a high exposure the first term of (21) will be small relative to the second term, and when exposure is low the direct employment loss is much higher than the indirect loss due to the spread of infection. It is also important to bear in mind that employment losses can vary considerably over the course of the epidemic.

Figure 4 shows the time profile of the simulated values of employment losses,  $\ell_t(\lambda)$ , for selected values of  $\lambda = 0.5, 0.25$  and  $0.1$ , with  $\alpha = 1$ . We focus on exposure rates of 50% and less, since our estimates of  $\lambda$  to be discussed tend to be rather small. The losses are computed with daily employment rates set to  $e_t = 0.6$ , which is approximately equal to the mean ratio of employment to population in the US during the last quarter of 2019. As before, the simulated values for  $i_t(\lambda)$  are obtained using the SIR model with the parameters  $R_0 = 3, \gamma = 1/d = 1/14$ , and the initial values  $i_1(\lambda) = \lambda/1000$ , and  $i_2(\lambda) = [1 - \gamma + (\gamma R_0/\lambda) s_1(\lambda)] i_1(\lambda)$ , where  $s_1(\lambda) = \lambda - i_1(\lambda)$ .

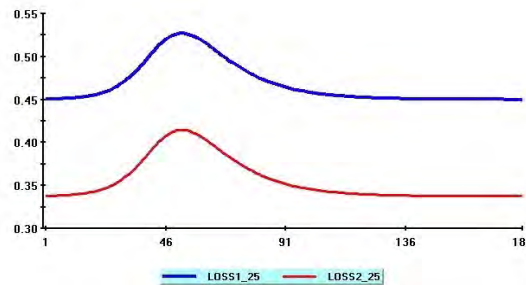
As to be expected, employment losses mount up as the rate of exposure to the disease is reduced from 50% to 25% and right down to 10%. It is also evident from Figure 4 that with the flattening of the infection curve, as  $\lambda$  is reduced, employment losses stabilize and remain high for the duration

of the epidemic. However, as noted earlier, the extent of the losses from reducing  $\lambda$  very much depends on  $\alpha$ . As can be seen from Figure 4, when  $a = 1$  the losses can be quite substantial, as everyone who is isolated has a full charge on the economy. When  $a = 2$ , the adverse effects of social distancing are somewhat mitigated, but could still be considerable for values of  $\lambda$  below 25%. See Figure 5 which shows the simulated employment losses for  $a = 1$  (blue) and  $a = 2$  (red) with  $\lambda = 0.25$ .

**Figure 4:** Simulated employment losses for  $\alpha = 1$  and the values of  $\lambda = 0.5$  (blue), 0.25 (red) and 0.10 (green)



**Figure 5:** Simulated employment losses for  $\lambda = 0.25$  and the values of employment loss elasticity,  $a = 1$  (blue) and  $a = 2$  (red)



A summary of average simulated employment losses for different values of  $\lambda$  and  $\alpha$  is provided in Table 1. In this table we also give estimates for  $\lambda = 1$  (case of no social distancing) and  $\lambda = 0.75$  representing a moderate degree of social distancing. We also computed the simulated losses allowing for voluntary social distancing, but the results in Table 1 were not much affected. The results confirm that average losses over the duration of the epidemic (simulated to be 120 days) can be significant, but can be somewhat mitigated by working from home and by enabling a select group of workers to take part in productive activities under medical supervision (through regular testing for the disease) and by providing the necessary protective equipment for their own and other people's safety.

**Table 1:** Simulated average employment loss (in per cent per annum) due to epidemic under different social distancing ( $\lambda$ ) and economic impact ( $\alpha$ ) scenarios

Employment loss elasticity $\alpha$	Social distancing coefficient ( $\lambda$ )				
	1.0	0.75	0.50	0.25	0.10
1.0	3.6	7.7	11.8	15.9	18.4
1.5	3.6	5.2	8.9	13.9	17.4
2.0	3.6	4.0	6.8	12.2	16.6

Notes: This table reports results of a simulation of the epidemic under different social distancing ( $\lambda$ ) and economic impact ( $\alpha$ ) scenarios. The epidemic is simulated using SIR model with  $R_0 = 3$  and  $\gamma = 1/14$ .  $\lambda$  is the fraction of the population exposed to the virus.  $\alpha$  determines the economic cost of the isolation measures, as defined by  $(1 - \lambda)^\alpha$ . The losses are given in per cent per annum over 120 days which is the simulated length of the epidemic.

The calibration of  $\lambda$  is a complicated undertaking and could differ across economies. In the case of the U.S., it is possible to estimate  $\lambda$  from the recently stated aims by US administration to limit the number of fatalities due to the COVID-19 to less than 200,000. Assuming a death rate of 1%, this requires limiting the cumulative number of infected cases to  $C^* = 200,000/0.01 = 20,000,000$ . For a given  $\lambda$  and the reproduction ratio of  $R_0 = 3$ , we have  $C^*/P_{US} = 2\lambda/3$ , which gives the estimate  $\lambda_{US} = (20/320)(3/2) = 0.094$ , assuming a US population of 320 million. The implied value of  $\lambda_{US}$

would need to be even lower if a higher death rate is assumed, as the current US data suggests.<sup>4</sup> With  $\lambda_{US}$  at 10%, the employment loss over the duration of the epidemic (estimated to be around 120 days), could be as much as 18.4% at an annual rate when  $\alpha = 1$ , but gets reduced to 16.6 per cent per annum when  $\alpha = 2$ .

## 5 Fitting the modified SIR model to the data: estimation of removal and exposure rates

Whilst calibration can be helpful in counterfactual analysis, it is also desirable to obtain estimates of  $\lambda$  from realized outcomes. This is fortunately possible using data on COIVD-19 from Chinese provinces over the period January to March 2020. We also report estimates for a selected number of countries, but these estimates should be considered as preliminary since at the time of writing many of these epidemics are still unfolding. The attraction of using data from Chinese provinces is two-fold. First we have complete daily time series data that cover the full duration of the epidemics with slightly different start dates. Second, we can investigate the differences in parameter estimates (particularly  $\lambda$ ) for the Hubei Province, the epicenter of the epidemic in China, as compared to the estimates for other provinces.

Our focus is on estimating the removal rate,  $\gamma$ , and the social distancing coefficient,  $\lambda$ . We base our estimation on equations (4) and the solution for  $i_t$  given by (11). However, it is widely acknowledged that in the absence of large scale testing and given the asymptomatic nature of the disease in the case of many infected individuals, the recorded numbers of infected and recovered cases of COIVD-19 most definitely underestimate the true numbers of such cases. Before proceeding therefore we need to address this challenge.

### 5.1 Adjusting for under-reporting and other measurement errors

To allow for under-recording of infected cases, and other related measurement errors, we distinguish between the *true* and reported (confirmed) measures. We denote the true measures of infected and

<sup>4</sup>At the time of writing the death rate of COIVD-19 in the U.S. is around 4% using reported number confirmed cases. But as argued below, due to under reporting of infected cases the true death rate is likely to be around 2%.

recovered cases by  $\tilde{C}_t$  and  $\tilde{R}_t$ , respectively, and denote the corresponding reported statistics by  $C_t$  and  $R_t$ . Let  $\pi_t$  be the ratio of confirmed to true cases, and suppose that

$$\pi_t = \pi e^{v_t - 0.5\sigma^2}, \tag{22}$$

where  $\pi$  ( $0 < \pi < 1$ ) is a fixed fraction, and  $v_t$  is  $IIDN(0, \sigma^2)$ . The assumption that  $\pi_t$  follows a log-normal distribution is made for convenience and can be relaxed, and ensures that  $E(\pi_t) = \pi$ . It is also worth noting that  $Var(\pi_t) = \pi^2(e^{\sigma^2} - 1)$ . The inverse of  $\pi$  measures the degree of under-reporting and is referred to as the multiplication factor (MF) in the literature—see, for example, Gibbons et al. (2014). It is also reasonable to expect that the same fraction,  $\pi_t$  applies to recovered cases. Under these assumptions we have

$$C_t = \pi_t \tilde{C}_t = \pi e^{v_t - 0.5\sigma^2} \tilde{C}_t, \quad \text{and} \quad R_t = \pi_t \tilde{R}_t = \pi e^{v_t - 0.5\sigma^2} \tilde{R}_t, \tag{23}$$

which also yield

$$I_t = C_t - R_t = \pi e^{v_t - 0.5\sigma^2} \tilde{I}_t, \tag{24}$$

where  $I_t$  and  $\tilde{I}_t$  are the reported and the true number of active cases, namely the number of individuals that remain infected in day  $t$ .

The theoretical equations (4) and (11) are derived in terms of the true measures,  $\tilde{i}_t = \tilde{I}_t/P$ , and  $\tilde{r}_t = \tilde{R}_t/P$ , but for estimation purposes they need to be cast in terms of the reported statistics, namely  $i_t = I_t/P$  and  $r_t = R_t/P$ . Using (23) and (24) in the equation for the recovery rate, (4), we have

$$r_{t+1} = e^{v_{t+1} - v_t} (r_t + \gamma i_t),$$

which yields the following estimating equation

$$r_{t+1} = \rho r_t + (\gamma\rho) i_t + \varepsilon_{t+1}, \tag{25}$$

where  $\rho = e^{\sigma^2}$ , and under the assumption that  $v_t$  are  $IIDN(0, \sigma^2)$ , it follows that  $E(\varepsilon_{t+1} | r_t, i_t) = 0$ .

It is interesting to note that the MF,  $1/\pi$ , does not enter the equation for  $r_{t+1}$ , and both of the unknown parameters,  $\sigma^2$  and  $\gamma$  can be estimated from the OLS regression of  $r_t$  on  $r_{t-1}$  and  $i_t$ .

Similarly, using (24) to replace the true values  $\tilde{i}_t$  in (11) we obtain

$$i_{t+1} = (i_t^2/i_{t-1}) \rho^3 + \left( \frac{\rho^2 \gamma R_0}{\pi \lambda} \right) [i_t i_{t-1} (1 - \gamma) - \rho i_t^2] + \xi_{t+1}, \quad (26)$$

where  $\rho = e^{\sigma^2}$ ,  $E(\xi_{t+1} | i_t, i_{t-1}) = 0$ . For a given value of  $\rho$ ,  $\gamma$  and  $R_0$  the above non-linear regression can be used to provide estimates of  $\pi \lambda$ . Thus, to estimate  $\lambda$  we need to make an assumption regarding,  $\pi$ , which we address below.

## 5.2 Estimates of recovery and social distancing rates

We allow recovery rates,  $\gamma_j$ , to differ across Chinese provinces reflecting possible differences in their demographics and the availability of medical facilities. Let  $\gamma_j$  be the recovery rate in province  $j$ , and consider the regressions<sup>5</sup>

$$r_{j,t+1} = \rho_j r_{jt} + (\gamma_j \rho_j) i_{jt} + \varepsilon_{j,t+1}, \text{ for } j = 1, 2, \dots, N, \quad (27)$$

where  $r_{jt}$  and  $i_{jt}$  are measured as

$$r_{jt} = (RE_{jt} + D_{jt})/P_j, \text{ and } I_{jt} = C_{jt} - RE_{jt} - D_{jt},$$

in which  $C_{jt}$ ,  $RE_{jt}$  and  $D_{jt}$  are daily time series data obtained from Johns Hopkins University Coronavirus Resource Center, corresponding to the cumulative number of confirmed, recovered and deceased cases for province/country  $j$ , respectively.<sup>6</sup>

<sup>5</sup>Here the recovery rate includes both the recovered and the deceased, and strictly speaking should be referred to as the *removal rate*. But in line with the literature we use "recovery rate" in place of the "removal rate".

<sup>6</sup>Available at [https://github.com/CSSEGISandData/COVID-19/tree/master/csse\\_covid\\_19\\_data](https://github.com/CSSEGISandData/COVID-19/tree/master/csse_covid_19_data).  $C_{jt}$  is the number of confirmed cases taken from file `time_series_covid19_confirmed_global.csv`,  $RE_{jt}$  is the number of recovered taken from file `time_series_covid19_recovered_global.csv`, and  $D_{jt}$  is the number of deceased taken from file `time_series_covid19_deaths_global.csv`.

### 5.2.1 Estimates for Chinese provinces

The estimates of  $\gamma_j$  for 21 Chinese provinces are summarized in Table 2.<sup>7</sup> As noted above, the estimation of  $\gamma$  does not depend on under-recording of infected cases, but could depend on the random component of the measurement equations (23) and (24). The extent of this type of mis-measurement is given by the estimates of  $\sigma_j$  which we also report in Table 2. Recall that  $\sigma_j^2 = \ln(\rho_j)$ , and  $\rho_j$ , for  $j = 1, 2, \dots, 21$  are identified from regressions, (27). As can be seen, the estimates of recovery rates,  $\gamma_j$ , do not differ much across the provinces and lie in the range of 0.033 (for Beijing) and 0.066 (for Hebei), with the mean across all the provinces given by  $\hat{\gamma}_{MG} = 0.046$ , with a standard error of 0.17%.<sup>8</sup> The random measurement errors are also relatively unimportant, with the estimates of  $\sigma_j$  falling within the range (0.06 – 0.10) across the 21 provinces.<sup>9</sup> The mean estimate,  $\hat{\gamma}_{MG} = 0.046$ , corresponds to around 22 days on average from infection to recovery or death, with the rather narrow 95% confidence interval of 20 to 23 days. Hubei and Beijing have the lowest recovery rates, and Hebei, Hunan and Guizhou provinces the highest. These estimates are all longer than the 14 days typically assumed in designing quarantine policies and, as we shall see, this has important implications for the estimates of the social distancing coefficient,  $\lambda$ .<sup>10</sup>

Next, we report estimates of  $\lambda_j$  by running the non-linear regressions in (26) for each province separately. We consider two choices for  $\rho$  and  $\gamma$ , namely the province-specific estimates,  $\hat{\rho}_j$ ,  $\hat{\gamma}_j$ , reported in Table 2, and the pooled estimate,  $\hat{\rho}_j = 1.0072$ ,  $\hat{\gamma}_{MG} = 0.046$ . Regarding the choice of  $R_0$ , we consider 2.5 and 3, which are in the range of values reported in the recent report from Imperial College, Ferguson et al. (2020). But we only report the results for  $R_0 = 3$ , to save space. The estimates of  $\lambda$  for other values of  $R_0$  differ only in scale and can be easily obtained if desired.

<sup>7</sup>We dropped those provinces where the number of active cases did not exceed 100 during the period up to the end of February. This leaves 21 provinces: Hubei, Guangdong, Henan, Zhejiang, Hunan, Anhui, Jiangxi, Shandong, Jiangsu, Chongqing, Sichuan, Heilongjiang, Beijing, Shanghai, Hebei, Fujian, Guangxi, Shaanxi, Yunnan, Hainan, and Guizhou.

<sup>8</sup>The standard errors for the mean group estimator,  $\hat{\gamma}_{MG} = n^{-1} \sum_{j=1}^n \hat{\gamma}_j$ , is computed using the formula given in Pesaran and Smith (1995), and as shown in Chudik and Pesaran (2019), they are robust to weak cross correlations across the provinces.

<sup>9</sup>It is indeed reassuring to note that all the 21 estimates of  $\rho_j$ , computed from separate regressions, are all larger than 1, and yield reasonable estimates for the standard error of the measurement errors, defined by  $\sigma_j = \sqrt{\ln(\rho_j)}$ .

<sup>10</sup>The medical evidence documented in Ferguson et al. (2020) implies a value for  $\gamma$  in the range 0.048 to 0.071, with our empirical evidence suggesting that values at the lower end of this range might be more appropriate.

Note from equation (26) that using time series data on  $i_t$ , we are only able to identify  $\pi\lambda/R_0$ , and other data sources must be used to set  $R_0$  and  $\pi$ .

Finally, we calibrate the proportion of under reporting,  $\pi$ , or its inverse,  $1/MF$ , using the data from the Diamond Princess cruise ship reported in Morbidity and Mortality Weekly Report, Moriarty et al. (2020). This case could be viewed as quasi-experimental. It is reported that out of 3,711 passengers and crew 712 had positive test results for SARS-Cov-2, with only 381 being symptomatic with the remaining 311 asymptomatic at the time of testing. Since all of those on board are tested, it is reasonable to assume that the true number of infected individuals is  $\tilde{C} = 712$ , and in the absence of complete testing the confirmed number of symptomatic cases  $C = 381$ , since those without any symptoms would have been overlooked in the absence of complete testing. These statistics suggest  $\hat{\pi} = C/\tilde{C} = 381/712 = 0.535$  or  $MF = 1.9$ , which we round to  $MF = 2$ . This estimate is preliminary but seems plausible when we consider the death rate reported for China and the death rate on Diamond Princess. It is widely recognized that the death rate of COVID-19 based on confirmed infected cases could be grossly over-estimated, again due to under testing, and under estimation of  $\tilde{C}$ . It is therefore interesting to see if we can obtain a death rate for China which becomes closer to the death rate observed on Diamond Princess of 1.3%, if we adjust upward the number of confirmed cases by  $MF = 2$ . Based on confirmed cases and the number of deaths in China (at the time of writing) the crude death rate is  $d_{China} = C/D = 3,335/81,865 = 4.07\%$ . But assuming that  $D = \tilde{D}$ , and setting  $MF = 2$ , the true death rate in China reduces to

$$\tilde{d}_{China} = \frac{\tilde{D}}{\tilde{C}} = \frac{D}{C} \cdot \frac{C}{\tilde{C}} = 2.03\%.$$

This is still somewhat larger than the death rate of 1.3% reported for Diamond Princess, but could still be close to the truth, noting that on average access to medical facilities for the passengers and crews on Diamond Princess might be better as compared to China where most of the fatalities occurred at the epicenter of the epidemic in Hubei province without much warning or preparation at the start of the epidemic. In view of these results we set  $\pi = 0.5$  and compute province-specific estimates of  $\lambda_j$  with  $R_0 = 3$  by running the regressions.<sup>11</sup>

<sup>11</sup>The death rate of COVID-19 in other countries where the epidemic is still at its early stages is likely to be further

Estimates of  $\lambda_j$  (per 100,000 of population) for Chinese provinces are reported in Table 3 using the full sample and a subsample. Initially, we focus on the full sample estimates. The left panel of Table 3 gives the results when the province-specific estimates of  $\rho_j$  and  $\gamma_j$  are used, whilst the right panel reports the estimates of  $\lambda_j$  based on the pooled estimates of  $\rho$  and  $\gamma$ , namely  $\hat{\rho}_j = \hat{\rho}_{MG} = 1.0072$ , and  $\hat{\gamma}_j = \hat{\gamma}_{MG} = 0.046$ . The reason for including the pooled estimates is to investigate the robustness of the exposure rates,  $\lambda_j$ , to the choice of the recovery rate and the extent of measurement errors. As it turns out, both sets of estimates are quite close, with the ones based on the pooled estimates slightly larger. The largest difference between the two sets of estimates is obtained for Hubei province (the epicenter of the epidemic), namely 16.31 (1.76) when we use province-specific estimates of  $\rho_j$  and  $\gamma_j$ , and 23.74 (2.74), when we use the pooled estimates ( $\hat{\rho}_{MG}$  and  $\hat{\gamma}_{MG}$ ).<sup>12</sup> Despite this difference, both estimates of  $\lambda$  for Hubei province have a high degree of precision and are statistically highly significant, with their 95% confidence interval overlapping. What is striking is the large difference between the estimates for Hubei and the rest of the Chinese provinces. Outside the epicenter the estimates of  $\lambda$  are much smaller in magnitude and range between 0.09 and 0.87, irrespective of whether we use province-specific or pooled estimates of  $\rho$  and  $\gamma$ . In fact the mean group estimates of  $\lambda$  across these provinces (excluding Hubei) are almost the same, namely 0.393 (0.05), and 0.389 (0.05), respectively. Thus on average the exposure rate in Hubei is estimated to be some 40 – 60 times higher than the average exposure rate of the provinces outside of the epicenter. This makes sense, since it is likely that it took the Chinese authorities some time before they managed to put into effect very stringent social distancing policies that were required to reduce  $\lambda$  substantially across China. Looking at the estimates of the province-specific exposure rates outside Hubei, we also see a remarkably low degree of heterogeneity consistent with a firm and homogenous imposition of social distancing policies, following what had been learned at the epicenter of the epidemic.

As can be seen from Figure 6, the regressions for  $i_{jt}$  fit reasonably well and trace the epidemic curves accurately for *all* 21 Chinese provinces that we consider. Here, it is also notable that the time to the peak of the epidemic curve is about 4 weeks for most provinces, and the time to completion is

biased upward due to the long delay (4 weeks or more) between infection and death.

<sup>12</sup>The figures in brackets are standard errors of the estimates.

around 8 weeks. It is clear that epidemic curves this flat could not have materialized if it were not for the very stringent social distancing policies implemented by the Chinese authorities, as reflected in the very low estimates of  $\lambda_j$  that we obtain, particularly once we consider provinces outside of the epicenter of the epidemic.

Thus far, we have focussed on Chinese data since they represent completed epidemic cycles across all 21 provinces. In contrast, at the time of writing, the peak of the epidemic has not been reached for other countries, where the first reported cases came a few weeks after China. So we now turn our attention to other countries, considering only those countries for which we have a sufficient history for a reliable estimation of  $\lambda$ . Before proceeding, for an accurate comparison with China, we report estimates of  $\gamma$  and  $\lambda$  for the same 22 Chinese provinces over a subsample ending on 20<sup>th</sup> of February (covering the initial stages of the epidemic before reaching its peak). For this subsample the estimates of  $\gamma$  (and  $\rho$ ) are summarized in Table 4, which are directly comparable to the full-sample estimates in Table 2. As can be seen, for  $\gamma$  we obtain much smaller estimates when we use the subsample as compared to the full sample, with a mean estimate of 0.018 compared to the full-sample estimate of 0.046, possibly reflecting the fact that before the peak of the epidemic the data do not capture the recoveries and deaths that will materialize in the following three weeks. It is therefore reasonable to expect that removal rates in other countries will converge to the very precise estimates for China that we have already reported for the full sample in Table 2.

Subsample estimates of  $\lambda$  are presented in Table 3. For  $\lambda$  the point estimates based on the two samples are very close, in line with the news reporting/anecdotal evidence of stringent and consistent implementation of social distancing. Remarkably, these estimates continue to be very precisely estimated. A visual comparison between the estimates of  $\lambda$  based on the full and the subsamples is given in Figure 7. As can be seen, the estimates of  $\lambda$  are essentially the same for the two sample periods, with the exception of the estimates for Shandong province where the subsample estimate of  $\lambda$  is larger than the full-sample estimate. This could be due to the fact that outside the epicenter, Shandong is the only province to experience a second wave in mid course, as is evident from the plot of active cases for Shandong in Figure 6.

**Table 2:** Estimates of the recovery rates ( $\gamma_j$ ) for Chinese provinces

	$\hat{\gamma}_j$	(s.e.)	$\hat{\rho}_j$	(s.e.)	$\hat{\sigma}_j$
Hubei	0.035	(0.0030)	1.0088	(0.0018)	0.09
Guangdong	0.042	(0.0032)	1.0070	(0.0018)	0.08
Henan	0.054	(0.0054)	1.0072	(0.0025)	0.08
Zhejiang	0.044	(0.0038)	1.0073	(0.0019)	0.09
Hunan	0.056	(0.0039)	1.0055	(0.0017)	0.07
Anhui	0.049	(0.0052)	1.0081	(0.0026)	0.09
Jiangxi	0.047	(0.0049)	1.0081	(0.0025)	0.09
Shandong	0.046	(0.0060)	1.0084	(0.0030)	0.09
Jiangsu	0.055	(0.0045)	1.0063	(0.0021)	0.08
Chongqing	0.043	(0.0039)	1.0077	(0.0021)	0.09
Sichuan	0.040	(0.0034)	1.0081	(0.0019)	0.09
Heilongjiang	0.043	(0.0052)	1.0086	(0.0030)	0.09
Beijing	0.033	(0.0042)	1.0053	(0.0028)	0.07
Shanghai	0.043	(0.0065)	1.0034	(0.0034)	0.06
Hebei	0.066	(0.0058)	1.0060	(0.0023)	0.08
Fujian	0.039	(0.0051)	1.0078	(0.0029)	0.09
Guangxi	0.037	(0.0051)	1.0093	(0.0031)	0.10
Shaanxi	0.044	(0.0051)	1.0074	(0.0027)	0.09
Yunnan	0.041	(0.0068)	1.0085	(0.0038)	0.09
Hainan	0.052	(0.0078)	1.0080	(0.0037)	0.09
Guizhou	0.056	(0.0079)	1.0049	(0.0038)	0.07
MG estimates	0.046	(0.0017)	1.0072	(0.0003)	0.08

Notes: Estimation is based on regression  $r_{j,t+1} = \rho_j r_{jt} + (\gamma_j \rho_j) i_{jt} + \varepsilon_{j,t+1}$ , where  $\sigma_j = \sqrt{\ln(\rho_j)}$ . See also (27). Sample is Jan-22 to March-31, 2020 ( $T = 70$ ) with the exception of Hubei which is estimated using the sample Jan-22 to Apr-6 ( $T = 76$ ).

**Table 3:** Estimates of exposure rates ( $\lambda_j$ ) per 100,000 population for Chinese provinces

( $\pi = 0.5, R_0 = 3$ )

	Using province-specific estimates $\hat{\rho}_j, \hat{\gamma}_j$				Using pooled estimates $\hat{\rho}_{MG}, \hat{\gamma}_{MG}$			
	Full sample		Subsample		Full sample		Subsample	
	$\hat{\lambda}_j$	(s.e.)	$\hat{\lambda}_j$	(s.e.)	$\hat{\lambda}_j$	(s.e.)	$\hat{\lambda}_j$	(s.e.)
Guangdong	0.441	(0.042)	0.431	(0.044)	0.491	(0.044)	0.484	(0.046)
Henan	0.610	(0.099)	0.571	(0.115)	0.501	(0.085)	0.457	(0.093)
Zhejiang	0.610	(0.079)	0.599	(0.110)	0.643	(0.084)	0.633	(0.117)
Hunan	0.663	(0.108)	0.677	(0.146)	0.468	(0.072)	0.472	(0.095)
Anhui	0.734	(0.159)	0.692	(0.157)	0.722	(0.168)	0.675	(0.164)
Jiangxi	0.846	(0.166)	0.770	(0.176)	0.868	(0.180)	0.786	(0.190)
Shandong	0.087	(0.008)	0.200	(0.034)	0.088	(0.008)	0.216	(0.040)
Jiangsu	0.389	(0.065)	0.399	(0.075)	0.297	(0.049)	0.300	(0.057)
Chongqing	0.586	(0.106)	0.583	(0.133)	0.644	(0.118)	0.642	(0.150)
Sichuan	0.166	(0.021)	0.165	(0.026)	0.211	(0.027)	0.213	(0.035)
Heilongjiang	0.364	(0.050)	0.364	(0.057)	0.414	(0.060)	0.420	(0.072)
Beijing	0.412	(0.077)	0.444	(0.127)	0.586	(0.096)	0.644	(0.163)
Shanghai	0.498	(0.106)	0.524	(0.156)	0.451	(0.079)	0.472	(0.115)
Hebei	0.215	(0.050)	0.205	(0.070)	0.126	(0.029)	0.115	(0.037)
Fujian	0.211	(0.042)	0.194	(0.041)	0.266	(0.053)	0.251	(0.054)
Guangxi	0.106	(0.030)	0.104	(0.045)	0.156	(0.049)	0.156	(0.076)
Shaanxi	0.213	(0.040)	0.199	(0.050)	0.227	(0.043)	0.213	(0.054)
Yunnan	0.108	(0.020)	0.095	(0.019)	0.130	(0.026)	0.116	(0.025)
Hainan	0.461	(0.079)	0.463	(0.108)	0.396	(0.069)	0.395	(0.094)
Guizhou	0.131	(0.034)	0.133	(0.046)	0.096	(0.023)	0.096	(0.031)
MG estimate	0.393	(0.050)	0.391	(0.047)	0.389	(0.050)	0.388	(0.047)
Hubei	16.306	(1.764)	16.164	(2.765)	23.743	(2.720)	23.584	(4.395)

Notes: Estimation is based on regressions  $i_{j,t+1} = \left(i_{jt}^2/i_{j,t-1}\right)\rho_j^3 + \rho_j^2 \left(\frac{\gamma_j R_0}{\pi \lambda_j}\right) \left[i_{jt} i_{j,t-1} (1 - \gamma_j) - \rho_j i_{jt}^2\right] + \xi_{jt+1}$ , for  $j = 1, 2, \dots, 21$  (provinces), with  $\rho_j, \gamma_j$  imposed equal to the country-specific estimates from Table 2 or their MG estimates from Table 2. The full sample is the same as in Table 2. The subsample is Jan-22 to Feb-20 ( $T = 30$ ).

Figure 6: Number of active cases in Chinese provinces ( $I_{jt}$ ) and fitted values

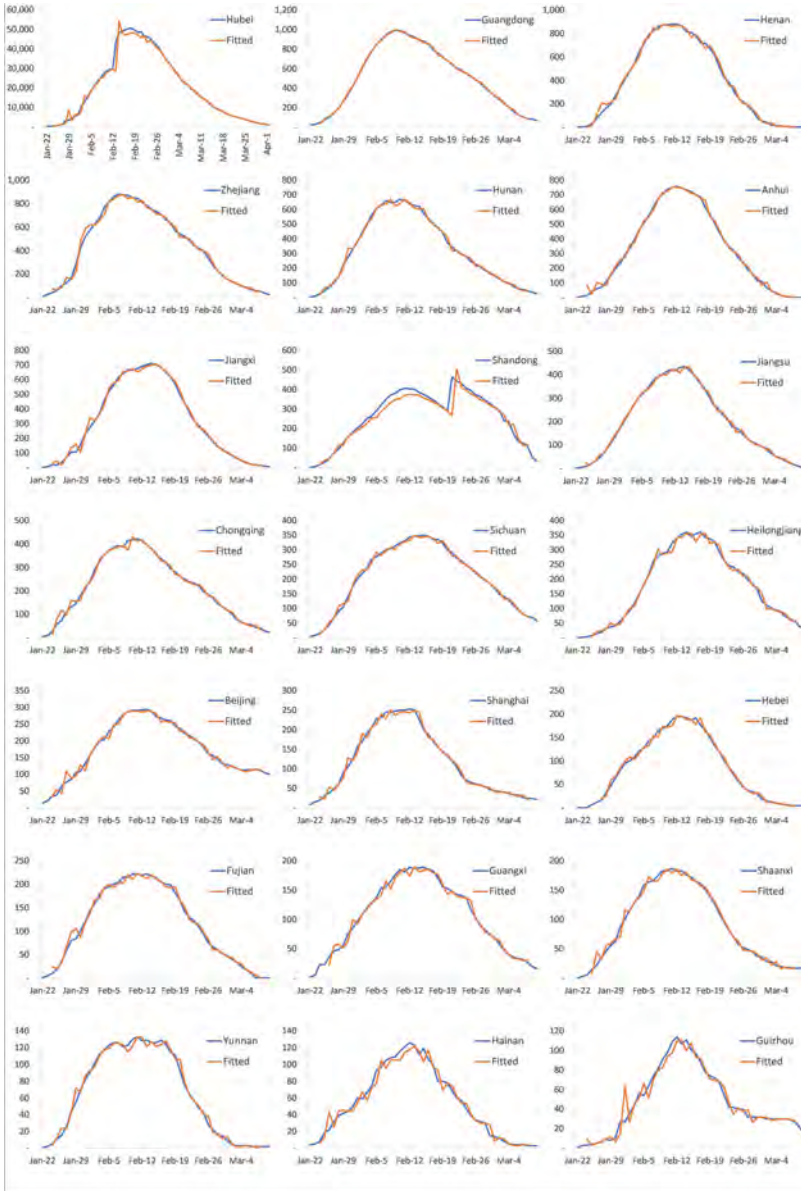
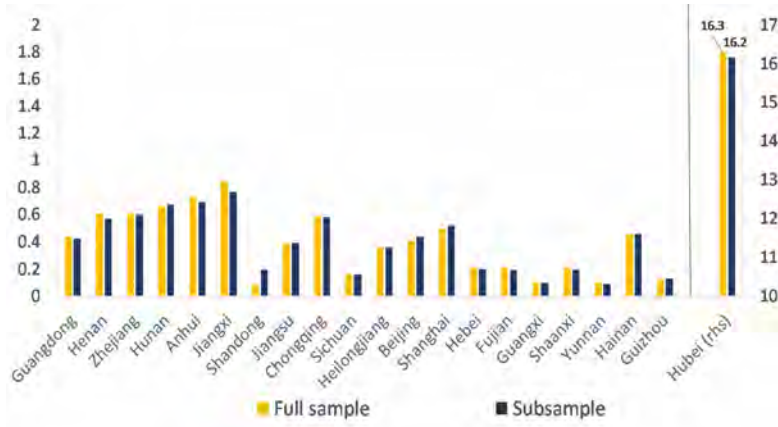


**Table 4:** Subsample estimates of recovery rates ( $\gamma_j$ ) for Chinese provinces using the sample ending Feb-20

	$\hat{\gamma}_j$	(s.e.)	$\hat{\rho}_j$	(s.e.)	$\hat{\sigma}_j$
Hubei	0.013	(0.0038)	1.0656	(0.0226)	0.25
Guangdong	0.022	(0.0037)	1.0587	(0.0104)	0.24
Henan	0.025	(0.0052)	1.0636	(0.0135)	0.25
Zhejiang	0.024	(0.0047)	1.0492	(0.0115)	0.22
Hunan	0.031	(0.0064)	1.0581	(0.0124)	0.24
Anhui	0.009	(0.0042)	1.1391	(0.0161)	0.36
Jiangxi	0.006	(0.0037)	1.1422	(0.0150)	0.36
Shandong	0.019	(0.0045)	1.0739	(0.0140)	0.27
Jiangsu	0.019	(0.0049)	1.1020	(0.0129)	0.31
Chongqing	0.019	(0.0038)	1.0840	(0.0109)	0.28
Sichuan	0.013	(0.0062)	1.0823	(0.0208)	0.28
Heilongjiang	0.016	(0.0077)	1.0785	(0.0373)	0.27
Beijing	0.014	(0.0063)	1.0681	(0.0231)	0.26
Shanghai	0.020	(0.0089)	1.0819	(0.0226)	0.28
Hebei	0.026	(0.0073)	1.0830	(0.0164)	0.28
Fujian	0.012	(0.0050)	1.0916	(0.0199)	0.30
Guangxi	0.009	(0.0079)	1.1034	(0.0373)	0.31
Shaanxi	0.010	(0.0042)	1.1194	(0.0156)	0.34
Yunnan	0.002	(0.0080)	1.1609	(0.0382)	0.39
Hainan	0.027	(0.0144)	1.0621	(0.0373)	0.25
Guizhou	0.038	(0.0140)	1.0434	(0.0349)	0.21
MG estimate	0.018	(0.0019)	1.0862	(0.0067)	0.29

Notes: Estimation is based on regression  $r_{j,t+1} = \rho_j r_{jt} + (\gamma_j \rho_j) i_{jt} + \varepsilon_{j,t+1}$ . See also (27). Sample is Jan-22 to Feb-20 ( $T = 30$ ).

**Figure 7:** Full sample and subsample estimates of exposure rate ( $\lambda$ ) per 100,000 population across Chinese provinces ( $\pi = 0.5, R_0 = 3$ )



Note: Full sample results are based on the same samples as in Table 2. The subsample estimates are based on the sample Jan-22 to Feb-20, 2020.  $\rho_j, \gamma_j$  are country-specific as estimated in Table 2.

### 5.3 Estimation results for selected countries

Bearing in mind the preliminary nature of these estimates using a subsample that covers the first phase of the epidemic, we now provide estimates for a selected number of countries with at least 30 days of reported active cases. Specifically, we consider South Korea, Iran and a selected number of European countries (Spain, Italy, France, Germany, United Kingdom, Belgium, Switzerland, and Austria).<sup>13</sup> Additional countries can be included as the epidemic spreads and moves to its later stages in the rest of the world.

The estimates of  $\gamma$  and  $\rho$  for these countries are summarized in Table 5. Estimates of  $\gamma$  are generally lower than the ones we obtain for Chinese provinces, using the full sample, implying longer removal times. In some cases, they are also less precisely estimated. Nevertheless, these country estimates are remarkably close to the estimates we obtained in Table 4 for Chinese provinces, when

<sup>13</sup>The fitting of epidemic curves for the United States or its counties is hampered by the lack of data for recovered cases. Due to the absence of minimally reliable data on recoveries, JHU stopped reporting these statistics at the US state level on March 9, 2020. Given the large variation in social distancing policies across US states and counties, it would be misleading to report a country-wide estimate of  $\lambda$  for the country as a whole.

we used the subsample. It is therefore reasonable to conjecture that the mean estimate of  $\gamma$  across European countries and elsewhere will end up converging to the mean estimate of  $\gamma = 0.046$  that we have provided for China using the full samples.

The estimates of exposure rates,  $\lambda$ , for the selected countries are summarized in Table 6, with the left panel giving the estimates using country-specific estimates of  $\rho$  and  $\gamma$  from Table 5, and the right panel using the pooled estimate of  $\rho$  and  $\gamma$  from Chinese provinces, namely  $\hat{\rho}_{MG} = 1.0072$ ,  $\hat{\gamma}_{MG} = 0.046$ , which are arguably closer to their true values. This choice is driven by our belief that the pooled estimates based on the full set of data from Chinese provinces provide a more reliable benchmark for these parameter values for countries with advanced scientific and medical capabilities and are possibly less likely to be biased as compared to the MG estimate for the selected countries in Table 5.

As can be seen, there is a great deal of heterogeneity in the estimates of  $\lambda$  across the selected countries, partly reflecting differences in the mitigation policies adopted. However, most of these estimates are much larger than those obtained for Chinese provinces ex-Hubei. Strikingly, and unfortunately, these estimates are 3-6 times larger than in Hubei, reflecting a massive failure at learning from the Chinese earlier experience with firm and uniform social distancing. With the exception of Iran, South Korea, and Austria the estimates of  $\lambda$  for the European countries in our sample are all either comparable or much higher than estimates we have obtained for the Hubei province. In particular, Italy, Spain and Belgium stand out with the largest estimates, all more than multiple times as high as Hubei. Again, remarkably, even though less precisely estimated than in the case of Chinese provinces sub-samples, these estimates continue to be relatively precise. We therefore have confidence that, as more data will become available, a very precise estimate of the actual degree of social distancing adopted will be measurable from the data.

**Table 5** Estimated values of recovery rates ( $\gamma_j$ ) for a selection of countries

	$\hat{\gamma}_j$	(s.e.)	$\hat{\rho}_j$	(s.e.)	$\hat{\sigma}_i$	Sample	$T$
Spain	0.054	(0.0015)	1.000	.	.	25-Feb to 12-Apr	46
Italy	0.026	(0.0010)	1.000	.	.	20-Feb to 12-Apr	51
France	0.035	(0.0025)	1.000	.	.	26-Feb to 12-Apr	45
Germany	0.045	(0.0124)	1.023	(0.022)	0.15	24-Feb to 12-Apr	47
United Kingdom	0.016	(0.0006)	1.000	.	.	24-Feb to 12-Apr	47
Iran	0.007	(0.0171)	1.081	(0.020)	0.28	20-Feb to 12-Apr	51
Belgium	0.041	(0.0056)	1.003	(0.013)	0.05	02-Mar to 12-Apr	40
Switzerland	0.037	(0.0098)	1.039	(0.018)	0.20	28-Feb to 12-Apr	43
Austria	0.023	(0.0037)	1.077	(0.010)	0.27	28-Feb to 12-Apr	43
South Korea	0.022	(0.0071)	1.020	(0.010)	0.14	19-Feb to 12-Apr	52
MG estimate	0.031	(0.0043)					

Notes: Estimation is based on regression  $r_{j,t+1} = \rho_j r_{jt} + (\gamma_j \rho_j) i_{jt} + \varepsilon_{j,t+1}$ .

**Table 6:** Estimated values of exposure rate ( $\lambda_j$ ) per 100,000 population for a selection of countries ( $\pi = 0.5, R_0 = 3$ )

	Using country-specific estimates $\hat{\rho}_j, \hat{\gamma}_j$		Using pooled estimates $\hat{\rho}_{MG}, \hat{\gamma}_{MG}$	
	$\hat{\lambda}_j$	(s.e.)	$\hat{\lambda}_j$	(s.e.)
Spain	457.9	(256.9)	117.8	(19.5)
Italy	252.4	(153.8)	117.8	(12.7)
France	25.8	(4.6)	34.5	(5.5)
Germany	23.6	(1.7)	43.9	(6.6)
United Kingdom	47.2	(18.2)	79.6	(13.0)
Iran	0.8	(0.1)	17.3	(2.9)
Belgium	172.9	(52.7)	120.8	(20.9)
Switzerland	24.8	(1.5)	65.4	(10.9)
Austria	6.8	(0.3)	47.7	(6.9)
South Korea	1.6	(0.2)	5.5	(0.8)
MG estimate	101.4	(37.4)	65.0	(23.7)

Notes: Estimation is based on regression  $i_{j,t+1} = (i_{jt}^2/i_{j,t-1}) \rho_j^3 + \rho_j^2 \left( \frac{\gamma R_0}{\pi \lambda} \right) [i_{jt} i_{j,t-1} (1 - \gamma) - \rho_i i_t^2] + \varepsilon_{t+1}$ , using the same sample as in Table 3. The left part of this table reports results using country-specific estimates  $\hat{\rho}_j, \hat{\gamma}_j$ , and the right part of this table uses pooled estimates  $\hat{\rho}_{MG}, \hat{\gamma}_{MG}$  from Table 2

## 6 Conclusions

This paper makes two related contributions. At the theoretical level, it integrates social distancing policies in a standard SIR model in order to evaluate their impact on both the COVID-19 epidemic and the associated employment costs. The framework distinguishes between mandatory and voluntary isolation. Critically, it is shown with simulations that, while targeted mandated policies can be very useful in flattening the epidemic curve, voluntary policies are relatively ineffective. Self-isolation can affect the epidemic curve, but only when it is close to its peak. We also show that mandating social distancing is very effective at flattening the epidemic curve, but is costly in terms of employment loss. However, if targeted towards individuals most likely to spread the infection, the employment loss can be somewhat reduced.

At the empirical level, using JHU daily COVID-19 statistics corrected for measurement errors, the paper provides estimates of province-specific recovery ( $\gamma$ ) and exposure ( $\lambda$ ) rates in China and in a selected number of countries, and shows that the rate of exposure to COVID-19 was around 40 – 60 times higher in Hubei at the epicenter of the epidemic compared to the rest of China. We find a very high degree of effective isolation, stable over time, and homogeneous across Chinese provinces. In contrast, we document lower and more heterogeneous degrees of effective isolation across European countries, and the degree of effective isolation turns out to be the lowest in Italy and Spain with an exposure some five times larger than our estimate for Hubei province, the epicenter of the epidemic in China.

As more and more reliable data becomes available, extending the empirical analysis to the United States and its metropolitan areas, as well as other countries worldwide, is an essential area of further research.

A further challenge is to relate the elasticity of employment loss,  $\alpha$ , to the way social distancing policies are implemented, including intensive testing and contact tracing. These are important topics of current and future research.

## References

- Atkeson, A. (2020). What will be the economic impact of COVID-19 in the US? Rough estimates of disease scenarios. NBER Working Paper No. 26867, <https://doi.org/10.3386/w26867>.
- Barro, R. J., J. F. Ursua, and J. Weng (2020). The coronavirus and the great influenza pandemic: Lessons from the "Spanish flu" for the coronavirus's potential effects on mortality and economic activity. NBER Working Paper No. 26866, <https://doi.org/10.3386/w26866>.
- Berger, D. W., K. F. Herkenhoff, and S. Mongey (2020). An SEIR infectious disease model with testing and conditional quarantine. NBER Working Paper No. 26901, <https://doi.org/10.3386/w26901>.
- Chudik, A. and M. H. Pesaran (2019). Mean group estimation in presence of weakly cross-correlated estimators. *Economics Letters* 175, 101 – 105. <https://doi.org/10.1016/j.econlet.2018.12.036>.
- Correia, S., S. Luck, and E. Verner (2020). Pandemics depress the economy, public health interventions do not: Evidence from the 1918 flu. Available at SSRN: <https://ssrn.com/abstract=3561560> or <https://doi.org/10.2139/ssrn.3561560>.
- Diekmann, O. and J. Heesterbeek (2000). *Mathematical Epidemiology of Infectious Diseases: Model Building, Analysis and Interpretation*. John Wiley & Son, New York, ISBN: 0471986828.
- Eichenbaum, M. S., S. Rebelo, and M. Trabandt (2020). The macroeconomics of epidemics. NBER Working Paper No. 26882, <https://doi.org/10.3386/w26882>.
- Fang, H., L. Wang, and Y. Yang (2020). Human mobility restrictions and the spread of the novel coronavirus (2019-nCoV) in China. NBER Working Paper No. 26906, <https://doi.org/10.3386/w26906>.
- Ferguson, N., P. Walker, C. Whittaker, and et al (2020). Impact of non-pharmaceutical interventions (NPIs) to reduce COVID19 mortality and healthcare demand. Imperial College London COVID-19 Reports, Report No. 9, 16 March 2020, available at <https://doi.org/10.25561/77482>.
- Flaxman, S., S. Mishra, A. Gandy, and et al. (2020). Estimating the number of infections and the impact of nonpharmaceutical interventions on COVID-19 in 11 European countries. Imperial College London COVID-19 Reports, Report No. 13, 30 March 2020, <https://doi.org/10.25561/77731>.
- Gibbons, C. L., M.-J. J. Mangen, D. Plass, and et al (2014). Measuring underreporting and underascertainment in infectious disease datasets: a comparison of methods. *BMC Public Health* 14:147, 1471–2458. <https://doi.org/10.1186/1471-2458-14-147>.
- Harko, T., F. S. Lobo, and M. Mak (2014). Exact analytical solutions of the susceptible-infected-recovered (SIR) epidemic model and of the SIR model with equal death and birth rates. *Applied Mathematics and Computation* 236, 184–194. <https://doi.org/10.1016/j.amc.2014.03.030>.
- Kermack, W. O. and A. G. McKendrick (1927). A contribution to the mathematical theory of epidemics. *Proceedings of the Royal Society of London* 22(772), 700–721. <https://doi.org/10.1098/rspa.1927.0118>.
- Kucharski, A. J., T. W. Russell, C. Diamond, Y. Liu, J. Edmunds, S. Funk, and R. M. Eggo (2020). Early dynamics of transmission and control of COVID-19: a mathematical modelling study. *The Lancet Infectious Diseases*. [https://doi.org/10.1016/S1473-3099\(20\)30144-4](https://doi.org/10.1016/S1473-3099(20)30144-4).
- Li, Q., X. Guan, P. Wu, X. Wang, L. Zhou, Y. Tong, ..., and Z. Feng (2020). Early transmission dynamics in Wuhan, China, of novel coronavirus-infected pneumonia. *New England Journal of Medicine* 382(13), 1199–1207. <https://doi.org/10.1056/NEJMoa2001316>.

- Linton, O. (2020). When will the Covid-19 pandemic peak? Cambridge Working Papers in Economics CWPE2025, available at: <http://www.econ.cam.ac.uk/research-files/repec/cam/pdf/cwpe2025.pdf>.
- Metz, J. A. J. (1978). The epidemic in a closed population with all susceptibles equally vulnerable; some results for large susceptible populations and small initial infections. *Acta Biotheoretica* 27, 75–123. <https://doi.org/10.1007/bf00048405>.
- Moriarty, L., M. Plucinski, B. Marston, and et al. (2020). Public health responses to COVID-19 outbreaks on cruise ships - worldwide, February-March 2020. Morbidity and Mortality Weekly Report (MMWR), 26 March 2020, 69:347-352. <https://doi.org/10.15585/mmwr.mm6912e3>.
- Pesaran, M. H. and R. Smith (1995). Estimating long-run relationships from dynamic heterogeneous panels. *Journal of Econometrics* 68(1), 79–113. [https://doi.org/10.1016/0304-4076\(94\)01644-F](https://doi.org/10.1016/0304-4076(94)01644-F).
- Riou, J. and C. L. Althaus (2020). Pattern of early human-to-human transmission of Wuhan 2019 novel coronavirus (2019-ncov), December 2019 to January 2020. *Eurosurveillance* 25(4). <https://doi.org/10.2807/1560-7917.ES.2020.25.4.2000058>.
- Salje, H., D. A. Cummings, and J. Lessler (2016). Estimating infectious disease transmission distances using the overall distribution of cases. *Epidemics* 17, 10–18. <https://doi.org/10.1016/j.epidem.2016.10.001>.
- Satsuma, J., R. Willox, A. Ramani1, B. Grammaticos, and A. Carstea (2004). Extending the SIR epidemic model. *Physica A: Statistical Mechanics and its Applications* 336, 369–375. <https://doi.org/10.1016/j.physa.2003.12.035>.
- Stock, J. H. (2020). Random testing is urgently needed. Manuscript, available at: <http://www.igmchicago.org/covid-19/random-testing-is-urgently-needed/>.
- Wang, C., L. Liu, X. Hao, H. Guo, Q. Wang, J. Huang, ..., and T. Wu (2020). Evolving epidemiology and impact of non-pharmaceutical interventions on the outbreak of coronavirus disease 2019 in Wuhan, China. *medRxiv*. <https://doi.org/10.1101/2020.03.03.20030593>.

# The first weeks of the coronavirus crisis: Who got hit, when and why? Evidence from Norway<sup>1</sup>

Annette Alstadsæter,<sup>2</sup> Bernt Bratsberg,<sup>3</sup> Gaute Eielsen,<sup>4</sup> Wojciech Kopczuk,<sup>5</sup> Simen Markussen,<sup>6</sup> Oddbjørn Raaum<sup>7</sup> and Knut Røed<sup>8</sup>

Date submitted: 3 May 2020; Date accepted: 4 May 2020

*Using real-time register data we document the magnitude, dynamics and socio-economic characteristics of the crisis-induced temporary and permanent layoffs in Norway. We find evidence that the effects of social distancing measures quickly spread to industries that were not directly affected by policy. Close to 90% of layoffs are temporary, although this classification may change as the crisis progresses. Still, there is suggestive evidence of immediate stress on a subset of firms that manifests itself in permanent rather than temporary layoffs. We find that the shock had a strong socio-economic gradient, hit a financially vulnerable population, and parents with younger children, and was driven by layoffs in smaller, less productive, and financially weaker firms. Consequently though, the rise in unemployment likely overstates the loss of output associated with the layoffs by about a third.*

1 This article is part of the report from the research project “Temporary and permanent layoffs under Covid-19”. Thanks to the Norwegian Directorate of Labour and Welfare and Statistics Norway for supplying the registry data, to Trond Vigtel for assistance with the data, and to Maria Hoen for assistance with the linking of data from the O\*NET database to Norwegian occupation codes.

2 Norwegian University of Life Sciences.

3 Frisch Centre.

4 Norwegian Labor and Welfare Directorate.

5 Columbia University and CEPR.

6 Frisch Centre.

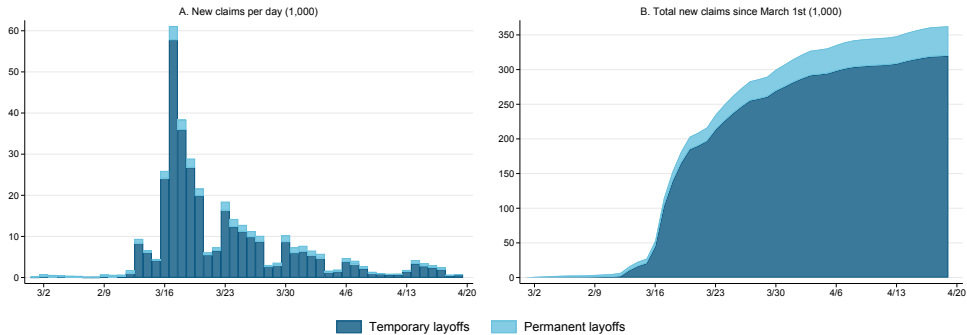
7 Frisch Centre.

8 Frisch Centre.

Copyright: Annette Alstadsæter, Bernt Bratsberg, Gaute Eielsen, Wojciech Kopczuk, Simen Markussen, Oddbjørn Raaum and Knut Røed

The coronavirus crisis hit fast all around the world. Its unprecedented nature and the response to it through social distancing led to massive reduction in economic activity. In Norway, where our data comes from, the measures were announced on March 12<sup>th</sup> and during the following few weeks 360,000 people (approximately 12% of the labor force) signed up for unemployment benefits, as Figure 1 demonstrates.

Figure 1: Unemployment benefits applications in Norway 3/1-4/19/2020



Note: Temporary and permanent layoffs refer to persons who have applied for unemployment benefits under the temporary or regular schemes of the UI program. Regular claims may include, in addition to dismissals, persons who have completed a fixed term employment contract. For each applicant we classify the person as temporarily or permanently laid off based on the latest filed application.

In the Norwegian context, workers filing for unemployment benefits may be laid off temporarily or permanently. Approximately 90 percent of the layoffs during the period covered here are temporary. That means that most of those applying for benefits retain employment relationships. There is, of course, a risk that temporary layoffs may turn into permanent layoffs later on. Berg et al. (2015), for example, shows that during the recession of 1993-95, about 15% of temporary layoffs did not return to the previous job. Previous studies also show that those exposed to unemployment during a temporary economic crisis have higher risk to be out of work in the longer term; see e.g. Yagan (2019).

On March 16, the Norwegian parliament agreed to change the rules for layoffs with immediate effect. Laid off workers will be paid full wages (up to an income limit of approximately NOK 600,000 — about USD 56,000) for the first 20 days. Afterwards, the benefits will be equal to 80% of income under NOK 300,000 and 62.4% for income between NOK 300,000 and 600,000. There is no compensation for lost income above NOK 600,000. Additionally, employers' responsibility for the first period of full pay was reduced from 15 to 2 days.

These changes in layoff regulations have been followed by additional crisis responses aimed at preventing bankruptcies, maintaining activity in municipalities and increased support for temporary training of laid off and unemployed.

We use almost real-time unemployment claims information linked to administrative registry data on past characteristics of individuals and firms to characterize which individuals and businesses were

most affected, how the effect unfolded over the first few weeks, and the role that policy played in the process.

In this article, we take a closer look at who was most affected by the crisis during the first few weeks, both by loss of work through temporary or permanent layoff, and by being exposed to infection risk through work with socially critical functions. The article delves into a research literature that has studied heterogeneous effects of economic crises; see, for example, Hoynes et al. (2012), who find that the financial crisis in the United States has particularly affected minority groups, youth, and those with low education. Studies from Germany, Britain and Norway have also shown that immigrants are particularly vulnerable to economic fluctuations (Dustmann et al, 2010; Bratsberg et al, 2010; 2018). However, the crisis we are facing now is unique, both in terms of how quickly it has occurred, how many are affected, and not least in its underlying origins. It is thus far from obvious that studies of previous economic fluctuations provide a good basis for assessing the distributional effects of the crisis we are currently experiencing.

This paper also contributes to emerging literature on the impact of the crisis on the labor market and it does so with real-time administrative data rather than relying on survey-based or partial industry-based information (see for example Adams-Prassl et al, 2020, Bartik et al 2020, and Coibion, Gorodnichenko and Weber, 2020).

We have six main findings. First, layoffs started in sectors of the economy directly affected by the policy measures but then quickly spilled over to the rest of the economy so that after 4 weeks 2/3 of layoffs are accounted for by businesses that were not directly targeted. Second, close to 90% of layoffs are temporary rather than permanent and while this classification may change as the crisis progresses, that is one glimmer of hope in the data. Third, while permanent layoffs are a minority, they still correspond to a 1.5 percentage point increase in unemployment — an unprecedented monthly change. Fourth, the layoffs have a strong socio-economic gradient and hit financially vulnerable populations. Fifth, there are hints of the important role of childcare — within firms, layoffs appear to be skewed toward workers with younger children, in particular toward women. Finally, layoffs are more common in less productive and financially weaker firms so that the employment loss may be overstating total output loss (although, the potential unobserved offsetting consideration is the possibility of underemployment of those that remained on the job).

## 1 The data

The primary database for this article is all individual unemployment benefit applications in Norway during the period from March 1<sup>st</sup> to April 19<sup>th</sup> 2020, with information on whether the applications concerned ordinary unemployment or temporary layoffs. This means that in practice the analysis will include wage earners, entitled to unemployment benefits. As the annual income limit for entitlement to unemployment benefit was lowered from approximately NOK 125,000 to NOK 75,000 in connection with the current crisis, some applicants are very low income. We do not have information on financial problems among self-employed persons and persons whose main income comes from contract work.

The population includes all persons residing in Norway as of January 1st 2019, and provides information about the employer (including industry), occupation, salary, previous income, education, age, sex, and country of birth, with links to spouse, children, and parents.

The employer has been identified on the basis of the so-called a-form, filed by all employers to the tax authority, in December 2019. The a-form includes information on occupation, current wages, and hours worked. Information on education is updated until October 2018, while information on previous income from all sources covers the period 1967-2017. The latter means that we can calculate total professional income so far in life quite precisely for the entire population.

As part of characterizing employees' occupations, we use information from O\*NET (see [www.onetonline.org](http://www.onetonline.org)), which, based on US data, provides a detailed description of the characteristics of various occupations. This information is then linked to the Norwegian standard for occupational classification (Hoen, 2016). In this article, one particular characteristic is of interest, namely the degree to which the job requires physical proximity to other people. Professions are described on a scale from 0 (do not work in the vicinity of others) to 100 (profession involves direct physical contact with others). This variable is standardized (in the US data), so that the average is equal to 0 and standard deviation is equal to 1.

Since our information on occupation and hourly wage is based on information somewhat back in time, some of the employed will be “misplaced.” This will happen for people who have switched jobs after December 2019. There are also some unemployment benefit applicants who cannot be matched to other data. This may be because they were not resident on January 1, 2019, or did not have a “normal” contract with an employer during 2019. Table 1 gives a more detailed description of the data. The analysis sample, described in column 1, consists of all wage recipients registered in 2019. Our data links enable us to capture a total of 330,492 of the 362,539 unemployment insurance applicants (91.2%) in the period in question; see columns (2) and (3). Among the approx. 32,000 applicants that we do not match, one half are not residents in the country as of January 1, 2019 (column 5). The rest fall out of our analysis because we cannot connect them to an employer in 2019 (column 4).

## 2 The Dynamics of the Crisis

Even though the crisis hit widely, it did not hit at random. In this section we look more closely at which employees had to bear the negative consequences in the first few weeks. We will first and foremost focus on who lost the job, through temporary or permanent layoffs. But we will also look at who might bear the brunt by continuing to work in jobs with the risk of incurring infection. This latter group consists of people in “socially critical” professions with a great deal of physical proximity to other people, such as health personnel, nursing and care staff, and staff in grocery stores.\*

Figure 2 shows the composition of layoffs by different types of policies. The initial measures requiring social distancing were announced on Thursday, March 12, and the layoffs responded immediately, with a big spike in claims immediately after the weekend on Monday March 16 when

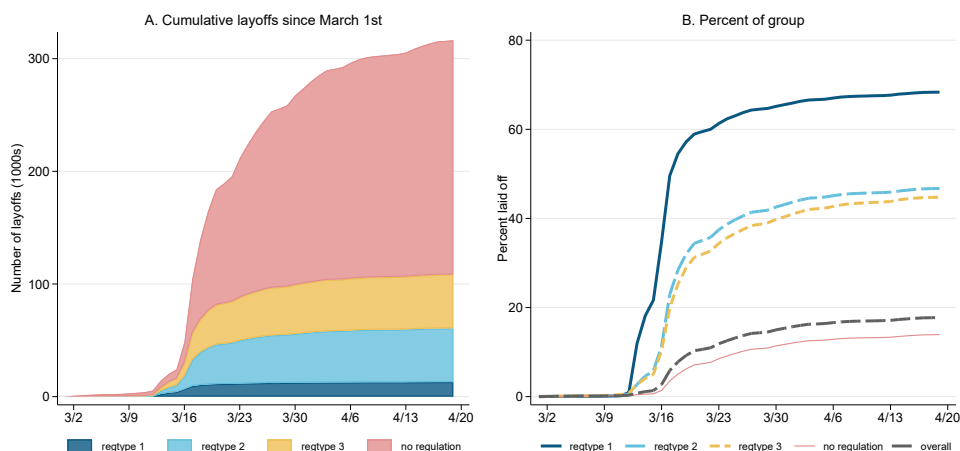
Table 1: Summary statistics

<i>Analysis sample</i>	UI benefit applicants 3/1 - 4/19/2020				
	<i>Analysis sample</i>	<i>Not included in analysis sample</i>			
	<i>Temporary layoff</i>	<i>Permanent layoff</i>	<i>Resident</i>	<i>Non resident</i>	
(1)	(2)	(3)	(4)	(5)	
Age	40.7	38.6	35.6	39.8	37.5
Female(%)	48.5	45.7	46.6	44.9	22.8
Norwegian-born(%)	82.7	75.7	65.6	74.8	7.6
Western Europe(%)	3.6	4.5	4.2	4.4	28.4
New EU country(%)	5.0	7.8	12.3	6.2	59.4
Other countries(%)	8.7	12.0	17.9	14.5	4.6
Education (years)	13.8	12.9	12.7	12.7	12.3
Income rank	56.1	52.6	41.4		
Hourly wage(NOK)	305.1	287.6	261.7		
Physical proximity index	0.307	0.275	0.474		
Observations	2,672,044	295,848	34,644	16,005	16,042

more generous rules (from both employee and employer's point of view) were announced.

We decompose this increase into four different categories. Group 1 includes individuals working in industries that were subject to the direct ban of activity (e.g., hairdressers, tattoo salons, bars). Group 2 includes workers of businesses that were subject to an implicit ban, typically from distancing restrictions (dentists, restaurants, etc), while Group 3 are workers of businesses that were subject to restrictions that prevented consumers from using those services, such as for hotels and airlines. Just 1% of workers were in Group 1, 5.7% in Group 2, 4.4% in Group 3, and 88.8% of workers were not subject to any direct regulation.

Figure 2: Layoffs by the type of restrictions

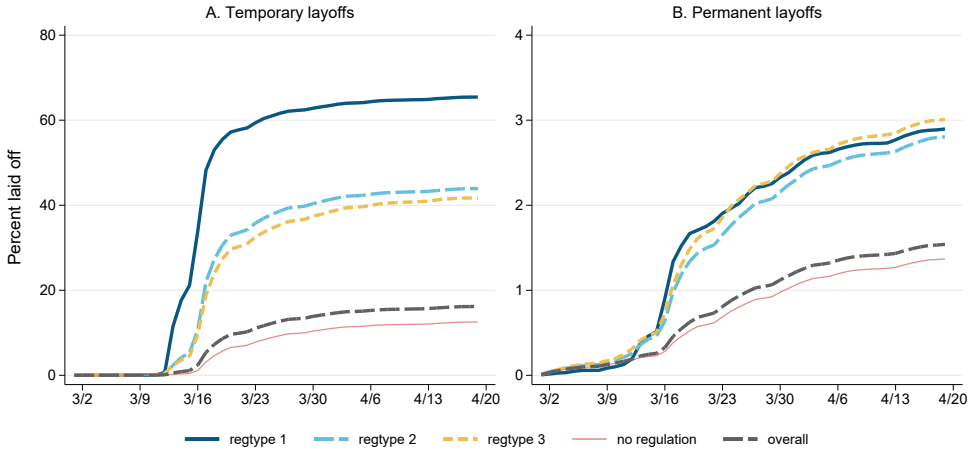


As a share of the group, layoffs in Group 1 were the largest, with close to 70% of the group laid off by the end of the period; the majority of them in the first few days. Groups 2 and 3 behaved similarly — a sizable immediate increase, a slower increase afterwards, reaching over 40% by the end of the period. These responses are not particularly surprising — they correspond to explicit or implicit restrictions on the activity. All three of these groups add up to a bit over 10% of employment but account for close to 1/3 of layoffs.

The remaining 2/3 of layoffs are accounted for by industries that did not face direct restrictions on their activity. Layoffs in that group were more spread out over time — they lagged layoffs in directly affected industries, but started building up a bit more gradually (although still with more than half of the layoffs over the whole period happening during the first week).

Figure 3 shows decomposition of layoffs into temporary and permanent ones. They do not follow the same time pattern — permanent layoffs build up more slowly over time. Of course, the size of the two groups is dramatically different. Permanent layoffs can be taken as a lower bound of employment ties that were severed permanently. In particular, the Norwegian system does not discourage temporary layoffs, so it is unlikely that permanent layoffs would revert to an employment relationship with the same employer at a later date. Viewed in that way, 1.5% of employment relationships in the whole economy ended permanently in the course of four weeks after March 12 — this would be a very large increase in unemployment at any time. In particular, a 1.5 percentage point increase is larger than any single month change in unemployment during the financial crisis.

Figure 3: Temporary and permanent layoffs by the type of restrictions



Speculating somewhat, permanent layoffs are likely to be revealing businesses in severe distress that are unlikely to survive the shock. One group of workers that may be permanently laid off are those on fixed term contracts that expire, but it is unlikely that they constitute the majority of the short-term effect. Otherwise, a permanent layoff in Norway requires the employer to pay severance, so that firms are expected to prefer temporary layoffs unless they are going bankrupt and this should be especially true at the time of a liquidity shock.

Figure 4: Layoffs by firm size and the type of restrictions

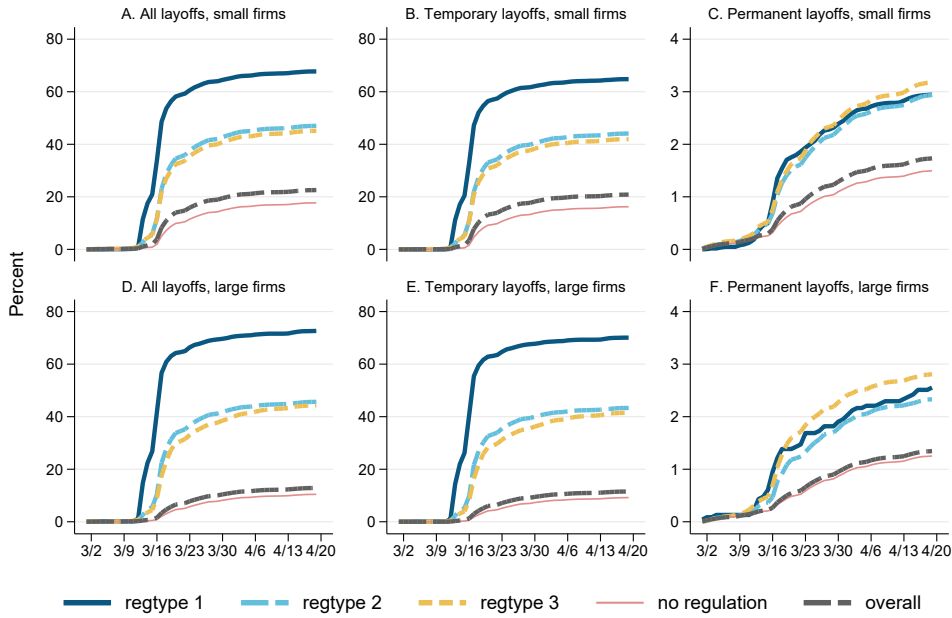
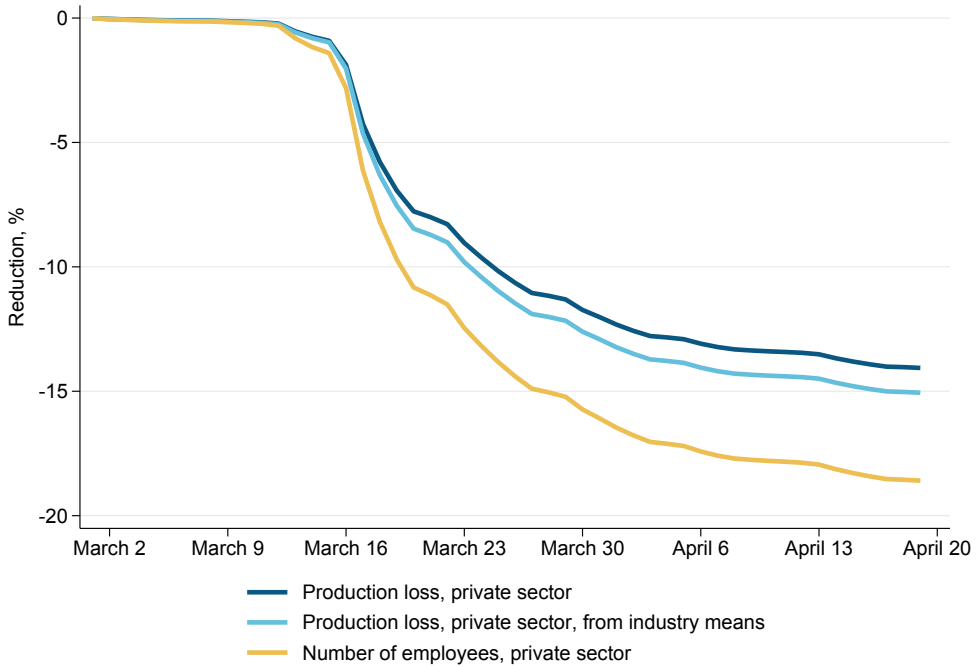


Figure 4 shows that the behavior of small and large firms (below/above the median of 63 employees) in industries affected directly by restrictions is quite similar, with about the same level of layoffs and their composition into temporary and permanent ones. The main difference between larger and smaller firms comes from the “no regulation” group in which small firms reacted much more strongly.

### 3 Production loss

How large is the magnitude of the shock in terms of lost output? While direct information on this is not yet available, we can provide a guess based on employment loss and measures of worker productivity. Worker productivity is measured as value added (profits plus total wage bill) per man-year. Figure 5 shows the production loss based on the assumption that all workers are equally productive, such that the percentage loss in production corresponds to that of employment (yellow line). This is likely an overestimate of the production loss because industries that are affected are likely less productive. Reweighting employment loss by the average industry-level productivity implies output loss of about 15% by the end of the period. Using a firm-specific measure of productivity allows for accounting for selection within industries. As expected (because less productive firms are more likely to lay off employees), it attenuates the effect somewhat further.

Figure 5: Production loss based on employment loss



Is change in labor employed a good proxy for production loss? Of course, this is not a prediction of the loss of output in general. It does not account for the fact that even workers who remain employed may be less productive than they would have been otherwise. Going in the other direction, in Norway workers may be laid off for a fraction of their time and some temporarily laid off workers may have returned to work by April 19. At this point, our data does not allow for observing that.

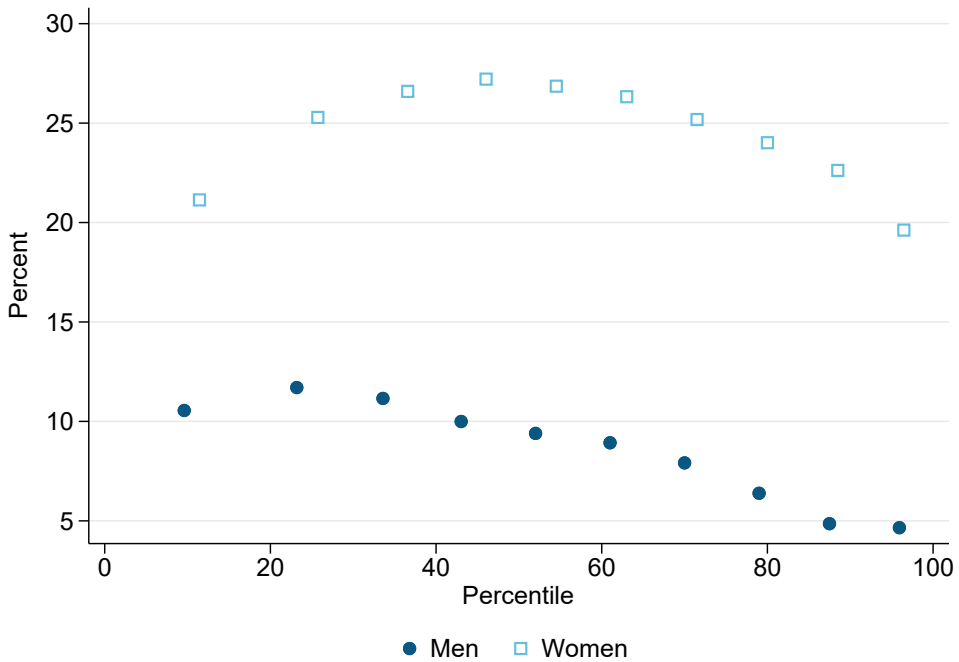
#### 4 The “social gradient” of the crisis

Figure 6 shows the incidence of socially critical risky work among all wage earners in Norway, based on their position in the age- and gender-specific distribution of total employment income throughout the professional career. Socially critical risky work is then defined as having a job of critical importance, in combination with a profession that requires physical closeness beyond the average in the whole economy. We divide the wage earners into ten equal groups by gender, according to their position in the age- and gender-specific income distribution.

The likelihood of holding an essential job with a high degree of physical proximity to others falls markedly with income levels, especially for men. There is also a remarkably large gender difference: Women are far more than men exposed to the combination of critical tasks and physical closeness

to others. As many as 24.5 percent of the female workers have such jobs, which is about twice the corresponding proportion for men.

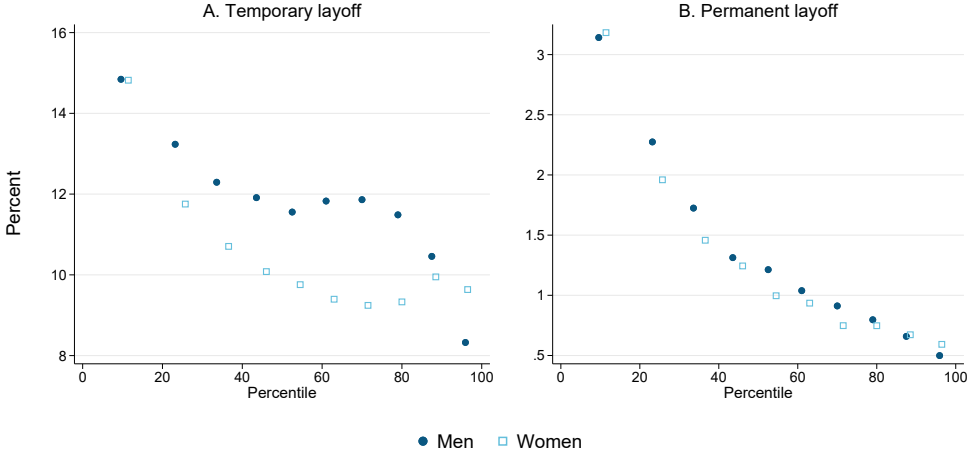
Figure 6: Share of employees in socially critical risk work, according to rank in age- and gender-specific distribution of lifetime income



Note: Critical function with a high degree of physical proximity is based on the coding of the ministries' list of personnel groups / positions covered by the exception to the main rule that children should be kept home from childcare and school to prevent the spread of infection, interacted with an indicator that the profession involves more physical closeness with others than the average. We have removed from this category 14,995 people classified as having an essential job, who were actually laid off or terminated in our data window. 63 percent of them come from one of the three professions salesperson in grocery / pharmacy / gas station, "other care worker," or bus and tram driver. The proportion with essential work with close physical proximity to others is 8.7 percent for men and 24.5 percent for women.

Figure 7 shows the extent of permanent and temporary layoffs for men and women by their position in the age and gender specific income distribution. We see that the likelihood of being hit by layoffs or termination falls sharply with income rankings. This social gradient is even more marked for permanent than for temporary layoffs. The probability of having permanently lost work during the first weeks of the coronavirus crisis is more than six times higher for people in the lower income deciles than at the top. The likelihood of being laid off is a little bit higher for men than for women.

Figure 7: Percentage of temporarily and permanently laid-off workers according to rank in age- and gender-specific distribution of lifetime income

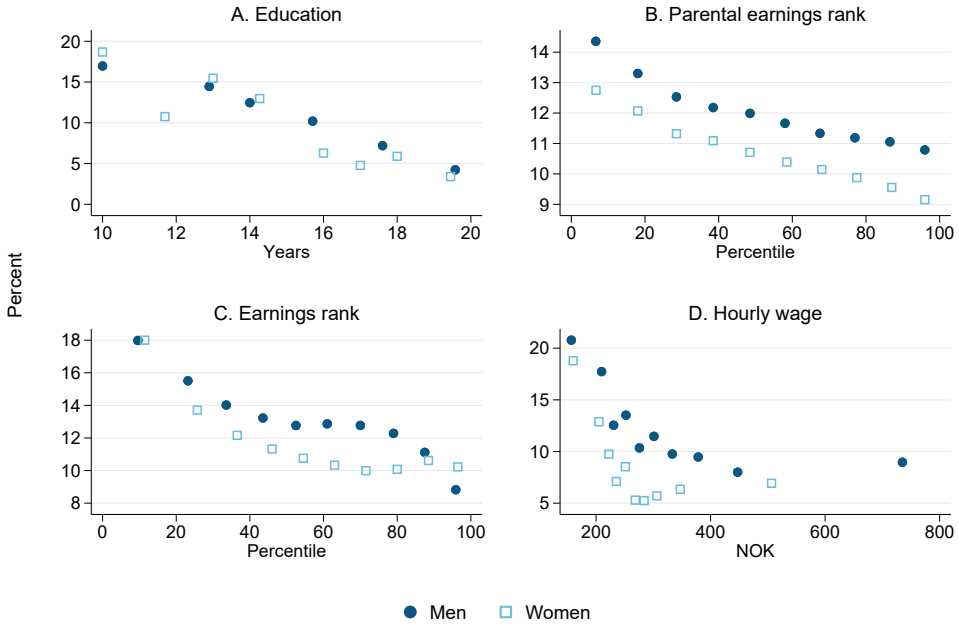


Note: The percentage of temporary layoffs in our data is 11.7 percent for men and 10.4 percent for women. Corresponding shares of permanent layoff are 1.3 percent for men and 1.2 percent for women. The income rank is based on lifetime income. It is calculated by summing up all income earned in the period 1967-2017 for all residents in Norway. Subsequently, all employees are divided into ten equal groups by ranking in the income distribution. This is done within each birth cohort and separately for men and women.

We will now take a closer look at who, in the period from March 1<sup>st</sup> to April 19<sup>th</sup>, lost the job on a temporary or permanent basis, and who applied for unemployment benefit. We will not separate between temporary and permanent unemployment benefits in what follows unless stated otherwise. The distinction between these two outcomes over the longer haul is not clear, as some of the temporary unemployed may end up being permanently dismissed

Figure 8 gives a broader idea of the socioeconomic composition of all the new claims during the first stage of the coronavirus crisis. We see that the social gradient is clear no matter how we capture socio-economic background. There is an overrepresentation among new unemployed people of low-income, low-education, and low hourly wages.

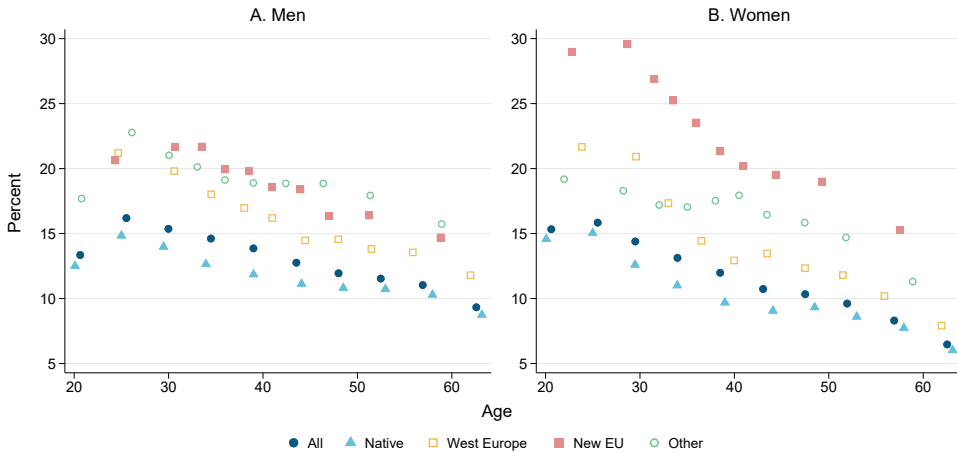
Figure 8: Layoffs by socioeconomic status



Note: Panel A shows the number of school years associated with the highest completed education on the horizontal axis. In panel B, the scale is the parent's income rank, and the location of the data points is determined by a division into 10 equal cells. Parents' income is measured at age 52-58 for all employees born before 1983, then the measurement window is shifted one year forward for each year the person is born after this. In Panel C, the income rank is based on their own "so far-in-life" professional income (up to 2017) and each birth cohort and gender are ranked separately. Both in panels B and C, the rankings were made within the entire population residing in Norway, while the division into 10 equal cells was made within the group of workers included in our analysis.

There is also a systematic pattern by age and country of birth. This is illustrated in Figure 9. There is a clear pattern that young people have been hit harder than the elderly, and that immigrants are more vulnerable than Norwegian-born.

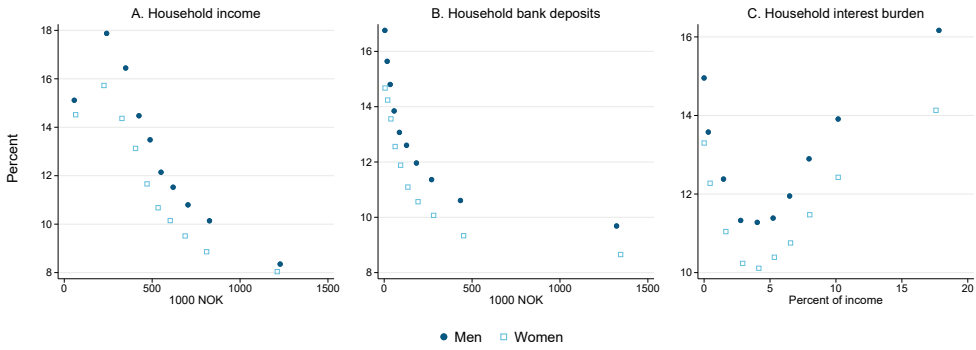
Figure 9: Layoffs by gender, age and country of birth



Note: Native includes children born in Norway by immigrant parents. In the group “Western Europe etc.,” Sweden, Germany and Denmark are the three largest country groups in the analysis sample. “New EU countries” includes countries with membership since 2004; Poland and Lithuania are the two largest country groups in the analysis sample. In the “Other” group, the Philippines, Thailand, Eritrea, Somalia and Iraq are the five largest country groups.

Within our data period, few wage earners have lost income during the crisis, since the laid off are secured full pay for the first 20 days up to an annual income of approximately NOK 600,000 (USD 56,000). However, if the crisis persists, there is a risk of significant loss of income for the laid-off and their families. The ability of families to manage a period of reduced (or lost) income will depend on how much income they used to have and access to liquid financial reserves. Figure 10 shows clear indications that the likelihood of being laid off or dismissed is higher for less financially secure households. This pattern is most clearly seen in panel A (household income) and B (the size of bank deposits), but there is also a clear systematic pattern when we look at the household’s interest burden relative to income. Those with the greatest interest burden are at the highest risk of being laid off or terminated. The U-shape is due to the fact that many people with particularly low financial resources also do not have debt, primarily because a large proportion of them do not own their own housing.

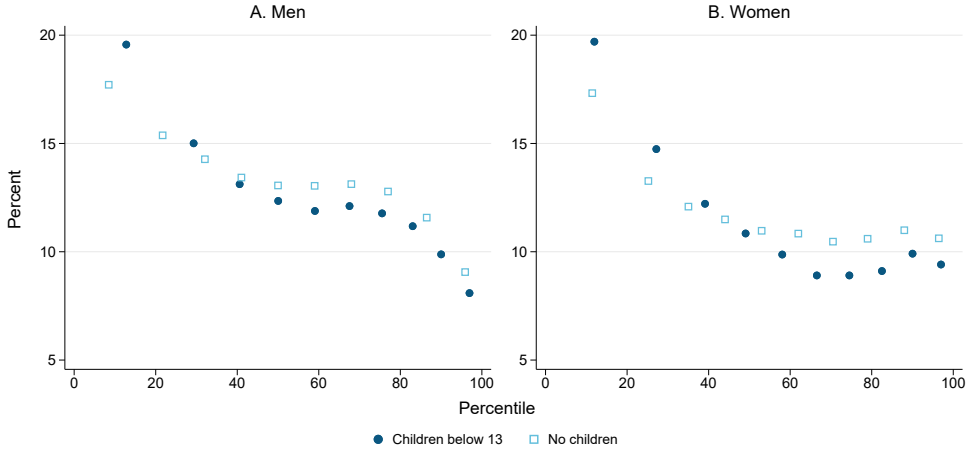
Figure 10: Layoffs by household income and total bank deposits



Note: Household income is adjusted for family composition (household income divided by the square root of the number of family members) .

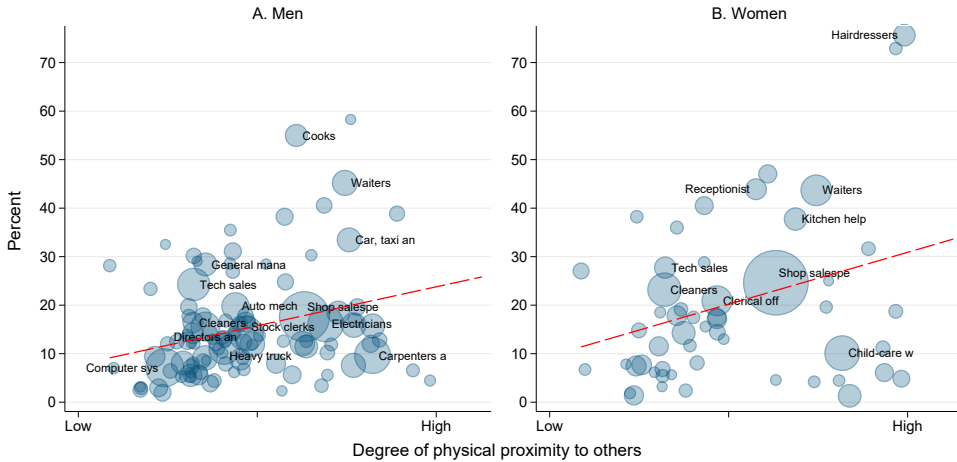
Having children is another important dimension of socioeconomic differences between families, both because of the implications for the behavior of parents and because of the potential of adverse outcomes for children. Figure 11 illustrates that families with children experienced a little bit higher rate of layoffs at the bottom of the distribution and a bit lower at the top. Figure 11 focuses on children under 13, because this is a group for which childcare considerations are very important. The interaction of the crisis with childcare is complex — on one hand, school closures have an obvious consequence of creating a childcare crisis as well. The crisis package in Norway adjusted the care benefit parents normally receive to look after their sick children to fit the current circumstances. The days were doubled for each parent, there was no requirement of the child being sick, and it allowed parents to transfer the days to the other parent in cases where one parent had socially critical work. This alleviated this problem somewhat. However, laid off workers by definition are not the ones that used the care benefit. At the same time, workers that can work from home have a (costly, but still) ability to take care of their own children while continuing to work. These considerations may be contributing to a different direction of the effect for lower and higher income individuals.

Figure 11: Layoffs depending on the presence of a child under 13 at home. By position in the age- and gender-specific lifetime earnings distribution



The discussion so far makes it clear that layoffs are strongly associated with a number of socioeconomic characteristics and result in a “social gradient” of the crisis. The social gradient mainly arises as a result of the underlying social gradient in the professional structure in Norway. The first phase of the coronavirus crisis affected people in occupations involving close physical contact with other people, but without essential jobs. This pattern follows, to some extent, directly from the authorities’ decision to close or restrict some types of businesses that involve the risk of spreading the virus, such as hairdressing salons and restaurants. The result of this is shown in Figure 12, where we show the proportion of laid-off workers by occupation, with occupations placed on the horizontal axis according to the extent to which they involve physical proximity with other people. The size of each data point is proportional to the size of the occupational group in our data, and for some of the largest occupational groups we have applied a professional designation in the figure. Figure 12 illustrates a clear positive correlation between physical proximity in the profession and the proportion of layoffs among both women and men.

Figure 12: Layoffs by occupation and the profession’s tendency to involve physical proximity with others



Note: Physical proximity at work is based on information provided by O\*NET; see further description in section on data. The data is limited to occupations in the private sector; occupation - gender combinations with fewer than 2,500 individuals are excluded from the figure. The figures also show the regression fit of industry-gender-specific unemployment claims on physical proximity, weighted by the number of workers in the occupation. The regression coefficient is 3.73 [0.69] for men and 4.97 [0.83] for women.

Do industry and occupation specific impacts fully account for the presence of the gradient? We investigate this question by regressing the likelihood of layoffs on individual characteristics and a set of progressively more detailed fixed effects in Table 2. The sample is restricted to private sector employees only. Without accounting for any firm or occupational characteristics, the multivariate analysis confirms the relevance of education and hourly wage. It also indicates that younger workers and those with shorter tenure were more strongly affected. There is an indication here that women were more affected (this is in contrast to Figure 7 that includes both public and private sector employees), and so were parents. Adding occupational or industry fixed effects attenuates gender, education, tenure and wage effects, but they remain statistically significant. Accounting for industry or occupation characteristics flips the sign of the age effect, suggesting that within industries or occupations it may be older workers that are more strongly affected, for a given tenure. Firm and combined firm and occupation effects attenuate most of these further somewhat.

An intriguing finding is the effect of having young children that remains almost unaffected once firm and job fixed effects are controlled for. Furthermore, while the gender difference for those without children disappears, the gender interaction with children becomes stronger. Once firm and occupational differences are accounted for, the gender effect is only associated with the presence of young children: women with young children are more likely to be laid off and this is a within-firm and within-occupation effect. This potentially points to the employers accounting for childcare in making layoff decisions, either unilaterally or in cooperation with employees who may prefer

temporary layoff in the presence of childcare obligations. It may also reflect employers’ belief that the productivity of female workers would be most strongly affected by child care obligations due to school and kindergarten closures, although it remains puzzling why temporary layoffs rather than the adjusted care benefit would be used.

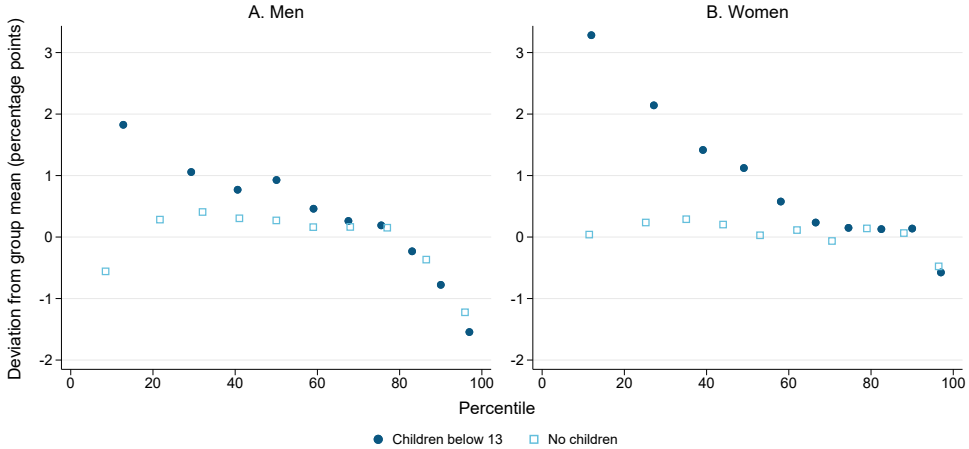
Table 2: Socio-economic characteristics and layoffs. Private sector.

	(1)	(2)	(3)	(4)	(5)
	OLS	Fixed Effects			
		Occupation	Industry	Firm	Firm and occupation
Female	5.246*** (0.345)	1.264*** (0.209)	0.518*** (0.156)	0.348*** (0.125)	0.158 (0.107)
Child under 13	1.012*** (0.134)	1.016*** (0.108)	1.102*** (0.106)	0.908*** (0.0901)	0.844*** (0.0874)
Female and child under 13	0.103 (0.232)	0.800*** (0.178)	1.346*** (0.163)	1.256*** (0.159)	1.242*** (0.154)
Age	-0.0265** (0.0108)	0.0317*** (0.00755)	0.0644*** (0.00660)	0.0495*** (0.00590)	0.0490*** (0.00608)
Education (years)	-1.106*** (0.0559)	-0.343*** (0.0255)	-0.357*** (0.0249)	-0.122*** (0.0180)	-0.0882*** (0.0174)
Tenure	-0.185*** (0.0246)	-0.143*** (0.0160)	-0.124*** (0.0130)	-0.103*** (0.00994)	-0.0967*** (0.00966)
Log hourly wage	-4.649*** (0.275)	-3.114*** (0.182)	-2.366*** (0.165)	-1.147*** (0.122)	-1.038*** (0.119)
N	1723833	1723833	1723833	1723833	1723833
# Fixed effects		349	571	149963	149963+349
R <sup>2</sup>	0.020	0.129	0.184	0.434	0.439

Note: The sample is restricted to private sector workers. Dependent variable is an indicator variable set to 100 if laid off between 3/1 and 4/19. The sample mean of the dependent variable is 18.1%. Standard errors are clustered within firms and reported in parentheses. Significance level of 1% is denoted by \*\*\*, 5% by \*\* and 10% by \*.

Figure 13 illustrates that this gender and parental effect is not an artifact of the choice of controls. It shows the deviation of the likelihood of layoffs from firm-specific means (residuals from regression of the layoff indicator on firm fixed effects) for men and women, separately for those with and without children under 13. The effect of having a child under 13 is stronger for women than for men and in each case it is driven by workers at the bottom of the distribution.

Figure 13: Within-firm relationship between having children under 13 and layoffs. By position in the age- and gender-specific lifetime earnings distribution

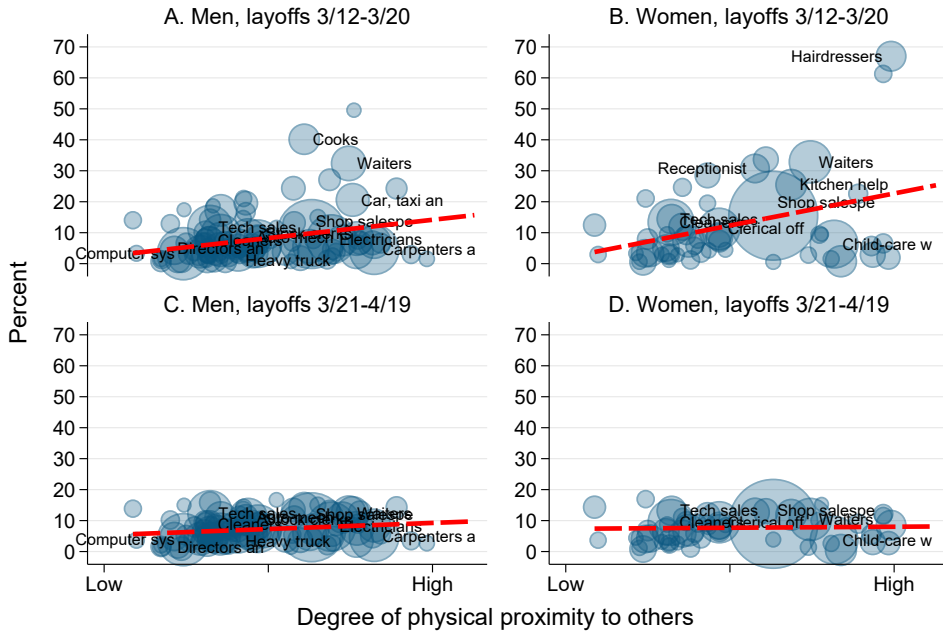


Note: The Figure shows the average residuals from regression of layoff indicator on firm fixed effects and should be interpreted as a deviation from firm-specific layoff rate.

## 5 The driving forces behind lay off decisions

The relevance of physical proximity for layoff decisions is natural, but it masks the dynamics that these considerations played. As Figure 14 demonstrates, this association applies to the immediate effect of the lockdown measures. The top panels show the relationship during the first 9 days after lockdown measures were introduced, the bottom ones show it in the weeks that followed. The association is much stronger in the initial weeks. A one standard deviation increase in physical proximity requirements of an occupation is associated with a very significant 2.75 percentage point increase in layoffs for men (t-stat of over 5) and 4.82 percentage point increase for women (t-stat of over 6). The effect weakens afterwards to 0.92 for men (still significant with t-stat of 4) and a small and insignificant one for women. While physical proximity plays a large role in the initial impact, it becomes less of a factor over time, suggesting the presence of spillovers to other parts of the economy.

Figure 14: Layoffs by occupation and the profession’s tendency to involve physical proximity with others, over time

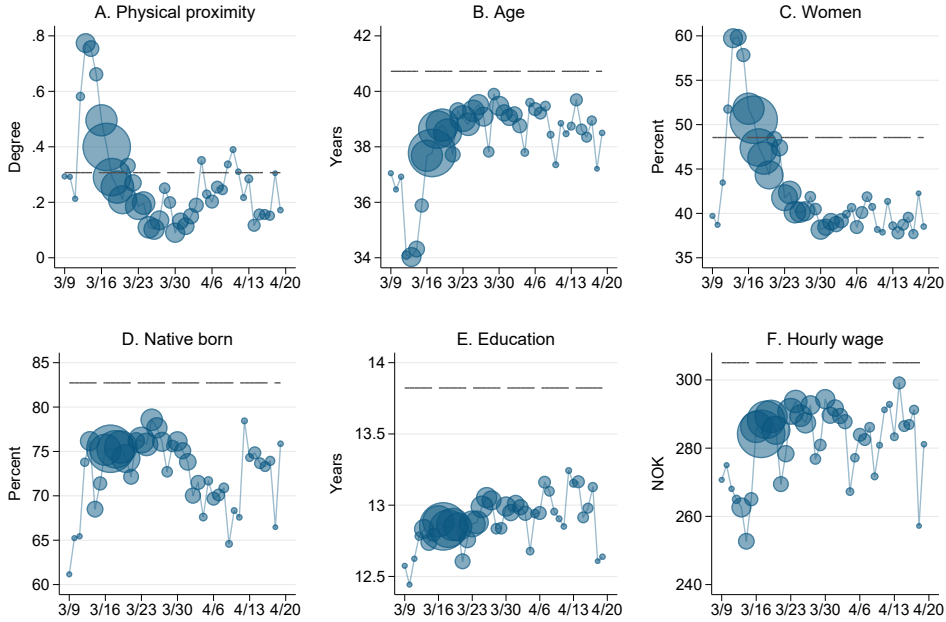


Note: See Figure 12. The regression coefficients are 2.75 [0.50] and 0.92 [0.23] for men and 4.82 [0.67] and 0.15 [0.23] for women.

As the economic crisis spreads both internationally and through the economy through falling demand for goods and services from the first affected businesses, we expect jobs with low physical proximity and contagion risk to be affected as well. This is also what we find in the data. In Figure 15 we visualize how the composition of the new unemployment insurance applicants has changed day by day after the layoff wave took off in earnest on Friday 13 March. While physical proximity was a driving factor in the early days, the importance of this was greatly diminished in just a few days. As the crisis spread through the economy, we also see that the average age is increasing and the proportion of women is falling. In particular, while in the first few days of the crisis layoffs were skewed toward females, this initial effect reversed quickly and by the end of the period more men than women were laid off altogether.

When it comes to indicators of the social gradient, the picture is more mixed, and the variations from day to day are rather moderate (note the scales on the vertical axes). We still see signs that the average hourly wage among the laid-off increased somewhat during the first week. For all socio-economic indicators, the affected individuals fall below the mean of the characteristic in the analysis sample.

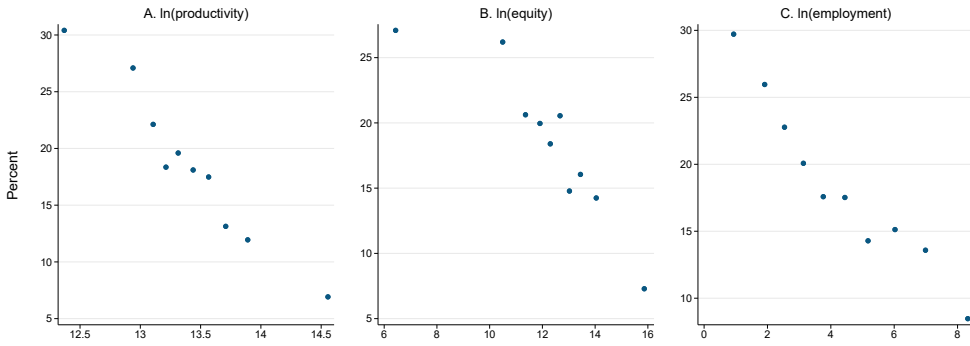
Figure 15: Characteristics of laid-off workers - day by day 3/3-4/19



Note: The size of the circles is proportional to the number of layoffs on each day. The definitions of “physical proximity at work” are described in more detail in the section on databases. See also note to Figure 8. The figures also show the mean value of each characteristic as a dashed line.

Which firms responded most strongly? Figure 16 shows the relationship between layoffs and a set of firm characteristics: productivity, equity and employment. In each case there is a very strong negative relationship between these proxies for the strength of a firm and layoffs.

Figure 16: Characteristics of firms and layoffs



Note: Each point corresponds to a decile of the distribution. Productivity is measured by value added. Employment represents the number of full-time equivalent workers.

Table 3 shows that this association is strong and statistically significant and it persists even within industries.

Table 3: Characteristics of firms and layoffs

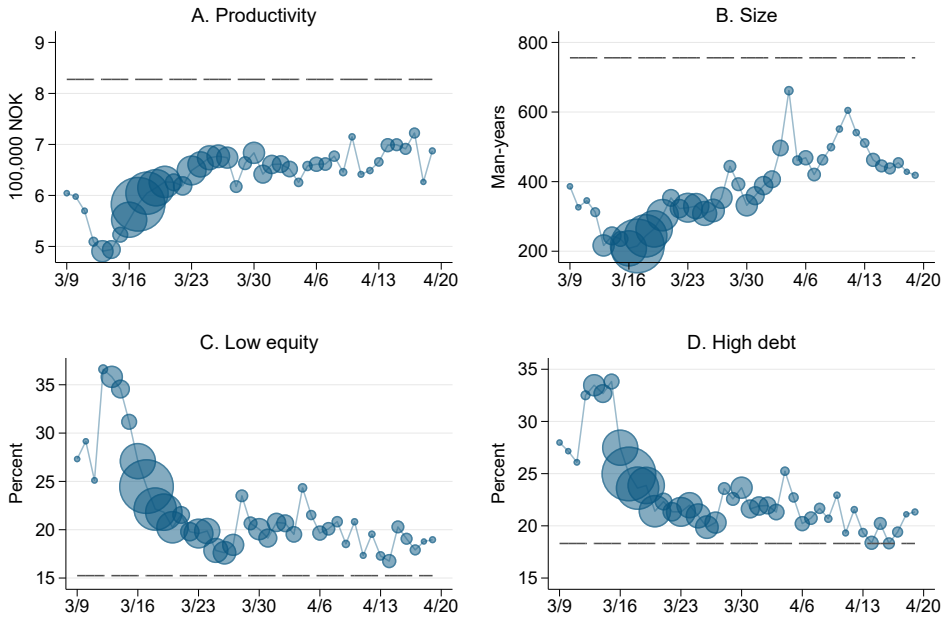
	(1)	(2)	(3)	(4)
	OLS	Industry FE	OLS	Industry FE
Log productivity	-10.13*** (0.54)	-3.86*** (0.39)	-6.90*** (0.61)	-3.00*** (0.38)
Log equity per worker			-1.17*** (0.20)	-0.74*** (0.17)
Log employment (No. FTE)			-2.13*** (0.21)	-1.52*** (0.14)
N	1,415,131	1,415,131	1,343,602	1,343,602
R-sq	0.023	0.169	0.040	0.176
#Industry FE		536		532

Note: The sample is restricted to private sector workers working for firms that can be linked to the 2017 accounting data. Dependent variable is an indicator set to 100 for workers laid off between March 1<sup>st</sup> and April 19<sup>th</sup>. Productivity is calculated as operating profit plus labor costs divided by the number of man-years, where man-years are calculated on the basis of a-forms filed in 2019 and accounting figures are based on the annual accounts for 2017. Employment is measured as the number of man-years (FTE) and calculated from a-forms filed in 2019. Standard errors are clustered within firms and reported in parentheses. Significance level of 1% is denoted by \*\*\*, 5% by \*\* and 10% by \*.

Figure 17 shows a timeline focusing on the characteristics of the companies that are laying off employees. In Panel A we see that the problems affect companies with higher and higher labor productivity (measured by total wages and profits per full-time equivalent), in Panel B that they affect larger and larger companies, and in Panels C and D that fewer and fewer of the laid-off

workers come from companies with low equity and high debt.

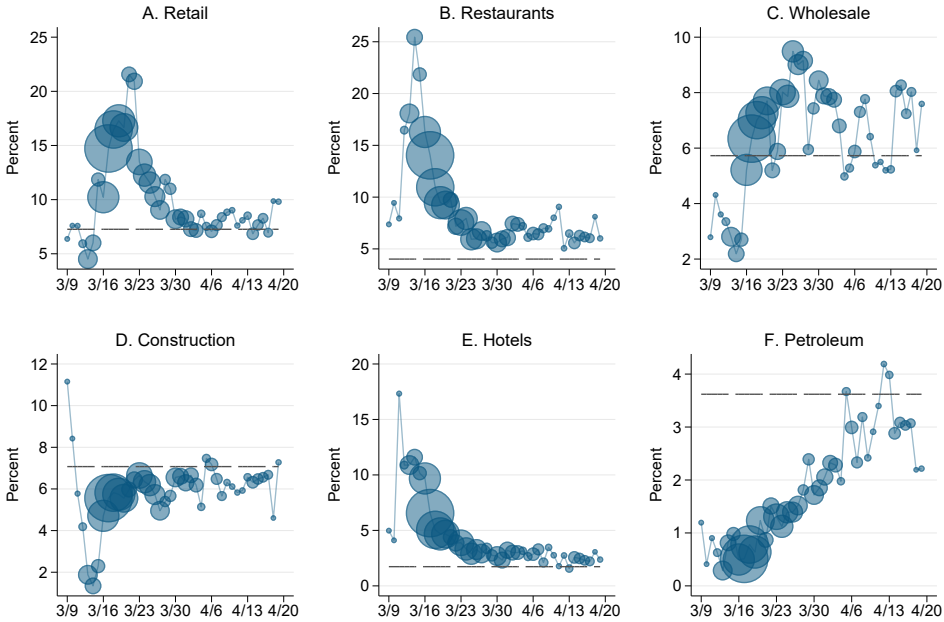
Figure 17: Characteristics of private-sector enterprises laying off workers - day by day in the period 3/3-4/19



Note: The size of the circles is proportional to the number of layoffs on each day. In Panel A, productivity is calculated as operating profit plus labor costs divided by the number of man-years, where man-years are calculated on the basis of a-forms in 2019 and accounting figures are based on the annual accounts for 2017. In panel B, the number of man-years is calculated from a-forms filed in 2019. In Panel C, low equity is defined as equity below NOK 40,000 per full-time equivalent. In Panel D, high debt is high debt defined as debt that exceeds eight times equity. The figures also show the mean value of each characteristic as a dashed line.

Figure 18 shows the extent of layoffs in selected industries, affected by the crisis in very different ways. Hotels and restaurants were among the first industries directly affected, and during the first days they accounted for 30-35% of the new unemployment benefit applications. In just over a week, this percentage dropped to about 10%. Soon after, layoffs in the retail sector followed. They were accompanied by layoffs among wholesalers that then continued in the following weeks. Layoffs in construction were not as important initially, but then continued at a level about proportional to the industry share. It appears that the petroleum industry has been more indirectly affected by a dramatic fall in oil prices than the domestic response to the crisis, as indicated by the absence of extensive layoffs during the first weeks of the crisis. The sector accounted for only 0.7% of new unemployment claims during the initial nine days of the crisis, and 1.8% of all layoffs between March 21 and April 19.

Figure 18: Layoffs in different industries over time



Note: The petroleum industry with 3.6 percent of total private-sector employment comprises extraction of crude oil and natural gas, drilling and other services related to extraction, construction of platforms and modules, furnishing and installation work and supply bases. The horizontal line represents the share of employment accounted for by a given industry

## 6 Summary and conclusion

The coronavirus crisis struck broadly, but not randomly. There are clear systematic patterns in which workers are most affected. The public sector is so far shielded from layoffs, but there are many public employees in socially critical and risk-exposed professions, especially in the health and care sectors. Here, women are far more exposed than men, and people with low incomes are more exposed than those with high incomes.

Among all employees, we find that the risk of layoffs or dismissals during the first phase of the crisis is higher the lower the education, income, hourly wage and social class background of an employee. While initially, women bear the brunt of the layoffs due to their over-representation in sectors explicitly targeted by social distancing policy measures, over time this effect was more than offset as the rest of the economy responded. Males are more exposed to layoffs than women, because more men work in the private sector. Within the private sector, the gender effect is associated with the presence of young children: women with young children are more likely to be laid off comparing workers within the same firm and occupation by means of fixed effects. This

points to the importance of childcare in understanding the labor market impact of the crisis (see also Dingel, Patterson and Vavra, 2020).

As the crisis spreads, both internationally and across sectors domestically, we see signs that unemployment seekers are coming from ever-increasing occupations in the private sector. The companies that are laying off have also changed over time. While industries such as tourism and businesses with low productivity and equity dominated the first few days, we see a trend towards more “average” businesses being affected.

The Norwegian context is also useful in judging the extent to which the crisis is expected to be permanent. In the short term, about 1/10th of layoffs are classified as “permanent” and correspond to severing employment relationships. The remaining layoffs are temporary. While the incentives to lay off workers permanently are not strong even for firms in distress, as temporary layoffs may be converted to permanent later on and permanent layoffs may trigger severance obligations, this decomposition gives at least some reasons for hope that the great majority of layoffs in countries where this choice is not as easily available (such as the US) may in fact be reversible.

## References

Adams-Prassl, A., Boneva, T., Golin, M., and Rauh, C. (2020) Inequality in the Impact of the Coronavirus Shock: Evidence from Real Time Surveys, IZA Discussion Paper 13183.

Bartik, A., Bertrand, M., Lin, F., Rothstein, J., and Unrath, M. (2020) Labor Market Impacts of COVID-19 on Hourly Workers in Small- and Medium-Sized Businesses: Four Facts from Homebase Data., Online at <https://irle.berkeley.edu/labor-market-impacts-of-covid-19-on-hourly-workers-in-small-and-medium-sized-businesses-four-facts-from-homebase-data-2/>, accessed on 4/30/2020.

Berg, H., Larsen, K. A., Klingenberg, S., og Solheim, Ø. B. (2015) Permitteringer og avgang fra arbeidslivet. Rapport 2015-007 Proba samfunnsanalyse.

Bratsberg, B., Raaum, O., and Røed, K. (2010) When Minority Labor Migrants Meet the Welfare State. *Journal of Labor Economics*, Vol. 28, No. 3, 633-676.

Bratsberg, B., Raaum, O., and Røed, K. (2018) Job Loss and Immigrant Labor Market Performance. *Economica*, Vol. 85, 124-151.

Coibion, O., Gorodnichenko, Y., and Weber, M. (2020) Labor Markets During the COVID-19 Crisis: A Preliminary View, NBER Working Paper No. 27017.

Direktoratet for samfunnsikkerhet og beredskap (2016) Samfunnets kritiske funksjoner. HR 2350.

Dingel, J., Patterson, C., and Vavra, J. (2020) Childcare Obligations Will Constrain Many Workers When Reopening the US Economy. Becker Friedman Institute for Economics at University of Chicago, Working Paper 2020-46.

Dustmann, C., Glitz, A., and Vogel, T. (2010) Employment, Wages, and the Economic Cycle: Differences between Immigrants and Natives. *European Economic Review*, Vol 54, No. 1, 1-17.

Hoen, M. (2016) Occupational crosswalk, data and language requirements. Working Paper 1/2016. The Ragnar Frisch Centre for Economic Research.

Hoynes, H. Miller, D. L., and Schaller, J. (2012) Who Suffers During Recessions? *Journal of Economic Perspectives*, Vol. 26, No. 3, 27-48.

NAV (2020) Statistics on unemployment insurance applications. Updated daily at 10am on <http://www.nav.no>.

Yagan, D. (2019) Employment Hysteresis from the Great Recession. *Journal of Political Economy*, Vol. 127, No. 5, 2505-2558.

# Pandemic recession: L-shaped or V-shaped?<sup>1</sup>

Victoria Gregory,<sup>2</sup> Guido Menzio<sup>3</sup> and David Wiczer<sup>4</sup>

Date submitted: 29 April 2020; Date accepted: 1 May 2020

*We develop and calibrate a search-theoretic model of the labor market in order to forecast the evolution of the aggregate US labor market during and after the coronavirus pandemic. The model is designed to capture the heterogeneity of the transitions of individual workers across states of unemployment, employment and across different employers. The model is also designed to capture the trade-offs in the choice between temporary and permanent layoffs. Under reasonable parametrizations of the model, the lockdown instituted to prevent the spread of the novel coronavirus is shown to have long-lasting negative effects on unemployment. This is so because the lockdown disproportionately disrupts the employment of workers who need years to find stable jobs.*

1 Any views expressed are those of the authors and not those of the U.S. Census Bureau. The Census Bureau's Disclosure Review Board and Disclosure Avoidance Officers have reviewed this information product for unauthorized disclosure of confidential information and have approved the disclosure avoidance practices applied to this release. This research was performed at a Federal Statistical Research Data Center under FSRDC Project Number 1819. Delegated Authority Number: CBDRB-FY19-P1819-R8293. The authors are grateful to Gianluca Violante for sharing some data, and to Zach Bethune, Dirk Krueger, Iacopo Morchio, Venky Venkateswaran for comments.

2 NYU Department of Economics.

3 NYU Department of Economics.

4 Stony Brook University Department of Economics.

Copyright: Victoria Gregory, Guido Menzio and David Wiczer

# 1 Introduction

In March 2020, the US entered a “lockdown” so as to prevent the spread of the novel coronavirus. The vast majority of residents of the United States have been ordered to stay at home. Most retail businesses have been ordered to shut down. Most workers have been ordered to stay away from their place of work. Not surprisingly, during March and April of 2020, the number of claims for unemployment benefits has sky-rocketed, exceeding in two months only the total from the entirety of the Great Recession. Is the enormous number of workers entering unemployment going to flow back into the ranks of the employed once the lockdown restrictions are lifted? Or are these workers going to remain unemployed long after the lockdown is removed? In this paper, we develop and quantify a framework to analyze and forecast the evolution of the labor market during and after the coronavirus pandemic. We find that, under reasonable parametrizations of the model, even a 3-month long lockdown is going to have long-lasting negative effects on unemployment.

Our framework is a search-theoretic model of the labor market in the spirit of Pissarides (1985) and Mortensen and Pissarides (1994). Workers endogenously transition across states of employment and unemployment, as well as from one employer to another. Workers search for jobs when they are unemployed. Workers search for more productive jobs when they are employed, albeit with a lower intensity. Workers move from employment into unemployment when their productivity falls below some threshold. If the productivity is low for transitory reasons, some workers and firms may suspend production but maintain the option of resuming it, albeit at some cost and imperfectly. As in Gregory, Menzio and Wiczer (2020), workers are ex-ante heterogeneous with respect to their baseline productivity, the distribution of the component of productivity that is idiosyncratic to their match with a particular employer, and with respect to their ability to search the labor market. The search process that brings workers and vacant jobs into contact is directed by wages, as in Moen (1997) and Menzio and Shi (2011).

According to our model, the lockdown—which we describe as a temporary decline in labor productivity—causes some employment relationships to be terminated, some to be suspended, and others to continue. Intuitively, terminated relationships are those in which the surplus becomes negative because of the lockdown. Continuing and suspended relationships are those in which the surplus remains positive in spite of the lockdown. A relationship is suspended rather than continued if its productivity during the lockdown is low enough that the firm and the worker prefer collecting unemployment benefits rather than continuing production and maintaining strong ties.

Once the lockdown is lifted, the speed of the recovery, depends on three factors: (i) the fraction of workers who, at the beginning of the lockdown, enter unemployment while maintaining a relationship with their employer; (ii) the rate at which inactive relationships dissolve during the lockdown; (iii) the rate at which workers who, at the end of the lockdown, are not recalled by their previous employer can find new, stable jobs. In turn, factors (i) and (ii) depend on the costs associated with maintaining and reactivating a temporarily inactive relationship, on the ability of the employer to survive the lockdown without revenues, and on the rate of decay in the quality of a temporarily inactive relationship. Factor (iii) depends on the job-finding rate of the non-randomly selected group of workers who are permanently laid off during the lockdown.

Depending on parameters, the model can generate either a V-shaped recession—one in which the

unemployment rate quickly returns to its baseline level once the lockdown restrictions are lifted—or an L-shaped recession—one in which the unemployment rate takes several years to return to its pre-lockdown level. As a matter of theory, a V-shaped recession occurs if: (a) workers who enter unemployment are in a suspended relationship with their previous employer and maintain it throughout the lockdown; or (b) workers who, by the end of the lockdown, have no relationship to their previous employer can quickly find a new, stable job. In contrast, an L-shaped recession occurs if: (a) many workers flow into unemployment without maintaining ties to their previous employer; and (b) these workers cannot quickly find a new, stable job.

We calibrate the model using data from the Longitudinal Employer and Household Dynamics (LEHD) and the Survey of Income and Program Participation (SIPP) to capture three features of the labor market: (i) the fact that workers differ systematically with respect to the duration of their unemployment spells, and with respect to the tenure length of their jobs; (ii) the prevalence of different types of workers in different industries; (iii) the increase in unemployment across industries in March and April 2020. We find 3 distinct types of workers. At one extreme, there are “stable” workers with high productivity, short unemployment spells, and a high probability of staying on a job for more than 2 years. At the other extreme, there are “fickle” workers with low productivity, long unemployment spells, and a low probability of staying on a job for more than 2 years. We find that the prevalence of “fickle” workers varies a lot across industries and happens to be concentrated in some of the industries hit hardest by the lockdown.

Using the calibrated framework, we measure the shape of the pandemic recession. We model the recession as 3-months lockdown—which affects differently the productivity of workers in different industries—followed by a 12-month period of uncertainty—during which productivity is back to normal but there is a risk of a second lockdown. Throughout the lockdown and uncertainty phases, unemployment benefits are augmented by special federal programs. We find that the recession has an L-shape. The finding is easy to explain. First, even when the cost of maintaining and reactivating a suspended employment relationship is fairly small—in the order of less than a month of the worker’s value added—the fraction of workers whose employment relationship is permanently terminated is about 35%. This is consistent with survey evidence, which finds that between 40 and 50% of the workers who have entered unemployment during the first month of the lockdown have no expectation of being recalled to their previous job (see, Adams-Prassl et al. 2020 and Bick and Blandin 2020). Second, the workers who are permanently laid-off are disproportionately of the “fickle” type, who need to search for several years in order to find a long-lasting job. Interestingly, increasing the length of the lockdown from 3 to 6 months does not significantly affect the behavior of unemployment 4 years out.

We believe that our simulation represents a lower bound on the effect of the pandemic on unemployment. Indeed, we abstract from several important channels that are likely to slow down the recovery of unemployment. First, it is unlikely that the lockdown will be entirely lifted after 3 months and that, once lifted, productivity will immediately return to its normal level. Second, even employment relationships that are kept active throughout the lockdown are likely to break down at a rate higher than normal due to bankruptcies. Third, contractual frictions may cause some viable employment relationships to break down during the lockdown. A leading example of contractual frictions are rigid wages (see, e.g., Hall 2005, Gertler and Trigari 2009, or Menzio and Moen 2010), minimum wages, or costs to renegotiate contracts in the face of unforeseen contingencies.

The paper contributes to recent work on the economic consequences of the pandemic. A non-exhaustive list of this line of work is Alvarez, Argente and Lippi (2020), Atkeson (2020), Berger, Herkenhoff and Mongey (2020), Eichenbaum, Rebelo and Tradandt (2020), Fernandez-Villaverde and Jones (2020), Garibaldi, Moen and Pissarides (2020), Glover et al. (2020), Guerrieri et al. (2020), Kapicka and Rupert (2020), Kaplan, Moll and Violante (2020), Jones, Philippon and Venkateswaran (2020). Compared with this literature, the focus of our paper is on forecasting the aggregate dynamics of the labor market starting from the disaggregate and heterogeneous dynamics of individual workers. Compared with this literature, we are also silent about optimal policy. We believe that a derivation of the “optimal” unemployment rate during a pandemic would require calculations that, while surely important, fall well outside the scope of our expertise.

## 2 Environment and Equilibrium

In this section, we present our model of the labor market. The basic structure of the model is the same as in Menzio and Shi (2010, 2011). Firms and workers come together in the labor market through a search process directed by the terms of employment contracts. Firms search the market by posting employment contracts for their vacancies. Workers search the market by seeking vacancies offering the desired employment contract. Matches between firms and workers are heterogeneous with respect to their quality, which gives employed workers a motive for searching not only off but also on the job. We add two new ingredients to this basic structure. First, we allow for the possibility that workers are ex-ante heterogeneous. In particular, different types of workers are heterogeneous with respect to their productivity, the distribution of match quality from which they sample, and their ability to search. As documented in Ahn and Hamilton (2019), Morchio (2020), Kudlyak and Hall (2019) and Gregory, Menzio and Wiczer (2020), there are systematic differences across workers in their UE (unemployment to employment), EU (employment to unemployment) and EE (employer to employer) rates. Second, we allow for the possibility that workers and firms might temporarily deactivate their match, while retaining the option of resuming production at a later date. As documented in Fujita and Moscarini (2017), workers frequently return to their previous job after a spell of unemployment. As we shall see, these two new ingredients are critical to understand the aggregate dynamics of the labor market.

### 2.1 Environment

The labor market is populated by a positive measure of workers and firms. Workers are ex-ante heterogeneous with respect to their type  $i = 1, 2, \dots, I$ , which affects their productivity, unemployment income, and their search and learning processes. A worker of type  $i$  maximizes the present value of income, discounted at the factor  $\beta \in (0, 1)$ . A worker of type  $i$  earns some income  $b_i$  when he is unemployed, and some income  $w_i$  when he is employed. The unemployment income  $b_i$  is a combination of unemployment benefits, transfers, and income value of leisure. The employment income  $w_i$  is determined by the worker’s employment contract. The measure of workers of type  $i$  is  $\mu_i \geq 0$  and the total measure of workers is 1.

Firms are ex-ante homogeneous. A firm maximizes the present value of profits, discounted at the factor  $\beta$ . A firm operates a constant returns to scale technology which turns the labor supply of a worker of type

$i$  into  $y_i z$  units of output, where  $y_i$  is a component that is common to all pairs of firms and workers of type  $i$ , and  $z \in Z$  is a component that is specific to a particular firm-worker pair. The first component is the source of persistent differences in the productivity of different types of workers. The second component is the source of worker's job mobility. We refer to the second component of productivity as the quality of a firm-worker match.

The labor market is organized in a continuum of submarkets indexed by the vector  $x = \{v, i\}$ , where  $v \in R$  denotes the lifetime utility promised by firms to workers hired in submarket  $x$ , and  $i \in \{1, 2, \dots, I\}$  denotes the type of workers hired by firms in submarket  $x$ .<sup>1</sup> Associated with each submarket, there is an endogenous vacancy-to-applicant ratio  $\theta_i(v) \in \mathbb{R}_+$ . If a worker searches in submarket  $x = \{v, i\}$ , he finds a vacancy with probability  $p(\theta_i(v))$ , where  $p$  is a strictly increasing, strictly concave function with  $p(0) = 0$  and  $p(\infty) = 1$ . A vacancy in submarket  $x = \{v, i\}$  meets an applicant with probability  $q(\theta_i(v))$ , where  $q$  is a strictly decreasing function with  $q(\theta) = p(\theta)/\theta$ ,  $q(0) = 1$  and  $q(\infty) = 0$ .

The state of the economy is described by some exogenous state  $s \in S$  and by the endogenous distribution of workers across employment states. The exogenous state  $s$  evolves stochastically, and its realization may affect the type-specific productivity  $y_i$  and the type-specific unemployment income  $b_i$ . To understand the endogenous distribution of workers across employment states, note that a worker may be unemployed without the option to recall its old job, unemployed with the option to recall a match of unknown quality, unemployed with the option to recall a match of known quality, employed in a match of unknown quality, or employed in a match of known quality. Let  $u_i$  be the measure of unemployed workers without the option to recall their old job,  $m_i$  the measure of unemployed workers with the option to recall a job with unknown quality,  $q_i(z)$  the measure of unemployed workers with the option to recall a job with known quality  $z$ ,  $n_i$  the measure of employed workers in a match of unknown quality, and  $g_i(z)$  the measure of employed workers in a match of known quality  $z$ . Overall, the state of the economy is described by  $\psi \equiv \{s, u_i, m_i, q_i, n_i, g_i\}$ .

Every period comprises six stages: learning, separation, recall, search, matching and production. In the first stage, a worker of type  $i$  who is employed in a match with an unknown idiosyncratic component of productivity discovers the quality of the match with probability  $\phi_i \in [0, 1]$ . The idiosyncratic component of productivity  $z$  is a random draw from a probability density function  $f_i : Z \rightarrow \mathbb{R}_+$  with a mean normalized to 1.

In the second stage, an employed worker of type  $i$  becomes unemployed with probability  $d_e \in [\delta, 1]$ . The probability  $d_e$  is specified by the worker's employment contract. The lower bound  $\delta$  represents the probability that the worker has to leave the match for exogenous reasons (e.g., worker relocation). Similarly, an unemployed worker with a recall option loses contact from his old employer with probability  $d_q \in [\delta_q, 1]$ , where  $d_q$  is specified by the worker's employment contract. The lower bound  $\delta_q$  represents the probability that the worker and the firm lose contact for exogenous reasons (e.g., firm bankruptcy, decline in the quality of the match while inactive, loss of contact while physically separated, etc...).

In the third stage, an employed worker of type  $i$  becomes unemployed with a recall option with proba-

<sup>1</sup>We assume that a worker knows his own type and so does the market. The second part of the assumption may appear unrealistic to some readers, but it does greatly simplify the model. In particular, the assumption allows us to abstract from issues of signaling—the worker distorting his behavior so as to convince the market that his type is better than what it actually is—as well as from issues of inference—the firms trying to assess the probability distribution of a worker's type by examining his employment history and performance on the job.

bility  $\ell \in [0, 1]$ , where  $\ell$  is specified by the worker's contract. Similarly, an unemployed worker with a recall option returns to his old job with probability  $h \in [0, 1]$ , where again  $h$  is a prescription of the employment contract. When a worker recalls his old job, he and his employer have to pay a fixed cost  $C_i \geq 0$ , which captures the physical costs of resuming production.

In the fourth stage, a worker gets the opportunity to search the labor market with a probability that depends on his type and on his employment status. If a worker of type  $i$  is unemployed without a recall option, he gets to search with probability  $\lambda_u^i \in [0, 1]$ . If the worker is unemployed with a recall option, he gets to search with probability  $\lambda_q^i \in [0, \lambda_u^i]$ . If the worker is employed, he gets to search with probability  $\lambda_e^i \in [0, \lambda_u^i]$ . Whenever the worker gets to search, he chooses which submarket  $x$  to visit. In the same stage, firms choose how many vacancies to open in submarket  $x = \{v, i\}$  at the unit cost  $k_i > 0$ .

In the fifth stage, workers and firms searching in submarket  $x = \{v, i\}$  meet bilaterally. When a firm and a worker of type  $i$  meet in submarket  $x$ , the firm offers to the worker an employment contract that is worth  $v$  in lifetime utility. If the worker accepts the offer, he becomes employed by the firm under the rules of the contract. If the worker rejects the offer—which is an off-equilibrium event—he returns to his previous employment status. When a firm and a worker of type different from  $i$  meet in submarket  $x$ , the firm does not offer an employment contract to the worker.

In the last stage, an unemployed worker without a recall option enjoys an income of  $b_i$  units of output. An unemployed worker with a recall option enjoys an income of  $b_i$  units of output, while the worker's old employer pays a cost  $c_i$  to maintain the recall option alive. The flow cost  $c_i$  is meant to capture the overhead expenditures that the firm has to incur in order to keep the job available to the worker. A worker of type  $i$  employed in a match of unknown quality produces, in expectation,  $y_i$  units of output. A worker of type  $i$  employed in a match of known quality  $z$  produces  $y_i z$  units of output. The worker's consumption is  $w_i$ , which is determined by the employment contract. After production and consumption take place, next period's state,  $\hat{s}$ , is drawn from the probability density function  $h : S \times S \rightarrow \mathbb{R}_+$  with  $h(\hat{s}, s)$  denoting the probability density of  $\hat{s}$  conditional on  $s$ .

We assume that employment contracts maximize the joint value of a firm-worker match, i.e. the sum of the worker's lifetime utility and the firm's present value of profits generated by the worker. We also assume that the domain of the employment contract includes not only the employment relationship proper, but also the time during which a worker is unemployed with the option of reactivating the relationship.<sup>2</sup> As discussed in Menzio and Shi (2011), there are many contractual environments with the property that the contract that maximizes the profit of the firm subject to providing the worker any given lifetime utility also maximizes the joint value of the match. We abstract from contractual incompleteness caused by either wage rigidities or missing contingencies.

## 2.2 Equilibrium

To define equilibrium, we need to introduce some additional pieces of notation. Let  $U_i(\psi)$  denote the value of unemployment without recall for a worker of type  $i$ . Let  $\tilde{Q}_i(\psi)$  denote the joint value to the worker

<sup>2</sup>It is straightforward to develop a version of the model in which the firm and the worker do not act cooperatively during a temporary separation. In keeping with the "contractual efficient" spirit of the paper, though, we decided to assume that an employment contract regulates also this phase of the firm-worker relationship.

and the firm from a temporarily inactive match (i.e. the worker is unemployed with the option to recall). Similarly,  $Q_i(z, \psi)$  denotes the joint value to the worker and the firm from a temporarily inactive match of known quality  $z$ . Lastly, Let  $\tilde{V}_i(\psi)$  and  $V_i(z, \psi)$  denote, respectively, the joint value of an active match of unknown quality and quality  $z$ . All value functions are evaluated at the beginning of the production stage.

In what follows, we will suppress the dependence of the value functions from  $i$  and  $\psi$  in order to keep the notation light. The value for an unemployed worker without a recall option is

$$U = b(s) + \beta E_{\hat{\psi}} \left\{ U + \lambda_u^i \max_v \{ p(\theta(v))(v - U) \} \right\}. \tag{1}$$

In the current period, the worker's income is  $b(s)$ . In the next period, the worker gets an opportunity to search with probability  $\lambda_u$ . If the worker searches in submarket  $v$ , he meets a firm with probability  $p(\theta(v))$ , in which case his continuation lifetime utility is  $v$ . If the worker does not get the opportunity to search, or if the search is unsuccessful, his continuation value is  $U$ .

The joint value of an active match of quality  $z$  between a worker and a firm is

$$V(z) = y(s)z + \beta E_{\hat{\psi}} \left\{ \max_d \left\{ dU + (1 - d) \max_{\ell} \left\{ \ell Q(z) + (1 - \ell) \left[ V(z) + \lambda_e \max_v p(\theta(v))(v - V(z)) \right] \right\} \right\} \right\} \tag{2}$$

In the current period, the sum of the worker's income and firm's profit is  $y(s)z$ . In the next separation stage, the worker moves into unemployment with probability  $d$ . In this case, the worker's continuation value is  $U$  and the firm's continuation profit is zero. In the next recall stage, the worker and the firm deactivate the match with probability  $\ell$ , in which case their joint continuation value is  $Q(z)$ . The worker and the firm keep the match active with probability  $1 - \ell$ . In this case, the worker gets an opportunity to search with probability  $\lambda_e$ . If the worker searches in submarket  $v$ , he meets a new employer with probability  $p(\theta(v))$ . In this case, the worker's continuation value is  $v$  and the firm's continuation value is 0. If the worker does not get to search or if the search is unsuccessful, the joint continuation value is  $V(z)$ . Note that, since employment contracts are bilaterally efficient,  $d$ ,  $\ell$  and  $v$  are chosen so as to maximize the joint value of the match.

The joint value of an active match of unknown quality is

$$\begin{aligned} \tilde{V} &= y(s) \\ &+ \beta(1 - \phi) E_{\hat{\psi}} \left\{ \max_d \left\{ dU + (1 - d) \max_{\ell} \left\{ \ell \tilde{Q} + (1 - \ell) \left[ \tilde{V} + \lambda_e \max_v \left\{ p(\theta(v)) (v - \tilde{V}) \right\} \right] \right\} \right\} \right\} \\ &+ \beta \phi E_{\hat{\psi}} \left\{ \sum_z f(z) \max_d \left\{ dU + (1 - d) \max_{\ell} \left\{ \ell Q(z) + (1 - \ell) \left[ V(z) + \lambda_e \max_v \left\{ p(\theta(v)) (v - V(z)) \right\} \right] \right\} \right\} \right\}. \end{aligned} \tag{3}$$

In the current period, the joint income of the match is  $y(s)$  (in expectation). With probability  $1 - \phi$ , the firm and the worker do not discover the quality of the match. With probability  $\phi$ , the firm and the worker discover the quality  $z$  of the match, where  $z$  is drawn from the  $f$  distribution. Conditional on discovering or nor discovering the match quality, the firm and the worker choose  $d$ ,  $\ell$  and  $v$  to maximize the joint value.

The joint value of a temporarily inactive match of quality  $z$  between a worker and a firm is

$$Q(z) = b(s) - c + \beta E_{\psi} \left\{ \max_d \left\{ dU + (1-d) \max_h \left\{ h [V(z) - c] + (1-h) \left[ Q(z) + \lambda_q \max_v p(\theta(v))(v - Q(z)) \right] \right\} \right\} \right\} \quad (4)$$

In the current period, the sum of the worker's income and firm's profit is  $b(s) - c$ . In the next separation stage, the worker moves into permanent unemployment with probability  $d$ . In this case, the worker's continuation value is  $U$  and the firm's continuation profit is zero. If the next recall stage, the worker and the firm reactivate the match with probability  $h$ , in which case their joint continuation value is  $V(z) - c$ . The worker and the firm keep the match inactive with probability  $1 - h$ . In this case, the worker gets an opportunity to search with probability  $\lambda_q$ . If the worker searches in submarket  $v$ , he meets a new employer with probability  $p(\theta(v))$ . In this case, the worker's continuation value is  $v$  and the firm's continuation value is 0. If the worker does not get to search or if the search is unsuccessful, the joint continuation value is  $Q(z)$ .

The joint value of a temporarily inactive match of unknown quality is

$$\tilde{Q} = b(s) - c + \beta E_{\psi} \left\{ \max_d \left\{ dU + (1-d) \max_h \left\{ h [\tilde{V} - c] + (1-h) \left[ \tilde{Q} + \lambda_q \max_v p(\theta(v))(v - \tilde{Q}) \right] \right\} \right\} \right\} \quad (5)$$

The expression above is analogous to (4) and requires no comment.

The tightness  $\theta(v)$  of submarket  $v$  is such that

$$k \geq q(\theta(v)) [\tilde{V} - v], \quad (6)$$

and  $\theta(v) \geq 0$ , with the two inequalities holding with complementary slackness. The left-hand side of (6) is the cost to a firm from opening a vacancy in submarket  $v$ . The right-hand side is the benefit to the firm from opening a vacancy in submarket  $v$ . The benefit is the probability that the firm fills its vacancy,  $q(\theta(v))$ , times the firm's value from filling a vacancy,  $\tilde{V} - v$ , i.e. the joint value of a match between the firm and a worker net of the lifetime utility promised by the firm to the worker.

We can easily characterize the solution of the search problems in (1)-(5). These problems have the common structure

$$\max_v p(\theta(v))(v - r), \quad (7)$$

where  $r$  denotes the value of the worker's current employment status. For any  $v$  such that  $\theta(v) > 0$ , (6) implies that  $v$  is equal to  $-k\theta(v) + p(\theta(v))\tilde{V}$ . For any  $v$  such that  $\theta(v) = 0$ ,  $p(\theta(v))$  is equal to zero. From these observations, it follows that (7) can be written as

$$\max_v -k\theta(v) + p(\theta(v))(\tilde{V} - r). \quad (8)$$

Now, notice that, for all  $\theta \geq 0$ , there exists a  $v$  such that  $\theta(v) = \theta$ . Thus, by changing the choice variable from  $v$  to  $\theta$  in (8), we do not enlarge the choice set. Conversely, for all  $v$ , there exists a  $\theta \geq 0$  such that  $\theta = \theta(v)$ . Thus, by changing the choice variable from  $v$  to  $\theta$  in (8), we do not shrink the choice set. From

these observations, it follows that (8) can be written as

$$\max_{\theta \geq 0} -k\theta + p(\theta)(\tilde{V} - r). \quad (9)$$

From the above formulation, it follows immediately that a worker employed in a match of unknown quality has no reason to actively search.

To formulate the laws of motion for the distribution of workers across employment states, we need some notation describing the policy functions. We denote as  $d_e(z)$  and  $d_q(z)$  the optimal probability that a worker employed in an active or inactive match of quality  $z$  moves into unemployment. We denote as  $d_e(\emptyset)$  and  $d_q(\emptyset)$  denote that probability for a worker employed in an active or inactive match of unknown quality. We denote as  $\ell(z)$  and  $\ell(\emptyset)$  the optimal probability that an active match of known or unknown quality becomes inactive. We denote as  $h(z)$  and  $h(\emptyset)$  the optimal probability that an inactive match of known or unknown quality becomes active. We denote as  $\theta_u$ ,  $\theta_q(z)$ ,  $\theta_e(z)$  the optimal search strategy for an unemployed worker without a recall option, an unemployed worker with an option to recall a match of quality  $z$ , and an employed worker in a match of quality  $z$ .

The law of motion for the measure of unemployed workers without recall is

$$\begin{aligned} \hat{u} = & u(1 - \lambda_u p(\theta_u)) + \sum_z d_e(z) [g(z) + n\phi f(z)] \\ & + \sum_z d_q(z) q(z) + n(1 - \phi) d_e(\emptyset) + m d_q(\emptyset) \end{aligned} \quad (10)$$

The law of motion for the measure of workers employed in an active match of unknown quality is

$$\begin{aligned} \hat{n} = & u \lambda_u p(\theta_u) + \sum_z (1 - d_e(z))(1 - \ell(z)) \lambda_e p(\theta_e(z)) [g(z) + n\phi f(z)] \\ & + \sum_z (1 - d_q(z))(1 - h(z)) \lambda_q p(\theta_q(z)) q(z) \\ & + n(1 - \phi)(1 - d_e(\emptyset))(1 - \ell(\emptyset)) \\ & + m(1 - d_q(\emptyset)) [h(\emptyset) + (1 - h(\emptyset)) \lambda_q p(\theta_q(\emptyset))] \end{aligned} \quad (11)$$

The law of motion for the measure of workers employed in an active match of known quality  $z$  is

$$\begin{aligned} \hat{g}(z) = & [g(z) + n\phi f(z)] (1 - d_e(z))(1 - \ell(z))(1 - \lambda_e p(\theta_e(z))) \\ & + q(z)(1 - d_q(z)) h(z) \end{aligned} \quad (12)$$

The law of motion for the measure of unemployed workers with the option to recall a match of quality  $z$  is

$$\begin{aligned} \hat{q}(z) = & q(z)(1 - d_q(z))(1 - h(z))(1 - \lambda_q p(\theta_q(z))) \\ & + [g(z) + n\phi f(z)] (1 - d_e(z)) \ell(z) \end{aligned} \quad (13)$$

Lastly, the law of motion for the measure of unemployed workers with the option to recall a match of unknown quality is

$$\begin{aligned} \hat{m} = & m(1 - d_q(\emptyset))(1 - h(\emptyset))(1 - \lambda_q p(\theta_q(\emptyset))) \\ & + n(1 - \phi)(1 - d_e(\emptyset)) \ell(\emptyset) \end{aligned} \quad (14)$$

All of the above expressions are easy to understand.

A Recursive Equilibrium (RE) is such that: (i) the value functions  $\{U, \tilde{V}, V, \tilde{Q}, Q\}$  satisfy the Bellman

Equations (1)-(5); (ii) the policy functions  $\{d_e, d_q, \theta_u, \theta_e, \theta_q, \ell, h\}$  satisfy the optimality conditions in (1)-(5); the distribution of workers across employment states  $\{u, m, n, q, g\}$  follows the laws of motion (10)-(14). A Block Recursive Equilibrium (BRE) is a RE such that the value and policy functions depends on the aggregate state of the economy  $\psi$  only through the exogenous state  $s$ , and not through the endogenous distribution of workers across employment states. A Block Recursive Equilibrium is much easier to solve, as it requires solving a system of functional equations with the one-dimensional state  $s$  as an aggregate state variable. As proved in Menzio and Shi (2011) in the context of a similar model, there exists a BRE, the BRE is unique, and there exists no other equilibrium that is not block-recursive.

### 3 Calibration

Using data from the Longitudinal Employer and Household Dynamics (LEHD) over the period 1997-2014, we apply a  $k$ -mean algorithm to group workers based on to their similarity with respect to the frequency and duration of unemployment spells and the number and length of jobs.<sup>3</sup> The algorithm identifies 3 types of workers, which we shall refer to as  $\alpha$ ,  $\beta$  and  $\gamma$ . About 55% of workers are of type  $\alpha$ . For a worker of type  $\alpha$ , the duration of a job is less than a year with probability 30%, and more than 2 years with probability 50%. For a worker of type  $\alpha$ , unemployment spells are short. About 25% of workers are of type  $\beta$ . For a worker of type  $\beta$ , the duration of a job is less than a year with probability 40%, and more than 2 years with probability 40%. For a worker of type  $\beta$ , unemployment spells are longer than for  $\alpha$ -workers. About 20% of the workers are of type  $\gamma$ . For a worker of type  $\gamma$ , the duration of a job is less than a year with probability 65%, and more than 2 years with probability 15%. These workers have the longest duration of unemployment. Workers of different types also have different average earnings. Specifically, the average earnings for  $\beta$ -workers are 70% compared to the average earnings for  $\alpha$ -workers. The average earnings for  $\gamma$ -workers are about 50% compared to the earnings for  $\alpha$ -workers. The worker type characteristics described above are the key calibration targets<sup>4</sup>

Let us review the parameters that describe the non-stochastic steady state of the model. These parameters are summarized in Table 1. Preferences are described by the discount factor,  $\beta$ , and by the flow unemployment income,  $b_i$ . Production is described by the type-specific component of productivity,  $y_i$ , and by the distribution of the match-specific component of productivity,  $f_i$ . We specialize the distribution  $f_i$  to be a Weibull distribution with shape  $\alpha_i$  and scale  $\sigma_i$ , shifted to have a mean of 1. Learning is described by the probability  $\phi_i$  with which a worker and a firm discover the component of productivity that is idiosyncratic to their match.

Search is described by the probability that a worker can search the labor market when unemployed without a recall option,  $\lambda_u^i$  and when employed,  $\lambda_e^i$ . Further, search depends on the vacancy cost,  $k_i$ , and on the job-finding probability function,  $p(\theta)$ . We normalize  $\lambda_u^i$  to 1. We specialize  $p(\theta)$  to have the form  $\min\{\theta^\gamma, 1\}$ , where  $\gamma$  is the elasticity of the job-finding probability with respect to tightness.

<sup>3</sup>In the LEHD, we cannot distinguish between unemployment and non-employment. We identify unemployment as a spell without earnings that lasts less than 2 years. In the LEHD, we only have quarterly observations and, thus, we cannot directly measure short unemployment spells. We impute an unemployment spell between two jobs by comparing earnings in the first job and earnings in the second job. If, during the transition from the first to the second job, there is a quarter in which earnings are lower than the minimum of the typical earnings in the two jobs, we impute an unemployment spell.

<sup>4</sup>Details about the calibration algorithm are available upon request.

Parameter	Value	Description
$\beta$	0.996	discount factor
$b_i$	(0.661, 0.563, 0.458)	flow unemployment income
$y_i$	(1, 0.623, 0.459)	type-specific productivity
$\alpha_i$	(4, 4, 1)	shape of $f_i$
$\sigma_i$	(0.117, 0.203, 0.08)	standard deviation of $f_i$
$\phi_i$	(0.25, 0.225, 0.25)	probability match quality is discovered
$\lambda_e^i$	(0.344, 0.763, 0.70)	probability an employed worker searches
$\lambda_u^i, \lambda_q^i$	1	probability an unemployed worker searches
$k_i$	(12.54, 25.92, 5.37)	vacancy posting cost
$\gamma$	0.5	elasticity of job-finding rate wrt tightness
$\delta$	0.005	exogenous separation probability
$\delta_q$	0.10	probability recall option is lost
$c_i$	(0.05, 0.031, 0.023)	cost of maintaining recall option
$C_i$	(0.25, 0.156, 0.115)	cost of reactivating a match

Table 1: Model Parameters

The recall process is characterized by the parameters  $\lambda_q$ , the probability that an unemployed worker with a recall option can search the labor market,  $\delta_q$ , the probability that an unemployed worker loses his recall option, and by  $c_i$  and  $C_i$ , the flow cost of maintaining the recall option and the fixed cost of exercising the recall option. None of these parameters affect the non-stochastic steady-state, because absent aggregate shocks, there are no firm-worker matches that are temporarily inactive. We shall discuss our choice of the parameters describing the recall process in a few pages.

Now, let us describe our calibration strategy in broad strokes. We use the empirical duration of unemployment spells to calibrate  $k_i$ . We use the empirical distribution of job durations to calibrate  $\alpha_i$ ,  $\sigma_i$  and  $\phi_i$ . We normalize  $y_\alpha = 1$  and choose  $y_\beta$  and  $y_\gamma$  to match the difference in average earning between different types of workers. As suggested by Hagedorn and Manovskii (2008) and Hall and Milgrom (2009), the proper interpretation of  $b_i$  is the sum of an unemployment benefit,  $\zeta_i$ , and the income value of leisure,  $\ell$ . We choose the unemployment benefit for workers of type  $i$  to be equal to 40% of the average labor income for workers of type  $i$ , which is the typical replacement rate of unemployment insurance in the US. We choose the value of leisure,  $\ell$ , so that, in the average of the whole population of workers, the flow value of unemployment is equal to 65% of labor income, a percentage that Hall and Milgrom (2008) argue is reasonable for the US economy. We tentatively set  $\delta$  to 0.5% per month. We tentatively set  $\gamma$  to 0.5. Neither of these parameters has much of an effect on our simulation results.

## 4 Simulating the Pandemic Recession

To describe and simulate the pandemic recession, we stratify the model by 2-digit industry. Using data from the Survey of Income and Program Participation (SIPP), we compute the distribution of job durations industry by industry. We choose the fraction of workers of type  $\alpha$ ,  $\beta$  and  $\gamma$  in industry  $j$  to minimize the distance between the distribution of job durations in industry  $j$  in the data and in the model. We carry out the minimization subject to a constraint requiring that the sum of workers of type  $\alpha$ ,  $\beta$  and  $\gamma$  across

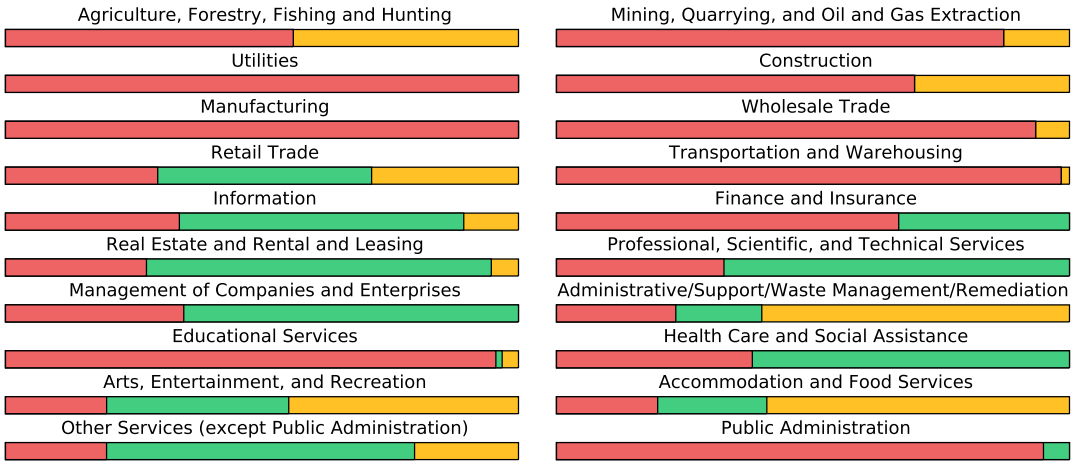


Figure 1: Proportion of workers of type  $\alpha$  (pink),  $\beta$  (green), and  $\gamma$  (yellow)

all industries is equal with the fraction of workers of type  $\alpha$ ,  $\beta$  and  $\gamma$  in the LEHD. Figure 1 shows the distribution of types by industry.

To describe the pandemic recession, we assume that the economy can be in one of three states: lockdown ( $s_L$ ), uncertainty ( $s_U$ ), or recovery ( $s_R$ ). Intuitively, the lockdown state is meant to capture the current phase of severe restrictions on economic activity. The uncertainty state is meant to capture a phase in which restrictions on economic activities are lifted, but there is a risk of returning to the lockdown state (because of, say, a second wave of infections). The recovery state is meant to capture a permanent return to normalcy (because of, say, an effective vaccine is discovered). The three states differ with respect to productivity and unemployment income. In the lockdown state, the productivity  $y_i$  of  $i$ -workers employed in industry  $j$  is multiplied by some factor  $A_{L,j}$ , which is typically smaller than 1 and captures the (industry-specific) effect of restrictions on economic activity. The unemployment income is multiplied by some factor  $B_L > 1$ , which captures the increase in unemployment benefits granted by the CARES Act. In the uncertainty state, the productivity of  $i$ -workers employed in industry  $j$  returns to its normal value, i.e.  $A_{U,j} = 1$ . The unemployment income, however, is still multiplied by some factor  $B_U > 1$  to capture the idea that the increase in the generosity of unemployment benefits may outlast the lockdown. In the recovery state, both productivity and unemployment income return to their normal values, i.e.  $A_{R,j} = 1$  and  $B_R = 1$ . When the aggregate state is  $s_L$ , the probability of moving to  $s_U$  is 75% per month and the probability of moving to  $s_R$  is zero. When the aggregate state is  $s_U$ , the probability of returning to  $s_L$  is 13% per month, and the probability of moving to  $s_R$  is 6.5%. The  $s_R$  state is absorbing.

There are several parameters that have yet to be chosen in order to simulate the recession. We calibrate the vector of productivity shocks  $A_{L,j}$  so that: (a) the aggregate unemployment rate increases by 19 percentage points during the lockdown—which we take it to be a sensible guess based on the number of unemployment insurance claims during March and April 2020; and (b) the relative increase in the unemployment rate across industries matches the relative flow of new unemployment claims across industry—which we measure for the states of Washington, Texas, Ohio and Nebraska. We set the unem-

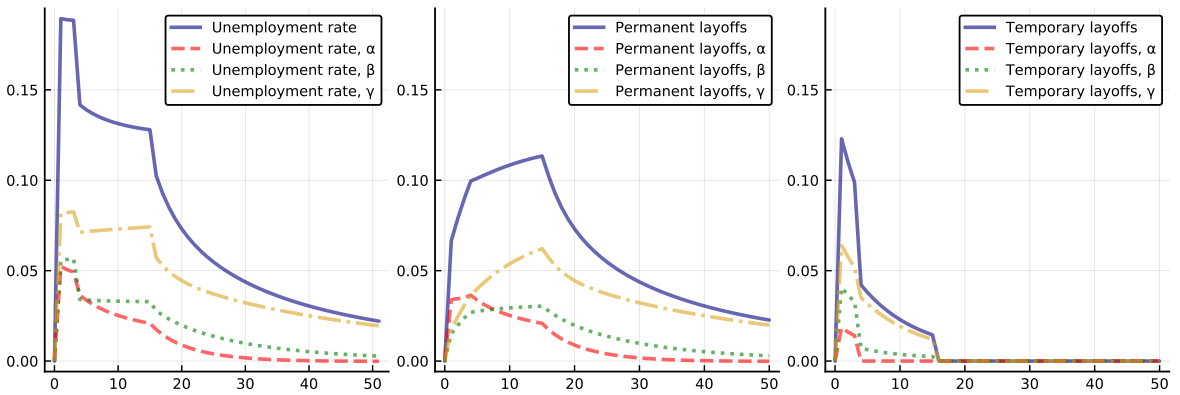


Figure 2: Baseline simulation of pandemic

Covid Economics 15, 7 May 2020: 88-109

employment income shock  $B_L$  to 1.3 or, equivalently, 1,000 US\$ per month. This is less than what offered by the CARES act because we want to capture, albeit crudely, the fact that not all unemployed workers will be awarded the additional benefits. In the baseline, we set  $B_U$  to 1.3, but we present results for other values as well.

The parameters describing the process of recall require some guesswork. We assume that unemployed workers with the option to recall their old job have the same probability of searching the labor market as unemployed workers without such an option, i.e.  $\lambda_q^i = \lambda_u^i$ . We assume that the rate at which a firm-worker match exogenously breaks down when it is temporarily inactive is 10% per month, i.e.  $\delta_q = 0.1$ . The particular values chosen for  $\lambda_q$  and  $\delta_q$  do not have a significant impact on the simulation of the pandemic. In contrast, the cost of maintaining the option of recall,  $c_i$ , and the cost of exercising the recall option,  $C_i$ , play an important role. Intuitively, both costs affect the trade-off between permanently terminating or temporarily deactivating a firm-worker match when its productivity is depressed by the lockdown. The relative magnitude of the two costs affects the trade-off between recalling a temporarily deactivated match as soon as the lockdown is lifted or only when the risk of a lockdown is eliminated. Indeed, if  $C_i = 0$ , the match can be activated and deactivated at no cost and, thus, the decision will be essentially determined by a static comparison between  $b(s) - c$  and  $y(s)z$ . If, in contrast,  $C_i > 0$ , the firm and the worker are discouraged from deactivating and reactivating their match often.

Figure 2 illustrates the simulation of the pandemic recession under our baseline calibration. For the purposes of the simulation, we assume that the economy is in the lockdown state for 3 months, in the uncertainty state for 12 months, and in the recovery state afterwards. Panel (a) plots the unemployment rate, measured in deviation from the steady-state. Panel (b) plots the fraction of workers who are unemployed without a recall option (permanently laid-off), measured in deviation from the steady state. Panel (c) plots the fraction of workers who are unemployed with a recall option (temporarily laid-off), measured in deviation from the steady state. The dashed lines in the three panels show the decomposition of the aggregates by type of worker.

As the economy enters the lockdown, the unemployment rate increases by 19 percentage points. About 13 percentage points of the increase are due to temporary separations between workers and firms, the

remaining 6 percentage points are due to permanent separations. As the economy exits the lockdown, approximately half of the workers on temporary layoff are recalled by their previous employer. Moreover, the UE rate increases and the unemployed workers on permanent layoff start flowing back into employment. Overall, during the 12 months between the exit from the lockdown state and the entry into the recovery state, the unemployment rate falls by about 5 percentage points. As the economy enters the recovery state, all remaining workers on temporary layoffs are recalled. Moreover, the UE rate returns to its pre-lockdown level. Thus, the unemployment rate starts its descent towards its old steady-state level.

Even though the lockdown lasts for as little as 3 months, the unemployment rate is still about 5 percentage points above its steady-state level 30 months after the beginning of the pandemic. Similarly, the unemployment rate is still about 2.5 percentage points above its steady-state level 50 months after the beginning of the pandemic. A recession with this kind of slow recovery is sometimes dubbed an “L-shaped” recession. The slow pace of the recovery is caused by the ex-ante heterogeneity of workers. As can be seen from Panel (a), the excess unemployment for  $\alpha$ -workers subsides fairly quickly. This is because  $\alpha$ -workers have a high UE rate and, once they find a job, they are likely to keep it for a long time. The excess unemployment for the  $\gamma$ -workers, however, subsides much more slowly. This is because  $\gamma$ -workers have a low UE rate and, once they find a job, they are unlikely to keep it for a long time. Thus, the increase in unemployment among  $\gamma$ -workers takes years to be reabsorbed as many of them go through multiple cycles of unemployment and short-term employment.

It is worth noting that  $\gamma$ -workers are the largest contributor to the initial increase in aggregate unemployment, even though they are the smallest group in the overall population. In contrast,  $\alpha$ -workers are the smallest contributor to the initial increase in aggregate unemployment, even though they are the largest group in the overall population. Intuitively,  $\gamma$ -workers have the smallest gains from trade in the labor market and, hence, their employment is most susceptible to a negative productivity shock and to an increase in the generosity of unemployment benefits. In contrast,  $\alpha$ -workers have the largest gains from trade in the labor market and, hence, their employment is least susceptible to the lockdown. Moreover, as one can see from Figure 1 and Table 2,  $\gamma$ -workers are overrepresented in some of the industries that are hit hardest by the lockdown. Indeed, the average productivity shock for a  $\gamma$ -worker is 10% larger than for  $\alpha$ -workers.

It is also worth pointing out that the share of temporary layoffs is highest for  $\gamma$ -workers (approximately 75%) and lowest for  $\alpha$ -workers (approximately 35%). There is a clear intuition behind this result. It takes a long time for an unemployed  $\gamma$ -worker to find a “stable” match, i.e. a match with an idiosyncratic component of productivity that is high enough to make the worker stop searching for something better. Thus, a firm and a  $\gamma$ -worker in a “stable” match prefer to remain in contact (at the costs  $c$  and  $C$ ) rather than to permanently separate. In contrast, it takes a relative short time for an unemployed  $\alpha$ -worker to find a new “stable” match. Thus, a firm and an  $\alpha$ -worker prefer to permanently terminate their relationship rather than to remain in contact.

The role played by the ex-ante heterogeneity of workers in shaping the recovery can be seen in the dynamics of the unemployment rate in different industries. Panel (a) in Figure 3 shows the excess unemployment rate in construction—an industry with a large fraction of  $\gamma$ -workers. Panel (b) shows the excess unemployment rate in manufacturing—an industry with a large fraction of  $\alpha$ -workers. Even though the

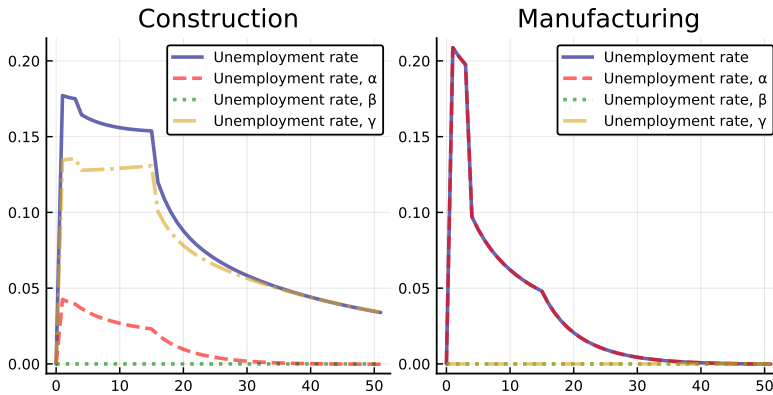


Figure 3: Unemployment dynamics in selected industries

initial increase in unemployment is higher in manufacturing, the recovery is much faster because  $\alpha$ -workers are more likely to find stable employment after the lockdown is lifted. In the Appendix, we present the behavior of the unemployment rate in every industry.

Table 2 shows the industry-specific productivity shocks that we infer from our calibration. The calibrated shocks depend on the composition of workers in the industry—which we estimate from the SIPP—and on the magnitude of the increase in unemployment benefit claims—which we observe for March and April 2020 for several states. As a sanity check, we compare our calibrated productivity shocks with two measures of the exposure of an industry to the lockdown. The first measure is the fraction of workers in industry  $j$  that can work remotely. This measure is constructed from the occupational index of “teleworkability” constructed by Dingel and Neiman (2020) using the ONET and then projected on industry  $j$  based on its occupational composition. The second measure is a definition of “essential work” for the state of Pennsylvania, where essential workers are those exempted from the lockdown.<sup>5</sup>

Figure 4 contains a scatter plot of the calibrated productivity shock and the fraction of “teleworkable” labor (panel a) and the scatter plot of the calibrated productivity shock and the fraction of “essential” labor (panel b) across 2-digit industries. As one would have hoped, both relationships are negative. Also note that the employment-weighted average productivity shock in the model is about 35%. The employment-weighted average of the fraction of labor that cannot be done remotely is 45%. The employment-weighted average of the fraction of labor that is both non-essential and cannot be done remotely is 27%. We find it reassuring that our model generates an average shock that is in the same order of magnitude as the fraction of labor that is susceptible to the lockdown.

As mentioned earlier, the recall costs  $c_i$  and  $C_i$  determine the fraction of workers in permanent and temporary layoffs. Thus, for a given increase in the unemployment rate, the recall costs affect the speed of the recovery. Specifically, the higher are the recall costs, the lower is the fraction of temporary layoffs and the slower is the recovery. It is then important to build some confidence in our choice of  $c_i$  and  $C_i$ . In our baseline calibration, we set  $c_i = 0.05 \cdot y_i$  and  $C_i = 0.25 \cdot y_i$  and found that 65% of the increase in unemployment during the lockdown was due to temporary layoffs and 35% to permanent layoffs. This

<sup>5</sup>There is nothing special about Pennsylvania. The list of essential work in other states is quite similar.

Industry	$\Delta u_j$ (%)	$A_j$
Agriculture, Forestry, Fishing and Hunting	3.85	1.2
Mining, Quarrying, and Oil and Gas Extraction	12.29	0.67
Utilities	1.06	1.11
Construction	18.06	0.75
Manufacturing	21.0	0.37
Wholesale Trade	11.82	0.53
Retail Trade	26.25	0.59
Transportation and Warehousing	12.37	0.49
Information	9.8	0.96
Finance and Insurance	1.33	1.16
Real Estate and Rental and Leasing	18.51	0.61
Professional, Scientific, and Technical Services	9.17	0.75
Management of Companies and Enterprises	5.58	1.04
Administrative/Support/Waste Management/Remediation	18.57	1.06
Educational Services	8.12	0.68
Health Care and Social Assistance	21.0	0.49
Arts, Entertainment, and Recreation	55.7	0.13
Accommodation and Food Services	49.06	0.34
Other Services (except Public Administration)	47.62	0.21
Public Administration	0.0	1.24

Table 2: Industry-level unemployment increases and calibrated productivity shocks

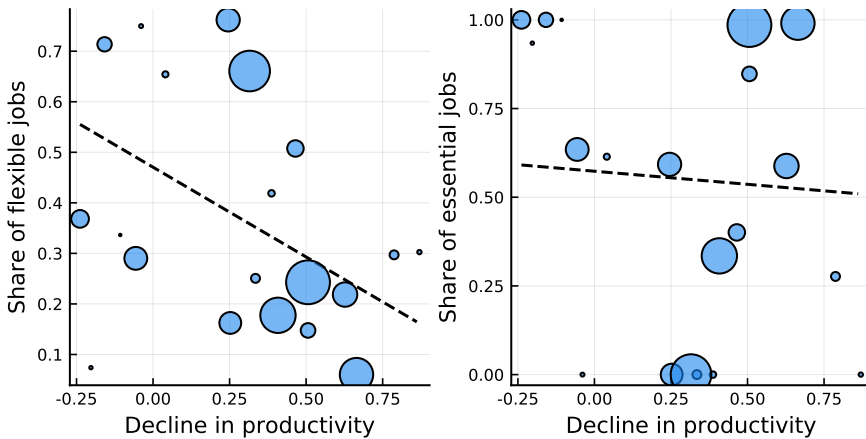


Figure 4: Calibrated productivity shocks vs. flexible and essential jobs

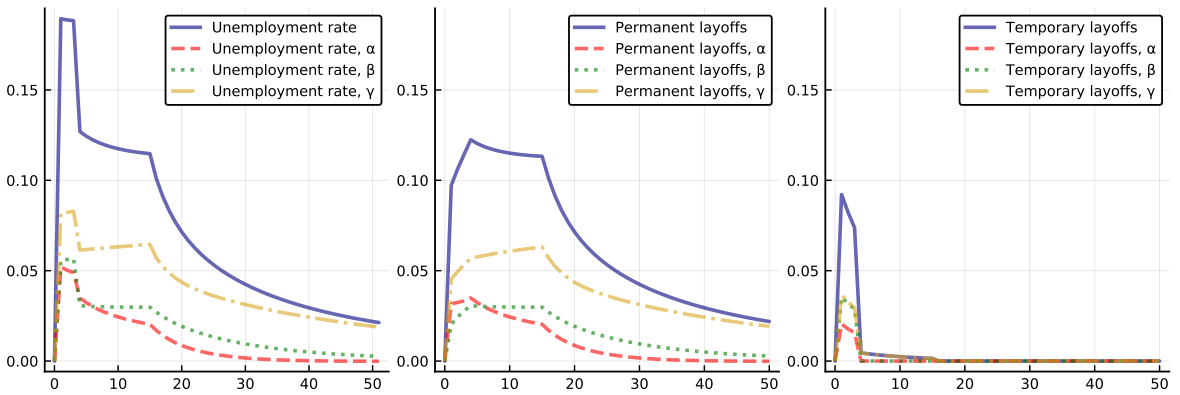


Figure 5: Simulation of pandemic with  $c_i = 0.15 \cdot y_i$  and  $C_i = 0$

Covid Economics 15, 7 May 2020: 88-109

finding is in line with the survey evidence on layoffs during the early stages of the pandemic. Adams-Prassl et al. (2020) survey a representative sample of individuals in the US, conducting multiple waves of interviews during the first weeks of the pandemic. Individuals could report whether they had lost their job in a permanent way or been furloughed, implying the expectation of being called back. As of the Apr 23 data, the ratio of temporary to permanent lay-offs was 3 : 2. Bick and Blandin (2020) conduct a similar survey, again asking whether individuals who separated from their employer expected the layoff to be temporary. They found approximately 50% of separations were expected to be temporary. Overall, our calibration of  $c_i$  and  $C_i$  is conservative, in the sense that our model generates more temporary lay-offs than what found in these surveys.

The ratio between the cost of exercising the recall option,  $C_i$ , and the cost of maintaining the recall option,  $c_i$ , affects the time at which temporarily deactivated relationships are recalled. Figure 5 shows the simulation of the recession for  $c_i = 0.15 \cdot y_i$  and  $C_i = 0$ , rather than for  $c_i = 0.05 \cdot y_i$  and  $C_i = 0.25 \cdot y_i$ . By lowering the cost of exercising the recall option while increasing the cost of maintaining the recall option, the fraction of layoffs that are temporary and permanent does not change by much (it goes from 65 : 35% to about 50 : 50%). For this reason, the medium-term effects of the lockdown do not change by much either (the excess unemployment rate 50 months out is still about 2.5%). However, the timing of recalls does change. In particular, most of temporarily laid-off workers are recalled as soon as the lockdown is lifted.

From the perspective of policy, it is interesting to see the effect of extending the lockdown. Figure 6 below illustrates the results of the simulated recession when the economy is kept under lockdown for 6 months rather than 3, and the period of uncertainty lasts 9 rather than 12 months. Because of the extended lockdown, the unemployment rate remains close to its peak for a longer period of time. Yet, once the economy enters the recovery state, the unemployment rate is essentially the same as in the baseline calibration. In this sense, extending the lockdown does not seem to have nefarious effects on unemployment in the medium-run. We urge our readers, however, to take this finding with a grain of salt, as it may depend on our conservative assumptions about the effect of the lockdown on the survival rate of temporarily deactivated relationships.

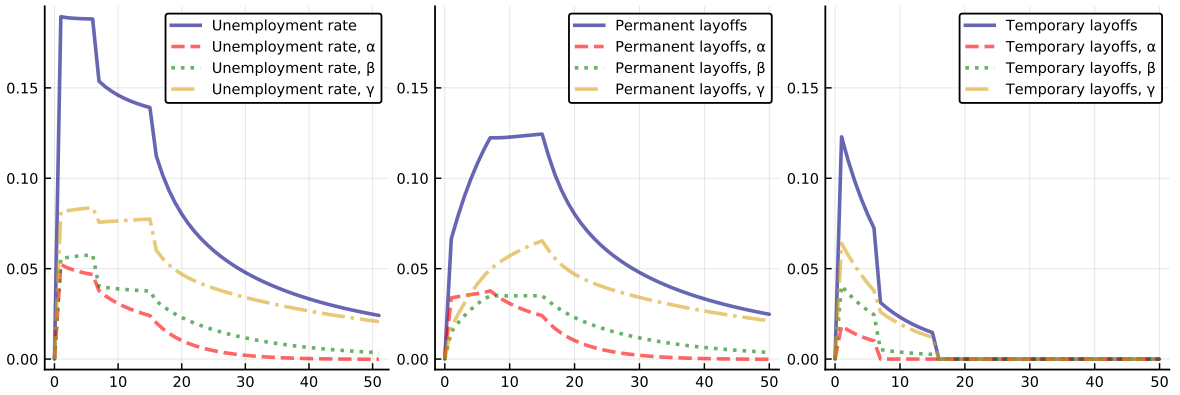


Figure 6: Simulation of pandemic with 6 months of lockdown, 9 months of uncertainty

Covid Economics 15, 7 May 2020: 88-109

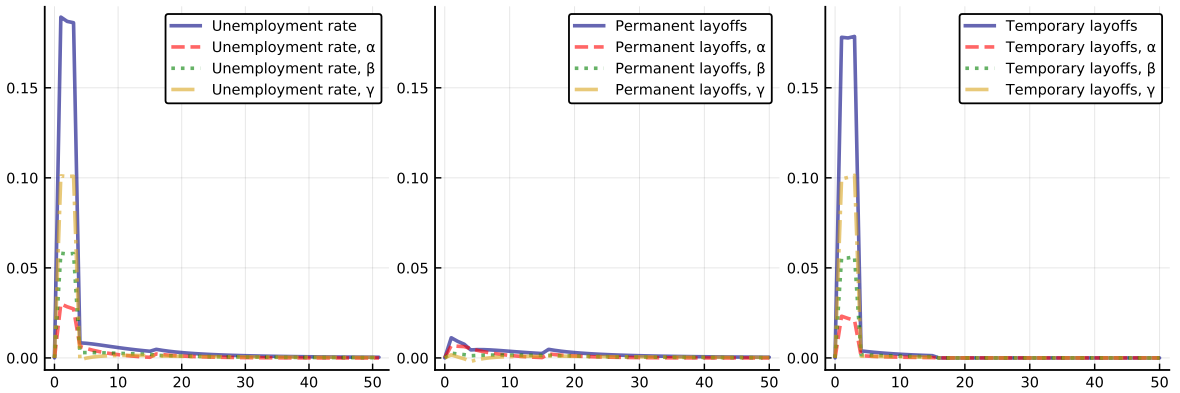


Figure 7: V-shaped simulation of pandemic

Lastly, we want to point out that the model can also generate a “V-shaped” recession, i.e. a recession in which the initial increase in unemployment is quickly reabsorbed after the end of the lockdown. The model generates a V-shaped recession when the initial increase in unemployment is almost entirely driven by temporary layoffs and, as soon as the lockdown is over, firms find it optimal to recall all of the temporarily laid-off workers.<sup>6</sup> Hence, the model generates a V-shaped recession when  $c_i$  and  $C_i$  are small and  $B_U$  is close to 1.

Figure 7 illustrates the simulation of the pandemic recession with  $c_i = C_i = 0$  and  $B_U = 1$ . As the economy enters the lockdown, the unemployment rate increases by 19 percentage points. About 18 percentage points of this increase are due to temporary separations between workers and firms, while the remaining 1 percentage point is due to permanent separations. As the economy exits the lockdown, nearly all of the workers on temporary layoff are recalled by their employers, and the unemployment rate returns

<sup>6</sup>In principle, the model could also generate a V-shaped recession if the vast majority of workers entering unemployment during the lockdown were of type  $\alpha$ . However, our calibration of the type distribution across industries and of the shock distribution across industries rules out this possibility.

within 1 percentage point of its steady-state level.

While the model can generate a V-shaped recession, it does so by producing some implausible outcomes. First, 95% the initial increase in the unemployment rate is due to temporary layoffs and only 5% is due to permanent layoffs. In the recent surveys of Adams-Prassl et al. (2020) and Bick and Blandin (2020), at least 40% of workers who became unemployed at the beginning of the recession state to have no expectation of being recalled by their previous employer. Second, when the costs associated with temporary layoffs are low, it takes a smaller productivity shock to generate the same increase in unemployment during the lockdown. Indeed, the employment-weighted productivity shock required to generate a 19 percentage point increase in unemployment is only 1.4%. This is an order of magnitude lower than the employment-weighted average of work that cannot be done remotely (45%), and much lower than the employment-weighted average of the fraction of work that is both non-essential and cannot be done remotely (27%).

Let us conclude by pointing out that underneath the results presented in this section—results that are aggregated either at the economy level or at the industry level—there is a wealth of additional results about individual workers, including the size of their earnings losses during the lockdown and the speed at which these losses are recouped.<sup>7</sup> We decided not to report these disaggregated results not because we deem them uninteresting, but for the sake of conciseness.

---

<sup>7</sup>Let us just say that our model does an excellent job at reproducing the size of earnings losses documented in Jacobson, LaLonde and Sullivan (1993) and Davis and von Wachter (2011).

# A Unemployment rate IRFs by industry

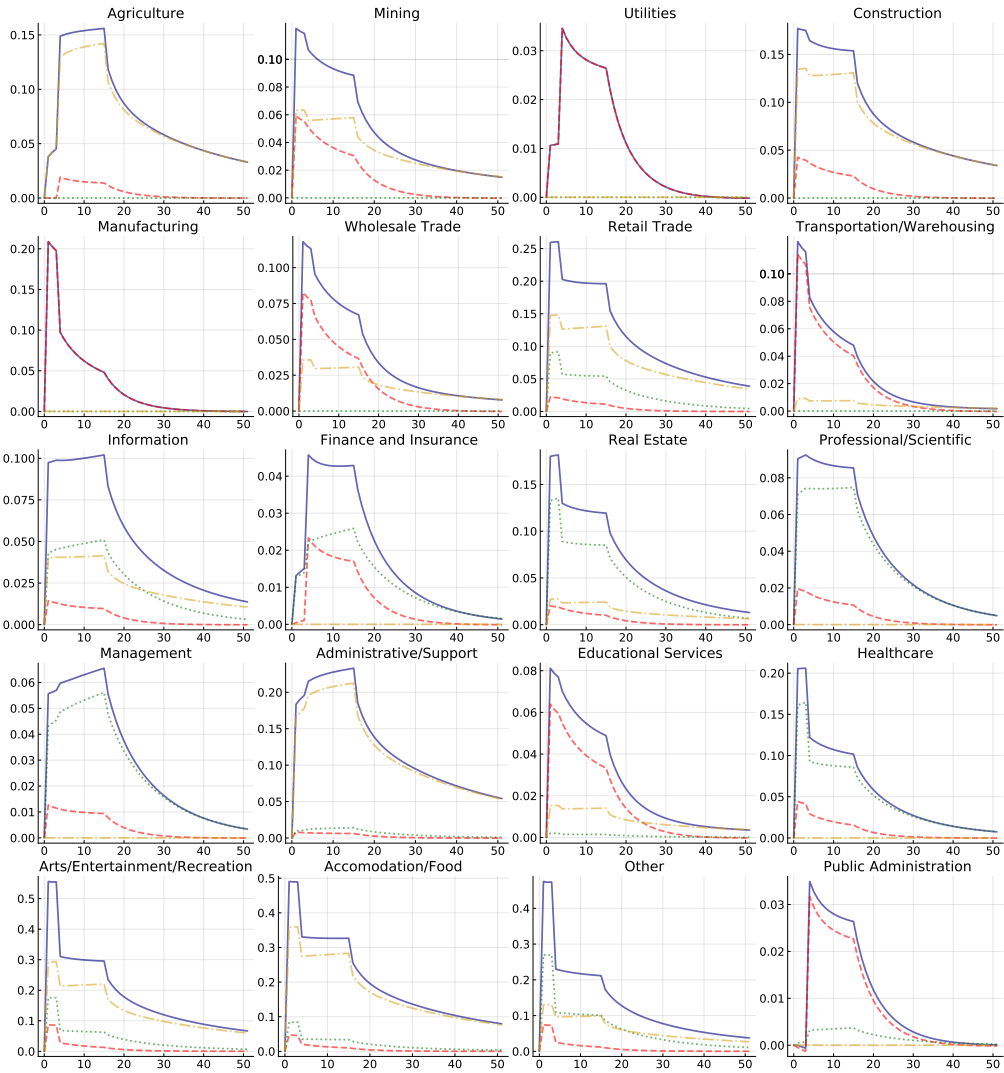


Figure 8: Pandemic simulation by industry

Covid Economics 15, 7 May 2020: 88-109

## References

- [1] Adams-Prassl, A., T. Boneva, M. Golin, and C. Rauh. 2020. "Inequality in the Impact of the Coronavirus Shock: Evidence from Real Time Surveys". Manuscript, Oxford University.
- [2] Ahn, H., and J. Hamilton. 2019. "Heterogeneity and Unemployment Dynamics" *Journal of Business & Economic Statistics*.
- [3] Alvarez, F., D. Argente, and F. Lippi. 2020. "A simple planning problem for COVID-19 lockdown." Manuscript, University of Chicago.
- [4] Atkeson, A. 2020. "What Will Be the Economic Impact of COVID-19 in the US? Rough estimates of disease scenarios." Manuscript, UC Los Angeles.
- [5] Berger, D., K. Herkenhoff, and S. Mongey. 2020. "An SEIR Infectious Disease Model with Testing and Conditional Quarantine." Manuscript, University of Chicago.
- [6] Bick, and Blandin. 2020. "Real Time Labor Market Estimates During the 2020 Coronavirus Outbreak." Manuscript, Arizona State University.
- [7] Davis, S., and T. von Wachter. 2011. "Recessions and the Costs of Job Loss." *Brookings Papers on Economic Activity*.
- [8] Dingel, J., and B. Neiman. 2020. "How Many Jobs Can Be Done at Home?" *Covid Economics*.
- [9] Eichenbaum, M., S. Rebelo, and M. Trabandt. 2020. "The Macroeconomics of Epidemics." Manuscript, Northwestern University.
- [10] Fernandez-Villaverde, J., and C. Jones. 2020. "Estimating and Simulating a SIRD Model of COVID-19 for Many Countries, States, and Cities." Manuscript, University of Pennsylvania.
- [11] Fujita, S., and G. Moscarini. 2017. "Recall and Unemployment." *American Economic Review* 107: 3875-3916.
- [12] Garibaldi, P., E. Moen, and C. Pissarides. 2020. "Modelling Contacts and Transitions in the SIR Epidemics Model." *Covid Economics*.
- [13] Gertler, M., and A. Trigari. 2009. "Unemployment Fluctuations with Staggered Wage Bargaining." *Journal of Political Economy* 117: 38-86.
- [14] Glover, A., J. Heathcote, D. Krueger, and J.-V. Ríos-Rull. 2020. "Health versus Wealth: On the Distributional Effects of Controlling a Pandemic." *Covid Economics*.
- [15] Gregory, V., G. Menzio, and D. Wiczer. 2020. "Heterogeneous Workers and Aggregate Fluctuations." Manuscript, New York University.
- [16] Guerrieri, V., G. Lorenzoni, L. Straub and I. Werning. 2020. "Macroeconomic Implications of COVID-19: Can Negative Supply Shocks Cause Demand Shortages?" Manuscript, MIT.

- [17] Hagedorn, M., and I. Manovskii. 2008. “The Cyclical Behavior of Unemployment and Vacancies Revisited.” *American Economic Review*, 98: 1692–706.
- [18] Hall, R., 2005. “Employment Fluctuations with Equilibrium Wage Stickiness.” *American Economic Review*, 95: 50-65.
- [19] Hall, R., and P. Milgrom. 2008. “The Limited Influence of Unemployment of the Wage Bargain.” *American Economic Review*, 98: 1653–74.
- [20] Jacobson, L., R. LaLonde, and D. Sullivan. 1993. “Earnings Losses of Displaced Workers.” *American Economic Review*, 83: 685-709.
- [21] Jones, C., T. Philippon, and V. Venkateswaran. 2020. “Optimal Mitigation Policies in a Pandemic: Social Distancing and Working from Home.” Manuscript, New York University.
- [22] Kapicka, M., and P. Rupert. 2020. “Labor Markets during Pandemic.” Manuscript, UC Santa Barbara.
- [23] Kaplan, G., B. Moll, and G. Violante. 2020. “The Pandemic According to HANK.” Manuscript, University of Chicago.
- [24] Kudlyak, M., and R. Hall. 2019. “Job-Finding and Job-Losing: A Comprehensive Model of Heterogeneous Individual Labor-Market Dynamics Paper.” FRB San Francisco WP No. 19-05.
- [25] Menzio, G., and E. Moen. 2010. “Worker Replacement.” *Journal of Monetary Economics*, 57: 623-636.
- [26] Menzio, G., and S. Shi. 2010. “Block Recursive Equilibria for Stochastic Models of Search on the Job.” *Journal of Economic Theory* 145: 1453-1494.
- [27] Menzio, G., and S. Shi. 2011. “Efficient Search on the Job and the Business Cycle.” *Journal of Political Economy* 119: 468–510.
- [28] Menzio, G., I. Telyukova and L. Visschers. 2016. “Directed Search over the Life Cycle.” *Review of Economic Dynamics*, 19: 38-62.
- [29] Moen, E. 1997. “Competitive Search Equilibrium.” *Journal of Political Economy*, 105: 385-411.
- [30] Morchio, I. 2020. “Work Histories and Lifetime Unemployment.” *International Economic Review* 61.
- [31] Mortensen, D., and C. Pissarides. 1994. “Job Creation and Job Destruction in the Theory of Unemployment.” *Review of Economic Studies* 61: 397–415..
- [32] Pissarides, C. 1985. “Short-Run Equilibrium Dynamics of Unemployment, Vacancies and Real Wages.” *American Economic Review* 75: 676–90.
- [33] Shimer, R. 2005. “The Cyclical Behavior of Unemployment and Vacancies.” *American Economic Review* 95: 25–49.

# Equilibrium social distancing<sup>1</sup>

Flavio Toxvaerd<sup>2</sup>

Date submitted: 30 April 2020; Date accepted: 1 May 2020

*This paper presents an economic model of an epidemic in which susceptible individuals may engage in costly social distancing in order to avoid becoming infected. Infected individuals eventually recover and acquire immunity, thereby ceasing to be a source of infection to others. Under non-cooperative and forward-looking decision making, equilibrium social distancing arises endogenously around the peak of the epidemic, when disease prevalence reaches a critical threshold determined by preferences. Spontaneous, uncoordinated social distancing thus acts to 'flatten the curve' of the epidemic by reducing peak prevalence. In equilibrium, social distancing stops once herd immunity sets in, but acts to extend the duration of the epidemic beyond the benchmark of a non-behavioral epidemiological model. Comparative statics with respect to the model parameters indicate that the curve becomes flatter (i) the more infectious the disease is and (ii) the more severe the health consequences of the disease are for the individuals.*

1 Generous feedback from Harjoat Bhamra, Frederick Chen, Eli Fenichel, Chryssi Giannitarou, Robert Rowthorn and Anthony Yates is gratefully acknowledged.

2 University Lecturer, Faculty of Economics, University of Cambridge.

Copyright: Flavio Toxvaerd

F. TOXVAERD

“...[the Black Death made people] shun and flee from the sick and all that pertained to them, and thus doing, each thought to secure immunity for himself”.

- Boccaccio's *The Decameron* (1353)

## 1. INTRODUCTION

The world is currently gripped by the COVID-19 pandemic. At the time of writing, there is no vaccine available against this virus and no antiviral therapies to increase the speed of recovery. The only available strategies to stem the spread of the disease are behavioral interventions such as *social distancing*. Social distancing refers to any non-pharmaceutical intervention, taken by individuals or by policy makers, which acts to decrease the contact rate between infected and susceptible individuals.<sup>1</sup> Reducing the contact rate is often held to be the central tool to “*flatten the curve*”, i.e. to reduce disease incidence and hence the number of infected individuals. In some countries such as the United Kingdom, governments have refrained from directly imposing restrictions on individuals and have instead appealed to citizens to act in the interests of society and to voluntarily withdraw from the public space. The question is then, when left to their own devices, how much social distancing will there be in equilibrium? And how does this depend on biological and preference parameters? The United Kingdom's response to the COVID-19 pandemic and the scientific research underlying it is heavily predicated on behavior changes that reduce the contact rate in the population (see Ferguson et al., 2020, Ferguson et al. 2006 and Halloran et al., 2008). The overwhelming focus of governments' responses to the epidemic on behavioral responses of the population makes it incumbent upon researchers to be clear about how and why individuals act as the epidemic unfolds. What are their constraints and incentives? Will they voluntarily comply with directions given by public health officials or do governments need to compel certain behaviors, as has now been seen across the world?

On current evidence, much of the thinking around social distancing is based on epidemiological simulations and modeling that eschew a nuanced analysis of human behavior in the face of epidemics. Specifically, most of the modeling is based on assumptions about how individuals will behave under a set of interventions such as travel restrictions, school closures and bans on sporting and cultural events and mass gatherings. But since behavior is the central issue, we must be careful about how we model it and strive to incorporate behavioral considerations more fully into our analysis of disease control. We cannot simply rely on traditional analyses that do not model behavior but augment these with ad-hoc interventions that rely on guesses about compliance rates. The standard epidemiological models are an excellent starting point for analysis, but must be made complete by fully integrating them with more sophisticated models of human decision-making and behavior. Empirical evidence shows that individuals indeed respond to disease outbreaks by changing behavior (see e.g. Kumar et al. 2012, Bayham et al., 2015, Bayham and Fenichel, 2016 and references therein).

Lauren Gardner, a public health expert and modeler of epidemics at Johns Hopkins, recently stated that

“When people change their behavior, [epidemiological] model parameters are no longer applicable.”<sup>2</sup>

<sup>1</sup>When social distancing is imposed on a sub-population by a government, it is often referred to as *quarantines*; when it is voluntary and chosen by individuals themselves, it is known as *self-isolation*.

## EQUILIBRIUM SOCIAL DISTANCING

In other words, we must revisit the traditional models to fully account for human behavior. This paper is a contribution towards this goal.

This paper analyzes social distancing by means of a continuous-time, infinite-horizon economic-epidemiological model of an infectious disease. A closed population of individuals face a disease of the susceptible-infected-removed variety, which is an appropriate setting for analyzing the spread of COVID-19.<sup>3</sup> At each instant, individuals non-cooperatively decide whether to engage in costly social distancing and in doing so, trade off the benefits of social interactions against the risk of contracting the communicable disease.

I find that each individual's optimal strategy is described succinctly in terms of a threshold infection probability, which depends on aggregate disease prevalence. For sufficiently low disease prevalence, as may be found at the beginning or the end of an epidemic, the risks from social interactions are small and thus individuals choose not to socially distance themselves. For higher levels of disease prevalence, the risk of exposure may outweigh the benefits and so individuals switch to social distancing. In this case, aggregate equilibrium disease prevalence remains constant through time until sufficiently many individuals have gone through the cycle *susceptible*  $\rightarrow$  *infected*  $\rightarrow$  *recovered* to cause disease prevalence to fall without further social distancing. In a sense, individuals' equilibrium social distancing decisions act as a flow rate regulator between healthy and recovered individuals, where the underlying uncontrolled flow rates are determined by the biological features of the disease.

The analysis emphasizes that while the equilibrium extent of social distancing is not socially optimal, aggregate equilibrium infection across the epidemic is lower than what a traditional non-economic epidemiological analysis would suggest. In other words, a purely non-behavioral model would tend to overstate the severity of the epidemic relative to one that features rational behavior. While this by no means implies that equilibrium is socially optimal, it does mean that the worst-case scenario under a laissez-faire policy is not that predicted by purely biological considerations.<sup>4</sup>

To further contrast the predictions of the economic model with those of a purely epidemiological model, I characterize the equilibrium dynamics in terms of several properties of the aggregate disease dynamics, namely in terms of *peak prevalence*, *duration* and *final size distribution*. I find that equilibrium social distancing will tend to reduce peak prevalence, increase duration and decrease cumulative incidence, which can be thought of as an inverse measure of herd immunity. Interestingly, I find that the comparative statics predictions of the economic model are the reverse of those in the uncontrolled epidemiological model. For example, peak prevalence and cumulative incidence are both *increasing* in the infectiousness of the disease in the biological model, whereas they are *decreasing* in the economic model. This is because the endogenously determined social distancing decisions of the individuals react to higher infectiousness by engaging in more protective behavior.

The formal economic analysis of social distancing is sparse. Sethi (1978) analyzes the

<sup>2</sup><https://www.nytimes.com/2020/03/13/us/coronavirus-deaths-estimate.html?referringSource=articleShare>

<sup>3</sup>This model is also known as that of a general epidemic. See Kermack and McKendrick (1927) for the original treatment. Disease-induced deaths can be incorporated explicitly in the model but are not considered in order to simplify the exposition.

<sup>4</sup>In the present model, equilibrium will not be socially optimal since individuals do not internalize the positive externalities that flow from their decisions to socially distance themselves.

problem of a social planner in the context of the simpler susceptible-infected-susceptible SIS model of disease in which recovered individuals are not immune to further infection. Chen et al. (2011), Gersovitz and Hammer (2004), Gersovitz (2010) and Toxvaerd (2019) consider equilibrium social distancing in the SIS model under decentralized decision-making, while Rowthorn and Toxvaerd (2015) consider the interaction between social distancing and treatment with antivirals, both in equilibrium and under central planning. Toxvaerd and Rowthorn (2020) consider the equilibrium and socially optimal inducement of immunity via vaccination and treatment. Reluga (2010) analyzes a differential game model of social distancing with a finite horizon, no discounting and (eventual) vaccination. Chen (2012) studies social distancing in the susceptible-infected-recovered SIR model under more general matching functions than the standard mass-action specification used in the epidemiological literature and finds that for some specifications of the matching function, there may be scope for multiple Nash equilibria at each point in time, making it difficult to predict the course of the epidemic.

In contrast to these papers, I consider an SIR framework in which individuals are perfectly forward-looking but where each is small relative to a large population, thereby side-stepping the difficulties involved in differential games. Furthermore, in the present setting there is a unique equilibrium path through the epidemic, allowing me not only to predict the course of the epidemic (within the model) but also to perform meaningful comparative statics with respect to biological and preference parameters. Last, Fenichel et al (2011) and Fenichel (2013) consider social distancing in the SIR model when individuals have concave utility functions. Fenichel (2013) considers the properties of decentralized equilibrium and socially optimal social distancing when susceptible, infected and recovered individuals can vary their exposure levels differentially. He argues that in such a setting, a second-best policy that requires all individuals to socially distance themselves to the same extent may be inferior to a *laissez-faire* policy. Here, the main focus is on the differences between the dynamics under equilibrium behavior and those in the uncontrolled epidemiological model. In addition, the dependence of the dynamics on preference parameters is explored and the present results are thus complementary to his analysis.

The paper is organized as follows. In Section 2, I present the economic-epidemiological model and briefly review the classical analysis of the susceptible-infected-recovered model. This is to set the stage for the subsequent analysis of individual decision-making and characterization of equilibrium dynamics under social distancing, contained in Section 3. In Section 4, I discuss the results and conclude.

## 2. THE MODEL

The model is an economic extension of the classical *susceptible-infected-recovered* model and is simple to describe. Time is continuous and runs indefinitely. A closed population consists of a continuum  $[0, 1]$  of infinitely lived individuals who can at each instant  $t \geq 0$  each be in one of three states, namely *susceptible* or *infected* or *recovered*. The measure of susceptible individuals is  $S(t)$ , the measure of infected (and infectious) individuals is  $I(t)$  and the measure of recovered individuals is  $R(t)$ . Because the population size is normalized to one, these measures can be interpreted as fractions. Henceforth,  $I(t)$  shall be referred to as *disease prevalence*.

At each instant, the population mixes homogeneously. This corresponds to pair-wise random matching where each individual has an equal chance of meeting any other indi-

## EQUILIBRIUM SOCIAL DISTANCING

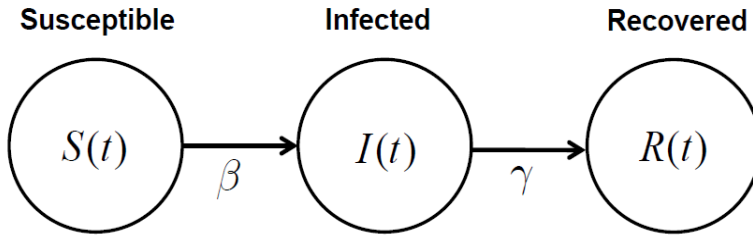


Figure 1: States and Flows in the SIR Model.

vidual, irrespective of the health status of the two matched individuals. A match between an infected and a susceptible individual may infect the susceptible. The rate at which infection is transferred in such a match, absent social distancing, is denoted by  $\beta > 0$ . This parameter captures the infectivity of the disease. Recovered individuals are immune to further infection and also cannot carry the disease. Coupled with the assumption of homogeneous mixing, this means that the aggregate rate at which susceptible individuals become infected is given by  $\beta I(t)S(t)$ . This means that the rate of new infection, or *disease incidence*, is proportional to disease prevalence. The basic model compartments with states and flow rates is illustrated in Figure 1.

Last, infected individuals spontaneously recover at rate  $\gamma \geq 0$ . This means that on aggregate, the rate at which recovery occurs is  $\gamma I(t)$ . Throughout, I will maintain the following assumption:

**Assumption 1:**  $\beta > \gamma \geq 0$ .

This assumption makes the analysis more interesting and will be explained below. To model the possibility of engaging in social distancing, assume that the individuals can affect the rate of infection by controlling the rate at which they expose themselves to infection. In particular, at each instant  $t \geq 0$ , each individual  $i \in \mathcal{S}(t)$  non-cooperatively chooses exposure level  $\varepsilon_i(t) \in [0, 1]$ , at personal cost  $(1 - \varepsilon_i(t))c \geq 0$ . Effectively, this reduces the rate of infection for the individual to  $\varepsilon_i(t)\beta I(t)$ . This formalization captures the notion that, *ceteris paribus*, exposure is desirable. Equivalently, this means that engaging in social distancing is costly to the individual. In this analysis, infected and recovered (and therefore immune) individuals have no private benefits from social distancing and are assumed to not engage in any preventive efforts.

To complete the economic model, assume that the individuals in the susceptible, infected and recovered classes earn flow payoffs  $\pi_S$ ,  $\pi_I$  and  $\pi_R$  respectively and discount the future at rate  $\rho > 0$ . It will be assumed that

$$\pi_S \geq \pi_R \geq \pi_I$$

In contrast to most of the literature on controlled epidemics, I allow for the possibility that  $\pi_S > \pi_R$ . This case captures the possibility of after-effects, i.e. that although an individual recovers from the disease, it may have negative long-term consequences on

health and well-being to have been infected.

In what follows, I will impose the following restriction:

**Assumption 2:**  $c < \frac{\beta}{(\rho+\gamma)(\rho+\beta)} [(\rho + \gamma) \pi_S - \pi_I + (\gamma/\rho)\pi_R]$ .

This assumption ensures that social distancing is state dependent in equilibrium.

**2.1. The Epidemiological Benchmark.** In this subsection, the classical SIR model will briefly reviewed. This is to help build intuition for the equilibrium analysis and to better contrast the equilibrium dynamics with those in the uncontrolled biological model.

The dynamics of the epidemic is described by the following system of differential equations:

$$\dot{S}(t) = -\beta I(t)S(t) \tag{1}$$

$$\dot{I}(t) = I(t) [\beta S(t) - \gamma] \tag{2}$$

$$\dot{R}(t) = \gamma I(t) \tag{3}$$

$$S(t) = 1 - I(t) - R(t) \tag{4}$$

$$S(0) = S_0 > \gamma/\beta, \quad I(0) = I_0, \quad S_0 + I_0 = 1 \tag{5}$$

It follows from the equations that  $\dot{S}(t) \leq 0$  and  $\dot{R}(t) \geq 0$ , but it turns out that the evolution of disease prevalence  $I(t)$  is non-monotonic. The restriction that  $S_0 > \gamma/\beta$  ensures that the epidemic can take hold in the population. With this assumption in place, the overall behavior of the system can be described as follows. The measure of susceptible individuals  $S(t)$  decreases over time while the measure of recovered individuals increases over time. In contrast, the measure of infected individuals initially increases, peaks when  $S(t) = \gamma/\beta$  and then tends to zero. The basic evolution of the uncontrolled, non-behavioral SIR epidemic is illustrated in Figure 2.

Let  $\bar{I}$  denote the *peak prevalence* of the epidemic. The level  $\bar{I}$  is the highest possible disease prevalence when there is no social distancing whatsoever. Peak prevalence for the SIR epidemic is

$$\bar{I} \equiv S_0 + I_0 - \frac{\gamma}{\beta} + \frac{\gamma}{\beta} \log \left( \frac{\gamma}{\beta S_0} \right) \tag{6}$$

The SIR model cannot be fully characterized analytically. Nevertheless, the limiting distribution of health states can be characterized, which shall prove useful in the analysis of the economic model below. Well-known steps lead to the central result in epidemiology that the final epidemic size is characterized by the equations<sup>5</sup>

$$S(\infty) = 1 - R(\infty) = S(0) \exp(-R(\infty)\mathcal{R}_0) \geq 0 \tag{7}$$

where  $\mathcal{R}_0 \equiv \beta/\gamma$  is the *basic rate of reproduction*.

The basic rate of reproduction represents how many secondary infections are caused by the insertion of a single infected individual into a fully susceptible population. The second equation in (7) defines  $R(\infty)$  implicitly and the first equation defines  $S(\infty)$  as the residual, which is possible since  $I(\infty) = 0$ . The limiting proportions  $S(\infty)$  and  $R(\infty)$

<sup>5</sup>See Brauer and Castillo-Chavez (2012).

EQUILIBRIUM SOCIAL DISTANCING

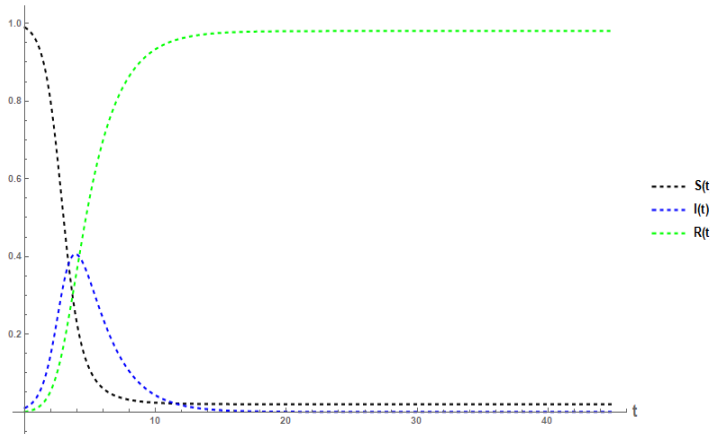


Figure 2: Dynamics of susceptible, infected and recovered in classical SIR model.

are easily found for particular parameterizations of the model. As is to be expected, cumulative incidence  $R(\infty)$  is an increasing function of the infectivity parameter  $\beta$  and a decreasing function of the rate of spontaneous recovery  $\gamma$ .

There are two important insights that follow from equation (7). First, in the limit the disease must die out and no infected individuals remain. Second, and more importantly, when the disease dies out, there is generically a positive measure of susceptibles remaining in the population. This shows that what causes the disease to die out is not that there is eventually a lack of susceptibles that can be infected. Rather, it dies out because the measure of recovered individuals, which must grow over time, becomes so large that the contact between infected and susceptible individuals becomes too rare for the infection to be passed on. Infected individuals have increasingly long sequences of matches with recovered individuals (or between themselves) and so, on expectation, will recover before having the opportunity to pass on the infection to a susceptible individual. Thus with increasing frequency, the chains of infection are broken. The remaining susceptible individuals are said to be protected by *herd* (or *population*) immunity as they benefit from the protection that the recovered individuals give.

The basic rate of reproduction plays a central role here. If  $\mathcal{R}_0 < 1$ , then infection cannot take hold in the population. If  $\mathcal{R}_0 > 1$ , then infection first flares up and then tapers off. In the characterization of equilibrium social distancing, the basic rate of reproduction will play a prominent role as well, not as an aim in itself, but as a feature of the equilibrium dynamics.

The economic version of the model inherits a number of simplifying assumptions from the classical model. First, there is only one disease and one level (or severity) of infection. In particular, this rules out the possibility of superinfection by different strains of the disease. Second, the *incubation period* has zero length. This means that the moment that an individual is infected coincides with the onset of symptoms, so no infected individual acts under the mistaken belief that he or she is susceptible. Last, once an individual becomes infected, he or she immediately becomes infectious to other individuals (i.e. the *latency period* has zero length). Relaxing any of these assumptions

constitutes possible extensions of the present work.

Last, the analysis is based on the implicitly assumption that only susceptibles ever engage in social distancing, as strictly self-interested infected or recovered individuals face no risks from social interactions.

### 3. EQUILIBRIUM SOCIAL DISTANCING

In making a decision on how much preventive effort to engage in, the individual must trade off the net benefits of remaining susceptible (through costly prevention) and the net benefits of exposure (with its inherent risks of becoming infected). But since the transition from infected to recovered is beyond the influence of the individual, he or she may treat the problem as one with only two (health) states, namely *susceptible* and *non-susceptible*.

Let  $\mathcal{S}(t)$  denote the set of susceptibles at time  $t \geq 0$ . For an individual  $i \in \mathcal{S}(t)$ , the social distancing decision influences his or her probability of becoming infected. Let  $p_i(t) \in [0, 1]$  denote that probability at instant  $t \geq 0$ . The problem to be solved by a susceptible individual is then given by

$$\max_{\varepsilon_i(t) \in [0,1]} \int_0^\infty e^{-\rho t} \{ (1 - p_i(t)) [\pi_S - (1 - \varepsilon_i(t))c] + p_i(t) \rho V_I \} dt \tag{8}$$

$$s.t. \quad \dot{p}_i(t) = \varepsilon_i(t) \beta I(t) (1 - p_i(t)), \quad p_i(0) = p_{i0} \tag{9}$$

where the value of transitioning into the infected state can be calculated as<sup>6</sup>

$$V_I = \frac{1}{\rho + \gamma} \left[ \pi_I + \gamma \frac{\pi_R}{\rho} \right] \tag{10}$$

The value can be understood as follows. Once infected, the individual experiences flow utility  $\pi_I$  until he or she recovers. From then on, the individual earns flow utility  $\pi_R$  in perpetuity. The recovery date is governed by a Poisson process with rate  $\gamma$  and cannot be influenced by the individual.<sup>7</sup> The value  $V_I$  is simply the expected discounted lifetime utility of an individual in the infected state. Last, observe that

$$\lim_{\gamma \rightarrow 0} V_I = \frac{\pi_I}{\rho}, \quad \lim_{\gamma \rightarrow \infty} V_I = \frac{\pi_R}{\rho} \tag{11}$$

In steady state,  $\dot{p}_i(t) = 0$ . Assuming that the agent has positive exposure, this means that in steady state, *either* the individual has become infected at some point in time  $t \geq 0$  so  $p_i(t) = 1$  (but has recovered since), *or* infection has died out so  $I(t) = 0$  before the individual became infected, in which case he or she remains susceptible in perpetuity.

Note that no individual can influence the evolution of disease prevalence and this is thus taken as exogenously given. Thus each individual's problem is solved on the background of the aggregate evolution of the infectious disease. This is in turn described by the following modified logistic growth equation, which is a function of the aggregate

<sup>6</sup>See the Appendix for the derivation.

<sup>7</sup>For equilibrium models with treatment augmented recovery, see Rowthorn and Toxvaerd (2015) for the SIS case with no immunity and Toxvaerd and Rowthorn (2020) for the SIR case with immunity.

EQUILIBRIUM SOCIAL DISTANCING

social distancing efforts across the population of susceptibles:

$$\dot{I}(t) = I(t) [\varepsilon(t)\beta S(t) - \gamma], \quad \varepsilon(t) \equiv \int_{i \in S(t)} S(t)^{-1} \varepsilon_i(t) di \tag{12}$$

Letting  $\eta(t)$  denote the current-value costate variable, the individual’s current-value Hamiltonian is given by

$$H = p_i(t) \frac{1}{\rho + \gamma} [\rho\pi_{\mathcal{I}} + \gamma\pi_{\mathcal{R}}] + (1 - p_i(t))[\pi_{\mathcal{S}} - (1 - \varepsilon_i(t))c] + \eta(t)\varepsilon_i(t)\beta I(t)(1 - p_i(t)) \tag{13}$$

The optimality condition, supposing that  $p_i(t) < 1$ , is given by

$$\frac{\partial H}{\partial \varepsilon_i(t)} = \eta(t)\beta I(t) + c = 0 \tag{14}$$

Thus the privately optimal policy for an individual (i.e. his or her best response function) is given by

$$\varepsilon_i(t) = \begin{cases} 0 & \text{for } -\eta(t)\beta I(t) > c \\ \varepsilon & \text{for } -\eta(t)\beta I(t) = c \\ 1 & \text{for } -\eta(t)\beta I(t) < c \end{cases} \tag{15}$$

for any constant  $\varepsilon \in [0, 1]$ . At first blush, this may seem like a bang-bang type solution but as will become clear, in equilibrium the solution will have a *bang-singular-bang* nature. This means that for some intervals of time (or equivalently, for some levels of disease prevalence), the best response of individuals will be bang-bang and switch between  $\varepsilon_i^*(t) = 0$  and  $\varepsilon_i^*(t) = 1$ . But during a phase around the peak of the epidemic, the best responses will be a singular solution determined by the aggregate measure of susceptibles remaining in the population.

The evolution of the current-value multiplier is given by

$$\dot{\eta}(t) = \rho\eta(t) - \frac{\partial H}{\partial p_i(t)} \tag{16}$$

$$= \eta(t) \left[ \rho + \varepsilon_i(t)\beta I(t) \right] + \left[ \pi_{\mathcal{S}} - \frac{\rho\pi_{\mathcal{I}} + \gamma\pi_{\mathcal{R}}}{\rho + \gamma} - (1 - \varepsilon_i(t))c \right] \tag{17}$$

Using the indifference condition (14) with the equation  $\dot{\eta}(t) = 0$  to eliminate  $\eta(t)$  yields the critical threshold of disease prevalence

$$I^* \equiv \frac{\rho c}{\beta \left( \pi_{\mathcal{S}} - \frac{\rho\pi_{\mathcal{I}} + \gamma\pi_{\mathcal{R}}}{\rho + \gamma} - c \right)} \tag{18}$$

Under Assumption 2,  $I^* \in (0, 1)$ .<sup>8</sup> Now the optimal strategy of a susceptible individual can be expressed in terms of disease prevalence as follows:

<sup>8</sup>Assumption 2 ensures that  $I^* < 1$ . The assumption also implies the weaker condition  $(\rho + \gamma)c < [(\rho + \gamma)\pi_{\mathcal{S}} - \pi_{\mathcal{I}} + (\gamma/\rho)\pi_{\mathcal{R}}]$ , which ensures that  $I^* > 0$ .

	$\beta$	$\gamma$	$c$	$\rho$	$\pi_S$	$\pi_I$	$\pi_R$
$I^*$	-	+	+	+/-	-	+	+
$\bar{I}$	+	-	0	0	0	0	0

Table 1: Comparative statics of peak prevalence levels.

$$\varepsilon_i(t) = \begin{cases} 0 & \text{for } I(t) > I^* \\ \varepsilon & \text{for } I(t) = I^* \\ 1 & \text{for } I(t) < I^* \end{cases} \quad (19)$$

for any constant  $\varepsilon \in [0, 1]$ .

The comparative statics of the threshold value  $I^*$  and peak prevalence  $\bar{I}$  are listed in Table 1.

It is noteworthy that peak prevalence  $\bar{I}$  for the purely biological model is increasing in the infectiousness of the disease  $\beta$ , while the maximum equilibrium prevalence  $I^*$  is in fact decreasing in  $\beta$ . Similarly, peak prevalence is decreasing in the recovery rate  $\gamma$  in the biological model but increasing in  $\gamma$  in the economic model. Thus the economic and the biological models offer sharply different predictions about how the characteristics of the disease will influence the course of the epidemic. That increased infectiousness will decrease individuals' incentives to self-protection is a feature also seen in the work of Philipson and Posner (1993), Geoffard and Philipson (1996), Fenichel (2013) and Toxvaerd (2019). It can be understood as follows.

Controlling for behavior, i.e. *holding behavior fixed*, higher infectiousness necessarily leads to more infected individuals. This is intuitive and in fact what the classical epidemiological model predicts. But in the behavioral model, behavior is *not fixed* but endogenously determined and changes as the environment changes. This is because the society in the economic model is populated by utility maximising individuals who each weigh the costs and benefits of social distancing. For these individuals, as the infectiousness increases, social distancing becomes more attractive because exposure now leads to a higher probability of becoming infected. As a result, individuals respond to increased infectiousness by scaling back exposure and socially distancing themselves. On aggregate, this behavioral response acts to curb disease incidence and hence decrease peak prevalence.

**3.1. No Social Distancing Scenario.** Next, I turn to the characterization of the equilibrium social distancing choices and the concomitant behavior of the dynamics of the epidemic. There are two cases to consider, namely  $I^* < \bar{I}$  and  $I^* \geq \bar{I}$  and each scenario will be characterized in turn. When  $I^* \geq \bar{I}$ , the disease is not very serious as seen from the perspective of individuals themselves and thus they never engage in any social distancing. That is, disease prevalence in the uncontrolled biological model never reaches levels that prompt individuals to engage in preventive effort. The equilibrium path of disease prevalence therefore exactly coincides with that in the classical SIR model, with infection peaking at  $\bar{I}$ . This is not a trivial case, since it highlights an important feature of continual prevention. Namely, in this type of equilibrium, it is quite possible that a very large proportion will become infected at some point along the way, and that all individuals know this. The key reason for there not being an incentive to engage in

EQUILIBRIUM SOCIAL DISTANCING

social distancing is that the intertemporal distribution of infections is sufficiently spread out, i.e. the infection curve is already sufficiently flat, such that at no given moment is the probability of infection sufficiently high to merit costly prevention. In a nutshell, what matters for prevention is the *intensity* of the epidemic rather than the *duration* of the epidemic.

**3.2. Social Distancing Scenario.** In the case where  $I^* < \bar{I}$ , equilibrium becomes more complicated. Denote by  $S^*(t)$ ,  $I^*(t)$  and  $R^*(t)$  the paths of susceptible, infected and recovered individuals under equilibrium social distancing and define the following threshold values:

$$\underline{t} \equiv \min\{t \geq 0 : I(t) = I^*\} \tag{20}$$

$$\bar{t} \equiv \min\{t \geq 0 : S^*(t) = \gamma/\beta\} \tag{21}$$

Disease prevalence will be defined as *naturally decreasing* if disease incidence is negative in the absence of social distancing. In other words, disease prevalence is naturally decreasing when even with no preventive behaviour, there are sufficiently few remaining susceptibles to ensure that the number of infected individuals declines. Then, the uncontrolled epidemic becomes naturally decreasing at time  $\tilde{t}$ , defined implicitly by

$$\tilde{t} \equiv \min\{t \geq 0 : S(t) = \gamma/\beta\}$$

Because social distancing induces (weakly) lower disease incidence for all  $t$ , it has to be that  $I^*(t) \leq I(t)$ . But this implies that

$$S^*(\tilde{t}) > S(\tilde{t}) = \gamma/\beta$$

In other words, at the point in time at which disease prevalence on the uncontrolled path starts decreasing, the equilibrium disease incidence would be positive (i.e. disease prevalence would *increase*) were the individuals to cease social distancing. This means that in a sense, in equilibrium social distancing prolongs the duration of the epidemic. To use a phrase much discussed in recent policy debates, in equilibrium the individuals will act to “*flatten the curve*” out of an uncoordinated desire for self-preservation.

Equilibrium behavior can now be characterized as follows:

**Proposition:** If  $I^* < \bar{I}$ , then in a symmetric equilibrium, exposure at time  $t \geq 0$  for each individual  $i \in \mathcal{S}(t)$  is given by

$$\varepsilon_i^*(t) = \begin{cases} \frac{\gamma}{\beta S(t)} & \text{for } t \in (\underline{t}, \bar{t}) \\ 1 & \text{for } t \notin (\underline{t}, \bar{t}) \end{cases} \tag{22}$$

**Proof:** From the best response function of the individuals, it follows that if  $I(t) > I^*$ , then all individuals will engage in full social distancing, thereby bringing down disease incidence. Similarly, if  $I(t) < I^*$ , then all individuals will fully expose themselves to infection, thereby increasing disease incidence. There are two cases to consider. If disease prevalence is naturally decreasing, then full exposure will continue to be optimal indefinitely. If disease prevalence is not naturally decreasing, then it will move towards the level  $I^*$ . Therefore, in equilibrium, disease prevalence must remain constant until it

Covid Economics 15, 7 May 2020: 110-133

becomes naturally decreasing. Setting  $\dot{I}(t) = 0$  yields the required aggregate exposure level (and thus the individual mixing probabilities) as

$$\varepsilon^*(t) = \frac{\gamma}{\beta S(t)} \quad (23)$$

and the result follows ■

The Proposition shows that in equilibrium, individuals engage in no social distancing until a sufficiently large proportion of the population has become infected. Once it has taken sufficient hold, they switch to a mixed strategy equilibrium in which they attach increasingly high probability to no social distancing. The probability increases as the measure of susceptibles decreases. One can view the strategy of individuals as akin to a thermostat that switches off and on as the temperature is above or below a desired level. An immediate result of the Proposition is as follows:

**Corollary:** During the equilibrium social distancing phase, individuals gradually reduce their social distancing efforts despite the infection probability not decreasing.

This result is noteworthy because it shows that in equilibrium, during the social distancing phase it is the measure of remaining susceptibles that determines the level of social distancing, *not the number of infected individuals*. In fact, during this plateau phase, disease incidence stays constant at the critical threshold  $I^*$  and equilibrium social distancing effort decreases as the measure of susceptibles decreases. During the social distancing phase, i.e. when the best responses are on the singular segment, efforts to decrease exposure to infection are strategic substitutes in that any individual would respond to more social distancing by others with an increase in exposure. The mixed strategy-singular solution nature of equilibrium during the social distancing phase is similar in nature to the steady state equilibrium behavior in Toxvaerd (2019). In that paper, the disease is of the susceptible-infected-susceptible variety and thus individuals cannot obtain immunity. As a consequence, in steady state  $S(t)$  remains constant through time and thus the mixed strategy weights in the singular solution are constant. In contrast, with immunity, the measure of susceptibles must decrease over time, explaining why the equilibrium mixing probabilities must change as time progresses and the state of the epidemic changes.

The the equilibrium path for disease prevalence and the associated equilibrium social distancing efforts are illustrated in Figure 3, which also displays the path of disease prevalence in the uncontrolled biological model for comparison. As can be seen in the figure, at the early stages of the epidemic, individuals choose not to make any social distancing efforts (i.e. they choose to fully expose themselves). This reflects the fact that as disease prevalence is initially very low (and thus the infection risk from exposure commensurately small), individuals do not find social distancing measures worthwhile. Similarly, when the epidemic has run its course and infection has almost died out, individuals will again opt for full exposure. But at the height of the epidemic, during the phase in which the uncontrolled epidemic would have peaked, individuals spontaneously act and engage in social distancing, causing a dampening effect on disease incidence and prevalence.

**Corollary:** The equilibrium trajectory of the disease during the social distancing phase

EQUILIBRIUM SOCIAL DISTANCING

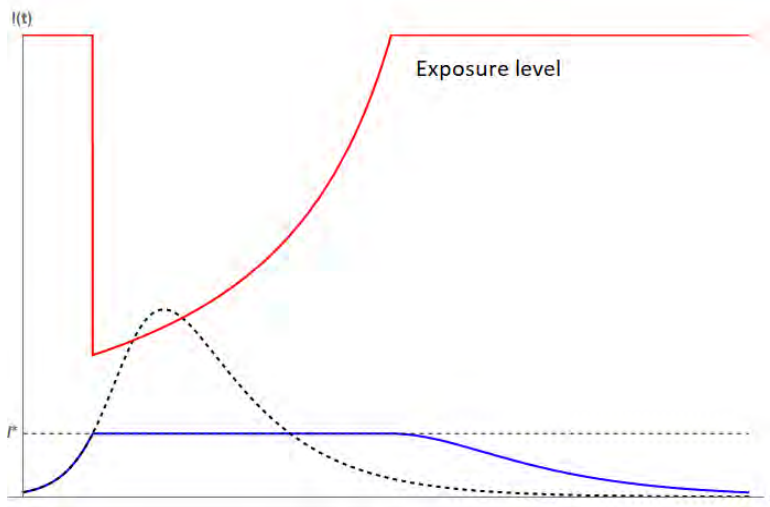


Figure 3: Equilibrium disease prevalence and social distancing across stages of epidemic. The blue curve shows disease prevalence and the red curve shows aggregate exposure.

is characterized by the system of differential equations

$$\dot{S}^*(t) = -\beta \epsilon^*(t) I^* S^*(t) = -\beta \left( \frac{\gamma}{\beta S^*(t)} \right) I^* S^*(t) = -\gamma I^* \tag{24}$$

$$\dot{I}^*(t) = 0 \tag{25}$$

$$\dot{R}^*(t) = \gamma I^* \tag{26}$$

As an aside, the model also has an equilibrium in asymmetric strategies. All that is required on the equilibrium path during the social distancing phase is that on the horizontal segment of the curve, aggregate exposure must equal  $\epsilon^*(t)$ ; it does not matter how this comes about. Since on this segment the individuals are indifferent between full social distancing and full exposure, they are willing to mix between strategies. But it is also consistent with equilibrium to have a fraction  $\epsilon^*(t)$  exposing themselves fully and have the remainder  $(1 - \epsilon^*(t))$  fully socially distancing themselves.

For ease of comparison of disease paths between the non-controlled biological model and the equilibrium under social distancing, Figures 4, 5 and 6 show the evolution of individuals in each health state separately, while Figure 9 at the end of the paper shows all the paths superimposed.

The dynamic equations in the Corollary show another interesting feature, namely that during the social distancing phase, the measure of susceptible individuals decreases linearly at a rate  $-\gamma I^*$ , while the measure of recovered individuals increases linearly at rate  $\gamma I^*$ . In addition, one sees that the rates of change are proportional to the critical threshold  $I^*$ . In other words, we can relate the speed of change over time during the social distancing phase to the magnitude of the biological and preference parameters. For example, an increase in infectivity  $\beta$  will cause the susceptibles to decrease more sharply

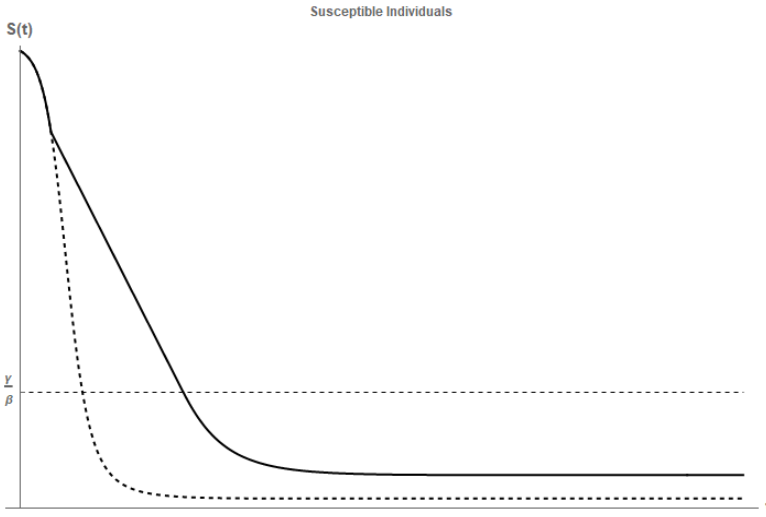


Figure 4: Paths of susceptible individuals across epidemic. Dashed curve shows path in epidemiological model; solid curve shows equilibrium path in economic model.

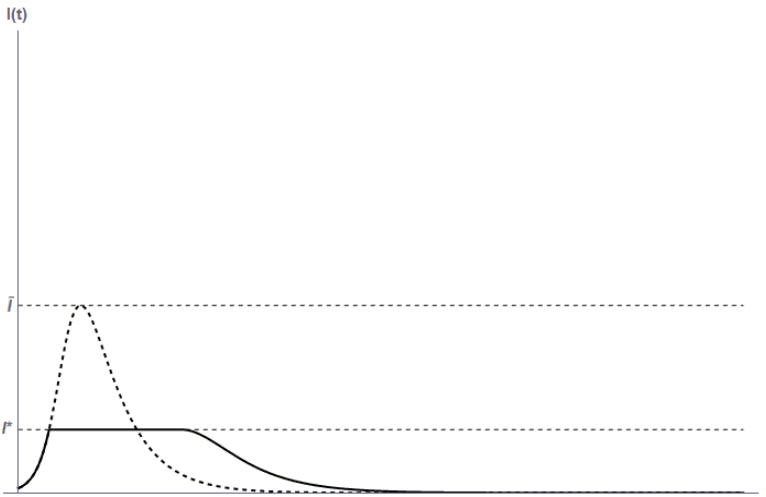


Figure 5: Paths of infected individuals across epidemic. Dashed curve shows path in epidemiological model; solid curve shows equilibrium path in economic model.

Covid Economics 15, 7 May 2020: 110-133

EQUILIBRIUM SOCIAL DISTANCING

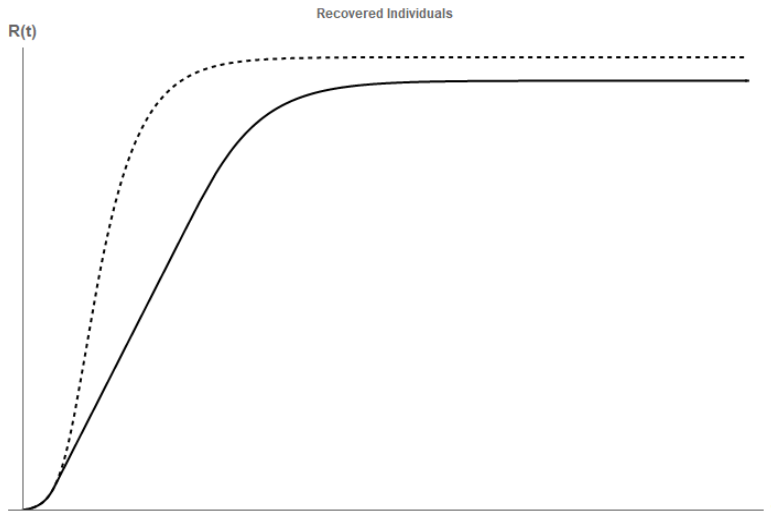


Figure 6: Paths of recovered individuals across epidemic. Dashed curve shows path in epidemiological model; solid curve shows equilibrium path in economic model.

and the recovered to increase more sharply. Similarly, the more severe the disease is, as measured by lower flow utility while infected  $\pi_I$ , will likewise make susceptibles decrease faster and that of the recovered increase faster. The linear segments on the  $S^*(t)$  and  $R^*(t)$  curves can be verified in Figures 4 and 6.

Next, consider how a change in the preference parameters influences the social distancing decisions in equilibrium and how they alter the trajectory of the disease over time. We will do this in terms of effects on peak prevalence and on the duration of the plateau phase with elevated disease prevalence. To trace the effects of changes in the preference parameters, we can simply determine how they influence the critical threshold  $I^*$  and then see what effect this has on the aggregate dynamics. Since the method of analysis is the same for each of the parameters, I will perform this exercise only for a change in the flow payoff  $\pi_I$  that an individual earns when it is infected. This case is illustrated in Figure 7, which shows the effects on the trajectory of infected people when  $\pi_I$  is lowered. This corresponds to making the disease more severe in that it has more dire health consequences. All other parameters are kept fixed. The benchmark case is shown as a solid black curve while the modified case is shown as a solid blue curve. The dashed black curve shows the uncontrolled benchmark for reference. Because the disease is now more severe, individuals have reduced tolerance to infection. This is reflected in a downward shift in the critical threshold  $I^*$ . But this means that social distancing kicks in earlier in equilibrium and also serves to extend the duration of the epidemic (in the sense described earlier). As will be explored further below, this also has consequences for the limiting distribution of the epidemic. As will become clear, although the phase of relatively high disease prevalence is thus increased, the actual number of infected individuals across the epidemic (i.e. cumulative incidence) actually decreases.

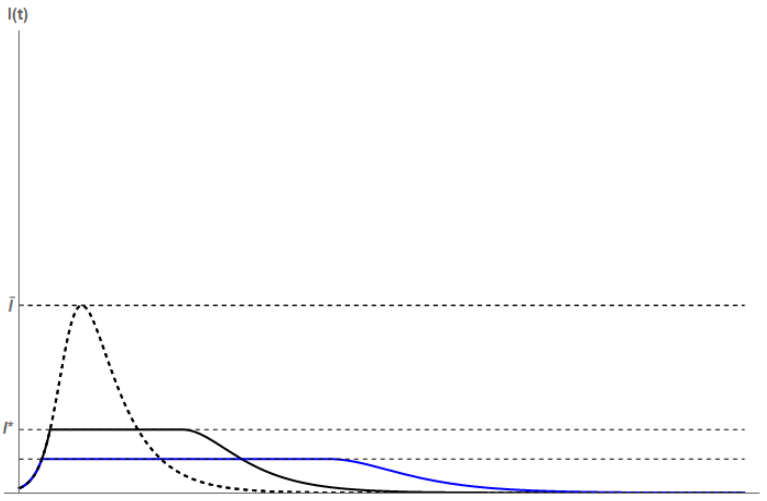


Figure 7: How parameters change the intensity and duration of the epidemic under equilibrium social distancing. Plot shows the evolution of susceptible individuals in the benchmark model in solid black and the evolution when the disease is more severe ( $\pi_I$  is lower) in solid blue.

**Analysis of the limiting distribution.** Till now, I have focused on the evolution of the epidemic across time, which is useful to analyze inter-dependencies between the compartments, growth rates and time-domain properties of the disease. But the time dimension is less useful for determining the limiting properties of the disease, such as the cumulative incidence (i.e. the total number of infected individuals across the epidemic) and how the eventual number of immune and susceptible individuals depend on the initial conditions. For that purpose, and to further compare the equilibrium disease dynamics with social distancing to those under the uncontrolled biological model, it is useful to consider the evolution of infections in the  $(S(t), I(t))$ -plane. This is done in Figure 8. For an arbitrary point in this diagram, the measure of recovered individuals  $R(t)$  is residually determined. For this purpose, note that the dynamics in  $(S(t), I(t))$ -space are characterized by the equation<sup>9</sup>

$$I(t) = S_0 + I_0 - S(t) + \frac{\gamma}{\beta} \log \left( \frac{S(t)}{S_0} \right) \tag{27}$$

To understand the figure, assume that  $R_0 = 0$  and pick an initial point  $(S_0, I_0)$ . This point is denoted by  $a$  on the curve. I will first describe the uncontrolled dynamics in the absence of social distancing and then contrast them with the dynamics in equilibrium. Starting from the initial point  $a$ , infection picks up and the susceptible population decreases, moving the state of the system along the dashed curve peaking at point  $f$  and ending in some point  $(S(\infty), I(\infty))$ , denoted by  $g$ . There are two important points to

<sup>9</sup>See Hethcote and Waltman (1973), who uses this type of diagram to illustrate the effects of an initial pulse vaccination of a fraction of the susceptible population.

EQUILIBRIUM SOCIAL DISTANCING

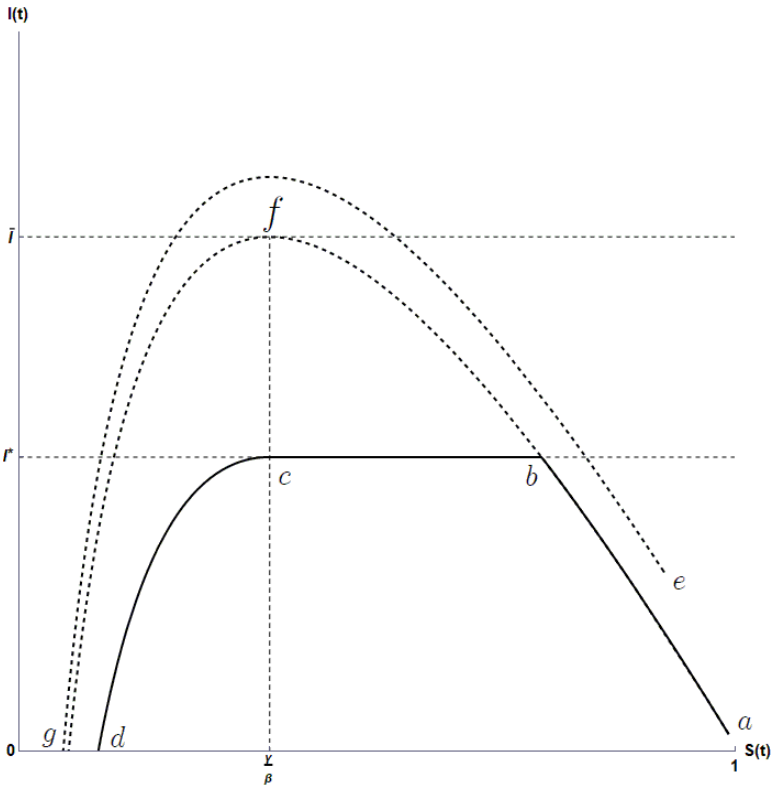


Figure 8: Disease dynamics in the  $(S(t), I(t))$ -plane. Dashed curve shows path in epidemiological model; solid curve shows equilibrium path in economic model.

notice.

First, the curve showing the uncontrolled dynamics has its maximum at  $S(t) = \gamma/\beta$ , irrespective of the initial condition. In other words, all the curves describing the epidemic in  $(S(t), I(t))$ -plane achieve their maximum at the same value of susceptibles. This will turn out to be important for the characterization of the equilibrium dynamics. If one chooses another initial state  $(S'_0, I'_0)$  with  $I'_0 > I_0$ , indicated by  $e$ , then the resulting curve is simply shifted upwards and never intersects the initial curve. The dynamics under this higher initial disease prevalence settles on a lower value for  $S(\infty)$ , as can be verified from the equation that characterizes the final distribution. But note that the shifted curve also has its maximum at  $S(t) = \gamma/\beta$ .

Second, generically, the curves intersect the  $S(t)$ -axis at a point  $(S(\infty), I(\infty))$  at which  $I(\infty) = 0$  and  $S(\infty) > 0$ . In other words, the disease dies out asymptotically, some individuals remain susceptible and  $R(\infty) = 1 - S(\infty)$  become infected at some point during the epidemic but eventually recover. The limiting fraction  $R(\infty)$  measures the aggregate incidence (or total case count) of the epidemic. Next, consider the movement along the  $I(t)$ -dimension. As is clear from the curve, infection initially increases to the point when  $S(t) = \gamma/\beta$  and then decreases.

It is important to emphasize that the speeds along these different uncontrolled disease curves differ and depend on the initial conditions and the parameters  $\beta$  and  $\gamma$  (see Hethcote and Waltman, 1973 for details). As will be shown below, the speed of movement in equilibrium is lower than that in the biological model, as social distancing serves to reduce the speed by suppressing disease incidence.

Next, I turn to the dynamics under endogenous social distancing. In Figure 8, I plot the horizontal line corresponding to the equilibrium cutoff  $I^* < \bar{I}$ . In equilibrium, the initial dynamics from the point  $a$  coincide with those of the biological model until the point  $b$ , where  $I(t) = I^*$ . At that point, the equilibrium and uncontrolled biological paths diverge as the individuals start to socially distance themselves. They do so to an extent that keeps  $I(t)$  constant at the critical level. Thus in equilibrium after the initial stage, the dynamics move horizontally leftward till the point  $c$ , at which no further social distancing is desired by the individuals. As described above, this happens when the infection becomes naturally decreasing. But on the diagram, one readily verifies this must happen at a point where  $S^*(t) = \gamma/\beta$ . Thus once point  $c$  is reached, individuals cease social distancing and thus the dynamics going forward coincide with those of the uncontrolled biological model but with the modified initial condition  $(S_0, I_0) = (\gamma/\beta, I^*)$ . The equilibrium path thus ends at point  $d$ , which can be confirmed to lie strictly to the right of point  $g$ .

In both the uncontrolled biological model and in the model with social distancing, the infection dies out only asymptotically. Thus the end of the disease cannot be said to occur faster under social distancing than it otherwise would have under a purely non-behavioral model. What is possible though is to determine when the disease starts decreasing naturally under the two scenarios. In the diagram, it is clear that this happens when the fraction of remaining susceptibles reaches the critical threshold  $\gamma/\beta$ . But note that along the uncontrolled biological trajectory, the speed of movement along the curve in the  $(S(t), I(t))$ -plane is

$$\dot{S}(t) = -\beta I(t)S(t) \tag{28}$$

$$= -\beta \left[ S_0 + I_0 - S(t) + \frac{\gamma}{\beta} \log \left( \frac{S(t)}{S_0} \right) \right] S(t) \tag{29}$$

In contrast, during the social distancing phase, the speed of movement is

$$\dot{S}(t) = -\beta I^* S(t) \tag{30}$$

But since  $I^*(t) \leq I^*$  for all  $t \geq 0$ , it follows that the starting point of declining infection happens with a delay under social distancing. Another way to see that infection is suppressed under social distancing is to recall that in the uncontrolled biological model, the churn rate is

$$\frac{\beta S(t)}{\gamma} \tag{31}$$

In other words, each individual who recovers is replaced by  $\beta S(s)/\gamma$  new infected individuals. The dependence of this conversion ratio on the fraction of susceptibles  $S(t)$  is exactly what causes infection to first increase and then decrease. In contrast, under social

EQUILIBRIUM SOCIAL DISTANCING

	$\beta$	$\gamma$	$c$	$\rho$	$\pi_S$	$\pi_I$	$\pi_R$
$S^*(\infty)$	+	-	-	+/-	+	-	-
$R^*(\infty)$	-	+	+	-/+	-	+	+
$S(\infty)$	-	+	0	0	0	0	0
$R(\infty)$	+	-	0	0	0	0	0

Table 2: Comparative statics of final size distributions.

distancing, the churn rate is

$$\frac{\varepsilon^*(t)\beta S(t)}{\gamma} = \frac{\frac{\gamma}{\beta S(t)}\beta S(t)}{\gamma} = 1 \tag{32}$$

In other words, equilibrium exposure is set such that each individual who recovers is replaced by exactly one new individual who is infected.

The suppression of incidence in equilibrium also has effects on the progression of susceptible and recovered individuals. Once social distancing kicks in, as fewer people become infected, the measure of susceptibles declines less steeply. At the same time, the measure of recovered grows less rapidly.

Note that since the curves in the  $(S(t), I(t))$ -plane do not intersect, we can use the intersection between the lines  $I(t) = I^*$  and  $S(t) = \gamma/\beta$  to determine the effects of changes in parameters on the final size distribution. E.g., for two distinct such intersection points (which differ because we vary one of the underlying parameters), we can rank the resulting limiting distributions by following the curves from the initial intersection points to the  $S(t)$ -axis to find the corresponding  $S(\infty)$ -values.

Using the comparative statics of the critical threshold  $I^*$  in Table 1, we find the corresponding effects that the biological and preference parameters have on the final size distribution in the uncontrolled biological model and in the equilibrium in the economic model. These are given in Table 2.

These comparative statics again show that the results from the equilibrium model may reverse those of the uncontrolled biological model. For example, increasing infectiousness  $\beta$  or decreasing the recovery rate  $\gamma$  leads to higher cumulative incidence in the biological model but to lower cumulative incidence in the economic model. The comparative statics with respect to the preference parameters have no biological counterpart and so for these, no comparison is possible.

4. DISCUSSION

This paper has considered the equilibrium amount of social distancing in the context of the well-known SIR epidemiological model. While simple, this model allows for an intuitive and clean analysis of the tradeoffs involved in individuals' decision-making on social distancing. There are several ways in which the analysis can be enriched. First, rather than consider a linear cost of social distancing, other cost structures can be considered. The main insights are robust to this extension. With increasing convex costs of social distancing, individuals would continually adjust to increasing disease prevalence in the population.<sup>10</sup> Second, the paper has not offered a full welfare analysis of the equilibrium.

<sup>10</sup>Note also that although costs (and thus the current-value Hamiltonian) is linear, the symmetric equilibrium is characterised by a singular solution during the social distancing phase. Thus exposure

## F. TOXVAERD

It is immediately clear that the equilibrium is in fact not social welfare maximizing. The reason is a classical one in this type of model, namely that the individuals in the population do not internalize the positive externalities flowing from social distancing. Third, and most interestingly, the analysis has been based on the assumption of a well-mixed population in which all that matters are the fractions of susceptible, infected and recovered. A richer model would consider a population with explicit social structure. This would open up for the possibility that the incentives to socially distance oneself may depend on one's position in the social network. Such an analysis may also be useful in informing policy, such as the socially optimal design and micro-targeting of quarantines.

Last, the population in this model has been assumed to be homogeneous. With a population that is heterogeneous along some dimension, the qualitative nature of the analysis would be similar, but aggregate social distancing would change more continuously, creating a gradual increase and subsequent decrease in social distancing. To see this, suppose that individuals were heterogeneous in how much they suffered from infection. In that case, different individuals would have different tolerances to infection risk and this would mean that each individual would start socially distance itself at different levels of disease prevalence. Initially, only the very risk intolerant in the population would start socially distancing but as prevalence increases further, additional individuals would join them. In this manner, aggregate social distancing would be phased in more smoothly than in the homogeneous population case, in which all switch to social distancing at the same time. The heterogeneous population case also suggests the interesting possibility of free-riding by the more risk tolerant on the efforts of the less risk tolerant. As the latter start socially distancing themselves, disease incidence is curbed somewhat, thus protecting those individuals who have not yet reached their individual social distancing thresholds. In fact, disease prevalence may be curbed so much by the initial social distancing efforts of the risk intolerant that the most tolerant may never have to engage in any social distancing and they would in effect be free-riding on the preventive efforts of those who do.

---

levels in fact vary continuously with the state during this phase.

EQUILIBRIUM SOCIAL DISTANCING

A. APPENDIX

In this Appendix, I derive the value of transitioning into the infected state. Let the recovery date for an infected individual be denoted by  $T$ . This date arrives according to a Poisson process with rate  $\gamma \geq 0$ .

The value we seek to characterize, namely the net present value of being infected at instant  $t \geq 0$  is

$$V_I = \int_t^T e^{-\rho u} \pi_I du + \int_T^\infty e^{-\rho u} \pi_R du \tag{33}$$

Consider a utility flow  $\pi$  which can take two values,  $\pi_I$  and  $\pi_R$ . At time  $t$ , the utility flow starts off with  $\pi = \pi_I$ . Over the time interval  $[t, t + dt)$ , the probability of the utility flow switching to  $\pi_R$  is  $\gamma dt$  and so the probability of the utility flow not switching  $\pi_I$  is  $1 - \gamma dt$ . Define

$$V_I^t = E_t \int_t^\infty e^{-\rho(u-t)} s_u du \tag{34}$$

and assume that  $s_t = \pi_I$ . We do so because for the case where  $s_t = \pi_R$ , we know that the utility flow gets stuck at  $\pi_R$  and so

$$E_t \int_t^\infty e^{-\rho(u-t)} \pi_R du = \pi_R E_t \int_t^\infty e^{-\rho(u-t)} du = \frac{\pi_R}{\rho} \tag{35}$$

Observe also that  $V_I^t$  is independent of  $t$ , by virtue of the infinite horizon and so  $V_I^t = V_I$ . Therefore

$$V_I = \pi_I dt + (1 - \gamma dt) e^{-\rho dt} V_I + \gamma dt e^{-\rho dt} \frac{\pi_R}{\rho} \tag{36}$$

$$V_I = \pi_I dt + [1 - (\rho + \gamma) dt] V_I + \gamma dt \frac{\pi_R}{\rho} + o(dt) \tag{37}$$

$$0 = \pi_I dt - (\rho + \gamma) V_I dt + \gamma dt \frac{\pi_R}{\rho} + o(dt) V_I dt = \frac{\pi_I + \gamma \frac{\pi_R}{\rho}}{\rho + \gamma} dt + o(dt). \tag{38}$$

In the continuous-time limit, we obtain

$$V_I = \frac{1}{\rho + \gamma} \left[ \pi_I + \gamma \frac{\pi_R}{\rho} \right] \tag{39}$$

and the result follows ■

## REFERENCES

- [1] BAYHAM, J., N. V. KUMINOFF, Q. GUNN AND E. P. FENICHEL (2015): Measured Voluntary Avoidance Behaviour During the 2009 A/H1N1 Epidemic, *Proceedings of the Royal Society B*, 282: 20150814.
- [2] BAYHAM, J. AND E. P. FENICHEL (2016): Capturing Household Transmission in Compartmental Models of Infectious Disease, in: Chowell, G., Hyman, J.M. (Eds.), *Mathematical and Statistical Modeling for Emerging and Re-emerging Infectious Diseases*, Springer, ebook, 329-340.
- [3] BRAUER, F. AND C. CASTILLO-CHAVEZ (2012): *Mathematical Models in Population Biology and Epidemiology*, 2nd edition, Springer.
- [4] CHEN, F. (2012): A Mathematical Analysis of Public Avoidance Behavior During Epidemics Using Game Theory, *Journal of Theoretical Biology*, 302, 18-28.
- [5] CHEN, F., M. JIANG, S. RABIDOUX AND S. ROBINSON (2011): Public Avoidance and Epidemics: Insights from an Economic Model, *Journal of Theoretical Biology*, 278, 107-119.
- [6] FENICHEL, E.P., C. CASTILLO-CHAVEZ, M. G. CEDDIA, G. CHOWELL, P. A. GONZALEZ PARRA, G. J. HICKLING, G. HOLLOWAY, R. HORAN, B. MORIN, C. PERRINGS, M. SPRINGBORN, L. VELAZQUEZ AND C. VILLALOBOS (2011): Adaptive Human Behavior in Epidemiological Models, *Proceedings of the National Academy of Sciences*, 108, 6306-6311.
- [7] FENICHEL, E. P. (2013): Economic Considerations for Social Distancing and Behavioral Based Policies During an Epidemic, *Journal of Health Economics*, 32(2), 440-451.
- [8] FERGUSON, N. M. ET AL. (2006): Strategies for Mitigating an Influenza Pandemic, *Nature*, 442, 448-452.
- [9] FERGUSON, N. M. ET AL. (2020): Impact of Non-Pharmaceutical Interventions (NPIs) to Reduce COVID19 Mortality and Healthcare Demand, *Imperial College COVID-19 Response Team*.
- [10] GEOFFARD, P.-Y. AND T. J. PHILIPSON (1996): Rational Epidemics and Their Public Control, *International Economic Review*, 37(3), 603-624.
- [11] GERSOVITZ, M. (2010): Disinhibition and Immiserization in a Model of Susceptible-Infected-Susceptible (SIS) Diseases, *mimeo*.
- [12] GERSOVITZ, M. AND J. S. HAMMER (2004): The Economical Control of Infectious Diseases, *Economic Journal*, 114(492), 1-27.
- [13] HALLORAN, M. E. ET AL. (2008): Modeling Targeted Layered Containment of an Influenza Pandemic in the United States, *Proceedings of the National Academy of Sciences*, 105(12), 4639-644.

## EQUILIBRIUM SOCIAL DISTANCING

- [14] HETHCOTE, H. W. AND P. WALTMAN (1973): Optimal Vaccination Schedules in a Deterministic Epidemic Model, *Mathematical Biosciences*, 18(3-4), 365-381.
- [15] KERMACK, W. O. AND A. G. MCKENDRICK (1927): A Contribution to the Mathematical Theory of Epidemics, *Proceedings of the Royal Society A*, 115(772), 700-721.
- [16] KUMAR, S., S. CROUSE QUINN, K. H. KIM, L. H. DANIEL AND V. S. FREIMUTH (2012): The Impact of Workplace Policies and Other Social Factors on Self-Reported Influenza-Like Illness Incidence During the 2009 H1N1 Pandemic, *American Journal of Public Health*, 102(1), 134-140.
- [17] MORRIS, D. H., F. W. ROSSINE, J. B. PLOTKIN AND S. A. LEVIN (2020): Optimal, Near-Optimal, and Robust Epidemic Control, <https://arxiv.org/pdf/2004.02209.pdf>.
- [18] PHILIPSON, T. AND R. A. POSNER (1993): Private Choices and Public Health: The AIDS Epidemic in an Economic Perspective, *Harvard University Press*.
- [19] RELUGA, T. C. (2010): Game Theory of Social Distancing in Response to an Epidemic, *PLoS Computational Biology*, 6(5):e1000793.
- [20] ROWTHORN, R. AND F. TOXVAERD (2015): The Optimal Control of Infectious Diseases via Prevention and Treatment, *mimeo*.
- [21] SETHI, S. P. (1978): Optimal Quarantine Programmes for Controlling an Epidemic Spread, *Journal of the Operational Research Society*, 29(3), 265-268.
- [22] TOXVAERD, F. (2019): Rational Disinhibition and Externalities in Prevention, *International Economic Review*, 60(4), 1737-1755.
- [23] TOXVAERD, F. AND R. ROWTHORN (2020): On the Management of Population Immunity, *mimeo*.

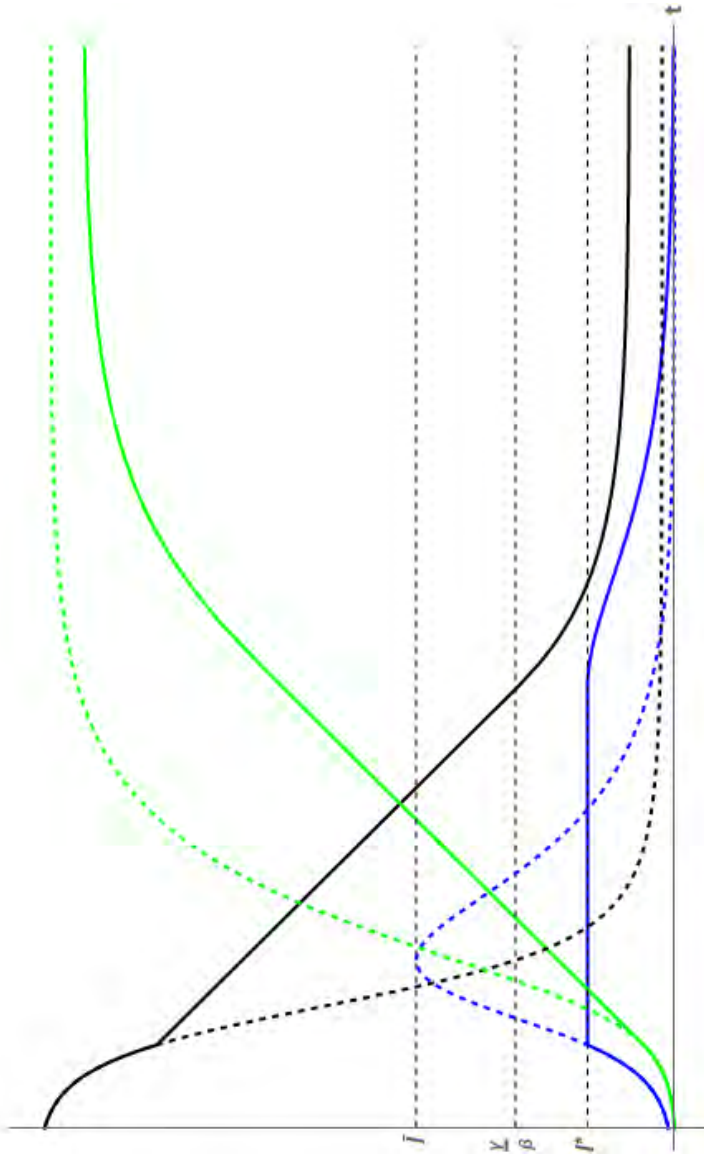


Figure 9: Paths of susceptible, infected and recovered individuals across epidemic. Dashed curves shows paths in epidemiological model; solid curves show equilibrium paths in economic model.

# Public firm borrowers of the US Paycheck Protection Program

Anna Cororaton<sup>1</sup> and Samuel Rosen<sup>2</sup>

Date submitted: 1 May 2020; Date accepted: 3 May 2020

*We provide an initial assessment of the US Paycheck Protection Program by studying the 273 public firms that received a total of \$929 million in loans between April 7-27, 2020. Despite receiving significant media coverage, these firms comprise 0.3% of the funds disbursed. Using guidelines specified by the US Small Business Administration, we document that about half of public firms were eligible to apply, of which 13% were eventual borrowers. Within the set of eligible firms, public firm borrowers tended to be smaller, have more employees, have fewer investment opportunities, have preexisting debt balances, and be located in a county with COVID-19 cases. Implementing additional eligibility requirements may help target funds towards the most constrained firms.*

<sup>1</sup> Assistant Professor of Finance, Cox School of Business, Southern Methodist University.

<sup>2</sup> Assistant Professor of Finance, Fox School of Business, Temple University.

Copyright: Anna Cororaton and Samuel Rosen

# 1 Introduction

The COVID-19 pandemic has caused widespread economic disruption in the US in the first few months of 2020. In response, the US federal government passed and signed into law the Coronavirus Aid, Relief, and Economic Security (CARES) Act on March 27, 2020 which provides over \$2 trillion dollars in relief funds to various sectors and industries in the US economy. One of the major provisions within the Act is the Paycheck Protection Program (PPP), a \$349 billion fund aimed at keeping workers employed by providing forgivable loans to businesses. The program is administered through the US Small Business Administration (SBA). On April 24, an additional \$310 billion was subsequently approved for the program, making PPP one of the largest economic stimulus programs in US history.

In this paper, we provide an initial assessment of the program by analyzing the public firms that received PPP loans. One of the primary reasons for focusing on public firms is the substantial media coverage regarding their loan approvals.<sup>1</sup> In fact, several large public companies, such as Ruth's Chris and Shake Shack, that received PPP loans that were subsequently returned after significant public pressure.<sup>2</sup> The argument has been that public firms do not need PPP funds because they have access to other sources of financing. In order to evaluate this argument, however, it is important to first understand the prepandemic financial condition of these borrowers. Fortunately, detailed financial information about public companies is readily available. We hope that the results of our empirical analysis can provide context to the policy discussion regarding the design or modification of the program moving forward.

In the first part of our analysis, we construct a list of public firms with PPP loans based on their disclosures to the Securities and Exchange Commission (SEC) and document three key facts. First, 273 public firms were granted \$929 million in PPP loans between April 7 and April 27. This represents a mere 0.3% of total funds allocated to the first round of the program. Second, we find that close to half of public firms were eligible for PPP loans based on the criteria outlined by the SBA. Third, 13% of these PPP-eligible public firms

---

<sup>1</sup>See, for example, Pacheco, Inti and Francis, Theo. "Public Companies Got \$500 Million in Small Business Loans." *The Wall Street Journal*. April 22, 2020.

<sup>2</sup>Wallace, Alicia. "Ruth's Chris will return its PPP loans after Treasury says public companies should repay." *CNN Business*. April 24, 2020.

eventually received PPP loans. Other concurrent research efforts document similar total PPP loan amounts to public firms.<sup>3</sup> Therefore the main contribution of this paper lies in understanding the set of PPP-eligible firms.

In the second part of our analysis, we investigate which firm-level characteristics are associated with PPP borrowing using a regression analysis. Overall, our findings suggest that PPP loans were granted to firms specifically targeted by the SBA. First, controlling for industry and location, we find that PPP borrowers tend to be smaller, but have more employees. PPP borrowers are also associated with fewer investment opportunities and fewer cash holdings. A firm with outstanding debt on their balance sheets is 5.3 percentage points more likely to be a PPP borrower, suggesting that preexisting banking relationships are an important determinant for borrowing. Lastly, we find that being located in a county with COVID-19 cases is associated with a 6.0 percentage point increase in the probability of receiving a PPP loan. In sum, PPP borrowers align with the characteristics of companies one would expect to seek assistance from the program.

Given that loans went to eligible firms, how should we view the PPP outcomes as a whole? Because PPP loans are targeted towards retaining workers at their prepandemic wage levels, we calculate the average loan amount per employee. From our data, public firms are able to allocate an average of \$17,758 for each employee. This amount is \$20,319 when we consider all PPP borrowers, regardless of being public or private. From this perspective, PPP loans appear to benefit workers similarly at both public and private firms.

However, we do not wish to downplay the news reports that continue to come out regarding the inability of many small firms to access PPP. Instead, we want to emphasize the need for additional eligibility requirements to direct policy towards aspects of the program that can have the largest potential impact. While the SBA modified its guidelines in late April discouraging large public companies from participating,<sup>4</sup> the program can implement further requirements based on a firm's financial health. Our results suggest that cash-to-assets and outstanding debt levels affect whether a firm borrowed. These requirements can

---

<sup>3</sup>See, among others, Meier and Smith (2020); the Washington Post article by O'Connell et al. "Public companies received \$1 billion in stimulus funds meant for small businesses" from May 1, 2020; and <http://trumpbailouts.org/>.

<sup>4</sup>Specifically, the SBA highlighted that loans must be "necessary to support the ongoing operations of the Applicant." See <https://home.treasury.gov/system/files/136/Paycheck-Protection-Program-Frequently-Asked-Questions.pdf> for details.

also be applied to private firms if the SBA wants to target the most constrained firms. Seru and Zingales propose a similar targeted approach through programs for wages, interest payments, and rent.<sup>5</sup>

Our study is one of the first to empirically investigate the PPP, an unprecedented stimulus program directly aimed at small businesses. Meier and Smith (2020) analyze a similar set of PPP borrowers but they do not consider SBA eligibility or provide overall context to the program. The authors refer to the loans as “bailouts” rather than loans, suggesting the funds are channeled directly to equity holders. Granja, Makridis, Yannelis, and Zwick (2020) use loan-level data from the SBA to study the geographic distribution of PPP funds. They find that PPP funds did not flow to communities that were more adversely affected by the pandemic. We view their results as complementary to ours given that they focus on lenders and the location of borrowers while we focus on the features of borrowers.

Our paper also contributes to growing literature on the impact of COVID-19 on firms. Fahlenbrach, Rageth, and Stulz (2020) find that firms with less financial flexibility faced more negative stock returns in the first few months of 2020. Acharya and Steffen (2020) study the use of credit lines by firms. Albuquerque, Koskinen, Yang, and Zhang (2020) explore how firms with high Environmental and Social (ES) ratings fared in early 2020. Bartik, Bertrand, Cullen, Glaeser, Luca, and Stanton (2020) focus on small businesses and document that over seventy percent of businesses anticipated using the PPP program as of March 26, 2020, and expected funds to significantly influence other business decisions. Also using survey data, Humphries, Neilson, and Ulyssea (2020) find that the smallest businesses were less aware of the PPP compared to larger firms. Baker, Bloom, Davis, and Terry (2020) quantify the significant increase in economic uncertainty in early 2020 using market-, news-, and survey-based measures. Sedláček and Sterk (2020) estimate the effects on startup activity and employment. Rio-Chanona, Mealy, Pichler, Lafond, and Farmer (2020) quantify supply and demand shocks at the industry level.

Finally, our paper contributes to the growing literature that seeks to understand the economic impact of COVID-19. Alon, Doepke, Olmstead-Rumsey, and Tertilt (2020) consider the implications of the impending COVID-19-based recession for gender equality.

---

<sup>5</sup><https://promarket.org/the-stimulus-package-is-too-expensive-and-poorly-targeted-the-waste-contained-in-the-cares-act>.

Giglio, Maggiori, Stroebel, and Utkus (2020) gauge investor short- and long-run expectations through a survey. Inoue and Todo (2020) show how the contractionary effects of lockdown policies can propagate to other cities. Alfaro, Chari, Greenland, and Schott (2020) show that unanticipated changes in predicted infections during the SARS and COVID-19 pandemics forecast aggregate equity market returns. Croce, Farroni, and Wolfskeil (2020) quantify the exposure of major financial markets to news shocks about global contagion risk accounting for local epidemic conditions. Many studies consider the effects of COVID-19 and potential policy responses in a macroeconomic framework (Caballero and Simsek, 2020; Eichenbaum, Rebelo, and Trabandt, 2020; Castro, Miguel Faria e, 2020; Glover, Heathcote, Krueger, and Ríos-Rull, 2020; Krueger, Uhlig, and Xie, 2020; Ludvigson, Ma, and Ng, 2020). Other studies explore the observed economic impact from previous pandemics (Carillo and Jappelli, 2020; Correia, Luck, and Verner, 2020; Daniel Lewis and Stock, 2020; Dahl, Hansen, and Jense, 2020).

The rest of this paper is organized as follows. Section 2 describes the PPP program in more detail. Section 3 describes the construction of our dataset, while 4 analyzes the data in detail. Section 5 concludes.

## 2 Background

The Payment Protection Program (PPP), administered and guaranteed by the US Small Business Administration (SBA), aims to provide immediate economic assistance to US individuals, families, and businesses affected by the COVID-19 pandemic by incentivizing small businesses to retain their workers. It was enacted as part of the Coronavirus Aid, Relief, and Economic Security (CARES) Act, which was signed into law on March 27, 2020. Of the over \$2 trillion in funds available through the CARES Act, \$349 billion was allocated to the PPP.<sup>6</sup>

Firms can allocate PPP loan funds for payroll, rent, mortgage interest, and utility expenses, with at least 75% to be used for paying employees for up to eight weeks. This loan

---

<sup>6</sup>Other programs that were previously available to small businesses for adverse situations were still available. This includes the Economic Injury Disaster Loan (EIDL) emergency program, providing up to \$10,000 per business, and the SBA Express Bridge Loan program, providing up to \$25,000 per business. In addition the SBA promised to pay 6 months of principal, interest, and fees for SBA loans that were disbursed prior to September 2020.

can be forgiven if the firm maintains its employee headcount or quickly rehires its employees while maintaining wages.<sup>7</sup> In addition, payments on this loan can also be deferred for six months, there are no fees associated with the loan, and no collateral or guarantees are required. Loans can also be prepaid without any penalties. The loan is a two year loan with an annual interest rate of 1% and is subject to a \$10 million cap.

SBA lenders, federally insured depository banks, federally insured credit unions, and Farm Credit System institutions were allowed to process PPP loans starting on April 3, 2020. All businesses (including nonprofits, independent contractors, self-employed individuals, and veterans organizations) with 500 or fewer employees can apply. In certain industries, businesses with more than 500 employees can apply if they meet revenue-based or employee-based size thresholds defined by the SBA.<sup>8</sup> In addition, all firms in the hotel and food services industries (NAICS code 72) with 500 or fewer employees per location are eligible to apply. At the time of implementation, there were no other requirements or certifications needed to qualify for a loan.<sup>9</sup>

Although the PPP was scheduled to be open until June 30, 2020, the SBA was overwhelmed with applications within days of the program opening on April 3. On April 16, the SBA announced \$342 billion had been allocated to over 1.6 million small business loans around the country (Small Business Administration, 2020). On April 21, Congress approved another stimulus package, allocating an additional \$310 billion for the PPP. Soon after on April 27, the SBA announced that it resumed taking PPP applications.

### 3 Data

Analyzing the types of public firms that borrowed from PPP requires firm-level data for both borrowers and firms eligible for the program. This section describes the data construction which proceeds in two steps. First, we identify PPP borrowers from their mandatory disclosure reports to the SEC. Second, we collect financial statement information for the set

<sup>7</sup>Payroll costs per employee are capped at \$100,000.

<sup>8</sup>For further detail, see the “Who Can Apply” section on the SBA website (<https://www.sba.gov/funding-programs/loans/coronavirus-relief-options/paycheck-protection-program>).

<sup>9</sup>Latest information about the PPP Program can be found on the SBA website: <https://www.sba.gov/document/support-faq-lenders-borrowers>, and the US Department of Treasury website: <https://home.treasury.gov/policy-issues/cares/assistance-for-small-businesses>.

of public firms and apply the SBA eligibility guidelines for PPP loans.

### 3.1 PPP Borrowers

We construct our list of public firms that borrowed through the PPP program using Form 8-K's submitted to the SEC and available through the EDGAR platform.<sup>10</sup> Form 8-K is a mandatory report of scheduled or unscheduled material information such as major events and/or corporate changes that are relevant to shareholders. An event such as taking out a large loan with a bank counts as a major event. Firms have four days to submit a Form 8-K from the triggering event. We first perform a textual search over all 8-K forms submitted in April 2020, including all attachments and exhibits, for the following keywords: "paycheck," "PPP," "small business administration," "SBA," "cares," and "emergency." We manually review the cases in which at least one of these terms is used and determine whether it represents a PPP loan. Finally, we collect the loan amount and date of the loan reported in the form.<sup>11</sup>

Between April 7 and April 27, 2020, we find 273 public firms that have availed of the PPP program. The list of firms, dates, and associated loan amounts is provided in Table A1 at the end of this paper. In total, public firms took out \$929 million in PPP loans. Relative to the \$349 billion amount designated by the CARES Act (section 2), public firms have comprised a small fraction (0.3%) of aggregate PPP loans.<sup>12</sup> Because PPP loans are targeted towards retaining workers at their prepandemic wage levels, we calculate the average loan amount per employee (table 1). From our data, public firms are able to allocate an average of \$17,758 for each employee. This amount is \$20,319 when we consider all PPP borrowers, regardless of being public or private. From this perspective, PPP loans appear to benefit workers similarly at both public and private firms.

<sup>10</sup>We download all 8-K reports from the EDGAR platform as of April 29, 2020.

<sup>11</sup>The PPP loan is often reported under the item "Entry into a Material Definitive Agreement."

<sup>12</sup>The calculation is almost identical when we use the latest data from the SBA; 1.66 million loans worth \$342.3 billion have been approved as of April 16, 2020 (Small Business Administration, 2020).

	All Firms	Public Firms
Total in US		
Number of Firms	5,996,900	5,544
Employment	128.59 mil	49.96 mil
PPP Eligible <sup>a</sup>		
Number of Firms	5,976,761	1,989
Employment	60.56 mil	3.49 mil
PPP Borrowers		
Number <sup>b</sup>	1,661,367	273
Employment <sup>c</sup>	16.83 mil	0.11 mil
Total Loan Amount	\$342,278.0 mil	\$929.2 mil
Averages		
PPP Loan Amount per Firm	\$206,022	\$3,403,663
PPP Loan Amount per Employee <sup>d</sup>	\$20,319	\$17,758

**Table 1.** Paycheck Protection Program in the Aggregate

Sources: 2017 Statistics of US Businesses conducted by the US Census, US Small Business Administration, Compustat.

<sup>a</sup>For all firms, we assume that firms with fewer than 500 employees are eligible for a PPP loan. For public firms, we apply the SBA criteria to Compustat data. There are fewer public firms in our regression analysis because of additional data requirements.

<sup>b</sup>For all firms, we report aggregate number of PPP loans. For public firms, we report number of distinct firms. Public firms may take on more than one PPP loan if it has multiple subsidiaries.

<sup>c</sup>For all firms, assume that the fraction of employees that accessed PPP is the same as the number of firms that accessed PPP =  $60.56m \cdot \frac{1,661,367}{5,976,761}$ . For public firms, this figure is based only on the 93% of firms for which we have employment data.

<sup>d</sup>For public firms, we report the average PPP loan amount per employee across firms.

### 3.2 PPP Eligible

We construct the list of PPP-eligible firms from Compustat. We apply the SBA guidelines which require that a firm meet criteria based on total dollar receipts or number of employees for its industry to the universe of public firms in the data. As an example, the SBA defines a firm in the farming industry as small if total dollar receipts are less than \$1 million, while a firm in the automobile manufacturing industry is small if it employs fewer than 1,500 employees.<sup>13</sup> For each firm in Compustat, we compute total dollar receipts as the sum of revenue (REVT) and the cost of goods sold (COGS) and use the most recent annual data

<sup>13</sup>The SBA small business size standards for each 6-digit NAICS code industry is found in <https://www.sba.gov/document/support--table-size-standards>.

available since September 2019.<sup>14</sup> We take the number of employees reported in EMP.<sup>15</sup> We restrict our sample to firms that satisfy the following criteria: nonmissing total assets, nonmissing revenue, with at least five employees, nonmissing 2-digit NAICS code. From the 5,544 firms that are active in 2019 in Compustat, 4,233 satisfy these criteria.

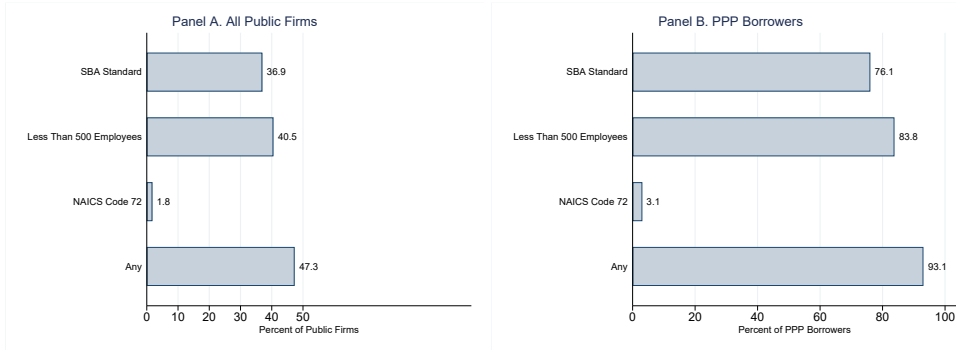


**Figure 1.** PPP Eligibility by SBA Criteria

This figure shows the fraction of firms that satisfy the eligibility criteria for PPP loans for the set of all public firms in Compustat (Panel A) and the set of PPP borrowers (Panel B). “SBA Standard” refers to the employee- and receipts-based guidelines for each 6-digit industry NAICS code imposed by the SBA. For certain industries, firms with up to 1,500 may be eligible. NAICS code 72 (Accommodation and Food Services) refers to the hotel and food services industry.

Of the public firms in Compustat, 2,020 (47.3%) satisfy at least one of the eligibility criteria specified by the SBA. We show the breakdown of this distribution for each of the specified criteria in figure 1 (panel A). In particular, 40.5% percent of public firms have fewer than 500 employees, while 36.9% satisfy the industry-specific standard based on either receipts or employees. A firm may satisfy the 500-employee threshold criteria but not the industry-specific SBA standard because the latter is more often based on total dollar receipts rather than employment. A firm may not satisfy the 500-employee threshold but may satisfy the industry-specific SBA standard based on the number of employees because the latter is often a higher number (as high as 1,500 employees).<sup>16</sup> Finally, a small fraction (1.8%) have

<sup>14</sup>For annual income statement values, we use the year-to-date value in the fourth fiscal quarter if available, or the sum of the trailing four quarterly values.

<sup>15</sup>EMP is only available in the annual Compustat data.

<sup>16</sup>500 out of 1,023 of the 6-digit NAICS codes listed in the SBA standards specify a criteria based on the number of employees. Of these codes, 306 (60%) have a threshold higher than 500 employees. See <https://www.sba.gov/document/support--table-size-standards>.

a 2-digit NAICS code of 72, which is the accommodation and food services sector.

We validate this methodology by applying it to the set of PPP-borrowers. We identify 93.1% of actual PPP borrowers as PPP-eligible, with many of the firms satisfying the 500-employee threshold criteria (figure 1, panel B). While we do not identify a few of the PPP borrowers to be eligible, we still include them in the analysis.

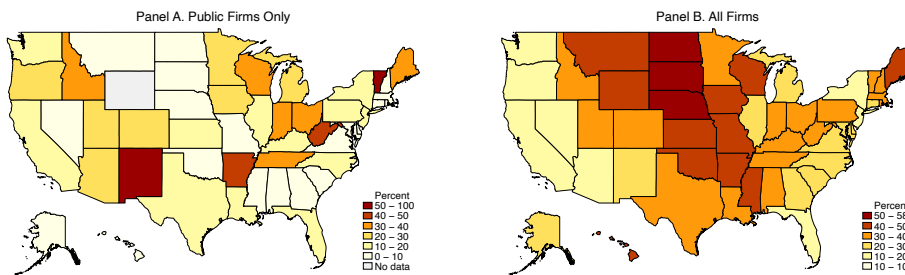


**Figure 2.** Fraction of PPP Eligible Firms that Borrowed, by State

Panel A shows the ratio of the number of public firms that are PPP borrowers (from their Form 8-K reports) to the number of public firms eligible for PPP loans (according to employee- and receipts-based size guidelines by industry from the SBA). Panel B shows the ratio of the number of PPP loans to the number of firms in that state with fewer than 500 employees according to the 2017 Statistics of US Businesses (a proxy for the number of firms eligible for PPP loans).

### 3.3 PPP Across States

PPP borrowers have been geographically distributed across the different states (figure 2). In panel A, we show the fraction of PPP-eligible public firms that borrowed from the program. We calculate this ratio based on the state of the firm's headquarters. For 21 states, less than 10 percent of PPP-eligible firms availed of SBA funding. New Mexico and Vermont have higher take up ratios, but only a few of the firms in our sample are headquartered in those states. For perspective, we show a similar figure for all firms across the country in panel B. In particular, we calculate the fraction of firms with fewer than 500 employees according to the 2017 Statistics of US Businesses (SUSB) that have taken PPP loans according to Small Business Administration (2020). There are close to 6 million firms with fewer than 500 employees across the US, which is a good proxy for the number of all firms eligible for PPP funding.

The maps point to several key takeaways. First, the number of PPP borrowers relative to PPP eligible firms is much higher across all firms compared to public firms. Given that 273 of loans were made to public firms, the vast majority of the 1.66 million issued PPP loans were in fact allocated towards non-public firms. Second, there is geographic dispersion in the percent of eligible firms that are PPP borrowers. In states along the west coast, fewer than 20% of small firms are PPP borrowers (California has the lowest at 15%), while more than half of businesses are PPP borrowers in less populous states (North Dakota is the highest at 58%). This suggests that allocating resources towards processing loans in more populous areas could address some of the bottleneck issues that the program is facing.

### 3.4 Final Data and Summary Statistics

To analyze the set of firms that are PPP-eligible and eventual borrowers, we merge the hand-collected information from the 8-K reports to Compustat. We use a link table of the firm identifier in the SEC filings (CIK) to the firm identifier in Compustat (GVKEY) provided by WRDS.<sup>17</sup> We use the following Compustat variables. A proxy for age (Years in Compustat) is defined as the difference in days between March 31, 2020 and the firms earliest DATADATE value, divided by 365. Return on assets is year-to-date net income (NIIY) for fourth fiscal quarter when available, or the trailing sum of quarterly net income (NIIQ) over the last four quarters divided by the moving average in total assets (ATQ) over the last four quarters.<sup>18</sup> Tobin's Q is defined as the sum of the market value of equity (MKVALTQ) and the difference between ATQ and common equity (CEQQ), all divided by ATQ. Cash to assets is cash (CHQ) divided by assets (ATQ). Total debt is the sum of long-term debt (DLTTQ) and current liabilities (DLCQ), where missing values are assumed to be zero. We define a positive debt dummy to be equal to 1 if a firm has over \$1,000 in total debt. For PPP borrowers, we compute the size of the loan relative to their expenses and liquidity. Annualized operating expense and SG&A are defined as the year-to-date value (XOPRY

<sup>17</sup>The Central Index Key (CIK) identifier is given to an individual, company, or foreign government by the US Securities and Exchange Commission (SEC). Several PPP borrowers (Acquired Sales Corp.; ARC Group, Inc.; Cool Holdings, Inc.; Duos Technologies Group, Inc.; Emerald Biosciences, Inc.; Galaxy Gaming, Inc.; Lodging Fund REIT III, Inc.; Luvu Brands, Inc.; Oblong, Inc.; Pharmacy Value Management Solutions, Inc.; SCI Engineered Materials, Inc.; XG Sciences, Inc.) do not appear in Compustat and are left out of the analysis.

<sup>18</sup>Missing assets are ignored for the moving average calculation.

and XSGAY) for fourth fiscal quarter when available, or the trailing sum of the quarterly values (XOPRQ and XSGAQ) over the last four quarters. We divide the annualized values by 6 because PPP loans are meant to cover 8 weeks of expenses.

Panel A: PPP-Eligible Nonborrowers

	<i>N</i>	Mean	SD	10%	50%	90%
Assets, \$ mil	1664	1411.71	5854.76	8.92	153.11	2956.55
Employees	1664	2001.26	18895.57	12.50	105.00	685.00
Years in Compustat	1664	15.48	11.90	4.00	11.01	34.27
Return on Assets, %	1664	-37.02	80.67	-98.33	-8.84	8.77
Tobin's Q	1664	4.04	8.48	0.88	1.83	7.47
Cash / Assets, %	1664	24.87	27.08	0.90	14.13	71.51
Debt / Assets, %	1664	32.42	32.36	0.00	21.54	87.99
Positive Debt Dummy	1664	0.93	0.25	1.00	1.00	1.00

Panel B: PPP Borrowers

	<i>N</i>	Mean	SD	10%	50%	90%
Assets, \$ mil	250	133.49	348.37	8.86	49.76	283.93
Employees	250	428.98	1133.55	23.50	136.50	779.50
Years in Compustat	250	19.54	12.77	5.01	17.76	38.32
Return on Assets, %	250	-33.57	56.02	-99.56	-12.63	8.22
Tobin's Q	250	2.34	2.42	0.80	1.52	4.80
Cash / Assets, %	250	21.07	21.73	1.56	14.26	52.27
Debt / Assets, %	250	34.40	30.54	0.94	25.94	86.63
Positive Debt Dummy	250	0.97	0.17	1.00	1.00	1.00
PPP Borrowing, \$ mil	250	3.46	3.60	0.53	2.18	8.21
PPP Borrowing / 8wk Oper. Expense, %	243	30.57	16.68	12.84	28.59	50.00
PPP Borrowing / 8wk SG&A, %	220	107.54	149.53	24.54	63.79	247.35
PPP Borrowing / Cash, %	250	420.51	2863.42	6.72	32.33	369.47

Panel C: COVID-19 Exposure Indicators

	Nonborrowers	Borrowers
Positive COVID-19 Cases	0.820	0.948
Any County-Wide Policy	0.663	0.772
- Business Closure	0.080	0.060
- Emergency Declaration	0.643	0.740
- Safer-At-Home	0.326	0.416
<i>N</i>	1664.000	250.000

**Table 2.** Summary Statistics

This table shows summary statistics for balance sheet and income statement information from Compustat used in the regression analysis for the full sample of PPP-eligible firms (Panel A) and PPP borrowers (Panel B). The number of COVID-19 cases by county is taken from the New York Times COVID-19 data repository and the data on local government policies is taken from the National Association of Counties. See section 3 for more details.

We use available data as of December 31, 2019, and take data as of September 30, 2019 when December data is not available. We winsorize return on assets, Tobin's Q, and debt

ratio at the 1st and 99th percentiles. For our empirical analysis, 106 firms that are eligible for PPP do not have sufficient data. This includes nine PPP borrowers.<sup>19</sup> We also use data that captures exposure to the pandemic. We merge the number of COVID-19 cases on a county level from the New York Times COVID-19 data repository.<sup>20</sup> We also merge in the exposure of a firm to various government-mandated closures and policies taken from the National Association of Counties (NACO).<sup>21</sup>

We provide summary statistics for firms in our empirical analysis in table 2. Due to data limitations, we focus on the set of firms who are PPP-eligible but did not borrow (1,664 firms in panel A) and PPP borrowers (250 firms in panel B). These tables provide a preview of the results we formally show in section 4. PPP borrowers are smaller on average, both in terms of total assets and number of employees, and about 4 years older on average. These firms also appear to be relatively more profitable, have less cash on hand, have fewer growth opportunities as represented by Tobin's Q. PPP loans are usually less than both 8-week operating expense and 8-week SG&A.

Panel C shows the exposure of both types of firms to the COVID-19 pandemic. We see that 94.8% of PPP borrowers are located in counties with at least one COVID-19 case, compared to 82.0% for PPP nonborrowers. In terms of the government policies in the county of the headquarters of the firm, a lower fraction of borrowers faced business closure policy, but a higher fraction faced either an emergency declaration and a safer-at-home policy. An emergency declaration is made when a government official feels that urgent is needed, often involving seeking federal assistance and resources. Safer-at-home policies prohibit outside gatherings of more than ten people and direct residents to remain at home unless engaging in "essential activities," which is as specified by county. Business closure policies are similar. According to NACO, the primary difference being that "safer at home policies explicitly restrict the movement and activities of individual residents, while business closure policies only restrict the activities of businesses."<sup>22</sup>

<sup>19</sup>These PPP borrowers with insufficient data are American Res Corp, Edison Nation Inc, Janel Corp, NioCorp Developments Ltd, Onewater Marine Inc, Rhino Resource Partners LP, SRAX Inc, Transportation & Log Sys Inc, and Vistagen Therapeutics Inc.

<sup>20</sup>See <https://github.com/nytimes/covid-19-data>. We use a mapping for the zip code available in Compustat to the FIPS county code.

<sup>21</sup>See <https://ce.naco.org/?dset=COVID-19&ind=Emergency%20Declaration%20Types>.

<sup>22</sup>[https://www.naco.org/sites/default/files/documents/NACO-Brief\\_Safer\\_at\\_Home.pdf](https://www.naco.org/sites/default/files/documents/NACO-Brief_Safer_at_Home.pdf).

## 4 Empirical Analysis

In this section, we use firm-level regressions to analyze the firm characteristics and local conditions associated with PPP borrowers. Specifically, we run regressions of the following form:

$$\text{PPP Borrower}_{i,j} = \alpha + \beta X_i + \gamma \text{COVID-19}_j + \epsilon_j. \quad (1)$$

Here,  $\text{PPP Borrower}_{i,j}$  is a dummy variable that is equal to 1 if firm  $i$  with headquarters located in county  $j$  received a PPP loan. We include a vector of firm-level variables,  $X_i$ , that are computed as of the end of 2019 to measure firm characteristics prior to the onset of the pandemic. These variables are described in section 3 and include size (total assets and employees), age (years in Compustat), profitability (return on assets), investment opportunities (Tobin's Q), cash-to-assets ratio, and a positive debt indicator. The vector  $\text{COVID-19}_j$  denotes the exposure of the firm to the pandemic and to county-level policies in response to the pandemic. The coefficients capture the change in probability that a PPP-eligible firm was a PPP borrower given a one unit change in the corresponding independent variable.

We present our main results in table 3 in which we progressively add our controls. Column (1) includes firm-level controls, while (2) includes industry fixed effects. We include a measure of exposure to COVID-19 cases and government policy dummies in columns (3) and (4), respectively. Our benchmark specification with all firm-level and county-level variables is in column (5). Table 3 shows that firm characteristics significantly determine the likelihood that a PPP-eligible public firm is also a borrower. We focus on the direction of the coefficients rather than on the magnitudes. First, we show that PPP borrowers tend to be smaller (negative coefficient on Log Assets). All else equal however, borrowers have more employees (positive coefficient on Log Employees), and are older (positive coefficient on Log Years in Compustat). Profitability does not appear to be a significant determinant of whether the firm is a borrower. However, firms with more growth opportunities as of the end of 2019, as captured by Tobin's Q, are less likely to be borrowers from the program. Importantly, this measure does not incorporate the dramatic declines in market value in early in the first few months of 2020. Unsurprisingly, firms with a higher cash-to-assets ratio are less likely to require immediate relief funding from the government, and are therefore

less likely to be PPP borrowers. This result, however, is only weakly significant. Finally, PPP borrowers are more likely to have outstanding debt on their balance sheets (positive coefficient on Positive Debt Dummy). Specifically, the presence of debt on a firm's balance sheet is associated with a 5.3 percentage point higher probability of receiving a PPP loan. We interpret this finding as the the firm is also more likely to have an existing relationship with a bank, increasing the likelihood of obtaining a PPP loan in a timely fashion.

	(1)	(2)	(3)	(4)	(5)
Log Assets	-0.058*** (-12.49)	-0.051*** (-7.77)	-0.050*** (-7.80)	-0.051*** (-7.90)	-0.051*** (-7.89)
Log Employees	0.035*** (6.22)	0.035*** (4.31)	0.034*** (4.24)	0.035*** (4.35)	0.034*** (4.27)
Log Years in Compustat	0.031*** (3.54)	0.026*** (2.82)	0.024*** (2.60)	0.026*** (2.85)	0.024*** (2.64)
Return on Assets	0.000 (1.30)	0.000 (0.44)	0.000 (0.64)	0.000 (0.62)	0.000 (0.74)
Tobin's Q	-0.006*** (-9.21)	-0.007*** (-8.59)	-0.006*** (-8.20)	-0.007*** (-8.32)	-0.006*** (-8.07)
Cash / Assets	-0.001*** (-3.19)	-0.001* (-1.89)	-0.001* (-1.65)	-0.001* (-1.79)	-0.001 (-1.64)
Positive Debt Dummy	0.062** (2.47)	0.051* (1.96)	0.051** (1.98)	0.053** (2.04)	0.053** (2.06)
Positive COVID-19 Cases Dummy			0.073*** (4.71)		0.060*** (3.50)
Business Closure Policy Dummy				-0.036 (-1.32)	-0.046* (-1.67)
Emergency Declaration Dummy				0.033* (1.87)	0.027 (1.53)
Safer-at-home Policy Dummy				0.028 (1.45)	0.016 (0.77)
Industry FE	No	Yes	Yes	Yes	Yes
R <sup>2</sup>	0.095	0.113	0.118	0.118	0.122
N	1914	1914	1914	1914	1914

**Table 3.** Benchmark Regression Results

This table shows the coefficient estimates for OLS regressions in which the dependent variable is an indicator that equals 1 if the public firm is a PPP borrower. Balance sheet and income statement information are from Compustat, the number of COVID-19 cases by county is from the New York Times COVID-19 data repository, and the data on local government policies is taken from the National Association of Counties. See sections 3 and 4 for more details. Standard errors are heteroskedasticity-consistent. *t*-statistics are in parentheses. \* $p < 0.10$ ; \*\* $p < 0.05$ ; \*\*\* $p < 0.01$ .

The coefficients on the COVID-19 exposure variables describe county-level conditions that PPP borrowers likely faced. First, we find that being located in a county with COVID-

19 cases is associated with a 6.0 percentage point increase in the probability of receiving a PPP loan. This result suggests that the employees or customers of these firms were more directly affected by the pandemic, resulting in more need for economic relief funding from the government. Studying the 1918 Flu Pandemic in the US, Correia et al. (2020) find that direct exposure to the disease does negatively affect the local economy. Second, we see that only one out of the three county-level government policies appears to be associated with PPP borrowing. Specifically, business closure policies seem to be negatively associated with whether a PPP-eligible public firm was a borrower, although the statistical significance of even this result is weak. The negative coefficient may appear surprising, but recall that the PPP program is geared primarily towards retaining workers and maintaining their wage levels. Policies that force business closures means that a firm cannot satisfy a major requirement of the PPP funding, which is to pay employees. Hence, these firms would be less likely to apply.

We perform two sets of robustness exercises to show the consistency of our results. In table 4, we focus on different subsamples to address the concern that we are not capturing the right set of PPP-eligible firms. The first concern is that, despite our eligibility filtering, we may still be including many large firms in our sample. In column (2), we restrict the analysis to the subset of firms with total assets less than \$100 million. The estimates are largely similar relative to the benchmark in column (1), which is the same as column (5) of table 3. Assets become insignificant by construction, yet the key firm characteristics and exposure to COVID-19 remain statistically significant. Note that our sample size drops to less than half in this analysis. In column (3) of table 4, we focus on the set of firms with fewer than 500 employees. Recall that some of the SBA standards based on the number of employees consider firms in certain industries with more than 500 employees to be eligible for a PPP loan. In column (4), we only use data as of December 2019 without including September–November 2019 data if December data is unavailable. We do so to alleviate the concern that differences in the timing of Compustat reports might affect our results. In column (5) we focus on the industries that PPP borrowers are in (2-digit NAICS code 32 and 33, manufacturing, and 51, information) to alleviate the concern that industry-level variables are driving our results despite including industry fixed effects. In all these specifications, our key results continue to hold with similar magnitudes and significance.

	(1)	(2)	(3)	(4)	(5)
	Benchmark	Assets<100mil	Empl.<500	Dec2019 Only	Select Industries
Log Assets	-0.051*** (-7.89)	-0.015 (-1.02)	-0.045*** (-6.55)	-0.056*** (-7.83)	-0.066*** (-6.39)
Log Employees	0.034*** (4.27)	0.076*** (5.06)	0.039*** (4.03)	0.035*** (4.14)	0.055*** (4.57)
Log Years in Compustat	0.024*** (2.64)	0.029* (1.71)	0.021** (2.15)	0.017* (1.82)	0.032*** (2.67)
Return on Assets	0.000 (0.74)	-0.000 (-0.11)	0.000 (1.04)	-0.000 (-0.64)	0.000 (0.13)
Tobin's Q	-0.006*** (-8.07)	-0.003*** (-3.04)	-0.005*** (-6.52)	-0.008*** (-7.24)	-0.007*** (-7.17)
Cash / Assets	-0.001 (-1.64)	-0.001 (-1.57)	-0.000 (-1.32)	-0.001*** (-2.93)	-0.000 (-0.94)
Positive Debt Dummy	0.053** (2.06)	0.056 (1.46)	0.050* (1.87)	0.046 (1.61)	0.056* (1.84)
Positive COVID-19 Cases Dummy	0.060*** (3.50)	0.135*** (4.41)	0.071*** (4.02)	0.059*** (3.32)	0.102*** (4.43)
Log COVID-19 Cases					
Business Closure Policy Dummy	-0.046* (-1.67)	-0.028 (-0.56)	-0.047 (-1.60)	-0.048* (-1.68)	-0.047 (-1.32)
Emergency Declaration Dummy	0.027 (1.53)	0.015 (0.48)	0.033* (1.73)	0.038** (2.03)	0.034 (1.42)
Safer-at-home Policy Dummy	0.016 (0.77)	0.051 (1.46)	0.016 (0.70)	0.004 (0.17)	-0.001 (-0.04)
Industry FE	Yes	Yes	Yes	Yes	Yes
R <sup>2</sup>	0.122	0.134	0.123	0.135	0.114
N	1914	861	1628	1690	1182

**Table 4.** Robustness: Alternative Firm Samples

This table shows the coefficient estimates for OLS regressions in which the dependent variable is an indicator that equals 1 if the public firm is a PPP borrower. Column (1) is the benchmark from Table 3. Columns (2)-(3) focus on firms with total assets less than the specified threshold, (4) focuses on firms with fewer than 500 employees, (5) focuses on firms with a December 2019 filing date, and (6) focuses on manufacturing and information, which are the top industries for PPP borrowers in our sample. Balance sheet and income statement information are from Compustat, the number of COVID-19 cases by county is from the New York Times COVID-19 data repository, and the data on local government policies is taken from the National Association of Counties. See sections 3 and 4 for more details. Standard errors are heteroskedasticity-consistent.  $t$ -statistics are in parentheses. \* $p < 0.10$ ; \*\* $p < 0.05$ ; \*\*\* $p < 0.01$ .

In the second set of robustness checks, we consider alternative model specifications. Results are shown in table 5, where the benchmark specification is shown in column (1) for reference. In column (2), we include county-level fixed effects, which absorb our county-level exposure variables. We lose observations in this specification due to counties with no PPP borrowers. In columns (3) and (4), we run logit and probit models without any fixed effects,

respectively. The important takeaway from this table is that, once again, our key results from table 5 continue to hold.

	(1)	(2)	(3)	(4)
	OLS (Benchmark)	OLS	Logit	Probit
Log Assets	-0.051*** (-7.89)	-0.046*** (-5.59)	-0.689*** (-10.64)	-0.365*** (-9.16)
Log Employees	0.034*** (4.27)	0.027*** (2.70)	0.460*** (6.20)	0.225*** (4.78)
Log Years in Compustat	0.024*** (2.64)	0.024** (2.17)	0.218** (2.32)	0.127** (2.51)
Return on Assets	0.000 (0.74)	0.000 (0.67)	0.001 (0.69)	0.000 (0.60)
Tobin's Q	-0.006*** (-8.07)	-0.008*** (-6.61)	-0.168*** (-4.28)	-0.087*** (-4.52)
Cash / Assets	-0.001 (-1.64)	-0.001 (-1.38)	-0.004 (-1.26)	-0.003 (-1.59)
Positive Debt Dummy	0.053** (2.06)	0.043 (1.27)	0.893** (2.06)	0.441** (2.02)
Positive COVID-19 Cases Dummy	0.060*** (3.50)		1.078*** (3.36)	0.544*** (3.48)
Business Closure Policy Dummy	-0.046* (-1.67)		-0.461 (-1.48)	-0.259 (-1.59)
Emergency Declaration Dummy	0.027 (1.53)		0.273 (1.40)	0.163 (1.59)
Safer-at-home Policy Dummy	0.016 (0.77)		0.175 (1.01)	0.105 (1.11)
Industry FE	Yes	Yes	No	No
County FE	No	Yes	No	No
R <sup>2</sup>	0.122	0.220		
Pseudo R <sup>2</sup>			0.169	0.169
N	1914	1561	1914	1914

**Table 5.** Robustness: Alternative Model Specifications

This table shows the coefficient estimates for OLS regressions in which the dependent variable is an indicator that equals 1 if the public firm is a PPP borrower. Column (1) is the benchmark from Table 3. Column (2) includes county fixed effects, (3) is a logit regression specification, and (4) is a probit regression specification. Balance sheet and income statement information are from Compustat, the number of COVID-19 cases by county is from the New York Times COVID-19 data repository, and the data on local government policies is taken from the National Association of Counties. See sections 3 and 4 for more details. Standard errors are heteroskedasticity-consistent. *t*-statistics are in parentheses. \* $p < 0.10$ ; \*\* $p < 0.05$ ; \*\*\* $p < 0.01$ .

## 5 Conclusion

In the first few weeks of April 2020, 273 public firms have participated and borrowed a total of \$929 million from the Paycheck Protection Program (PPP). This corresponds to 0.3% of

the total \$349 billion in funding allocated by the Coronavirus Aid, Relief, and Economic Security (CARES) Act towards the program.

We document that close to half of public firms are eligible to apply for PPP funds and, of these firms, 13% received them. In this paper, we document the firm characteristics that are significantly associated with public firms that are PPP borrowers. These firms are smaller both in terms of total assets, but in fact larger in terms of number of employees. PPP firms also tend to be older, with less relatively less growth opportunities and relatively less cash in hand. Firms with outstanding debt, which may capture preexisting bank relationships, are also more likely to be borrowers.

While we do not take a stance on whether or not these firms should have gotten PPP assistance, we highlight the difference in the order of magnitude of funding that has been made available to private firms relative to public firms. It may be more useful to evaluate the size of the program and the eligibility requirements to address the continued inability of small and private firms to access funding. A natural first step is underway, in the form of \$310 billion additional funds for replenishing PPP. In addition, assessing the program geographically shows that small firms in certain states, especially along the coasts, are receiving relatively less funding compared to less populous states (about 15% of small firms in California compared to 58% in North Dakota). Reallocating resources geographically can also alleviate issues related to PPP access.

As data become available, we plan to build upon our analysis by looking at the second set of PPP borrowers. We are also interested in tracking the performance of PPP borrowers to see how the funds affected their business decision-making and financial outcomes. An understanding of the post-loan outcomes can help dictate future policy changes.

## References

- Acharya, V. V., and S. Steffen. 2020. The risk of being a fallen angel and the corporate dash for cash in the midst of COVID. *Covid Economics* 10.
- Albuquerque, R. A., Y. J. Koskinen, S. Yang, and C. Zhang. 2020. Love in the time of covid-19: The resiliency of environmental and social stocks. *Covid Economics* 9.
- Alfaro, L., A. Chari, A. N. Greenland, and P. K. Schott. 2020. Aggregate and Firm-Level Stock Returns During Pandemics, in Real Time. *Covid Economics* 4.

- Alon, T. M., M. Doepke, J. Olmstead-Rumsey, and M. Tertilt. 2020. The Impact of COVID-19 on Gender Equality. *Covid Economics* 4.
- Baker, S. R., N. Bloom, S. J. Davis, and S. J. Terry. 2020. COVID-Induced Economic Uncertainty. Working Paper 26983, National Bureau of Economic Research.
- Bartik, A. W., M. Bertrand, Z. B. Cullen, E. L. Glaeser, M. Luca, and C. T. Stanton. 2020. How Are Small Businesses Adjusting to COVID-19? Early Evidence from a Survey. Working paper.
- Caballero, R. J., and A. Simsek. 2020. A Model of Asset Price Spirals and Aggregate Demand Amplification of a “Covid-19” Shock. Working Paper 27044, National Bureau of Economic Research.
- Carillo, M. F., and T. Jappelli. 2020. Pandemic and local economic growth: Evidence from the Great Influenza in Italy. *Covid Economics* 10.
- Castro, Miguel Faria e. 2020. Fiscal Policy During a Pandemic. *Covid Economics* 2.
- Correia, S., S. Luck, and E. Verner. 2020. Pandemics Depress the Economy, Public Health Interventions Do Not: Evidence from the 1918 Flu. Working paper.
- Croce, M., P. Farroni, and I. Wolfskeil. 2020. When the Markets Get COVID: COntagion, Viruses, and Information Diffusion. Working paper.
- Dahl, C. M., C. W. Hansen, and P. S. Jense. 2020. The 1918 epidemic and a V-shaped recession: Evidence from municipal income data. *Covid Economics* 6.
- Daniel Lewis, K. M., and J. Stock. 2020. US economic activity during the early weeks of the SARS-Cov-2 outbreak. *Covid Economics* 6.
- Eichenbaum, M. S., S. Rebelo, and M. Trabandt. 2020. The Macroeconomics of Epidemics. Working Paper 26882, National Bureau of Economic Research.
- Fahlenbrach, R., K. Rageth, and R. M. Stulz. 2020. How valuable is financial flexibility when revenue stops? Evidence from the COVID-19 crisis. Working paper.
- Giglio, S., M. Maggiori, J. Stroebel, and S. Utkus. 2020. Inside the mind of a stock market crash. Working paper.
- Glover, A., J. Heathcote, D. Krueger, and J.-V. Ríos-Rull. 2020. Health versus Wealth: On the Distributional Effects of Controlling a Pandemic. *Covid Economics* 6.
- Granja, J., C. Makridis, C. Yannelis, and E. Zwick. 2020. Did the Paycheck Protection Program Hit the Target? Working paper.
- Humphries, J. E., C. Neilson, and G. Ulyssea. 2020. The Evolving Impacts of COVID-19 on Small Businesses Since the CARES Act. Discussion Paper 2230, Cowles Foundation.

- Inoue, H., and Y. Todo. 2020. The propagation of the economic impact through supply chains: The case of a mega-city lockdown to contain the spread of Covid-19. *Covid Economics* 2.
- Krueger, D., H. Uhlig, and T. Xie. 2020. Macroeconomic dynamics and reallocation in an epidemic. *Covid Economics* 5.
- Ludvigson, S. C., S. Ma, and S. Ng. 2020. Covid19 and the Macroeconomic Effects of Costly Disasters. Working Paper 26987, National Bureau of Economic Research.
- Meier, J.-M., and J. Smith. 2020. The COVID-19 Bailouts. Working paper.
- Rio-Chanona, R. M. d., P. Mealy, A. Pichler, F. Lafond, and J. D. Farmer. 2020. Supply and demand shocks in the COVID-19 pandemic: An industry and occupation perspective. *Covid Economics* 6.
- Sedláček, P., and V. Sterk. 2020. Startups and employment following the COVID-19 pandemic: A calculator. *Covid Economics* 13.
- Small Business Administration. 2020. Paycheck Protection Program (PPP) Report URL [https://www.sba.gov/sites/default/files/2020-04/PPP\\_Deck\\_copy.pdf](https://www.sba.gov/sites/default/files/2020-04/PPP_Deck_copy.pdf).

## A Appendix

**Table A1.** List of Public Firms with PPP Loans

N	Date Granted	Name	Amount (\$)	Industry
1	Apr 07	Ruths Hospitality Group	20,000,000	retail eating places
2	Apr 08	Fiesta Restaurant Group	10,000,000	retail eating places
3	Apr 08	Transportation And Logistics Systems	2,941,213	transportation
4	Apr 09	Graham	4,599,003	general industrial machinery equipment
5	Apr 09	Identiv	2,900,000	computer peripheral equipment nec
6	Apr 09	Silversun Technologies	3,150,832	business services nec
7	Apr 09	Windtree Therapeutics	546,600	biological products no diagnostic substances
8	Apr 10	Addvantage Technologies Group	2,915,000	wholesale durable goods
9	Apr 10	Air T	8,215,100	air courier
10	Apr 10	Blonder Tongue Laboratories	1,768,762	radio tv broadcasting communications equipment
11	Apr 10	Bsquare	1,600,000	business services nec
12	Apr 10	Careview Communications	781,800	radio tv broadcasting communications equipment
13	Apr 10	Cpi Aerostructures	4,795,000	aircraft part auxiliary equipment nec
14	Apr 10	Crawford United	3,679,383	industrial instruments for measurement display and control
15	Apr 10	Drive Shack	5,276,742	retail eating drinking places
16	Apr 10	Enservco	1,939,900	oil gas field nbc
17	Apr 10	Infinite Group	957,373	computer programming data processing etc
18	Apr 10	Inuvo	1,100,000	advertising
19	Apr 10	Joint	2,730,000	patent owners lessors
20	Apr 10	Legacy Housing	6,545,700	mobile homes
21	Apr 10	Lindblad Expeditions Holdings	6,600,000	transportation

22	Apr 10	Lodging Fund Reit Iii	286,100	real estate investment trusts
23	Apr 10	Mannkind	4,900,000	pharmaceutical preparations
24	Apr 10	Misonix	5,199,487	laboratory apparatus furniture
25	Apr 10	Mobivity Holdings	891,103	
26	Apr 10	Natural Gas Services Group	4,600,000	oil gas field nbc
27	Apr 10	Oblong	2,416,600	telephone communications no radio telephone
28	Apr 10	Optinose Us	4,400,000	pharmaceutical preparations
29	Apr 10	Phunware	2,850,336	computer processing data preparation
30	Apr 10	Potbelly Sandwich Works	10,000,000	retail eating places
31	Apr 10	Prodex	1,360,100	surgical medical instruments apparatus
32	Apr 10	Pulmatrix	616,795	pharmaceutical preparations
33	Apr 10	Sifco Industries	5,024,732	aircraft engines engine parts
34	Apr 10	Us Auto Parts Network	4,107,388	retail auto home supply stores
35	Apr 10	Vislink Technologies	1,167,700	communications equipment nec
36	Apr 10	Wave Life Sciences	7,234,890	pharmaceutical preparations
37	Apr 12	Frequency Electronics	4,964,810	instruments for meas testing of electricity elec signals
38	Apr 12	Polarityte Md	3,576,145	biological products no diagnostic substances
39	Apr 12	Srax	1,074,488	advertising agencies
40	Apr 13	Adamis Pharmaceuticals	3,191,700	pharmaceutical preparations
41	Apr 13	Bk Technologies	2,196,335	radio tv broadcasting communications equipment
42	Apr 13	Broadwind Energy	9,500,000	nonferrous foundries castings
43	Apr 13	Emmis Operating Company	4,753,000	radio broadcasting stations
44	Apr 13	Englobal	4,915,800	engineering services
45	Apr 13	Helius Medical Technologies	323,000	electromedical electrotherapeutic apparatus
46	Apr 13	Hepion Pharmaceuticals	176,585	pharmaceutical preparations
47	Apr 13	Hyrecar	2,004,175	auto rental leasing no drivers
48	Apr 13	Immuell	937,700	in vitro in vivo diagnostic substances
49	Apr 13	Intellicheck	796,100	prepackaged software
50	Apr 13	Livexlive Media	2,000,000	retail eating places
51	Apr 13	Marrone Bio Innovations	1,723,000	agriculture chemicals
52	Apr 13	Quantum	10,000,000	computer storage devices
53	Apr 13	Rave Restaurant Group	656,830	wholesale groceries related products
54	Apr 13	Rocky Mountain Chocolate Factory	1,400,000	sugar confectionery products
55	Apr 13	Vaso	3,610,900	electromedical electrotherapeutic apparatus
56	Apr 13	Zagg	9,443,728	retail misc retail
57	Apr 14	Accelerate Diagnostics	4,780,600	laboratory analytical instruments
58	Apr 14	Acquired Sales	149,623	prepackaged software
59	Apr 14	Astrotech	541,500	laboratory analytical instruments
60	Apr 14	Ballantyne Strong	3,173,900	photographic equipment supplies
61	Apr 14	Biolase	2,980,000	dental equipment supplies
62	Apr 14	Continental Materials	5,487,000	concrete gypsum plaster products
63	Apr 14	Dmc Global	6,700,000	misc primary metal products
64	Apr 14	Harte Hanks	10,000,000	direct mail advertising services
65	Apr 14	Kura Sushi Usa	5,983,290	retail eating places
66	Apr 14	Mikros Systems	753,300	measuring controlling devices nec
67	Apr 14	New Age Beverages	6,868,400	malt beverages
68	Apr 14	Permafex Environmental Services	5,666,300	hazardous waste management
69	Apr 14	Scientific Industries	563,700	laboratory analytical instruments
70	Apr 14	Sigma Labs	361,700	misc manufacturing industries
71	Apr 14	Superior Drilling Products	891,600	oil gas filed machinery equipment
72	Apr 14	Sw Seed Company	2,000,000	agriculture production crops
73	Apr 14	Ultralife	3,459,278	misc electrical machinery equipment supplies
74	Apr 14	Westell	1,637,522	telephone telegraph apparatus
75	Apr 14	Workhorse Group	1,411,000	motor vehicles passenger car bodies
76	Apr 15	Arc Group	6,064,560	patent owners lessors
77	Apr 15	Asure Software	8,855,605	computer integrated systems design
78	Apr 15	Audioeye	1,300,000	prepackaged software
79	Apr 15	Azur Rx Biopharma	180,000	pharmaceutical preparations
80	Apr 15	Cinedigm	2,151,800	video tape rental
81	Apr 15	Collectors Universe	4,200,000	business services nec
82	Apr 15	Culp	7,605,500	broadwoven fabric mills cotton
83	Apr 15	Dawson Geophysical Company	6,373,707	oil and gas field exploration
84	Apr 15	Eastside Distilling	1,438,100	beverages
85	Apr 15	Edison Nation	789,852	games toys childrens vehicles no dolls bicycles

86	Apr 15	Energy Services Of America	13,139,100	water sewer pipeline comm and power line construction
87	Apr 15	Hallador Energy Company	10,000,000	bituminous coal lignite mining
88	Apr 15	Intellinetics	838,700	prepackaged software
89	Apr 15	J Alexander S Holdings	15,100,000	retail eating places
90	Apr 15	Lgl Group	1,907,500	electronic components nec
91	Apr 15	Nortech Systems Orporated	6,100,000	electronic components nec
92	Apr 15	Ricebran Technologies	1,800,000	grain mill products
93	Apr 15	Senestech	645,700	agriculture chemicals
94	Apr 15	Spanish Broadcasting System	6,478,800	
95	Apr 15	Torotel	1,984,688	electronic coils transformers other inductors
96	Apr 15	Trovagene	305,000	biological products no diagnostic substances
97	Apr 15	Tsr	6,659,220	computer programming services
98	Apr 15	Veritone	6,491,300	computer processing data preparation
99	Apr 15	Wilhelmina International	1,847,700	management consulting services
100	Apr 16	Adma Biomanufacturing	5,400,000	biological products no diagnostic substances
101	Apr 16	Arcadia Biosciences	1,107,700	agriculture chemicals
102	Apr 16	Autoweb	1,380,000	computer programming data processing etc
103	Apr 16	Calamp	10,000,000	radio tv broadcasting communications equipment
104	Apr 16	Cool Holdings	3,098,000	wholesale electronic parts equipment nec
105	Apr 16	Digimarc	5,032,072	computer integrated systems design
106	Apr 16	Educational Development	1,447,400	wholesale misc nondurable goods
107	Apr 16	Flotek Industries	4,788,100	misc chemical products
108	Apr 16	Freightcar America	10,000,000	railroad equipment
109	Apr 16	Gulfslope Energy	100,300	crude petroleum natural gas
110	Apr 16	Intest	2,829,207	instruments for meas testing of electricity elec signals
111	Apr 16	Odyssey Marineexploration	370,400	water transportation
112	Apr 16	Perceptron	2,545,205	optical instruments lenses
113	Apr 16	Retractable Technologies	1,363,000	surgical medical instruments apparatus
114	Apr 16	Smithmidland	2,691,700	concrete products except block brick
115	Apr 16	Universal Stainless Alloy Products	10,000,000	steel works blast furnaces rolling mills coke ovens
116	Apr 16	Urenergy	893,300	gold silver ores
117	Apr 16	Usio	813,500	functions related to depository banking nec
118	Apr 17	Applied Optoelectronics	6,228,895	semiconductors related devices
119	Apr 17	Aquestive Therapeutics	4,830,000	pharmaceutical preparations
120	Apr 17	Bioanano Genomics	1,770,000	laboratory analytical instruments
121	Apr 17	Bridgeline Digital	1,047,500	prepackaged software
122	Apr 17	Conformis	4,719,800	orthopedic prosthetic surgical appliances supplies
123	Apr 17	Crh Medical	2,945,620	health services
124	Apr 17	Csp	2,180,600	computer integrated systems design
125	Apr 17	Cv Sciences	2,906,195	pharmaceutical preparations
126	Apr 17	Electronic Systems Technology	171,712	electronic components accessories
127	Apr 17	Encision	598,567	surgical medical instruments apparatus
128	Apr 17	Energy Focus	794,965	electric lighting wiring equipment
129	Apr 17	Galaxy Gaming	835,300	amusement recreation services
130	Apr 17	Gulf Island Fabrication	10,000,000	fabricated structural metal products
131	Apr 17	Intrepid Potash	10,000,000	mining quarrying of nonmetallic minerals no fuels
132	Apr 17	Limoneira Company	3,609,200	agriculture production crops
133	Apr 17	Micropacindustries	1,924,400	semiconductors related devices
134	Apr 17	Nanophase Technologies	951,600	misc primary metal products
135	Apr 17	Nio Developments	196,300	metal mining
136	Apr 17	Ramaco Resources	8,444,737	bituminous coal lignite mining
137	Apr 17	Sonotek	1,001,640	misc electrical machinery equipment supplies
138	Apr 17	Technical Communications	474,400	radio tv broadcasting communications equipment
139	Apr 17	Tecogen	1,874,200	air cond warm air heating equip comm indl refrig equip
140	Apr 17	Trans World Entertainment	2,017,550	retail computer prerecorded tape stores
141	Apr 17	Tss	889,858	management consulting services
142	Apr 17	Twin Disc Orporated	8,199,500	general industrial machinery equipment
143	Apr 18	Exone Company	2,193,512	printing trades machinery equipment
144	Apr 18	Forward Industries	1,356,570	plastics products nec
145	Apr 18	Harvard Bioscience	6,114,700	laboratory analytical instruments
146	Apr 18	Neos Therapeutics	3,582,800	pharmaceutical preparations
147	Apr 18	Ntn Buzztime	1,625,100	television broadcasting stations
148	Apr 18	Xg Sciences	825,000	plastics materials synth resins nonvulcan elastomers

149	Apr 19	Crown Crafts	1,963,800	broadwoven fabric mills cotton
150	Apr 19	Durect	2,037,395	pharmaceutical preparations
151	Apr 19	Janel	2,725,893	business services nec
152	Apr 19	Manning Napier	6,732,818	investment advice
153	Apr 19	Shake Shack	10,000,000	retail eating drinking places
154	Apr 20	Ampio Pharmaceuticals	543,900	pharmaceutical preparations
155	Apr 20	Art Sway Manufacturing Co	1,242,900	farm machinery equipment
156	Apr 20	Biolife Solutions	2,175,320	electromedical electrotherapeutic apparatus
157	Apr 20	Chembio Diagnostic Systems	2,980,000	pharmaceutical preparations
158	Apr 20	Crimson Wine Group	3,819,521	beverages
159	Apr 20	Cumberland Pharmaceuticals	2,187,140	pharmaceutical preparations
160	Apr 20	Cynergistek	2,825,500	business services nec
161	Apr 20	Ekso Bionics Holdings	1,085,630	general industrial machinery equipment nec
162	Apr 20	Fuelcell Energy	6,515,045	misc electrical machinery equipment supplies
163	Apr 20	Global Healthcare Reit	574,975	real estate investment trusts
164	Apr 20	Hallmark Financial Services	8,300,000	insurance carriers nec
165	Apr 20	Idt Domestic Telecom	10,000,000	telephone communications no radio telephone
166	Apr 20	Ikonic	1,214,500	photographic equipment supplies
167	Apr 20	Kopin	2,100,000	semiconductors related devices
168	Apr 20	Leaf Group	7,143,927	computer processing data preparation
169	Apr 20	Onewater Marine	14,151,797	retail auto home supply stores
170	Apr 20	Pf Industries	2,929,200	metalworking machinery equipment
171	Apr 20	Predictive Oncology	541,867	orthopedic prosthetic surgical appliances supplies
172	Apr 20	Sharps Compliance	2,183,187	hazardous waste management
173	Apr 20	Socket Mobile	1,058,700	electronic computers
174	Apr 20	Sonic Foundry	2,314,815	radio tv broadcasting communications equipment
175	Apr 20	Summer Energy Holdings	2,342,300	electric
176	Apr 20	Transmedics	2,249,280	electromedical electrotherapeutic apparatus
177	Apr 20	Zomedica Pharmaceuticals	527,360	pharmaceutical preparations
178	Apr 21	Advanced Emissions Solutions	3,300,000	misc chemical products
179	Apr 21	Alimera Sciences	1,777,502	pharmaceutical preparations
180	Apr 21	Amerinac Holding	3,083,000	wholesale hardware
181	Apr 21	Ashford Hospitality Trust	30,100,000	real estate investment trusts
182	Apr 21	Aviat Networks	5,911,000	radio tv broadcasting communications equipment
183	Apr 21	Avid Bioservices	4,400,000	pharmaceutical preparations
184	Apr 21	Braemar Hotels Resorts	15,800,000	real estate investment trusts
185	Apr 21	Celsion	632,220	pharmaceutical preparations
186	Apr 21	Cipherloc	365,430	computer processing data preparation
187	Apr 21	Crexendo	1,000,626	telephone communications no radio telephone
188	Apr 21	Curis	890,779	biological products no diagnostic substances
189	Apr 21	Cvd Equipment	2,415,970	special industry machinery nec
190	Apr 21	Endra Life Sciences	308,600	electromedical electrotherapeutic apparatus
191	Apr 21	Imac Holdings	1,691,520	specialty outpatient facilities nec
192	Apr 21	Image Sensing Systems	923,700	measuring controlling devices nec
193	Apr 21	Innovate Biopharmaceuticals	220,205	pharmaceutical preparations
194	Apr 21	Innovative Food Holdings	1,650,221	wholesale groceries general line
195	Apr 21	Lantronix	2,437,714	computer communications equipment
196	Apr 21	Luby S	10,000,000	retail eating places
197	Apr 21	Mateon Therapeutics	250,000	pharmaceutical preparations
198	Apr 21	Mimedx Group	10,000,000	surgical medical instruments apparatus
199	Apr 21	Nathans Famous	1,224,645	retail eating places
200	Apr 21	Neuronetics	6,360,327	surgical medical instruments apparatus
201	Apr 21	Omnitek Engineering	199,000	motor vehicle parts accessories
202	Apr 21	Profire Energy	1,074,030	oil gas filed machinery equipment
203	Apr 21	Red Lion Hotels	4,233,500	hotels motels
204	Apr 21	Servotronics	4,000,000	cutlery handtools general hardware
205	Apr 21	Sharpspring	3,234,000	prepackaged software
206	Apr 21	Telkonet	913,063	auto controls for regulating residential comml environment
207	Apr 21	Thermogenesis Holdings	646,300	laboratory apparatus furniture
208	Apr 21	Tomi Environmental Solutions	410,700	industrial organic chemicals
209	Apr 21	Vuzix	1,555,900	radio tv broadcasting communications equipment
210	Apr 21	Xeris Pharmaceuticals	5,090,000	pharmaceutical preparations
211	Apr 21	Zosano Pharma	1,610,000	pharmaceutical preparations
212	Apr 22	Allied Healthcare Products	2,375,000	orthopedic prosthetic surgical appliances supplies
213	Apr 22	American Resources	2,700,000	misc repair services
214	Apr 22	Ashford	3,300,000	management consulting services
215	Apr 22	Avalon Holdings	800,000	refuse systems

216	Apr 22	Castlight Health	10,000,000	computer processing data preparation
217	Apr 22	Cutera	7,135,348	electromedical electrotherapeutic apparatus
218	Apr 22	Emerald Biosciences	116,700	
219	Apr 22	Eyepoint Pharmaceuticals S	2,041,405	laboratory analytical instruments
220	Apr 22	Insignia Systems	1,054,200	advertising
221	Apr 22	Microvision	1,570,881	electronic components nec
222	Apr 22	Motusgi Holdings	780,942	surgical medical instruments apparatus
223	Apr 22	Novan	955,800	pharmaceutical preparations
224	Apr 22	Obalon Therapeutics	430,047	surgical medical instruments apparatus
225	Apr 22	Opgen	1,138,983	medical laboratories
226	Apr 22	Rhino Resources Partners LP	10,000,000	bituminous coal lignite surface mining
227	Apr 22	Sanara Medtech	583,000	orthopedic prosthetic surgical appliances supplies
228	Apr 22	Senseonics Holdings	5,800,000	industrial instruments for measurement display and control
229	Apr 22	Soleno Therapeutics	350,445	electromedical electrotherapeutic apparatus
230	Apr 22	Solitario Z	70,000	gold silver ores
231	Apr 22	Strata Skin Sciences	2,028,524	surgical medical instruments apparatus
232	Apr 22	Tetraphase Pharmaceuticals	2,285,830	pharmaceutical preparations
233	Apr 22	Vistagen Therapeutics	224,000	pharmaceutical preparations
234	Apr 23	Aehr Test Systems	1,678,789	instruments for meas testing of electricity elec signals
235	Apr 23	Alphatec Holdings	4,300,000	surgical medical instruments apparatus
236	Apr 23	Avinger	2,300,000	surgical medical instruments apparatus
237	Apr 23	Axogen	7,800,000	electromedical electrotherapeutic apparatus
238	Apr 23	Bioanalytical Systems	5,051,282	commercial physical biological research
239	Apr 23	Cleafield	3,700,000	telephone telegraph apparatus
240	Apr 23	Dolphin Entertainment	2,096,000	personal services
241	Apr 23	Duos Technologies Group	1,410,270	prepackaged software
242	Apr 23	Enzo Biochem	6,999,500	medical laboratories
243	Apr 23	Gigatronics Orporated	786,200	instruments for meas testing of electricity elec signals
244	Apr 23	International Isotopes	495,500	
245	Apr 23	Iridex	2,497,199	electromedical electrotherapeutic apparatus
246	Apr 23	Izea Worldwide	1,905,100	advertising
247	Apr 23	Lightwave Logic	410,700	misc plastic products
248	Apr 23	Marin Software Orporated	3,319,600	
249	Apr 23	Miragen Therapeutics	1,725,585	medical laboratories
250	Apr 23	Oncocyte	1,140,930	in vitro in vivo diagnostic substances
251	Apr 23	Park City Group	1,100,000	computer processing data preparation
252	Apr 23	Pharmabio Serv	1,931,700	
253	Apr 23	Pharmacy Value Management Solutions	1,243,840	hospital medical service plans
254	Apr 23	Precipio	787,200	laboratory analytical instruments
255	Apr 23	Sigmatron International	6,282,973	printed circuit boards
256	Apr 23	Xcel Brands	1,805,856	patent owners lessors
257	Apr 23	Zedge	217,900	prepackaged software
258	Apr 24	Black Ridge Oil Gas	112,925	crude petroleum natural gas
259	Apr 24	Bright Mountain Media	464,800	computer programming services
260	Apr 24	Capstone Turbine	2,610,200	
261	Apr 24	Conifer Holdings	2,744,667	fire marine casualty insurance
262	Apr 24	Escalade	5,627,500	
263	Apr 24	General Moly	365,034	metal mining
264	Apr 24	Myomo	1,077,590	orthopedic prosthetic surgical appliances supplies
265	Apr 24	Peck Electric Co	1,487,624	gas other combined
266	Apr 24	Realnetworks	2,870,568	computer programming services
267	Apr 24	Sci Engineered Materials	325,300	
268	Apr 24	Unique Fabricating Na	5,998,700	motor vehicle parts accessories
269	Apr 24	Viveve Medical	1,343,400	electromedical electrotherapeutic apparatus
270	Apr 25	Arch Therapeutics	176,300	surgical medical instruments apparatus
271	Apr 26	Luvu Brands	1,096,200	household furniture
272	Apr 27	Harrow Health	1,967,100	pharmaceutical preparations
273	Apr 27	Transenterix Surgical	2,815,200	surgical medical instruments apparatus

Note. This table lists public firms that have been granted PPP loans. All information is taken from their Firm 8-K reports to the SEC. Date refers to the day the loan was granted or approved.

# Assessing the consequences of quarantines during a pandemic<sup>1</sup>

Rikard Forslid<sup>2</sup> and Mathias Herzing<sup>3</sup>

Date submitted: 30 April 2020; Date accepted: 4 May 2020

*This paper analyzes the epidemiological and economic effects of quarantines. We use a basic epidemiological model, a SEIR-model, that is calibrated to roughly resemble the COVID-19 pandemic, and we assume that individuals that become infected or are isolated on average lose a share of their productivity. An early quarantine will essentially postpone but not alter the course of the infection at a cost that increases in the duration and the extent of the quarantine. A quarantine starting at a later stage of the pandemic reduces the number of infected persons and economic losses, but generates a higher peak level of infectious people. A longer quarantine dampens the peak of the pandemic and reduces deaths, but implies higher economic losses. Both the peak share of infectious individuals and economic losses are U-shaped in relation to the share of the population in quarantine. A quarantine covering a moderate share of the population leads to a lower peak, fewer deaths and lower economic costs, but it implies that the peak of the pandemic occurs earlier.*

1 Both authors are grateful for financial support from the Jan Wallander and Tom Hedelius Research Foundation.

2 Professor, Stockholm University and CEPR Research Fellow.

3 Senior lecturer, Stockholm University.

Copyright: Rikard Forslid and Mathias Herzing

## 1 Introduction

This paper analyzes the epidemiological and economic effects of quarantines. More specifically, our focus is on how the timing, duration and extent of a quarantine impact on the dynamics of a pandemic as well as on economic losses.

In the absence of a vaccine or efficient drugs, countries have to adopt old-fashioned practices to combat the COVID-19 pandemic. One such policy is the use of quarantines, which slow down the spread of the infection. This means that fewer individuals will be infected at the peak of the infection and that the peak will occur later in time. Both these effects are important in order to prevent the health care system from being completely overwhelmed. However, quarantines have substantial economic costs, as production closes down when workers are confined to stay at home.

Countries have adopted very different strategies when it comes to the use of quarantines. China implemented an almost complete quarantine or lockdown in Wuhan and in some other cities in the Hubei province on 23 January. On April 8 the lockdown officially ended. Many European countries have also been using quarantines of various degrees of restrictiveness. For instance, Italy that has been hit very hard by the COVID-19 infection has implemented a very restrictive quarantine. In the most affected town of Codogno (pop. 16,000), police cars blocked roads into and out of the quarantined area and erected barriers. In Switzerland schools and most shops were closed nationwide, and on 20 March all gatherings of more than five people in public spaces were banned. Denmark was among the first European countries to introduce lockdown measures, starting on 13 March; since mid-April a very slow and gradual reopening has been initiated. At the other end of the spectrum is Sweden that has not yet (end of April) imposed any quarantine, keeps schools open and still allows public gatherings of up to 50 people.

We will in this paper analyze the effects of quarantines of different extents and durations that are imposed at different points during a pandemic. We use a basic epidemiologic model, a SEIR-model, that is calibrated to roughly resemble the COVID-19 pandemic.<sup>1</sup> As in Atkeson (2020) we assume that individuals that become infected on average lose a share of their productivity, and that also quarantined individuals on average incur productivity losses. However, our qualitative results do not depend on the assumed values of productivity losses. Our main findings can be summarized as follows.

- 1) The implementation of an early quarantine will essentially postpone but not alter the course of the infection, at a cost that increases in the duration and the extent of the quarantine.
- 2) A later starting day reduces the total number of infected and dead individuals as well as the economic losses, but it generates a higher infectious peak level.
- 3) There is a trade-off between economic costs and health outcomes in terms of the duration of a quarantine. A longer quarantine either postpones the peak (if it is implemented relatively early) or dampens the peak and reduces deaths (if it starts at a later stage of the pandemic),

---

<sup>1</sup>This type of epidemiological model was introduced by Kermack and McKendrick (1927).

but implies higher economic losses.

4) The peak level of infectious people as well as economic losses are U-shaped in relation to the extent of a quarantine (the share of the population in quarantine). A quarantine of moderate extent, covering around half the population, leads to a lower peak, fewer deaths and lower economic costs than a more complete lockdown. However, it implies that the peak of infectious people occurs earlier.

Several recent papers analyze the implications of the policy response in relation to the COVID-19 pandemic. Dewatripont et al. (2020) discuss how to best use testing. Hall et al. (2020) analyze the optimal trade-off between consumption losses and pandemic deaths. Jones et al. (2020) studies the interaction of private and public mitigation efforts. Other policy options are discussed in Baldwin and Weder di Mauro (2020a) and Baldwin and Weder di Mauro (2020b). More closely related to us, a number of recent papers specifically analyze the consequences of isolation enforcement. Anderson et al. (2020) discuss how mitigation policies will affect the COVID-19 pandemic. Casares et al. (2020) calibrates a dynamic model for the Spanish economy. The study shows how isolation or quarantine slows down the speed of the contagion and reduces the number infected and dead. However, they do not consider the economic effects of quarantines. Piguillem et al. (2020) calibrate a SEIR- model to Italian data, and calculate the optimal path of a quarantine for different functional forms of the planner's utility function. Similarly Alvarez et al. (2020) and Gonzalez-Eiras and Niepelt (2020) employ optimal control theory to determine the optimal path of a quarantine that can be continuously varied. We do not calibrate our model to any particular country and do not use control theory to pin down an optimal path of isolation. Our purpose is instead to try to shed light on some of the underlying trade-offs between economic and health outcomes when a quarantine is implemented.

## 2 The Model

We employ a SEIR-model similar to Atkeson (2020). There are five categories of individuals: susceptible persons ( $S$ ) who have never been exposed to the virus; exposed persons ( $E$ ) who carry the virus, but are not yet infectious; infectious persons ( $I$ ); recovered persons ( $R$ ) who are no longer infectious and, possibly, have developed resistance to the virus; and deceased persons ( $D$ ). A susceptible individual becomes infected by infectious individuals at the rate  $\beta I$ . Exposed persons become infectious at rate  $\sigma$ . Infectious persons recover at rate  $\gamma$  and die at rate  $\delta$ . The dynamics of the SEIR-model can be summarized as follows:

$$\begin{aligned}\dot{S} &= -\beta SI, \\ \dot{E} &= \beta SI - \epsilon E, \\ \dot{I} &= \epsilon E - \gamma I - \delta I, \\ \dot{R} &= \gamma I, \\ \dot{D} &= \delta I.\end{aligned}$$

For simplicity it will be assumed that  $S$ ,  $E$ ,  $I$ ,  $R$  and  $D$  represent shares of the population, i.e.  $S(t) + E(t) + I(t) + R(t) + D(t) = 1$  at any point in time  $t$ .

Most countries have responded to the present Corona pandemic by imposing different types of quarantines, covering large parts of the population. In the context of the present model a quarantine would cover a constant share  $q$  of susceptible, exposed, infectious and recovered individuals over a certain period. The quarantined population would thus consist of the shares  $S_Q$ ,  $E_Q$ ,  $I_Q$  and  $R_Q$ . For simplicity we assume that there is no transmission of the virus among the quarantined population, i.e.  $S_Q(t)$  remains constant during the quarantine. In reality, the virus could be transmitted within quarantined families; allowing for a small rate of transmission among the quarantined population would not alter our analysis qualitatively. Quarantined exposed individuals become infectious at rate  $\sigma$ , and quarantined infectious individuals recover at rate  $\gamma$  and die at rate  $\delta$ . The dynamics during the quarantine can thus be summarized as follows:

$$\begin{aligned}\dot{S} &= -\beta SI, \\ \dot{E} &= \beta SI - \sigma E, \\ \dot{I} &= \sigma E - \gamma I - \delta I, \\ \dot{R} &= \gamma I, \\ \dot{D} &= \delta I + \delta I_Q \\ \dot{S}_Q &= 0, \\ \dot{E}_Q &= -\sigma E_Q, \\ \dot{I}_Q &= \sigma E_Q - \gamma I_Q - \delta I_Q, \\ \dot{R}_Q &= \gamma I_Q.\end{aligned}$$

After the quarantine has been terminated, the quarantined individuals join their corresponding groups, e.g.  $E_Q$  is added to  $E$ . Here, we do not account for quarantines that are introduced and lifted in steps. In reality, a government can vary the extent of a quarantine and let smaller groups of people return to normal life. However, there are infinitely many possibilities for implementing a quarantine. To keep our analysis transparent we only consider quarantines that take place once for a certain duration and covering a constant share of the population.

To assess the implications of a quarantine we will focus on the following measures:

- (i) The peak of the share of infected individuals  $I_{Peak}$ . From a public health perspective it is desirable to dampen the maximum number of infected persons.
- (ii) The day  $t(I_{Peak})$  when the peak of the share of infected individuals occurs. For the public health authorities a later day is preferable, because it allows hospitals to be better prepared.
- (iii) The share of the population that will have been infected and survived one year after the start of the pandemic, which is measured by the share of recovered individuals on day 365 of

the pandemic  $R(365)$ ; the share of deceased persons is obviously proportional to that number. To keep the number of infected and hence, deceased individuals low is one important objective.

(iv) The economic output during one year  $Y$ , from day 0 to day 365. In the absence of the pandemic it is assumed that productivity is 1 per individual and day, i.e. normalized total output would be 366 for the entire population. It is assumed that the productivity of susceptible, exposed and recovered individuals is 1 if there is no quarantine, whereas those in quarantine will have an average productivity  $b = 0.5$ , reflecting the fact that some individuals, e.g. individuals employed as manual workers, may have close to zero productivity, whereas other professions or tasks are easier to perform from home. Likewise infectious persons either have no or only mild symptoms or are sick at home or need costly treatment in a hospital. Their average productivity is decreased by a factor  $a$ , here set to  $a = 0.5$ . The productivity parameters determine the economic impact of the quarantine, but they do not affect the dynamic properties of the model.

Normalized total output at any day  $t$  is given by

$$Y(t) = S(t) + E(t) + R(t) + aI(t) + b[S^Q(t) + E^Q(t) + R^Q(t) + aI^Q(t)].$$

To assess the economic consequence of the pandemic,  $Y = \sum_{t=0}^{365} Y(t)$  will be measured. It is thus implicitly assumed that the pandemic only has short-term consequences in the sense that it only leads to lost output due to illness and, possibly, a quarantine. Long-term structural effects are therefore not accounted for. Once the pandemic is over, the economy reverts to the status quo ante.

### 3 Simulations

We do not intend to calibrate the infection dynamics to any particular country or case, but we do have the COVID-19 pandemic in mind, and we therefore chose parameter values that have been suggested for this infection. The average incubation period is 5 days, but it seems that you can spread the infection two days before that.<sup>2</sup> We therefore set  $\sigma = \frac{1}{3}$ . We also assume that it takes on average two weeks to recover, implying that  $\gamma = 1/14$ , and that 0.1% of infectious persons die, i.e.  $\delta = 0.001/14$ .<sup>3</sup> Finally, we have  $\beta = 0.2$  in the base case, which reflects the speed of the spread of the pandemic without a quarantine.<sup>4</sup>

<sup>2</sup>See He et al. (2020).

<sup>3</sup>This relatively optimistic value for  $\delta$  is consistent with the study by Bendavid et al. (2020). However, the choice of  $\delta$  has virtually no effect on the infection dynamics.

<sup>4</sup>This value of  $\beta$  is used by Alvarez et al. (2020).

### 3.1 Base case: no quarantine

The base case scenario has no quarantine. With our parameter values the pandemic dynamics during the course of one year looks as follows:

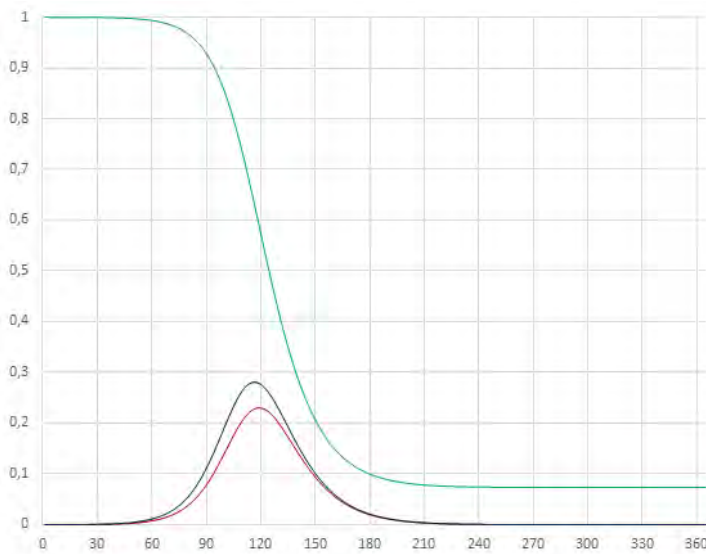


Figure 1. Pandemic dynamics in the absence of a quarantine

The horizontal axis measures days since the start of the pandemic, while the vertical axis measures shares of the population. The red curve represents the share of infectious individuals, the blue curve represents the share of infectious plus exposed individuals, and the green curve represents the share of infectious, exposed and susceptible individuals. That is, recovered and deceased individuals are represented by the area above the green curve; deceased people represent only a tiny fraction (0.1%) of these.

Assuming that at the start of the pandemic 0.01% had been exposed to the virus (i.e.  $S(0) = 0.9999$ ), the peak of infectious individuals would occur on day 118 and represent 23 per cent of the population. Moreover, a year after the pandemic started almost 93% would belong to the category of recovered (and possibly resistant) individuals, implying a share of 7% still being susceptible.

Furthermore, assuming that the average productivity of infectious individuals is given by  $a = 0.5$ , output would be reduced from 366 to 359.28, i.e. a fall of 1.84%, due to the pandemic.

### 3.2 Introducing a quarantine

When assessing the effects of a quarantine several factors are of interest:

- (i) timing, i.e. the start of the quarantine;
- (ii) the duration of the quarantine;
- (iii) the extent of the quarantine, i.e. how large a share of the population is covered.

We simulate below the importance of these factors using the same parameter values as above, and assuming an average productivity of quarantined persons given by  $b = 0.5$ .

#### 3.2.1 Timing of the quarantine

The following figure illustrates the pandemic dynamics in the absence of a quarantine (solid curves, the same as in figure 1) and for a thirty-day quarantine covering 80 per cent of the population starting on day 30 of the pandemic (dashed curves). At early stages of the pandemic the starting date of the quarantine has almost no effect on the dynamics; a later starting date will simply postpone the pandemic.

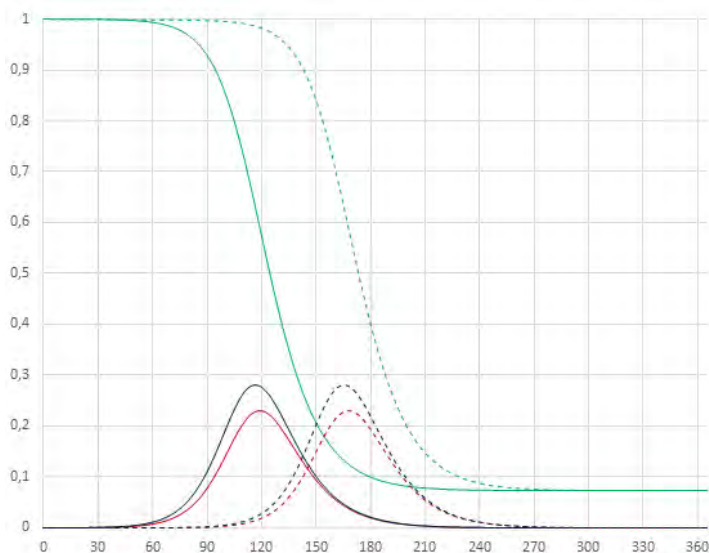


Figure 2. Pandemic dynamics with no quarantine and with a 30 day quarantine covering 80 per cent of the population starting on day 30

If the quarantine starts at a stage when the share of infectious individuals is increasing rapidly, the pandemic dynamics are affected differently, as illustrated by a quarantine starting

on day 90 in the following figure (dashed-dotted curves). In this case there will be a double-peak in the share of infectious individuals, as its rise is stopped, but it starts increasing again after the quarantine has been terminated.<sup>5</sup> In case the quarantine starts later, just before or after the peak of the share of infectious individuals has been reached, there will be a faster drop from the peak (see the dotted curves in the following figure). Both cases leads to fewer infected compared to the base case, and therefore to fewer deaths. The later quarantine leads to fewer being infected, but at the cost of a higher peak level of infectious individuals.

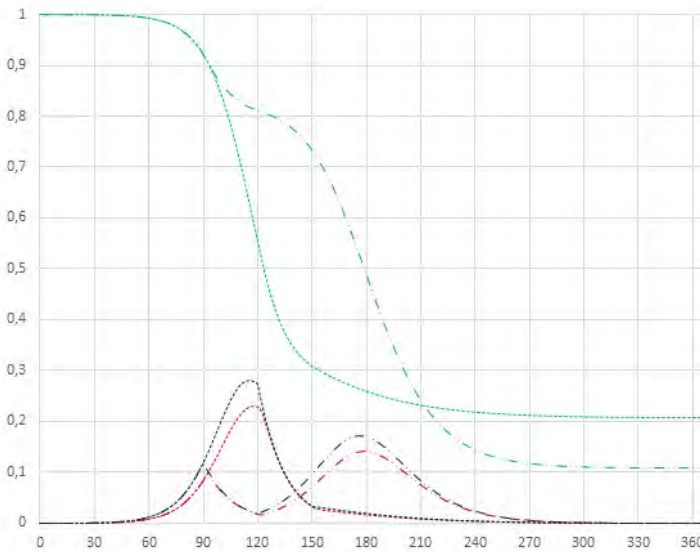


Figure 3. Pandemic dynamics for 30 day quarantines covering 80 per cent of the population starting on days 90 and 120

The following two figures illustrate how the peak level of the share of infectious individuals and the day when this peak level is reached are affected by the timing of a thirty-day quarantine covering 80 per cent of the population; the horizontal axis measures the day of the pandemic when the quarantine starts.

<sup>5</sup>This case is discussed by Anderson et al. (2020).

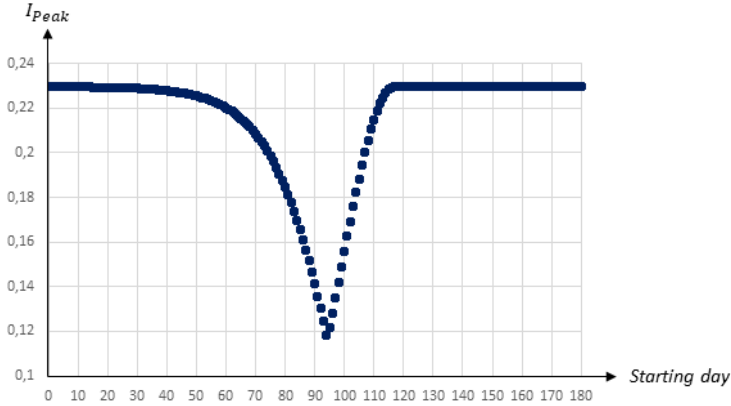


Figure 4. The peak level of infectious people in relation to the starting date of a 30 day quarantine covering 80 per cent of the population

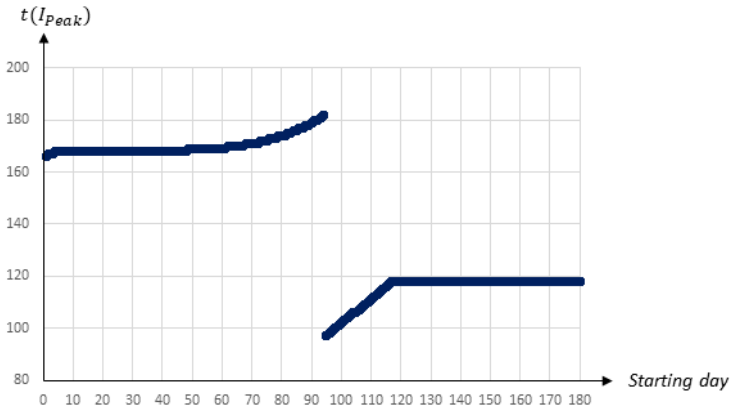


Figure 5. The day of the peak level of infectious people in relation to the starting date of a 30 day quarantine covering 80 per cent of the population

The perhaps most striking result is that there is a U-shaped relationship between the starting day of the quarantine and the maximum share of infectious individuals. An early quarantine primarily postpones the infection (see figure 2). Once lifted the infection runs its course, and, if there are still many susceptible in the population, the peak will be high. A late quarantine, just before or after the peak of the infection has passed, has no effect on the level of the peak (see figure 3). The peak of the infection is therefore mostly reduced by a quarantine in the midst

of the pandemic. This results in a double peak in the share of infectious persons, leading to a drop in the peak day as the first peak becomes larger than the second peak.

In the example above a quarantine starting on day 94 seems optimal in terms of reducing the peak level of infectious individuals; it decreases to less than 12 percent from almost 23 percent in the absence of a quarantine. This is a remarkably stable result; although peak levels obviously depend on the duration and the extent of a quarantine, those starting around this date generally yield the lowest peak levels.<sup>6</sup>

The following figures show the share of population that has recovered after the pandemic as well as the economic losses with respect to the starting date.

---

<sup>6</sup>For a 30 day quarantine covering only 20 per cent of the population the  $I_{Peak}$ -level would reach its minimum if it is started on day 93; however, the minimum  $I_{Peak}$ -level would be somewhat higher, at 0.15.

For a 60 day quarantine covering 80 per cent of individuals the  $I_{Peak}$ -level would also reach its minimum if implemented on day 93; in this case the minimum  $I_{Peak}$ -level would be somewhat lower, at 0.1086.

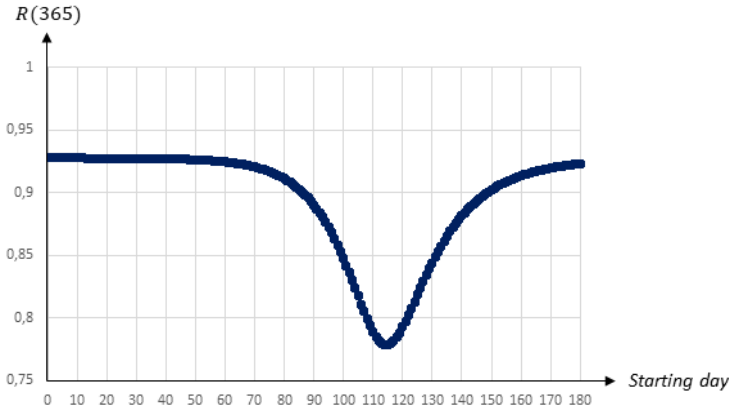


Figure 6. The share of population that has recovered one year after the start of the pandemic in relation to the starting date of a 30 day quarantine covering 80 per cent of the population

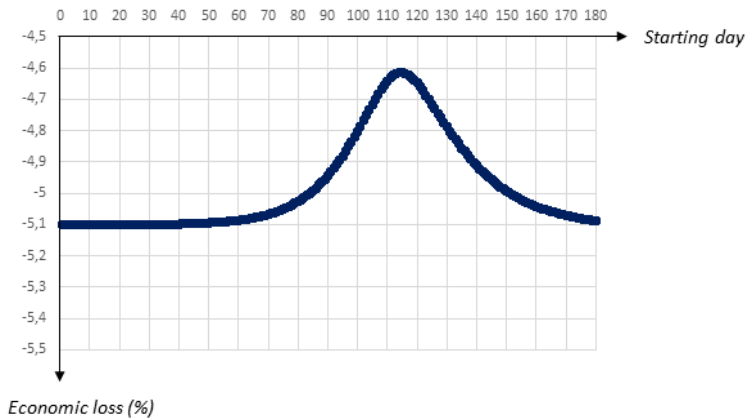


Figure 7. Economic losses in relation to the starting date of a 30 day quarantine covering 80 per cent of the population

There is a U-shaped relationship between the share of recovered individuals (and hence, also the share of deceased individuals) and the starting day of the quarantine. The lowest level is reached for a quarantine starting on day 114. In this case the share of the population that will have been infected and survived will be less than 78 per cent, as compared to almost 93 per cent in the absence of a quarantine. It is worth noting that herd immunity would be achieved

for any 30 day quarantine covering 80 percent of the population, regardless of the starting day.<sup>7</sup>

The relationship between the economic loss and the starting date is also U-shaped, with economic losses minimized for a quarantine starting on day 115. Interestingly there seems to be no trade-off between economic losses and averting fatalities. The total number of deaths and the economic losses are both minimized when the quarantine is implemented around day 114-115. Thus, to keep fatalities as well as economic losses low it seems optimal to postpone a quarantine to just before the share of infectious individuals reaches its peak. Again this result is stable; obviously levels depend on the duration and extent of a quarantine, but the general pattern is similar.<sup>8</sup> The downside, however, is that this policy does little to reduce the peak, and the implementation of this policy is therefore dependent on there being sufficient capacity in the health care system.

To summarize, there is a trade-off between lowering the peak level of infectious people on the one hand, and reducing fatalities as well as economic losses on the other hand. If the main goal is to lower the  $I_{Peak}$ -level an earlier quarantine starting day within this time frame is preferable, while a later starting day would be optimal if the main goal is to reduce fatalities and/or economic losses. An implication of this is that a high capacity for intensive care treatment in the health care system implies that the government can chose a strategy that leads to both fewer deaths and lower economic losses.

### 3.2.2 Duration of the quarantine

We now turn to the effect of the duration of a quarantine. We simulate quarantines that covers 80 per cent of the population. As demonstrated in the previous section, the timing of a quarantine impacts crucially on the pandemic dynamics. To analyze the effects of a quarantines duration we therefore distinguish between those implemented early and those started later, when the share of infectious individuals starts taking off.

Consider first the case of a quarantine that starts at a relatively early stage of the pandemic. The following figure illustrates the pandemic dynamics in the absence of a quarantine (solid curves) and on day 60 of the pandemic with different durations (30 days: dashed curves; 60 days: dashed-dotted curves; 90 days: dotted curves).

<sup>7</sup>The herd immunity threshold would be about 64% of the population given that  $R_0 = 2.8$ .

<sup>8</sup>For a 30 day quarantine covering only 20 per cent of the population the  $R(365)$ -value would be larger, reaching its minimum for one started on day 109 (at 0.875), while economic losses would be smaller, being minimized for a quarantine starting on day 111.

For a 60 day quarantine covering 80 per cent of individuals the  $R(365)$ -value would be smaller and minimized for one implemented on day 111 (at 0.668), while economic losses would be larger, being minimized for a quarantine starting on day 112.

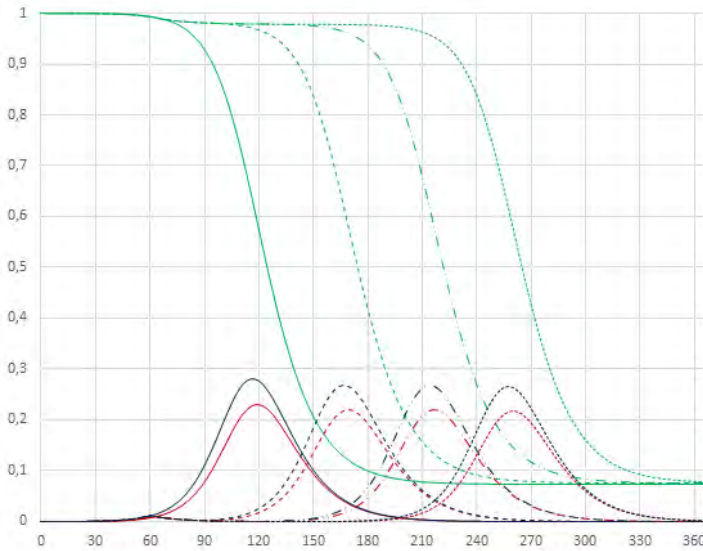


Figure 8. Pandemic dynamics for quarantines covering 80 per cent of the population starting on day 60 with different durations

The duration of a quarantine that starts relatively early, e.g. on day 60, pushes the dynamics forward, about 1.6 days per extra quarantine day, but has hardly any impact on the peak level of infectious individuals and the share of recovered persons after the pandemic has ended. Naturally a longer quarantine is associated with higher economic losses, about 0.1 percentage points for every extra day, as shown in the table below, which presents the  $I_{Peak}$ -level, the day when this peak is reached, the share of the population that will have been infected and survived, economic output and economic losses for quarantines of different durations. For example, Q60-74 indicates a quarantine starting on day 60 and ending on day 74.

	$I_{Peak}$	$t(I_{Peak})$	$R(365)$	$Y$	$dY/Y(\%)$
<b>No quarantine</b>	<b>0,229639</b>	<b>118</b>	<b>0,927533</b>	<b>359,2824</b>	<b>-1,83541</b>
<b>Q60-74</b>	0,222980	144	0,925365	353,3448	-3,45769
<b>Q60-89</b>	0,220134	169	0,924393	347,3839	-5,08635
<b>Q60-104</b>	0,218935	194	0,923933	341,4120	-6,71803
<b>Q60-119</b>	0,218358	217	0,923573	335,4361	-8,35078
<b>Q60-149</b>	0,217919	260	0,921169	323,4916	-11,6143

Table 1. Outcomes of quarantines of different durations, covering 80 per cent of the population and starting on day 60

A quarantine starting on the same day, but covering a smaller share of the population yields different results with respect to the duration. In particular, the share in isolation will impact substantially on the peak level, while having a smaller effect on the peak day and naturally leading to smaller economic losses (see section 3.2.3).

The impact of the duration of quarantines covering 80 per cent of the population is somewhat different when these start at a later stage, e.g. on day 90 of the pandemic, as illustrated in the following figure. The solid curves represent the absence of a quarantine, dashed curves represent a quarantine of 15 days duration, dashed-dotted curves represent a quarantine of 30 days duration and dotted curves represent a quarantine of 60 days duration.

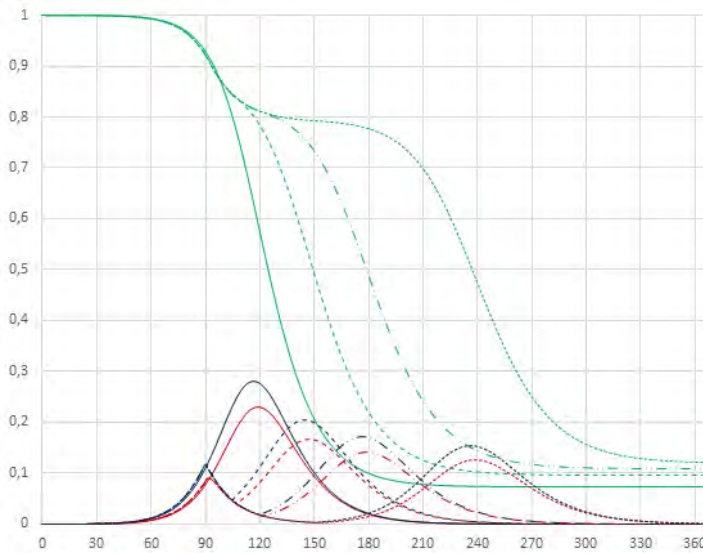


Figure 9. Pandemic dynamics for quarantines covering 80 per cent of the population starting on day 90 with different durations

All quarantines starting on day 90 lead to a double-peak in the share of infectious individuals, with the first peak occurring on day 90. The second, larger peak is pushed forward by around two days per extra quarantine day. The  $I_{Peak}$ -level decreases in the duration. The share of recovered individuals and deaths decrease in the duration of the quarantine. The following figures illustrate the impact of the duration (the number of days) of a quarantine on the peak level of infectious individuals and the day of the peak occurring.

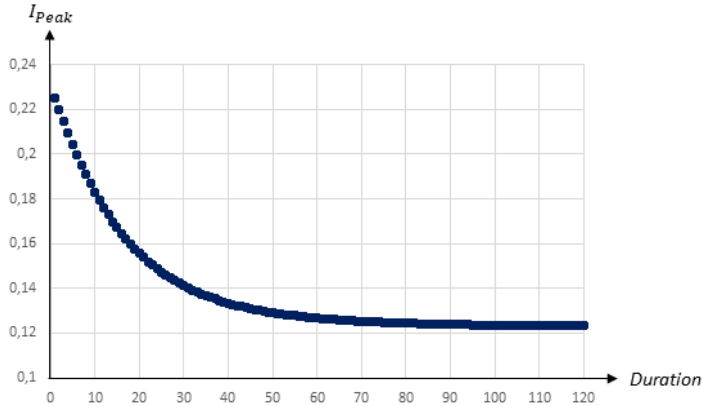


Figure 10. The peak level of infectious people in relation to the duration of a quarantine starting on day 90 and covering 80 per cent of the population

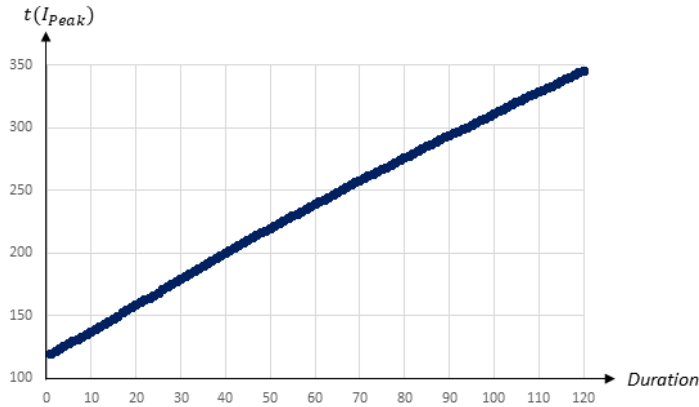


Figure 11. The day of the peak level of infectious people in relation to the duration of a quarantine starting on day 90 and covering 80 per cent of the population

While the peak day is almost linearly related to the duration, the peak level decreases at a decreasing rate in the duration. A quarantine lasting about 30 days reduces the peak level substantially; extending the quarantine beyond 30 days only marginally reduces the peak level,

but pushes the peak date forward. The following two figures illustrate the impact on the share of recovered individuals after one year and the economic losses in relation to the duration; since quarantines starting on day 90 and lasting more than 60 days lead to the pandemic not having ended after one years time, only the effects for durations up to 60 days are presented.

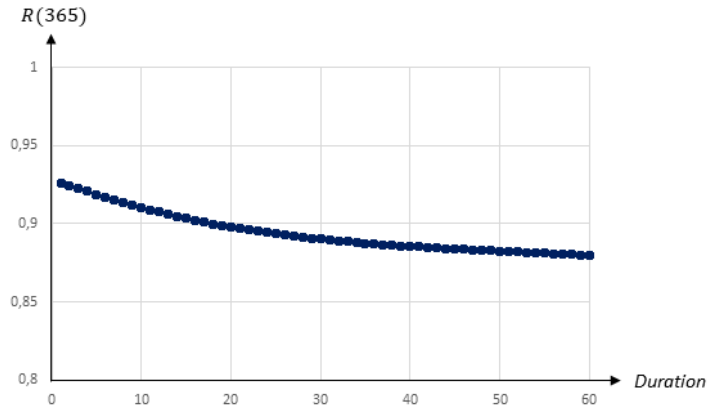


Figure 12. The share of population that has recovered one year after the start of the pandemic in relation to the duration of a quarantine starting on day 90 and covering 80 per cent of the population

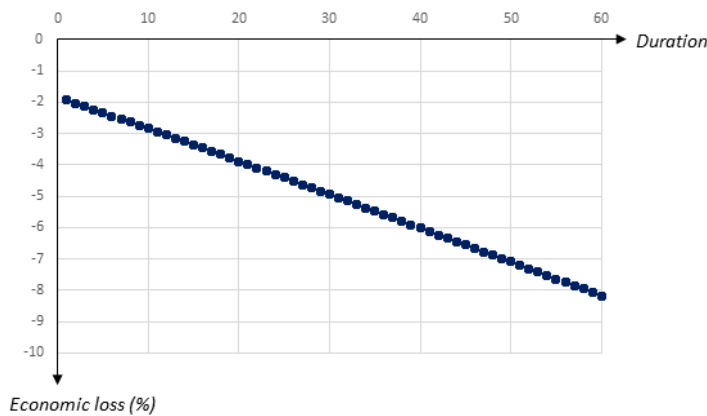


Figure 13. Economic losses in relation to duration of a quarantine starting on day 90 and covering 80 per cent of the population

The share of recovered individuals and hence, also the share of deceased persons is only marginally affected by the duration, whereas economic losses increase almost linearly in the

duration, by more than 0.1 percentage points for every extra quarantine day.

To summarize, longer quarantines imply larger economic losses. The main effect of a longer duration of a quarantine that is implemented at an early stage of the pandemic is to push the infection forward. For quarantines that start later, the peak level of infectious individuals is reduced by a longer duration, and so is the number of recovered and dead individuals. Thus, there is a relatively clear trade-off between economic costs and health outcomes in terms of the duration of a quarantine.

**3.2.3 Extent of the quarantine**

Finally, we vary the share of the population that is covered by the quarantine,  $q$ . Again we distinguish between quarantines starting early on and those starting later during the pandemic.

First, we consider quarantines starting relatively early, e.g. on day 60, and lasting for 60 days. The following figure illustrates the pandemic dynamics in the absence of a quarantine (solid curves) as well as for quarantines covering different shares of the population (20 per cent: dashed curves; 40 per cent: dashed-dotted curves; 60 per cent: dotted curves).

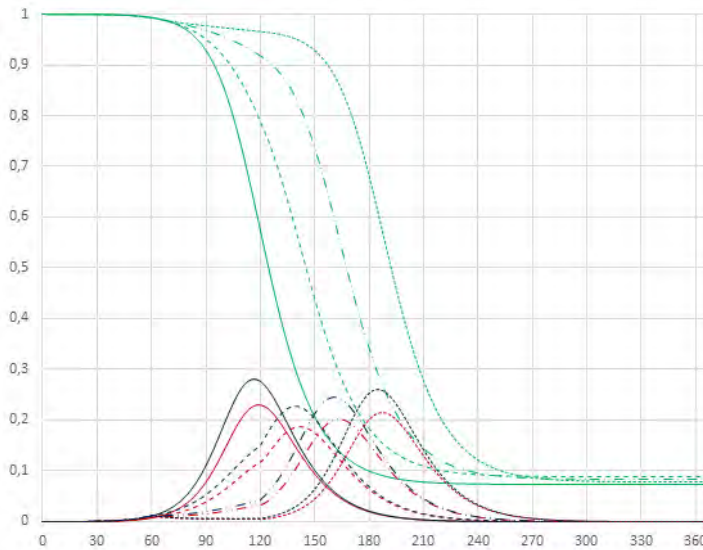


Figure 14. Pandemic dynamics for 60 day quarantines starting on day 60 and covering different shares of the population

An increase in the share of quarantined persons unambiguously pushes the  $I_{Peak}$ -day forward. The  $I_{Peak}$ -level first decreases somewhat, but eventually increases as a higher share of the population is covered by the quarantine. The share of recovered individuals remains stable

Covid Economics 1.5, 7 May 2020: 159-183

above 90 per cent. The following table summarizes results of simulations; a quarantine covering the entire population is obviously not realistic, but can be used as a benchmark.

	$I_{Peak}$	$t(I_{Peak})$	$R(365)$	$Y$	$dY/Y(\%)$
<b>No quarantine</b>	<b>0,229639</b>	<b>118</b>	<b>0,927533</b>	<b>359,2824</b>	<b>-1,83541</b>
<b>q=0.2</b>	0,185808	142	0,911491	353,4251	-3,43577
<b>q=0.4</b>	0,200683	163	0,917401	347,4115	-5,07882
<b>q=0.6</b>	0,213378	187	0,922015	341,4107	-6,71840
<b>q=0.8</b>	0,218358	217	0,923573	335,4361	-8,35078
<b>q=1.0</b>	0,219352	232	0,923614	329,4590	-9,98387

Table 2. Outcomes of quarantines of different extents, starting on day 60 and lasting for 60 days

Thus, the principal effect of increasing  $q$  for an early quarantine is to push the infection forward in time, but this is associated with substantial economic costs.

For quarantines starting a later stage of the pandemic the pattern is slightly different. The following figure illustrates the pandemic dynamics in the absence of a quarantine (solid curves) as well as for quarantines starting on day 90 of the pandemic, lasting for 60 days and covering different shares of the population (20 per cent: dashed curves; 35 per cent: dashed-dotted curves; 60 per cent: dotted curves).

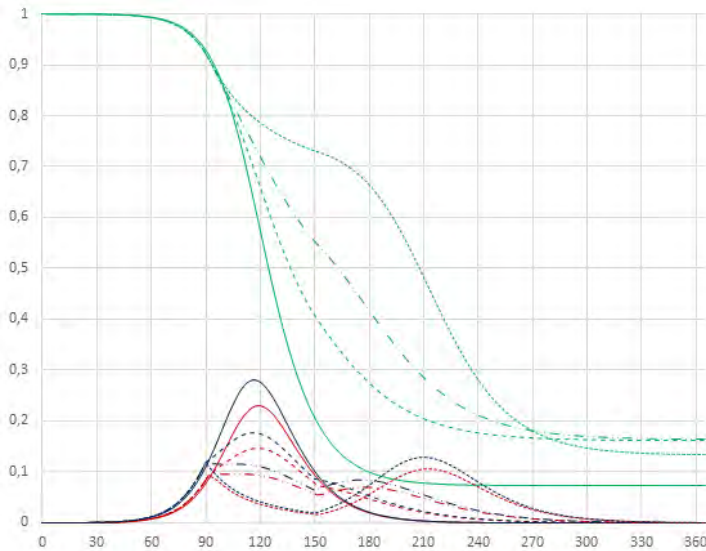


Figure 15. Pandemic dynamics for 60 day quarantines starting on day 90 and covering different shares of the population

A smaller share of quarantined individuals leads to flatter pandemic dynamics compared to the absence of a quarantine; in particular, the  $I_{Peak}$ -level is reduced substantially. For larger shares of quarantined individuals we obtain the familiar double-peak pattern, with the first peak occurring at the starting day of the quarantine. The second peak is actually lower for  $q = 0.35$  than for  $q = 0.6$ , as a higher share will already have become infectious once the quarantine is terminated. The following figures illustrate how the  $I_{Peak}$ -level and the  $I_{Peak}$ -day are affected by the extent of the quarantine.

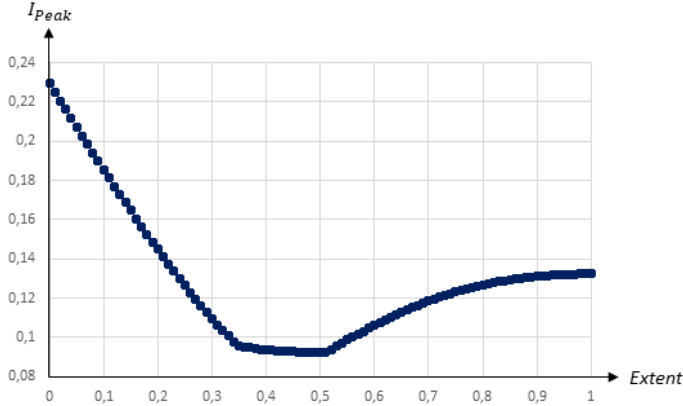


Figure 16. The peak level of infectious people in relation to the extent of a 60 day quarantine starting on day 90

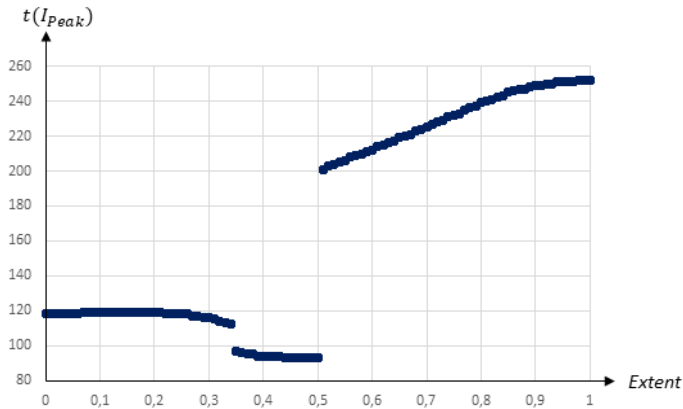


Figure 17. The day of the peak level of infectious people in relation to the extent of a 60 day quarantine starting on day 90

An increase in  $q$  initially reduces the  $I_{Peak}$ -level and has only a minor impact on the  $I_{Peak}$ -day.<sup>9</sup> Eventually an increase in  $q$  brings about the double-peaked pandemic pattern. A higher  $q$  is associated with an increase in the  $I_{Peak}$ -day, but also an increase in the  $I_{Peak}$ -level. The impact on the  $I_{Peak}$ -level is thus U-shaped, with a minimum reached for  $q = 0.5$  when the two

<sup>9</sup>Note that for quarantines covering around a third of the population the first peak resembles a plateau lasting for almost 30 days (see figure 15 when  $q = 0.35$ ). We therefore observe a drop in the peak-level day when  $q$  increases from 0.34 to 0.35, as the peak of this plateau shifts from day 112 to day 97.

peaks reach almost the same level. The following figures illustrate how the share of recovered individuals after one year and economic losses are affected by the extent of the quarantine.

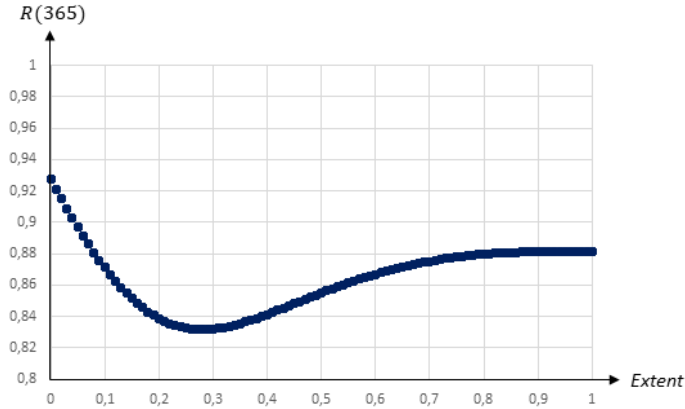


Figure 18. The share of population that has recovered one year after the start of the pandemic in relation to the extent of a 60 day quarantine starting on day 90

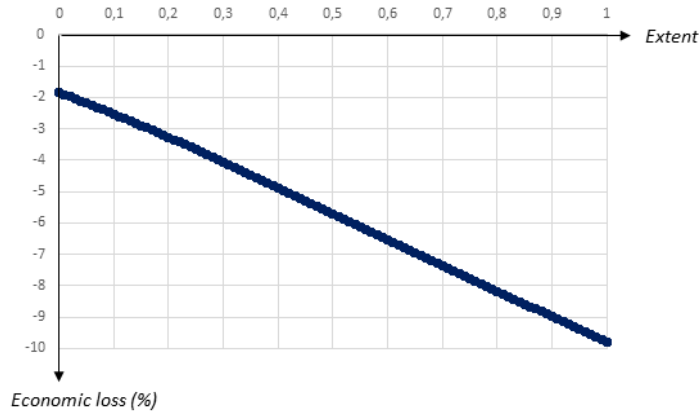


Figure 19. Economic losses in relation to the extent of a 60 day quarantine starting on day 90

The relationship between the share of recovered (and hence, also deceased) people after the pandemic and the extent of the quarantine is also U-shaped. More specifically, the number of deceased individuals is minimized for  $q = 0.28$ . Economic losses increase almost linearly in the share of quarantined persons, by almost 0.08 percentage points for every extra per cent being

quarantined.

For  $q \in [0.28, 0.5]$  there is a trade-off between lowering the  $I_{Peak}$ -level on the one hand and reducing the share of people that will have become exposed to the virus on the other hand. If the main goal is to minimize fatalities, a quarantine covering a smaller share of the population is optimal, while a quarantine covering almost half the population is preferable if the focus is on reducing the  $I_{Peak}$ -level.

To summarize, the main effect of increasing the share of the quarantined population when the quarantine starts at a relatively early stage of the pandemic is essentially that the peak infection day is pushed forward, but this comes at a substantial economic cost. A quarantine starting at a later stage, when the number of infectious individuals starts increasing rapidly, is associated with a U-shaped relationship between the peak level of infectious individuals and the extent of the quarantine, such that the peak level is reduced substantially for quarantines covering about half the population. At higher  $q$ -levels the peak is pushed forward, but this also leads to a higher peak level and higher economic losses. The share of deceased people is minimized for quarantines covering a rather small share of the population. Thus, there is a relatively strong case for limiting the extent of a quarantine, since this leads to a lower peak, fewer deaths and lower economic costs. However, such a policy would lead to an earlier peak of infectious people.

## 4 Conclusions

This paper considers some of the basic trade-offs between health outcomes and economic outcomes when a quarantine is implemented. For this purpose we employ a SEIR-model, calibrated to resemble the COVID-19 pandemic and coupled with the assumption that infected and quarantined individuals lose part of their productivity.

Our main findings can be summarized as follows. First, the implementation of an early quarantine will essentially postpone but not alter the course of the infection at a cost that increases in the duration and the extent of the quarantine. Second, a later starting day of a quarantine is optimal if the main goal is to reduce fatalities and economic losses, but it comes at the cost of a higher peak level of infectious people. The use of this strategy therefore depends on whether the health care system can deal with a high peak level. Third, there is a trade-off between economic costs and health outcomes when it comes to the duration of a quarantine. A longer quarantine either postpones the peak (if it is implemented relatively early) or dampens the peak and reduces deaths (if it starts at a later stage of the pandemic), but implies higher economic losses. Finally, there is a relatively strong case for limiting the extent of a quarantine. A less than complete quarantine leads to a lower peak, fewer deaths and lower economic costs. The flip side of this strategy is that the peak of infectious individuals occurs earlier.

To test the robustness of our results we have simulated pandemics with both higher and lower transmission rates. Qualitatively all our findings can be replicated for different pandemic dynamics. Thus, our conclusions regarding the timing, duration and extent of quarantines hold

generally.

## 5 References

### References

- Alvarez, F. E., D. Argente, and F. Lippi (2020). A simple planning problem for covid-19 lockdown. Technical report, National Bureau of Economic Research.
- Anderson, R. M., H. Heesterbeek, D. Klinkenberg, and T. D. Hollingsworth (2020). How will country-based mitigation measures influence the course of the covid-19 epidemic? *The Lancet* 395(10228), 931–934.
- Atkeson, A. (2020). What will be the economic impact of covid-19 in the us? rough estimates of disease scenarios. Technical report, National Bureau of Economic Research.
- Baldwin, R. E. and B. Weder di Mauro (2020a). *Economics in the Time of COVID-19*. CEPR Press.
- Baldwin, R. E. and B. Weder di Mauro (2020b). *Mitigating the COVID EconomicCrisis: Act Fast and Do Whatever It Takes*. CEPR Press.
- Bendavid, E., B. Mulaney, N. Sood, S. Shah, E. Ling, R. Bromley-Dulfano, C. Lai, Z. Weissberg, R. Saavedra, J. Tedrow, et al. (2020). Covid-19 antibody seroprevalence in santa clara county, california. *medRxiv*.
- Casares, M., H. Khan, et al. (2020). A dynamic model of covid-19: Contagion and implications of isolation enforcement. Technical report, Carleton University, Department of Economics.
- Dewatripont, M., M. Goldman, E. Muraille, and J.-P. Platteau (2020). Rapid identification of workers immune to covid-19 and virus-free: A priority to restart the economy. Technical report, Discussion paper, Universit Libre de Bruxelles.
- Gonzalez-Eiras, M. and D. Niepelt (2020). On the optimal "lockdown" during an epidemic. Technical report, CESifo.
- Hall, R. E., C. I. Jones, and P. J. Klenow (2020). Trading off consumption and covid-19 deaths. Technical report, Mimeo, Stanford University.
- He, X., E. H. Lau, P. Wu, X. Deng, J. Wang, X. Hao, Y. C. Lau, J. Y. Wong, Y. Guan, X. Tan, et al. (2020). Temporal dynamics in viral shedding and transmissibility of covid-19. *Nature Medicine*, 1–4.

Jones, C. J., T. Philippon, and V. Venkateswaran (2020). Optimal mitigation policies in a pandemic: Social distancing and working from home. Technical report, National Bureau of Economic Research.

Kermack, W. O. and A. G. McKendrick (1927). A contribution to the mathematical theory of epidemics. *Proceedings of the royal society of london. Series A, Containing papers of a mathematical and physical character* 115(772), 700–721.

Piguillem, F., L. Shi, et al. (2020). The optimal covid-19 quarantine and testing policies. Technical report, Einaudi Institute for Economics and Finance (EIEF).

# Short-term impact of COVID-19 on poverty in Africa

Gbêtondji Melaine Armel Nonvide<sup>1</sup>

Date submitted: 1 May 2020; Date accepted: 3 May 2020

*Less impacted than the rest of the world, the African continent is also facing the spread of Covid-19 and the numbers of confirmed cases are rising. This paper estimates the short-term impact of COVID-19 on poverty in Africa using the World Bank's PovcalNet dataset. Three scenarios were used including low, medium and high consumption contractions of 10%, 20% and 30%. The impact is estimated based on the US\$ 1.90 per day poverty line. First, the impact of COVID-19 is estimated for the whole Africa. Secondly, to account for the regional heterogeneity, the impact is estimated separately for the five regions in Africa. The results indicate that the number of poor people in Africa would increase by between 59 and 200 million due to contractions in consumption as a result of COVID-19 pandemic. In all three scenarios, West Africa and East Africa are the most affected by contractions in consumption due to the COVID-19 pandemic, while North Africa is the least affected among the five regions in Africa. The findings suggest that COVID-19 pandemic is a serious threat for achieving the Sustainable Development Goals (SDGs). Therefore, governments and international organizations should increase efforts in supporting the economic activities in all countries.*

<sup>1</sup> Research Fellow, Laboratoire d'Economie Publique, Université d'Abomey-Calavi.

Copyright: Gbêtondji Melaine Armel Nonvide

## 1. Introduction

The whole world is facing an unprecedented health crisis due to the Covid-19 pandemic. The virus has spread to 185 countries and regions since emerging in China last December. As of April 2020, there are more than 3 million cases infected with COVID-19 worldwide with the U.S. and Europe now the hardest-hit regions in the world. The ten (10) most affected countries are United States (US), Spain, Italy, France, Germany, United Kingdom, Turkey, Russia, Iran and China. China, which was initially the world center of the epidemic, registers less than 100 thousand cases while in the others countries, this bar is largely exceeded. For instance the US confirmed more than a million cases. In Africa, the number of COVID-19 cases has risen to about 30,000. North Africa remains the hardest-hit of the continent's five regions, followed by West, Southern, East, and Central. In term of countries, South Africa has 4,996 COVID-19 cases, Egypt has 4,100, Morocco 3,800, and Algeria has 3,100.

The consequences of this COVID-19 pandemic would be dramatic worldwide, both from a health and economic point of view. A global economic recession appears inevitable in 2020. African countries would not be spared from this global economic crisis. Recent studies that estimate the economic impact of the COVID-19 were done by International Food Policy Research Institute (IFPRI), the International Labour Organization (ILO), and the United Nations University World Institute for Development Economics Research (UNU-WIDER).

Employing the computable general equilibrium (CGE) model, the estimates of IFPRI done by Vos, Martin and Laborde (2020a, 2020b) show that a decrease of 1 percentage point in a global gross domestic product (GDP) would increase poverty (based on a poverty line of US\$1.90 per day) by between 14–22 million people in Sub-Sahara Africa and South Asia. However the impact would be greater in Sub-Sahara Africa. Also based on a CGE model, the work by ILO (2020) is focused on three scenarios: low, medium, and high global drops in GDP growth of 2, 4, and 8 per cent. In all cases, the three scenarios results indicate a substantial rise in global unemployment of between 5.3 million and 24.7 million from a base level of 188 million in 2019. The medium scenario suggests an increase of 13 million. The working poverty is also likely to increase significantly; under the mid and high scenarios, there will be between 20.1 million and 35.0 million more people in working poverty.

UNU-WIDER estimates by Sumner, Hoy and Ortiz-Juarez (2020) used the World Bank's PovcalNet dataset. Their estimates are based on three scenarios: low, medium, and high income or consumption contractions of 5, 10, and 20 per cent; and three poverty lines including

US\$1.90, US\$3.20 and US\$5.50 per day. The three scenarios results show an important increase in the number of poor relative to the 2018 figures, of between 80 million and 580 million people. Under the medium scenario, the increases in a number of poor people is between 180, and 280 million people. Sumner, Hoy and Ortiz-Juarez (2020) also show that the concentration of the potentially new poor under the US\$1.9/day and US\$3.2/day poverty lines would occur in the poorest regions of the world, notably in SSA and South Asia, which could accrue together between two thirds and 80–85 per cent of the total poor. For the higher poverty line of US\$5.5/day, about 40 per cent of the new poor could be concentrated in East Asia and Pacific, about a third in both SSA and South Asia combined, and about 10 per cent each in Middle East and North Africa and Latin America and the Caribbean.

This paper aims to estimate the potential short-term impact of COVID-19 on poverty in Africa. While previous studies (Sumner, Hoy and Ortiz-Juarez, 2020; Vos, Martin and Laborde, 2020a, 2020b) concluded on the greatest impact of COVID 19 in Sub Sahara Africa, this does not tell about the specific case of the regions in Africa. In fact, the regions are not affected in the same way as they have different levels of development and resilience. The study accounts for this heterogeneity by including the regions in the analysis. The five (5) regions in Africa are “Central Africa”, “North Africa”, “East Africa”, “Southern Africa” and “West Africa”.

The rest of the paper is structured as follows. Section 2 presents the methods of analysis followed by results and discussion in section 3. Finally, section 4 provides concluding remarks.

## 2. Methods of analysis

Data used in this study are from the World Bank’s PovcalNet dataset and were computed through the Stata’s PovcalNet interface (Castañeda et al. 2019; Sumner, Hoy and Ortiz-Juarez, 2020) at the global and regional levels in Africa. The data were aggregated using 2018 as the reference year. PovcalNet has income or consumption distributional data from more than 1500 household surveys spanning 1967-2018 and 166 economies<sup>2</sup>.

The data set allows to consider all the five regions in Africa. However, there are four (04) countries that were not covered by PovcalNet dataset. These include Somalia and Eritrea for East Africa, Equatorial Guinea for Central Africa and Liberia for North Africa. Thus, in total, fifty (50) countries distributed in five regions are included in this analysis (see annex 1 for the list of countries).

<sup>2</sup> <http://iresearch.worldbank.org/PovcalNet/methodology.aspx>

All the African countries have consumption data in the PovcalNet dataset except Seychelles which has an income data. These monetary data are expressed in PPP exchange rates from the 2011 International Comparison Program (Sumner, Hoy and Ortiz-Juarez, 2020). A poor people is defined as an individual whose daily consumption expenditure or income is less than an international poverty line of US\$ 1.90.

This study uses three scenarios of consumption drops as a result of the COVID 19 pandemic.

- a “Low scenario” where consumption drops by around 10 per cent;
- a “Mid scenario” where consumption decreases by 20 per cent;
- a “High scenario” where consumption reduces by around 30 per cent:

The study considers 10, 20 and 30 per cent contractions in consumption instead of 5, 10, and 20 per cent contractions used by Sumner, Hoy and Ortiz-Juarez (2020) because we believed that the impact of COVID-19 would be more pronounced in developing countries especially in Africa than the developed countries. The reason is that majority of the populations in Africa are poor and lives daily. Therefore this COVID-19 pandemic will have much more effect on the consumption and income levels of populations in Africa.

Following Sumner, Hoy and Ortiz-Juarez (2020), the reductions in consumption is captured by increasing the value of the poverty line consequently. This is because the individuals’ consumption levels from PovcalNet’s built-in database are not observed. Therefore, for a consumption decreases of  $x$  per cent, the poverty line  $z$  is adjusted upwardly as follows:

$$Z' = z (1 - x) \quad (1)$$

Where  $Z'$  is the adjusted poverty line.

The three scenarios were performed using a “povcalnet” command in STATA 15.

### 3. Results and discussion

To achieve the objective of the paper, we first estimate the impact of COVID-19 on the whole Africa. Secondly, to account for the regional heterogeneity, we estimate the impact separately for the five regions in Africa. All the estimations were performed based on the US\$ 1.90 per day poverty line.

Table 1 shows the increase in poverty as result of COVID-19 pandemic at the global level in Africa.

**Table 1.** Increase in poverty in Africa due to consumption drops as a result of COVID-19 pandemic

Percentage decreases in consumption	Number of poor people		Additional percentage points in poverty incidence	
	Percentage	Millions	Percentage	Millions
10%	40.3	502.8	4.7	58.6
20%	45.6	568.9	10	124.7
30%	51.5	642.5	15.9	198.3
Status quo			35.6%	

**Source:** Estimates based on PovcalNet

All other things being equal, a drops in consumption or income as a result of COVID-19 pandemic would lead to an increase in the global poverty headcount ratio in Africa. Under a decrease of 10% and relative to the reference year (2018), the poverty headcount ratio at US\$ 1.9 per day would increase by about 5 percentage points; meaning that under this low scenario, the whole Africa could experience an increase in the number of poor people in comparison to the status quo in 2018, by 59 million. Under the medium scenario, the result indicate an increase in poverty incidence by 10% equivalent of 124.7 million new poor people relative to the status quo. In the most extreme scenario, that is a consumption contraction of 30%, the poverty headcount ratio would increase by about 16%. This suggests that comparing to the status quo, Africa would experience an increase in the number of poor people by almost 200 million. The results of the three scenario reveal that the poverty incidence in Africa would increase by between 5 - 16%. In absolute terms this means that the number of poor people in Africa would increase by between 59 – 200 million.

Considering the fact that the impact of drops in consumption due to COVID-19 could differ depending on the regions, the impact is presented for the five regions in Africa (Table 2). In the case of Central Africa, Table 2 shows that under a decrease of 10% and relative to the reference year (2018), the poverty incidence at US\$ 1.9 per day would increase by about 4.5 percentage points; meaning that under this low scenario, in Central Africa the number of poor people would increase in comparison to the status quo in 2018, by 6.1 million. Under the medium scenario, the result indicate an increase in poverty incidence by 9 percentage points, equivalent of 12.4 million new poor people relative to the status quo. In the most extreme scenario (30% drops) the poverty headcount ratio would increase by about 13.7 percentage points. This suggests that comparing to the status quo, Central Africa would experience an increase in the number of poor people by almost 19 million. Similar results were found in

Southern Africa where the low scenario indicate an increase in the poverty incidence by about 4 percentage points, corresponding to an increase in the number of poor people by 8.3 million comparing to the status quo. For the medium scenario, the result indicate an increase in poverty headcount ratio by about 9 percentage points equivalent of 17.5 million additional poor people relative to the status quo. In the most extreme scenario, the poverty incidence would increase by about 13.5 percentage points, suggesting that Southern Africa would experience an increase in the number of poor people by 27.4 million.

The results of the low scenario (decrease of 10%) show that in the case of East Africa, the poverty incidence at US\$ 1.9 per day would increase by 6 percentage points, equivalent to 20.2 million increase in a number of poor people in comparison to the status quo in 2018. Under the medium scenario, the result indicate an increase in poverty incidence by about 13 percentage points equivalent of 43.2 million new poor people relative to the status quo. In the most extreme scenario, the poverty headcount ratio would increase by about 20.2 percentage points. This suggests that comparing to the status quo, East Africa would experience an increase in the number of poor people by 68.2 million. Similar results were found in West Africa. Indeed the low scenario indicate an increase in the poverty incidence by about 6 percentage points. This corresponds to an increase in the number of poor people by 21.8 million comparing to the status quo. For the medium scenario, the result indicate an increase in poverty incidence by about 12 percentage points equivalent of 45 million additional poor people relative to the status quo. In the most extreme scenario, the poverty incidence would increase by about 19 percentage points, suggesting that West Africa would experience an increase in the number of poor people by almost 71 million.

In the case of North Africa, a decrease of 10% in the consumption would increase the poverty headcount ratio by about 1.2 percentage points; meaning that under this low scenario, in North Africa the number of poor people would increase in comparison to the status quo in 2018, by 2.3 million. Under the medium scenario, the result indicate an increase in poverty incidence by 3.5 percentage points, equivalent to 6.7 million additional poor people relative to the status quo. In the most extreme scenario (30% drops) the poverty headcount ratio would increase by about 7 percentage points, suggesting that comparing to the status quo, North Africa would experience an increase in the number of poor people by 13.2 million.

**Table 2.** Increase in poverty by regions in Africa due to consumption drops as a result of COVID-19 pandemic

Percentage decreases in consumption	Number of poor people		Additional number of poor people	
	Percentage	Millions	Percentage	Millions
Central Africa				
10%	60.5	82.8	4.5	6.1
20%	65.1	89.1	9.1	12.4
30%	69.7	95.4	13.7	18.7
<b>Status quo</b>	56.0%			
East Africa				
10%	40.2	135.7	6.0	20.2
20%	47.0	158.7	12.8	43.2
30%	54.4	183.7	20.2	68.2
<b>Status quo</b>	34.2%			
North Africa				
10%	3.2	6.1	1.2	2.3
20%	5.5	10.5	3.5	6.7
30%	8.9	17.1	6.9	13.2
<b>Status quo</b>	2.0%			
Southern Africa				
10%	49.4	100.5	4.1	8.3
20%	53.9	109.6	8.6	17.5
30%	58.8	119.6	13.5	27.4
<b>Status quo</b>	45.3%			
West Africa				
10%	47.0	177.0	5.8	21.8
20%	53.1	200.0	11.9	44.8
30%	60.0	226.0	18.8	70.8
<b>Status quo</b>	41.2%			

**Source:** Estimates based on PovcalNet

Overall, the results of the three scenario indicate an increase of poverty in all the five regions. This increase is between 4.5 - 14 percentage points for Central Africa, 6 – 21 percentage points for East Africa, 1–7 percentage points for North Africa, 4 – 14 percentage points for Southern Africa, and between 5 – 19 percentage points for West Africa. In absolute terms this corresponds to an increase between 6 - 19 million for Central Africa, 20 – 69 million for East Africa, 2 – 14 million for North Africa, 8 – 28 million for Southern Africa, and between 21 – 71 million for West Africa.

Table 3 presents the share of additional poor for each region in the global increase in poverty in Africa.

**Table 3.** Share of poor by region in the global increase in poverty in Africa

Regions	Population (millions)	Number of additional poor people (millions)			Share in percentage		
		10%	20%	30%	10%	20%	30%
Central Africa	137.0031	6.1	12.4	18.7	10.4	10.0	9.4
East Africa	337.8018	20.2	43.2	68.2	34.4	34.6	34.4
North Africa	192.6497	2.3	6.7	13.2	4.0	5.4	6.7
Southern Africa	203.4939	8.3	17.5	27.4	14.1	14.0	13.8
West Africa	376.7934	21.8	44.8	70.8	37.1	36.0	35.7
Africa	1247.7419	58.7	124.6	198.3	100	100	100

**Source:** Estimates based on PovcalNet

Focusing on a 10% drops in consumption and under the US \$ 1.9 per day poverty line, Table 3 shows that about 71% of those additional poor would be located in two regions including East Africa (34.4%) and West Africa (37.1%). North Africa accounted for the lowest share with about 4% of the additional poor in Africa as a result of COVID-19 pandemic. Similar results were found with 20% and 30% decrease in consumption respectively. Based on the three scenario, West Africa and East Africa appear to be more affected by contractions in consumption due to the COVID-19 pandemic, while North Africa is the least affected among the five regions in Africa. This contrasts with the fact that North Africa is the hardest-hit of the continent's five regions in term of confirmed case of COVID-19. However, it can be noted that in contrast to the other regions, North Africa has benefited from a lower level of poverty.

#### 4. Conclusion

The COVID-19 pandemic continues to affect the African continent. Though the continent still accounts for relatively few confirmed cases, the numbers are rising. As African countries struggle to contain the virus, they are affected by the efforts of other countries doing the same, and the economic impacts of COVID -19 pandemic grow. This paper estimates the short-term impact of COVID-19 on poverty in Africa using the World Bank's PovcalNet dataset. Three scenario were proposed in this study: low, medium and high consumption contractions of 10%, 20% and 30% based on the US\$ 1.90 per day poverty line. The results of the three scenario show that, the poverty incidence in Africa would increase by between 5 - 16%. In absolute terms this means that the number of poor people in Africa would increase by between 59 – 200

million due to contractions in consumption as a result of COVID-19 pandemic. The results also indicate an increase in poverty between 4.5 - 14 percentage points for Central Africa, 6 – 21 percentage points for East Africa, 1–7 percentage points for North Africa, 4 – 14 percentage points for Southern Africa, and between 5 – 19 percentage points for West Africa. In absolute terms this corresponds to an increase between 6 - 19 million for Central Africa, 20 – 69 million for East Africa, 2 – 14 million for North Africa, 8 – 28 million for Southern Africa, and between 21 – 71 million for West Africa. Finally, based on the three scenario, West Africa and East Africa are the most affected by contractions in consumption due to the COVID-19 pandemic, while North Africa is the least affected among the five regions in Africa.

While interesting, these findings have important limitations. Using the PovcalNet dataset, the estimates are based on distribution neutral assumptions, and therefore some interactions with labour market, household-level responses to economic contractions, and government responses to COVID-19 pandemic are not accounted in the analysis. Also, the potential impact of COVID-19 could be bias (overestimated or underestimated) because the real impact may depend on how long the pandemic will last or the effectiveness of responses by governments and international organizations. Further studies should explore how responses from governments, international organizations and households can reduce the impact of COVID-19 pandemic. Despite all these, the findings are very useful and practical. These findings cast doubt on the fact that the impact of COVID-19 would be extreme. Thus, the study calls for rapid public policy (governments and international organizations) interventions to support the economic activities in all countries especially in African countries.

## Reference

- Castañeda Aguilar, R. A., Lakner, C., Prydz, E. B., Soler Lopez, J., Wu, R. and Zhao, Q. (2019). Estimating Global Poverty in Stata. The povcalnet command. Global Poverty Monitoring Technical Note 9. World Bank: Washington DC. <http://documents.worldbank.org/curated/en/836101568994246528/pdf/Estimating-Global-Poverty-in-Stata-The-Povcalnet-Command.pdf>.
- ILO (2020). COVID-19 and the world of work: impact and policy responses. International Labour Organization. [https://www.ilo.org/wcmsp5/groups/public/---dgreports/-dcomm/documents/briefingnote/wcms\\_738753.pdf](https://www.ilo.org/wcmsp5/groups/public/---dgreports/-dcomm/documents/briefingnote/wcms_738753.pdf).
- Sumner, A., Hoy, C. and Ortiz-Juarez, E. (2020). Estimates of the impact of COVID-19 on global poverty. UNU- WIDER Working Paper 2020/43. <https://www.wider.unu.edu/publication/estimates-impact-covid-19-global-poverty>.
- Vos, R., Martin, W. and Laborde, D. (2020a). How much will global poverty increase because of COVID-19?. <https://www.ifpri.org/blog/how-much-will-global-poverty-increase-because-covid-19>.
- Vos, R., Martin, W. and Laborde, D. (2020b). As COVID-19 spreads, no major concern for global food security yet. <https://www.ifpri.org/blog/covid-19-spreads-no-major-concern-global-food-security-yet>.

**Annex 1.** Countries list and codes

Countries	Codes
<b>Central Africa</b>	
1. Cameroon	CMR
2. Central African Republic	CAF
3. Chad	TCD
4. Congo Dem Rep	COD
5. Congo Rep	COG
6. Equatorial Guinea*	GNQ
7. Gabon	GAB
8. Sao Tome	STP
<b>East Africa</b>	
9. Burundi	BDI
10. Comoros	COM
11. Djibouti	DJI
12. Eritrea*	ERI
13. Ethiopia	ETH
14. Kenya	KEN
15. Rwanda	RWA
16. Seychelles*	SYC
17. Somalia	SOM
18. South Sudan	SSD
19. Sudan	SDN
20. Tanzania	TZA
21. Uganda	UGA
<b>North Africa</b>	
22. Algeria	DZA
23. Egypt	EGY
24. Libya*	LBY
25. Mauritania	MRT
26. Morocco	MAR
27. Tunisia	TUN
<b>Southern Africa</b>	
28. Angola	AGO
29. Botswana	BWA
30. Lesotho	LSO
31. Madagascar	MDG
32. Malawi	MWI
33. Mauritius	MUS
34. Mozambique	MOZ
35. Namibia	NAM
36. South Africa	ZAF
37. Eswatini	SWZ
38. Zambia	ZMB
39. Zimbabwe	ZWE
<b>West Africa</b>	
40. Benin	BEN
41. Burkina	BFA
42. Cabo Verde	CPV

43. Cote d'Ivoire	CIV
44. Gambia	GMB
45. Ghana	GHA
46. Guinea	GIN
47. Guinea Bissau	GNB
48. Liberia	LBR
49. Mali	MLI
50. Niger	NER
51. Nigeria	NGA
52. Senegal	SEN
53. Sierra Leone	SLE
54. Togo	TGO

**Note.** \* denotes countries that are not covered by the World Bank's PovcalNet dataset.